

**Hydroxy fatty acids: Structures and antifungal activities in foods**

by

Nuanyi Liang

A thesis submitted in partial fulfillment of the requirements for the degree of

Doctor of Philosophy

in

Food Science and Technology

Department of Agricultural, Food and Nutritional Science

University of Alberta

© Nuanyi Liang, 2020

## Abstract

Spoilage and mycotoxin production by mycelial fungi threatens global food security. Climate change and increasingly complex food value chains may exacerbate these concerns. Alternative or complementary antifungal agents for food and agricultural applications may alleviate problems associated with fungi. Hydroxy fatty acids (HFAs) are novel antifungal agents, however, due to the diversity in the molecular structures of hydroxy fatty acids from various sources, their structure-function relationships, modes of action, and potential applications, have not been fully investigated. In this work, several HFAs were extracted from two types of lactobacilli fermented cultures and four types of plant seed oils. HFAs were purified using solid-phase extraction (SPE) or high-speed counter-current chromatography (HSCCC). The purified HFAs were then characterized by LC-APPI-MS/MS and LC-ESI-MS/MS. Eight types of HFAs were tested to challenge the growth of common food-related fungi, including filamentous fungi and yeasts (Chapter 3-5). Structure-antifungal activity relationships demonstrated that the location of the hydroxy groups within a HFA determines its antifungal activity. Mono-HFAs with hydroxy group located at the middle of the fatty acid chain (C9-13) were found to have high anti-mold activities. Remarkably, filamentous fungi, but not yeasts, were sensitive to HFA with a hydroxy group in C9-13 location. To investigate the difference between HFA-resistant yeasts and -sensitive molds, the content of a cellular membrane fluidity modifier, ergosterol, was quantified. With one exception, the HFA-resistant yeasts tend to have high sterol content (Chapter 5). This structure-function relationship elucidated the application of HFA in preventing mold growth while allowing yeast viability and activities. This relationship also indicates that HFA mainly targets fungal strains with a relatively low ergosterol content, but other resistant mechanisms may also be involved.

A representative HFA was applied in sourdough bread to determine their efficacy *in situ* (Chapter 6). The anti-mold effect of ricinoleic acid was weaker in flaxseed-flour sourdough bread when compared to wheat-flour sourdough bread. In addition, collaborative work in plants indicated synergistic antifungal effects of coriolic acid with other plant components. These indicate that the antifungal activities of HFA can be affected by the matrixes of food and plants synergistically or antagonistically.

Due to the bacterial capacity to convert unsaturated fatty acids into HFA, the bacterial production of HFA and fatty acid metabolism *in situ* were also evaluated in a fermented sausage model with well-controlled microbiota (Chapter 7). HFAs were detected in the model sausages, but antifungal HFAs were not produced at levels that exert antifungal activity. This supports the compatibility of fermented sausage with the use of mold as ripening agents. Unpublished experimental data also documented that the antifungal activity of lactic acid bacteria in model dairy systems was not dependent on their ability to convert fatty acids to HFA.

Results presented in this thesis contribute to understanding the structure-function relationship of HFAs, their mode of action, and their application *in situ*. This can further enable the development of lipid-based antifungal approaches suitable for application in food and agriculture, which in turn has the potential to reduce food waste and so help to address the increasing global food and agricultural demands.

## Preface

This is an original work by Nuanyi Liang.

Chapter 2 is a book chapter published as “Liang, N., and Curtis, J. M. (2020) ‘Conventional and Current Methods for the Analysis of Hydroxy Fatty Acids.’ In *Lipidomics: Current and Emerging Techniques*. Royal Society of Chemistry, Cambridge, UK (pp. 175-222).” I performed literature review on the distribution of hydroxy fatty acids in nature and conventional and current methods for their analysis, and I wrote the chapter. Jonathan Curtis provided guidance during the writing and reviewed and revised several versions of the chapter.

Chapter 3 is an experimental work published as “Chen, Y. Y., Liang, N. Y., Curtis, J. M., & Gänzle, M. G. (2016). Characterization of linoleate 10-hydratase of *Lactobacillus plantarum* and novel antifungal metabolites. *Frontiers in Microbiology*, 7, 1561.” I performed analysis of hydroxy fatty acids, and performed fermentation, extraction, isolation and antifungal activity assay of hydroxy fatty acids together with Yuan Yao Chen; other experiments described in the chapter were performed by Yuan Yao Chen. The manuscript was written by Yuan Yao Chen, and revised by me, Curtis, J. M. & Gänzle, M. G. This work was also published in Yuan Yao Chen’s PhD thesis, “Chen, Y. Membrane lipid homeostasis and stress resistance in *Escherichia coli* and *Lactobacillus plantarum*. University of Alberta, 2017.”

Chapter 4 is an experimental work published as “Liang, N., Cai, P., Wu, D., Pan, Y., Curtis, J. M., & Gänzle, M. G. (2017). High-speed counter-current chromatography (HSCCC) purification of antifungal hydroxy unsaturated fatty acids from plant-seed oil and *Lactobacillus* cultures. *Journal of Agricultural and Food Chemistry*, 65(51), 11229-11236.” I performed the majority of lab work with support from Pengfei Cai and Datong Wu related to

purification of hydroxy fatty acids via HSCCC. The manuscript was written by me and revised by all authors.

Chapter 5 is an experimental work submitted as “Liang, N., Dacko, A., Tan, A. K., Xiang, S., Curtis, J. M., & Gänzle, M. G., An investigation into the relationship between the structures of monohydroxy unsaturated fatty acids and their antifungal activities.” to Food Research International. I conducted the majority of the lab work and mentored Andrea Dacko, who assisted the extraction of hydroxy fatty acids and antifungal test of some of the hydroxy fatty acids, Sheng Xiang, who assisted with the measurement of LAUDAN assay and antifungal test of some of the hydroxy fatty acids, and Alexander Tan, who conducted the analysis of sterol content. The manuscript was written by me and revised by all the other authors.

Chapter 6 is an experimental work published as “Quattrini, M.\*, Liang, N.\*, Fortina, M. G., Xiang, S., Curtis, J. M., & Gänzle, M. G. (2018). Exploiting synergies of sourdough and antifungal organic acids to delay fungal spoilage of bread. *International Journal of Food Microbiology* (\*: Both authors contributed equally to the manuscript.), 302, 8-14.” I participated in the experimental design and performed the fungi-challenging test in sourdough bread with addition of hydroxy fatty acids, with the assistance of Sheng Xiang, and provided mentorship to Mattia Quattrini, who performed the other experiments. The manuscript was written by Mattia Quattrini and revised by me and other co-authors.

Chapter 7 is currently prepared for submission to a peer-reviewed scientific journal. I conducted the identification and purification of hydroxy fatty acids, as well as the validation of LC-MS method and quantitation of fatty acids. Kaixing Tang and I performed the extraction of fatty acids from model sausages. The manuscript was written by me and revised by other co-authors. Statistical analysis was performed by Kaixing Tang with the assistance of Weilan Wang. The quantitation of hydroxy fatty acids has been published in Kaixing

Tang's MSc thesis, "Tang, K. Effect of starter culture on accumulation of taste active amino acids, free fatty acids, and on survival of pathogenic *Escherichia coli* in dry fermented beef sausages. University of Alberta, 2018."

Appendix 1 is a manuscript prepared for submission. Lucie Nečasová assisted the separation of gangliosides. Yuan Yuan Zhao and Jonathan Curtis contributed to the experimental design. The manuscript was written by Nuanyi Liang and revised by other coauthors.

*This thesis is dedicated to my grandparents, Neng Liang (梁能) and Yuezhen Liang (梁月贞),  
and to all of the love and kindness I receive in life.*

## Acknowledgements

Thank you, Dr. Michael Gänzle and Dr. Jonathan Curtis, for the enormous support and guidance. Your dedication to research and teaching, as well as your genuine caring for students, are truly amazing. You are always patient in explaining every piece of knowledge, even the most trivial one; you are always there to help, even in the busiest days; and you are always proud of us, even for the smallest achievement. You encourage us to try new things and explore without the fear of failure. Your unconditional support is really the best thing I can ask for from supervisors.

Thank you, my supervisory committee member, Dr. David Bressler for all of your help and advice. You have helped me grow as a scientist with a critical mind. Your outstanding work as both a scientist and an entrepreneur is truly inspiring.

Thank you, Dr. Xingfang Li and Dr. Steve Labrie for being my examiners and providing incredible feedbacks. Thank you, Dr. Feral Temelli for being an excellent chair in such a special time. Thank you, Dr. Stephen Strelkov and Dr. Randall Weselake for being my candidacy examiners and helped me expand my knowledge in plant science and lipid science. Thank you, Dr. Lingyun Chen for chairing my candidacy exam.

Thank you, all the collaborators, Dr. Yuanjiang Pan, Dr. Pengfei Cai, Dr. Datong Wu, Dr. Yuanyao Chen, Dr. Mattia Quattrini, Dr. Yuan Yuan Zhao, Kaixing Tang, Sabrina Strafella, Andrea Dacko, Alexander Tan, Sheng Xiang, Lucie Nečasová, Fangqin Hu, Azadeh Yasari, Dr. Stephen Strelkov and Dr. Nat Kav. I also want to thank Dr. Grigor Bantchev from United States Department of Agriculture. I feel very fortunate to work closely with incredibly intelligent, hardworking and dedicated scientists like you.

Thank you, Mitacs, for your generous financial supports. Your awards for me have let me pursue my dream as a scientist. Thank you, American Oil Chemists' Society and Canadian Institute of Food Science and Technology Scholarship Trust Fund for supporting my



participation in conferences, and the Western Grains Research Foundation and the Alberta Wheat Commission for the funding of some of the projects.

Thank you, all of my lab mates from the Lipid Chemistry Group, including Ereddad Kharraz, Dr. Si Mi, Anna Magdalena Hubmann, Vinay Patel, Beiyi Shen, Savanna Won, Dr. Xiaohua Kong, Dr. Tolibjon Omonov, Dr. Rami Akkad, Dr. Mohammad Hossein Tavassoli Kafrani, Siew Meng Liew, and I must thank again, Dr. Yuan Yuan Zhao. Thank you all for supporting me through all the ups and downs in the program.

Thank you, all the lab mates from the Food Microbiology Lab 2-50, especially Luis Rojas Tovar, Dr. Yalu Yan, Dr. David Simpson, Dr. Justina Zhang, Zhiying Wang, Gautam Gaur, Dr. Yuan Fang, Dr. Weilan Wang, Maria Solis Ares, Heather Vandertol-Vanier, Tingting Liu, Dr. Ying Hu, Dr. Januana Teixeira, Dr. Ziyi Hu, Jin Xie, Qing Li, Felicitas Pswaray, Oanh Nguyen, Lilian Morceli, Zhen Li, Vi Pham, Shaelyn Xu, Tongbo Zhu, Qixing Ou, Yan Yang, Dr. Jing Zhao, Dr. Hui Li and Dr. Fernanda Sanchez Maldonado. You are fantastic colleagues, amazing friends and continuous sources of inspiration.

I would also like to express my gratitude to my friends and family from China, especially my parents Guangping Liang (梁广平) and Qiancha Lu (芦倩茶). I am enormously thankful for the dearest friends and family from Edmonton, especially Steve To, Dinuka Gunaratne, Alireza Saidi-Mehrabad, Yuqi Zhang, and Dylan Ashley. Thank you all for your unconditional support for me throughout this amazing journey.

Finally, thank you to all the heroes that worked during the COVID-19 pandemic for fighting for us, in whatever role you play, and keeping us safe. Because of your dedication, I am able to finish this piece of work, and I hope, my own dedication to science and a better world will allow me to serve the society like you do.

## Table of Contents

<b>Abstract.....</b>	<b>ii</b>
<b>Preface.....</b>	<b>iv</b>
<b>Acknowledgements .....</b>	<b>viii</b>
<b>Table of Contents .....</b>	<b>x</b>
<b>List of Tables .....</b>	<b>xvii</b>
<b>List of Figures.....</b>	<b>xx</b>
<b>List of Abbreviations .....</b>	<b>xxvii</b>
<b>Chapter 1. Introduction .....</b>	<b>1</b>
<b>Chapter 2. Conventional and current methods for the analysis of hydroxy fatty acids ...</b>	<b>8</b>
<b>2.1 Introduction.....</b>	<b>8</b>
<b>2.2 Biological significance of hydroxy fatty acids .....</b>	<b>8</b>
2.2.1 Mono-HFAs with –OH near the –COOH (2- and 3-HFAs) .....	9
2.2.2 Mid-chain HFAs .....	11
2.2.3 Omega-HFAs .....	13
2.2.4 Di-HFAs and poly-HFAs.....	14
<b>2.3 Pre-treatment before HFA analysis .....</b>	<b>15</b>
<b>2.4 Conventional methods for hydroxy fatty acid analysis - GC based approaches ...</b>	<b>18</b>
2.4.1 Esterification (preparation of FAME).....	19
2.4.2 Derivatisation methods used to locate HFA hydroxy groups .....	21
2.4.3 Derivatization methods used to locate HFA unsaturation and other structural features.....	25
<b>2.5 Current methods for HFA analysis - LC/MS approaches .....</b>	<b>30</b>

2.5.1 Choices of LC mobile phase and stationary phase .....	31
2.5.2 Interpretation of mass spectra of HFAs .....	40
2.5.3 Online-derivatization for LC-MS analysis of HFA .....	47
<b>2.6 Summary for the analysis of hydroxy fatty acids, outlook on lipidomics and beyond .....</b>	<b>49</b>
<b>Chapter 3. Characterization of linoleate 10-hydratase of <i>Lactobacillus plantarum</i> and novel antifungal metabolites .....</b>	<b>51</b>
<b>3.1 Introduction.....</b>	<b>51</b>
<b>3.2 Materials and methods .....</b>	<b>52</b>
3.2.1 Bacterial strains and fermentation .....	52
3.2.2 DNA manipulations .....	53
3.2.3 Sequence and phylogenetic analysis of linoleate hydratases in lactobacilli .....	54
3.2.4 Cloning and heterologous expression of linoleate hydratases of lactobacilli .....	54
3.2.5 Purification of linoleate hydratases.....	56
3.2.6 Enzymatic activity assay and fatty acid analysis .....	56
3.2.7 Construction of <i>L. plantarum</i> TMW1.460 $\Delta$ lah by double-crossover mutagenesis	56
3.2.8 Determination of ethanol resistance.....	57
3.2.9 Determination of the membrane fluidity under ethanol stress.....	58
3.2.10 Physicochemical properties of cells surface .....	58
3.2.11 Extraction and purification of 13-HOE and 10-HOE .....	59
3.2.12 Determination of the antimicrobial activity of fatty acids .....	60
3.2.13 Statistical analysis.....	60
3.2.14 Accession numbers .....	61
<b>3.3 Results .....</b>	<b>61</b>
3.3.1 Identification of the products of linoleate conversion by lactobacilli.....	61

3.3.2 Phylogenetic analysis of linoleate hydratase .....	63
3.3.3 Characterization of linoleate 10-hydratase .....	64
3.3.4 Most lactobacilli require oleic acid or linoleic acid for growth.....	67
3.3.5 The effect of <i>lah</i> on stress tolerance in <i>L. plantarum</i> .....	67
3.3.6 The effect of <i>lah</i> on ethanol-dependent membrane fluidity in <i>L. plantarum</i> .....	67
3.3.7 Influence of <i>lah</i> on cell surface properties in <i>L. plantarum</i> .....	70
3.3.8 Antifungal properties of purified hydroxy fatty acids .....	71
<b>3.4 Discussion.....</b>	<b>73</b>
<b>Chapter 4. High-speed counter-current chromatography (HSCCC) purification of antifungal hydroxy unsaturated fatty acids from plant-seed oil and <i>Lactobacillus</i> cultures.....</b>	<b>77</b>
<b>4.1 Introduction.....</b>	<b>77</b>
<b>4.2 Materials and methods .....</b>	<b>79</b>
4.2.1 Chemicals and reagents.....	79
4.2.2 Microbial strains and culture conditions.....	79
4.2.3 Extraction of fatty acid mixtures from <i>Coriaria nepalensis</i> Wall. seed oil and from cultures of <i>L. plantarum</i> TMW1.460 $\Delta$ <i>lah</i> and <i>L. hammesii</i> DSM16381 .....	80
4.2.4 LC-MS and MS/MS analyses of fatty acids .....	81
4.2.5 Measurement of partition-coefficient ( <i>K</i> ) values.....	84
4.2.6 Purification of fatty acids by high-speed counter-current chromatography (HSCCC).....	85
4.2.7 Minimum-inhibitory-concentration (MIC) assay .....	85
<b>4.3 Results .....</b>	<b>86</b>
4.3.1 Identification and quantification of fatty acids in <i>Coriaria</i> seed oil and in the lipids extracted from <i>Lactobacillus</i> cultures.....	86

4.3.2 Optimization of HSCCC solvent systems and preparative separation of HUFA by HSCCC .....	93
4.3.3 Antifungal activity of mono-HUFA and other UFA.....	97
<b>4.4 Discussion.....</b>	<b>100</b>
<b>Chapter 5. An investigation into the relationship between the structures of monohydroxy unsaturated fatty acids and their antifungal activities .....</b>	<b>104</b>
<b>5.1 Introduction.....</b>	<b>104</b>
<b>5.2 Materials and methods .....</b>	<b>106</b>
5.2.1 Chemical materials.....	106
5.2.2 Microbial strains and culture conditions.....	107
5.2.3 Extraction and saponification of oils from plant seeds rich in HUFA.....	107
5.2.4 Purification and analysis of HUFA.....	108
5.2.5 Antifungal test of hydroxy fatty acids .....	110
5.2.6 Extraction and GC-MS quantitation of fungal sterols .....	111
5.2.7 Measurement of fungal membrane fluidity using Laurdan assay.....	112
5.2.8 Statistical analysis.....	113
<b>5.3 Results .....</b>	<b>113</b>
5.3.1 Extraction, HSCCC purification, and identification of antifungal HUFA from plant seed oil. ....	113
5.3.2 Antifungal activity of HUFA .....	122
5.3.3 Effect of HUFA on the fluidity of fungal membranes monitored by Laurdan .....	123
<b>5.4 Discussion.....</b>	<b>127</b>
<b>Chapter 6. Exploiting synergies of sourdough and antifungal organic acids to delay fungal spoilage of bread .....</b>	<b>133</b>
<b>6.1 Introduction.....</b>	<b>133</b>

<b>6.2 Materials and methods .....</b>	<b>135</b>
6.2.1 Strains and growth conditions.....	135
6.2.2 Antifungal activity assay.....	135
6.2.3 Sourdough fermentation and bread preparation.....	136
6.2.4 Bread challenge test against <i>P. roqueforti</i> and <i>A. niger</i> .....	137
6.2.5 Quantification of acetic acid with high performance liquid chromatography (HPLC).....	140
<b>6.3 Results .....</b>	<b>140</b>
6.3.1 MIC of preservatives and combination effects .....	140
6.3.2 Antifungal effect of organic acids addition to bread .....	141
6.3.3 Antifungal effect of sourdough addition to bread.....	143
<b>6.4 Discussion.....</b>	<b>147</b>
 <b>Chapter 7. Identification and quantitation of fatty acids in fermented sausage samples</b> .....	 <b>153</b>
<b>7.1 Introduction.....</b>	<b>153</b>
<b>7.2 Materials and methods .....</b>	<b>155</b>
7.2.1 Chemical and reagents .....	155
7.2.2 Preparation of beef sausage fermentation .....	156
7.2.3 Extraction of fatty acids from sausage sample .....	158
7.2.4 HPLC-MS and MS/MS analysis of fatty acids.....	158
7.2.5 Optimization of HSCCC solvent system and enrichment of HFAs from sausage sample using HSCCC .....	160
7.2.6 Methylation, silylation and GC-MS analysis of fatty acids.....	161
<b>7.3 Results .....</b>	<b>162</b>

7.3.1 Identification of hydroxy fatty acids in beef sausages fermented with <i>L. sakei</i> , or <i>L. sakei</i> and <i>S. carnosus</i> .....	162
7.3.2 Validation of analytical method for the analysis of fatty acids in sausage model	170
7.3.3 Comparison of fatty acid composition among different fermentation beef sausages .....	174
<b>7.4 Discussion.....</b>	<b>176</b>
<b>Chapter 8. General discussion and conclusions .....</b>	<b>181</b>
<b>8.1 Advancement in the analysis, separation and development of structure-function relationship of HUFA .....</b>	<b>181</b>
<b>8.2 Potential application of HUFA in food preservation .....</b>	<b>184</b>
<b>8.3 Potential application of HUFA in plant protection.....</b>	<b>188</b>
<b>8.4 Limitation and further research.....</b>	<b>192</b>
8.4.1 Further development of structure-function relationship and application of HUFA <i>in situ/in vivo</i> .....	192
8.4.2 Comprehensive characterization and quantitation of HUFA in fermented food matrixes.....	193
8.4.3 Further study on the mode of action and the resulting development of co-antifungal compounds .....	193
<b>References.....</b>	<b>195</b>
<b>Appendix 1: Advances in the preparative separation of gangliosides by high-speed counter-current chromatography (HSCCC).....</b>	<b>265</b>
<b>A1.1 Introduction.....</b>	<b>265</b>
<b>A1.2 Materials and methods .....</b>	<b>267</b>
A1.2.1 Reagents .....	267
A1.2.2 LC-MS/MS analysis of gangliosides .....	268

A1.2.3 Selection of the solvent system for HSCCC separation of gangliosides .....	269
A1.2.4 High-speed counter-current chromatography (HSCCC) separation of gangliosides.....	270
<b>A1.3 Results .....</b>	<b>272</b>
A1.3.1 LC-MS analysis of gangliosides to determine their partition coefficient ( $K_D$ value) in BuOH/MTBE/ACN/water solvent systems .....	272
A1.3.2 HSCCC separation of ganglioside with head-to-tail mode.....	275
A1.3.3 HSCCC separation of gangliosides in acidified solvent systems with dual-mode elution .....	285
<b>A1.4 Discussion.....</b>	<b>290</b>
<b>A1.5 Conclusions .....</b>	<b>293</b>



## List of Tables

Table 2.1. Examples of characteristic MS spectrum ions of TMS-FAME of C18 HFAs .....	26
Table 2.2. Ion transitions and retention times for HFA in LC-MS/MS analyses .....	34
Table 2.3. Examples of LC methods used in the analysis of HFA .....	37
Table 2.4. Characteristic product ions in the negative ion MS/MS spectra of HFAs.....	44
Table 3.1. Primers used in this study .....	55
Table 3.2. Comparison of products obtained from strain fermentation and enzymatic reaction with linoleic acid as substrate .....	63
Table 3.3. MICs of hydroxy fatty acids extracted from cultures of <i>L. hammesii</i> and <i>L.</i> <i>plantarum</i> $\Delta 10$ - <i>lah</i> and reference fatty acids (n=3).....	72
Table 4.1. MS transition and retention time of fatty acids in LC/ESI–MS/MS-MRM quantitative analysis.....	83
Table 4.2. Fatty acid content (% w/w) in lipid extracts from <i>C. nepalensis</i> seed oil and lipids extracted from <i>L. hammesii</i> and <i>L. plantarum</i> TMW1.460 $\Delta$ <i>lah</i> cultures.....	88
Table 4.3. Partition coefficients (K) of the target components in different hexane-ethyl acetate-methanol-water (H-E-M-W) solvent system.....	95
Table 4.4. Minimum inhibitory concentration (MIC) of coriolic acid against food spoilage and pathogenic fungi compared to linoleic acid and oleic acid. Data are shown as means $\pm$ standard deviation of triplicate independent experiments. ....	99
Table 4.5. Minimum inhibitory concentration (MIC) comparison of four mono-hydroxy fatty acids against <i>A. niger</i> and <i>P. roqueforti</i> . Data represent means $\pm$ standard deviation of triplicate independent experiments. ....	100

Table 5.1 HUFA analogues extracted from plant oils and <i>Lactobacillus</i> fermentation, or purchased, and their LC-MS/MS (multiple reaction monitoring, MRM) ion transitions, which were for construction of HSCCC chromatogram and the measurement of <i>K</i> value.....	115
Table 5.2 Partition coefficient ( <i>K</i> value) of 2-OH linoleic acid in the hexane/ethyl acetate/methanol/water (HEMWat) systems with different solvent ratios. Fatty acids, C16:0, C17:0, C18:0, C18:1, C18:2, C18:3, 2-OH C18:1, 2-OH C18:3 were measurement with LC-MS/MS (MRM) with the following ion transition: 255.2/255.2, 269.2/269.2, 283.2/283.2, 281.2/281.2, 279.2/279.2, 277.2/277.2, 297.2/251.2, 293.4/191.3.....	116
Table 5.3 Partition coefficient ( <i>K</i> ) of kamlolenic acid in hexane-ethyl acetate-methanol-water (HEMWat) systems with different solvent ratios. Fatty acids, beside the fatty acid mentioned above, 13-OH C18:2, mono-OH C18:0 and 18-OH C18:3 were monitored with the following ion transition and retention time: 295.2/195.1 (5.14 min), 299.2/299.2 (7.83 min), 293.2/263.2 (3.71 min).....	117
Table 5.4 Minimum inhibitory concentrations of various hydroxyl fatty acids against filamentous fungi. Results are presented as means ± standard deviation of triplicate independent experiments. ....	123
Table 6.1. Ingredients in bread formulation with chemical preservatives and their combinations.....	138
Table 6.2. Ingredients of sourdough bread. Wheat or flaxseed sourdoughs were fermented with <i>L. hammesii</i> , <i>L. plantarum</i> or <i>L. brevis</i> . 10% of the experimental sourdough was added to bread dough.....	139
Table 6.3. Effect of preservatives alone or in combination on the mould-free shelf life of bread. Preservatives were added as indicated in Table 6.1 to match their MIC <i>in vitro</i> . Data	

are shown as means  $\pm$  standard deviations of three independent experiments. Values in the same row that do not share a common superscript differ significantly ( $p < 0.05$ ). ..... 143

Table 6.4. Effect of sourdough on the pH and the mould-free shelf life of bread. The sourdough was fermented with *L. hammesii*, *L. plantarum* or *L. brevis*, with or without addition of 4% sucrose; *L. hammesii* sourdough was combined with calcium propionate (3.1 mM) or sorbic acid (0.16 mM). The challenge test was with two indicator strains. Data are shown as means  $\pm$  standard deviations of three independent experiments. Values obtained for different breads with the same indicator strain differ significantly if they do not share a common superscript ( $p < 0.05$ ). ..... 144

Table 7.1. MRM transition and optimized parameters for fatty acid standards ..... 163

Table 7.2. GC-MS information of methylated (FAME) or methylated and sialylated (TMS) hydroxy fatty acids..... 170

Table 7.3. Linear range of major fatty acids ..... 171

Table 7.4. Accuracy and precision (matrix effect) (triplicates) ..... 172

Table 7.5. Extraction recovery (duplicates) ..... 173

Table 7.6. Concentration of free fatty acids in sausages fermented with different starter cultures ..... 175

Table A1- 1. Multiple reaction monitoring (MRM) experiments of ganglioside individuals 272

Table A1- 2. Partition coefficient ( $K$  value) of gangliosides in the solvents system of butanol (BuOH)/methyl tert-butyl ether (MTBE)/acetonitrile (ACN)/water with/without addition of acetic acid..... 274

## List of Figures

Figure 2.1. Silylation reaction.....	22
Figure 2.2. Migration ions .....	24
Figure 2.3. Reaction of DMOX derivatization .....	25
Figure 2.4. Examples of MS spectra of DMOX-18-OH HFAs of A) C18:0, B) C18:1, and C) C18:2. (Spectra from <a href="http://www.lipidhome.co.uk/">http://www.lipidhome.co.uk/</a> ) <sup>242</sup> .....	28
Figure 2.5. LC-MS/MS-MRM analysis of oxylipins performed on a triple quadrupole MS ..	31
Figure 2.6. Normal-phase LC-MS extracted ions chromatogram of crude lipid extract from <i>Lactobacillus plantarum</i> .....	38
Figure 2.7. Silver ion chromatography-MS extracted ion chromatogram of the characteristics ions ( $[M+H-H_2O]^+$ , $m/z$ 295.2) of the FAME derivatives of 10-hydroxy-12-octadecenoic fatty acids extracted from <i>Lactobacillus hammesii</i> fermentation products. <sup>191</sup> The <i>trans</i> isomer (at 15.0 min) elutes ahead of the <i>cis</i> isomer (at 17.6 min). .....	39
Figure 2.8. Negative ion MS/MS spectra of 15-OH C20 analogues .....	43
Figure 2.9. Ozonolysis mechanism for an unsaturated FAME (left) and ozonolysis-APPI-MS spectrum and proposed fragmentation ion structures of FAME of 10-hydroxy-octadecenoic acid (right): (A) molecule ions $[M + H]^+$ $m/z$ 313; (B) fragment ion $m/z$ 227; and (C) fragment ion $m/z$ 195. ....	48
Figure 3.1. Fragmentation pattern and APPI-MS/MS spectra of hydroxy fatty acids produced when linoleic acid was used as substrate. (A) Mass spectrum of 10-hydroxy-12-octadecenoic acid; (B) mass spectrum of 13-hydroxy-9-octadecenoic acid; (C) mass spectrum of 10,13-dihydroxy octadecanoic acid.....	62
Figure 3.2. Phylogenetic tree of linoleate hydratases (LAHs). The evolutionary relationships are shown with scale bar line, which represents an evolutionary distance of 0.05. Linoleate	

10-hydratases reported in the literature are highlighted in red, linoleate 13-hydratases are highlighted in blue, and linoleate 10-hydratases that were characterized in this study are underlined. ....65

Figure 3.3. SDS-PAGE analysis of purified LAHs expressed from respective recombinant *Escherichia coli* BL21 (DE3) cells. Lane 1, LAH of *Lactobacillus reuteri*; lane 2, LAH of *Lactobacillus plantarum*; lane 3, molecular mass marker proteins (250, 150, 100, 75, 50, 37 and 25 kDa); lane 4, LAH of *Lactobacillus hammesii*; lane 5, LAH of *Lactobacillus spicheri*. ....66

Figure 3.4. Survival of *L. plantarum* and its *lah* deficient derivative under 20% ethanol treatment. *L. plantarum* TMW1.460 was incubated in mMRS-Tween80 (closed circles) or mMRS-Tween20 (open circles); *L. plantarum* TMW1.460 $\Delta$ *lah* was grown in mMRS-Tween80 (closed triangle) or mMRS-Tween 20 (open triangle) during treatment. Values obtained at the same treatment time that do not share common superscripts are significantly different ( $P < 0.05$ ). Data represent means  $\pm$  standard deviations of three independent experiments with duplicate determinations of cell counts. ....68

Figure 3.5. General polarization (GP) values of *L. plantarum* and its  $\Delta$ *lah* derivative stained with Laurdan under ethanol stress. *L. plantarum* TMW1.460 was cultivated in mMRS-Tween80 (closed circles) or mMRS-Tween 20 (open circles) prior to staining; *L. plantarum* TMW1.460 $\Delta$ *lah* strain was cultivated in mMRS-Tween80 (closed triangle) or mMRS-Tween 20 (open triangle) prior to staining. Values obtained at the same treatment time that do not share common superscripts are significantly different ( $P < 0.05$ ). Data represent means  $\pm$  standard deviations of three independent experiments with duplicate determinations of cell counts. ....69

Figure 3.6. Effect of 10-*lah* on cell surface properties of *L. plantarum* grown in different media. Cell surface hydrophobicity was measured using the MATS method. (A) *L. plantarum*

TMW1.460; (B) *L. plantarum* TMW1.460 $\Delta$ lah. White bar indicates % affinity to solvents when cells were grown in mMRS-Tween 20; gray bar indicated in mMRS (Tween 20) supplemented with 1 g/L oleic acid; black bar indicated in mMRS (Tween 20) supplemented with 1 g/L linoleic acid. Data represent means  $\pm$  standard deviations of three independent experiments. .... 71

Figure 4.1.  $^{13}\text{C}$  NMR spectrum of purified HUFA from *Coriaria nepalensis* seed oil (400MHz,  $\text{CDCl}_3$ ) (upper) compared to the according spectrum published in a previous literature (125MHz,  $\text{CDCl}_3$ ) (lower).<sup>350</sup> ..... 89

Figure 4.2.  $^1\text{H}$  NMR spectrum of purified HUFA from *Coriaria nepalensis* seed oil (400MHz,  $\text{CDCl}_3$ ) (upper) compared to the according spectrum published in a previous literature (500MHz,  $\text{CDCl}_3$ ) (lower).<sup>350</sup> ..... 90

Figure 4.3. COSY analysis of purified HUFA from *Coriaria nepalensis* seed oil (400MHz,  $\text{CDCl}_3$ ) (upper) compared to the according spectrum published in a previous literature (500MHz,  $\text{CDCl}_3$ ) (lower).<sup>350</sup> ..... 91

Figure 4.4. Negative-mode LC-APPI-MS/MS fragmentation spectra of antifungal fatty acids purified via HSCCC. (A) coriolic acid. (B) 10-hydroxy-12-octadecenoic acid (10-OH C18:1). (C) 13-hydroxy-9-octadecenoic acid (13-OH C18:1). The inserts indicate molecular structures and proposed fragmentation patterns. .... 92

Figure 4.5. ESI-MS/MS flow injection analysis of HSCCC purification fractions collected during HSCCC purification using solvent system of HEMWat (3.5:1.5:3.5:2, v/v/v/v). Panel A, fractionation of hydrolyzed *Coriaria* seed oil. Panel B, fractionation of lipids extracted from cultures of *L. hammessi*. Panel C, fractionation of lipids extracted from *L. plantarum* TMW1.460 $\Delta$ lah. The compositions of peaks of analytes of interest were monitored by different ion transition, i.e., coriolic acid and 13-OH C18:2 isomer (Q1/Q3=295.2/197.2),

ricinoleic acid (Q1/Q3=297.2/183.1), 10-OH C18:1 (Q1/Q3=297.2/185.1) and 13-OH C18:1 (Q1/Q3=297.2/197.1).....96

Figure 4.6. Negative-mode LC-APPI-MS total ion chromatogram (TIC) of antifungal fatty acids purified via HSCCC. Panel A. coriolic acid; Panel B. 10-OH C18:1 (10-hydroxy-12-octadecenoic acid); Panel C. 13-OH C18:1 (13-hydroxy-9-octadecenoic acid).....97

Figure 5.1. HSCCC chromatogram of saponified seed oil from various oil sources: (A) coriolic acid (13-hydroxy-9,11-octadecadienoic acid) from *Coriaria nepalensis* seed oil; (B) dimorphecolic acid (9-hydroxy-10,12-octadecadienoic acid) from *Dimorphotheca sinuata* seed oil; (C) kamlolenic acid (18-hydroxy-9,11,13-octadecatrienoic acid) from *Mallotus philippensis* seed oil; (D) 2-hydroxy-linolenic acid (2-hydroxy-9,12,15-octadecatrienoic acid) from *Thymus vulgaris* seed oil..... 118

Figure 5.2. LC-APPI-MS total ion chromatograms (1), and APPI-MS spectra (2) of ionized purified hydroxyl fatty acids (A) coriolic acid; (B) dimorphecolic acid; (C) kamlolenic acid; and (D) 2-hydroxy-linolenic acid..... 119

Figure 5.3. APPI-MS/MS spectra of [M-H]<sup>-</sup> ion and molecular structure of ionized purified hydroxyl fatty acids (A) coriolic acid; (B) dimorphecolic acid; (C) kamlolenic acid; and (D) 2-hydroxy-linolenic acid..... 121

Figure 5.4. Upper figure) Fungal membrane fluidity change in different concentration of ethanol, monitored by GP value using Laurdan assay; Lower figure) The measurement of fungal cell membrane fluidity of *Saccharomyces cerevisiae*, *Aspergillus niger* and *Penicillium roqueforti* under fatty acid (ricinoleic and oleic acid) or negative control treatment. Generalized polarization  $GP = (I_{440} - I_{490}) / (I_{440} + I_{490})$ , where  $I_{440}$  and  $I_{490}$  stood for fluorescent intensity under wavelengths of 440 nm and 490 nm, respectively. .... 125

Figure 5.5. Left figure) GC-MS quantitation of ergosterol extracted from food-related fungi (dry weight basis); Right figure) relationship between fungal ergosterol content and fungal MIC of coriolic acid. The abbreviation of fungi species represented the following strains: *Candida valida* (C.v), *Pichia membranefaciens* (P.m), *Saccharomyces cerevisiae* (S.c), *Candida albicans* (C.a), *Wickerhamomyces anomalus* (W.a), *Penicillium roqueforti* (P.r), *Aspergillus brasiliensis* (A.b), *Mucor plumbeus* (M.p), *Aspergillus niger* (A.n), and *Aspergillus clavatus* (A.c). The outlier (grey: □ C.a) was determined using Cook's distance >0.4 in SPSS software. .... 127

Figure 6.1. Minimum inhibitory concentration of acetic acid in combination with sorbic acid, propionic acid, phenyllactic acid, or ricinoleic acid. The minimum inhibitory concentrations were evaluated at a pH of 4.50. The results are shown as means ± standard deviations of three independent experiments. .... 141

Figure 6.2. Effect of sourdough in combination with ricinoleic acid on the mould-free shelf life of bread. Control bread was produced without addition of sourdough (white bars); *L. hammesii*-fermented sourdough bread was produced with addition of 2% linoleic acid during sourdough fermentation (white hatched bars); or with addition of 0.03% (gray bars), 0.08% (dark gray bars) or 0.15% ricinoleic acid (black bars) added at the bread stage. Experiments were done with wheat sourdough or flaxseed sourdough as indicated and *Penicillium roqueforti* and *Aspergillus niger* were used as challenge organisms. Data are shown as mean ± standard deviations of seven independent experiments. Values produced with the same sourdough and challenged with the same organism differ ( $p < 0.05$ ) if they do not share a common superscript. .... 146



Figure 7.1. A) LC-APPI-MS Extracted ion chromatogram (XIC) of  $m/z$  297 of sausage lipid in negative control, or sausage lipid fermented by *Lactobacillus sakei* and *L. sakei* + *S. carnosus*; 5 peaks observed in the chromatogram are label as peak a-e; B) LC-APPI-MSMS spectra of precursor ion of  $m/z$  297 of peak a-e in A, respectively..... 164

Figure 7.2. A) HSCCC chromatogram of hypothetical hydroxy fatty acids from sausages. Fractions were analyzed by FIA-ESI-MRM (TIC) of the fractions collected during HSCCC separation. HSCCC employed the solvent system of HEMW (4:1:4:1, v/v/v/v) with 0.1% acetic acid addition. B) HSCCC separation of hypothesized HFAs, monitored by LC-ESI-MSMS-MRM experiment. a) was analysis of original samples before separation and b)-g) were of different fractions collected from separation that was enriched with 6 individual hypothetical hydroxy fatty acids. .... 167

Figure 7.3. A) ESI-MS spectrum of hypothesized 2-OH C16:0 enriched fraction; B) EI-MS spectrum of hypothesized 2-OH C16:0 FAME structure; C) EI-MS spectrum of hypothesized silylated 2-OH C16:0 FAME structure; D) ESI-MS spectrum of hypothesized 2-OH C18:1; E) EI-MS spectrum of hypothesized 2-OH C18:1 FAME structure; F) EI-MS spectrum of hypothesized silylated 2-OH C18:1 FAME structure. .... 168

Figure A1-1. LC-MS/MS chromatogram of the porcine ganglioside mixture used in this work .....276

Figure A1-2. Head-to-tail mode HSCCC chromatograms of the ganglioside mixture using a BuOH/MTBE/ACN/water 3:1:1:5 , v/v/v/v solvent system with acetic acid added in the sample solution to 0.5% (v/v).....277

Figure A1-3. LC-MS/MS analysis of fractions collected from the head-to-tail mode HSCCC separation using the 3:1:1:5 solvent system shown in Figure A1-2. ....279

Figure A1-4 Head-to-tail mode HSCCC chromatogram of gangliosides mixture using a BuOH/MTBE/ACN/water 2:2:1:5, v/v/v/v solvent system with acetic acid added in the sample solution to 0.5% (v/v).....	280
Figure A1-5. LC-MS/MS analysis of fractions collected from the HSCCC separation using the 2:2:1:5 solvent system indicated in Figure A1-4. ....	282
Figure A1-6. Head-to-tail mode HSCCC chromatogram of GM1 mixture using a BuOH/MTBE/ACN/water 2:2:1:5, v/v/v/v solvent system with acetic acid added in the sample solution to 0.5% (v/v). The flow rate was 3 ml/min and fraction collection frequency was 3 min/tube. ....	284
Figure A1-7. LC-MS/MS analysis of A) GM1 (d36:1) and B) GM1 (d38:1) fractions separated using the BuOH/MTBE/ACN/water, 2:2:1:5 v/v/v/v solvent system indicated in Figure A1-6. (A) and (B) were fractions collected during the elution volume of 342-369 mL, and 414-900 mL. ....	284
Figure A1-8. Dual-mode HSCCC chromatogram of gangliosides mixture using a BuOH/MTBE/ACN/water 2:2:1:5, v/v/v/v solvent system with acetic acid added in the solvent system (A) or only in the lower phase (B) to 0.5% (v/v). ....	286
Figure A1-9. Dual-mode HSCCC chromatogram of gangliosides mixture using a BuOH/MTBE/ACN/water 2:4:3:8, v/v/v/v solvent system with acetic acid added in the lower phase to 0.5% (v/v).....	287
Figure A1-10. LC-MS/MS analysis of fractions collected from the dual-mode HSCCC separation using the 2:4:3:8 solvent system indicated in Figure A1-9. ....	288

## List of Abbreviations

- 10-HOE: 10-hydroxy-12-octadecenoic acid
- 13-HOE: 13-hydroxy-9-octadecenoic acid
- ACN: acetonitrile
- APPI: atmospheric pressure photo ionization
- BuOH: butanol
- CA: coriolic acid
- DMOX: 4,4-dimethyloxazoline
- EI: electron ionization
- ESI: electrospray ionization
- FAME: fatty acid methyl ester
- GC: gas chromatography
- GC-MS: gas chromatography coupled with mass spectrometry
- HEMWat or HEMW: hexane-ethyl acetate-methanol-water
- HFA: hydroxy fatty acid
- HPLC: high performance liquid chromatography
- HSCCC: high-speed counter-current chromatography
- HUFA: hydroxy unsaturated fatty acid
- $K$  or  $K_D$ : partition coefficient
- LAB: lactic acid bacteria
- LAH: linoleate hydratase
- LC: liquid chromatography
- LC-MS: liquid chromatography coupled with mass spectrometry
- LC-MS/MS: liquid chromatography coupled with tandem mass spectrometry
- MEA: malt extract agar

MTBE: methyl tert-butyl ether

MIC: minimum inhibitory concentration

mMRS: modified deMan-Rogosa-Sharpe

MRM: multiple reaction monitoring

MS: mass spectrometry

MS/MS: tandem mass spectrometry

NMR: nuclear magnetic resonance

OH: hydroxy

PD: potato dextrose

RA: ricinoleic acid

SPE: solid phase extraction

TIC: total ion chromatogram

TMS: trimethylsilyl

UFA: unsaturated fatty acid

XIC: extracted ion chromatogram

## Chapter 1. Introduction

Lipids, which are mainly comprised of water-insoluble fatty acid derivatives, are essential in cellular composition and energy metabolism. In addition, lipids have additional activities and regulatory functions in biological processes,<sup>1,2</sup> such as cell proliferation,<sup>3,4</sup> senescence,<sup>5,6</sup> apoptosis,<sup>7,8</sup> and the response to abiotic or biotic stress<sup>9,10</sup>. The advancement of knowledge on the biological activity of lipids is dependent on the improvement of separation<sup>11</sup> and analysis techniques<sup>2</sup> for lipids, e.g. solid- or liquid-liquid chromatography and tandem mass spectrometry, respectively. With these techniques, closely similar lipid structures can be isolated at both analytical and preparative scale, and thus their bioactivities can be distinguished in bioassays. Bioactivities in turn can also be matched to the exact molecular structures and the quantitation of these lipids, which can greatly further our understanding of their structure-function relationship. The structure-function relationship of bioactive lipids can be used in the further search, screening and optimizing production of the similar effective compounds to facilitate their application. As an example, in this work, antifungal lipids are being produced and characterized, and their activities are studied using these methods.

Antifungal lipids, largely hydroxy fatty acids,<sup>12,13</sup> are oxygenated products of lipids, which occur in plant and are involved in plant signaling of systemic resistance development to defense against phytopathogens.<sup>14</sup> Antifungal lipids are also produced in bacterial metabolism<sup>15</sup> but their ecological role remains unknown, although it is mainly associated with their detoxification of unsaturated fatty acids.<sup>16,17</sup> These plant- or bacterial-derived antifungal lipids have potential to be used as novel food preservatives, and hence can contribute to finding solutions for the problems of food waste caused by fungal spoilage.

The rising global population requires a substantial increase in food production.<sup>18</sup> This concern can be partially addressed by reducing food waste.<sup>19</sup> Fungal food spoilage

contributes significantly to the 1.3 billion tons of annual global food loss or waste at the retail or household levels.<sup>19, 20</sup> Its large impact on food can be attributed to the ability of fungi to survive and grow in environments and conditions that occur during food production, distribution and storage.<sup>21</sup> In addition, allergens caused by food spoilage fungi and the mycotoxin produced by them lead to concerns on food safety<sup>21</sup> and thus the additional cost in contamination management.<sup>22, 23</sup> The populations and virulence factors of spoilage fungi may constantly evolve with increasingly complex food value chains<sup>24</sup> and climate change.<sup>25</sup> Similar trends can be found in plant- and animal-pathogenic fungi, concerning public health, economics and ecology.<sup>26, 27, 28, 29</sup>

Common perishable or processed foods, such as fruits, vegetables, bread, cereals, nuts and refrigerated foods with longer storage lives are particularly susceptible to fungal spoilage.<sup>20, 21</sup> Mycotoxin contamination has also been found in pet food<sup>30</sup> and other animal feed.<sup>31</sup> Although hurdle technologies and prevention methods have been implemented, the elimination of fungal spoilage is still considered challenging.<sup>32</sup> Currently used food preservatives, such as sorbic acid or natamycin, impact food flavor and/or may be incompatible with the food industry's efforts to develop "clean-label" products.<sup>33, 34</sup> Thus, it is desirable to explore alternative strategies, like the use of antifungal lipids, for inhibiting fungal growth on agricultural commodities and food, to complement the current practices.

The functions of antifungal hydroxy fatty acids have been associated with plant self-defence<sup>12, 35, 36, 37</sup> and bacterial detoxification,<sup>17</sup> which make them suitable as an antifungal candidate in food and agricultural application. However, the knowledge of this group of antifungal hydroxy fatty acids has not yet been well associated with other more abundant sources of similar lipids. Hydroxy fatty acids (HFAs) from plants and microbial sources are structurally diverse.<sup>38, 39, 40</sup> However, how these HFAs perform as antifungals against food spoilage fungi is unknown. In addition, the sensitivity of fungi to HFAs was suggested to be

specific to the fungal strain,<sup>12, 13</sup> but no systematic study has been done to investigate the differences between fungal strains.

Antifungal HFAs are examples of an even larger group of antifungal metabolites of lactic acid bacteria.<sup>15, 20, 41</sup> The emerging use of lactic acid bacteria in antifungal applications is facilitated by the long history of safe consumption of lactic acid bacteria with fermented foods.<sup>42, 20</sup> Some strains of lactic acid bacteria show promising antifungal activities,<sup>20, 43, 44</sup> and data on the antifungal activity of purified metabolites with known structure is increasingly available.<sup>43, 44</sup> However, the commercial application of these lactic acid bacteria cultures or metabolites is still limited.<sup>20, 44, 45</sup>

The candidate antifungal metabolites of *Lactobacillus* can be categorized according to characteristics such as their abundance *in situ* compared to the active antifungal concentration, and their impact on food quality. Firstly, compounds like acetic acid are effective antifungals, with a low minimum inhibitory concentration (MIC) of 1.50 g/L against *Penicillium roqueforti* at pH 4.5<sup>33</sup> but also a strong taste/aroma contribution, with taste threshold of 0.2 g/L.<sup>46</sup> Two other *Lactobacillus* metabolites with similar characteristics are diacetyl,<sup>47</sup> which has an MIC of 0.075 g/L against *Penicillium* sp. nov. DCS 1541<sup>47</sup> but a taste threshold of 0.002-0.003 g/L,<sup>48</sup> and propionic acid<sup>49</sup> which has an MIC of 0.89 g/L against *Penicillium roqueforti* at pH 4.5,<sup>33</sup> but taste threshold of 0.1 g/L.<sup>46</sup> Other than aroma and flavor, the addition of these organic acids may also have dose-dependent effect on the volume, texture or appearance on food products.<sup>50</sup> Therefore, whilst these antifungals are relevant due to their potential production at the active concentration *in situ*,<sup>47, 49, 43</sup> they are only useful in foods when their alteration to the taste, texture or volume is tolerable.

Secondly, antifungal metabolites of LAB such as antifungal peptides<sup>51 44</sup> and hydroxy long-chain unsaturated fatty acids,<sup>15</sup> were produced *in situ* in concentrations well below those levels that are effective to inhibit fungal growth. These compounds may be relevant antifungal

candidates for external addition to a food matrix, either directly as the active compounds themselves, or via adding their precursors for conversion. In addition, such compounds may function with the assistance of other synergistically antifungal compounds which become available in the matrix. In fact, the low levels of production *in situ* compared to the MIC are commonly observed in LAB metabolites, such as for lactic acid and 2-hydroxy-(4-methylthio)butanoic acid.<sup>43</sup>

Thirdly, non-antifungal substrates added externally to the matrix can be converted into antifungals by the enzymatic activity of *Lactobacillus* spp. For example, phenylalanine has no antifungal activity, but it can be converted through aminotransferase and dehydrogenase<sup>52</sup> into the phenyllactic acid (PLA); PLA formation by lactobacilli was suggested to contribute to the extended shelf life of bread.<sup>53</sup> The conversion of non-antifungal linoleic acid into antifungal 10-OH C18:1<sup>15</sup> was successfully applied in extending the shelf life of bread for ~2 days against *P. roqueforti* FUA5055. However, the specific bacterial conversions rates to produce these antifungal *in situ* can vary,<sup>43</sup> and therefore it needs to be elucidated and optimized for different food matrixes to achieve antifungal purposes.

Last but not least, endogenous enzymatic or chemical conversions of food components in the food matrix can also result in antifungal products. The accumulation of these antifungals, such as coriolic acid<sup>15</sup> and cyclic di-peptides (2,5-diketopiperazines)<sup>54</sup> from bread, are independent of the addition of starter culture of lactic acid bacteria, but may work synergistically with their antifungal metabolites.

Therefore, although increasing number of antifungal metabolites of *Lactobacillus* have been discovered, all of them have their own technical barriers to further application. Different for bio-protective cultures targeting pathogenic bacteria,<sup>55</sup> the antifungal “toolset” for LAB is substantially smaller.<sup>56</sup> In many cases, the antifungal activity of LAB has not been attributed to specific compounds.<sup>57</sup> Hence, the species- or strain-specific antifungal properties of these



bacterial cultures cannot always be explained by their characterized antifungal metabolites, and therefore they are usually attributed to the synergistic effect of several compounds.<sup>58,57</sup> A better understanding on these metabolites and their synergistic effects will remove hurdles towards their applications in food, particularly by addressing the differences between *in vitro* and *in vivo* antifungal activity, their effects on sensory attributes of food, and the factors that allow their formation in food to active concentrations.<sup>20,45</sup>

The synergistic effect of LAB metabolites with the food matrixes is particularly relevant when plant-derived antifungal compounds are present. Plant stress responses trigger production of low amounts of antifungal HFA,<sup>35,37</sup> In contrast, some plants seed oils store high amount of HFA of great structural diversity,<sup>40,38</sup> from which HUFA can be purified for further study via, for instance, high-speed counter-current chromatography (HSCCC). HSCCC is a liquid-liquid chromatography that employs multi-layer coil planet centrifuge model,<sup>59</sup> and it has been a very useful tool to complements preparative LC<sup>59</sup> and to facilitate the development of structure-function relationships of bioactive compounds.<sup>60</sup> Since only limited number of bioactive lipids have been separated using the HSCCC preparative purification techniques, the transferability of this method is also demonstrated through the separation of sphingolipids (gangliosides) in Appendix 1, in addition to the separation of hydroxy fatty acids in Chapter 4, 5, and 7.

To address the knowledge gaps described above, experimentation described in this thesis aimed to test the following hypotheses:

### **Hypotheses:**

1. HSCCC separates bioactive lipids representing a wide spectrum of structural diversity (Chapter 4, 5, and 7; Appendix 1);

2. Hydroxy fatty acids (HFAs) inhibit the growth of food spoilage filamentous fungi and yeasts *in vitro* and in food products; the specific antifungal activity of HFA is structure-dependent and relates to their interaction with fungal membranes (Chapter 3, 4, 5, and 6);

3. Fermentation using LAB strains capable of unsaturated fatty acid conversion accumulates HFAs *in situ*; the molecular structures and concentrations of the HFAs produced *in situ* enable their antifungal activities (Chapter 6 and 7);

To test these hypotheses, the specific objectives were:

1) To purify 10-hydroxy-12-octadecenoic acid (10-HOE) and 13-hydroxy-9-octadecenoic acid (13-HOE) via solid phase extraction (SPE) from *Lactobacillus plantarum* TMW1.460 and *L. plantarum* TMW1.460 $\Delta$ *lah* cultures respectively. Then, to compare the antifungal activities of 10-HOE and 13-HOE against two common food spoilage fungi, *Penicillium roqueforti* and *Aspergillus niger*, with those of 13-hydroxy-9,11-octadecadienoic acid (coriolic acid), 12-hydroxy-9-cis-octadecenoic acid (ricinoleic acid) and non-HUFA 9,12-octadecadienoic acid (linoleic acid) (Chapter 3);

2) To purify 13-hydroxy-9,11-octadecadienoic acid (coriolic acid) from *Coriaria* seed oil using HSCCC, to test the antifungal spectrum of coriolic acid against food related yeasts and filamentous fungi and to compare this spectrum with the ones of 9,12-octadecadienoic acid (linoleic acid) and 9-octadecenoic acid (oleic acid) (Chapter 4);

3) To purify 9-hydroxy-10,12-octadecadienoic acid (dimorphecolic acid), 18-hydroxy-9,11,13-octadecatrienoic acid (kamlolenic acid), and 2-hydroxy-9,12,15-octadecatrienoic acid (2-hydroxy linolenic acid) from plant seed oils by HSCCC; to compare the profiles of their antifungal activities against food-related yeasts and molds to those of other HUFA, including coriolic acid, ricinoleic acid, microbial-converted HUFA (10-HOE and 13-HOE), 2-hydroxy oleic acid; to construct structure-function relationships for HUFA, and investigate their modes of action (Chapter 5);

4) To measure the antifungal activities of HUFA in flaxseed sourdough bread and wheat flour sourdough bread (Chapter 6);

5) To characterize HFAs and quantify non-HFA and HFA compositions in fermented sausage sample, in order to elucidate the impact of starter culture on the fatty acid metabolism in sausage fermentation (Chapter 7);

In addition, a preparative HSCCC separation of gangliosides was developed to separate gangliosides by classes, species, and homologues, which only differ in the composition or arrangement of saccharide monomers (glycoforms), or their ceramide moieties. This work is presented as Appendix 1.

## Chapter 2. Conventional and current methods for the analysis of hydroxy fatty acids

### 2.1 Introduction

Hydroxy fatty acids (HFAs) are important constituents of cellular structures.<sup>38, 61</sup> They are involved in processes such as the moderation of membrane fluidity,<sup>62</sup> single- or multi-cellular signaling processes<sup>14, 63</sup> and the self-defense of organisms.<sup>64, 65</sup> These bioactivities are often distinct from those of their non-hydroxy metabolic precursors or analogues.<sup>62, 66</sup> Furthermore, their presence is an indicator of the extent of lipid oxidation,<sup>67</sup> metabolic status,<sup>64, 68</sup> disease development<sup>69, 70</sup> and species identification.<sup>71, 72</sup>

Due to their low abundance (with a few notable exceptions, such as ricinoleic acid in castor oil and coriolic acid in *Coriaria* oil<sup>73</sup>), and to their complexity and susceptibility to isomerize and degrade, HFA profiles can be difficult to determine and quantify.<sup>74</sup> However, such information is critically important to understanding the biological processes in which they participate. This chapter is a summary of the progress that has been made to identify and quantify HFAs. It begins with a description of the biological significances of HFAs, which have stimulated interest in developing novel approaches to the qualitative and quantitative measurement of HFA species and profiles.

### 2.2 Biological significance of hydroxy fatty acids

Subtle changes to the molecular structure of HFAs, such as the number and/or position of –OH or –C=C– groups, can dramatically change their biochemical functions.<sup>12, 63</sup> Similarly, their presence in diverse lipid classes (e.g. as free fatty acids or in acylglycerols, phospholipids, sphingolipids, sterol esters etc.) may also result in different functions. These

HFA structure-function relationships may provide insight that is useful for understanding related biological processes, and for designing novel HFA applications. Although the main emphasis here is on the biological functions of HFAs, it should be noted that HFAs, especially from castor oil, are a very important feedstock for the oleochemical industry, as discussed elsewhere.<sup>39</sup>

### 2.2.1 Mono-HFAs with –OH near the –COOH (2- and 3-HFAs)

In animals, the physiological importance of 2-HFA is quite distinct from that of their non-hydroxy counterparts, such as in anticancer<sup>75, 76</sup> antitumor activity,<sup>77</sup> body weight reduction and blood pressure regulation.<sup>78, 79, 80, 82</sup> The mutation of the 2-hydroxylation enzyme (FA2H) is associated with a series of neurological disorders<sup>83, 84, 85, 86</sup>, which indicates the importance of 2-HFA lipids in regulating neural functions. CoA derivatives of 3-HFA (3-OH-acyl CoA) are universal intermediates of  $\beta$ -oxidation processes.<sup>87, 88</sup> The production, especially the “escape” of 3-HFA indicating incomplete  $\beta$ -oxidation, provides a diagnostic indicator of ischemic heart disease.<sup>69, 89</sup> In addition, 3(*R*)-hydroxy-5*Z*,8*Z*,11*Z*,14*Z*-eicosatetraenoic acid (3-HETE, or 3-OH C20:4) is a precursor of 3-OH prostaglandins, which are inflammatory compounds.<sup>89</sup>

In fungi, a high proportion of 2-HFA exists in sphingolipids, including ceramides, acidic sphingolipids and cerebroside.<sup>90, 91</sup> In the dimorphic fungus *Sporothrix schenckii*, 2-HFA has been found in galactocerebroside but only from its yeast form, suggesting a role for 2-HFA-containing sphingolipids in the morphological regulation of fungi.<sup>92</sup>

Fungal 3-HFA has been associated with survival and pathogenesis.<sup>93, 89, 94, 95</sup> For example, in human pathogenic yeasts, *Candida albicans*, 3(*R*)-hydroxy-tetradecanoic acid (3-OH C14:0) contributes to the important quorum sensing processes.<sup>96</sup> The production of 3-HFA is

also involved in the protection against animal predation,<sup>97</sup> release of sexual spores and yeast flocculation.<sup>94, 98, 99</sup> Interestingly, enzymatic oxidation of fungal 3-HETE results in the formation of mammalian oxylipins that are precursors of 3-OH-PGE<sub>2</sub>, a pro-inflammatory metabolite.<sup>100</sup> This indicates that 3-HFA may contribute to the interaction between fungal invasion and the mammalian immune system.

Similarly, in plants, 2-HFAs are also primarily found within sphingolipids.<sup>101, 102, 103, 104</sup> 2-HFAs are also rich in the leaves of *Gramineous* plants (*e.g.* > 40% of 2-OH C20:0 cerebrosides in the leaves of rice).<sup>104</sup> However, the forms of 2-HFA are not specified in many plant studies.<sup>105, 106</sup> It should be emphasized that, while some plants naturally accumulate 2-HFAs, recent studies showed that 2-HFAs are produced as a self-defense compounds under specific stresses, such as pathogen infections,<sup>107, 108, 37</sup> herbivory<sup>109</sup> or senescence.<sup>37</sup> In addition, 2-HFAs also have important plant physiological functions in regulating hormone homeostasis,<sup>107, 110</sup> suppression of stress-related cell death,<sup>102</sup> oxidative stress protection,<sup>107</sup> increase of plant chill-resistance,<sup>104, 111, 103</sup> and possibly more.

Long-chain (C14-C18) 3-HFAs have been found in several plant floral oils,<sup>112, 113, 114</sup> while very long chain 3-HFAs (C26-30) were found in the cuticular waxes of *Aloe arborescens* leaves.<sup>115</sup> The 3-OH C18:3 and C16:2 with conjugated double bond systems were found in green microalgae *Tydemania expeditionis*, which showed an inhibitory effect against tumor cell lines.<sup>116</sup> The biosynthesis and other sources of 3-HFAs have been described in detail.<sup>115</sup> However, it should be emphasized that in many cases, the occurrence of 3-HFA has yet to be explained in terms of their biological functions.

Unlike with eukaryotic cells, in bacteria, phospholipids<sup>117, 118, 119</sup> and lipopolysaccharides<sup>120, 121, 119</sup> are the main lipid forms containing 2-HFA, for gram-positive and gram-negative bacteria, respectively. Although sphingolipids are ubiquitous in eukaryotic cells, they are rare in bacterial membranes,<sup>122</sup> with the exception of a few bacteria such as *Sphingomonas*

*paucimobilus*<sup>123</sup> and *Sphingobacterium spiritivorum*.<sup>124</sup> In gram-negative bacteria, 2- and 3-HFA moieties are components of lipid A, an endotoxin located in the bacterial cell wall<sup>125, 126</sup>, and are also found in ornithine lipids.<sup>127</sup> In comparison, gram-positive bacteria produce 3-HFA containing acyl peptides as antibiotic compounds.<sup>88, 128, 129</sup> In addition, 2- and 3-HFA have characteristically been found to co-exist in many bacterial sources.<sup>130</sup> Their occurrence in bacteria has been used as a useful tool to investigate bacterial taxonomy<sup>131</sup> and origins,<sup>132</sup> as well as to identify environmental endotoxin producing strains,<sup>133</sup> to measure LPS content and activities<sup>134</sup> and to develop terrestrial proxies for the past environment.<sup>135</sup> In addition, it has also been described that 2-HFA plays a role in mediating the bacterial virulence, *e.g. via* bacterial toxin-binding<sup>136</sup> and the apoptotic effect exerted on human leukaemic cells.<sup>137</sup>

### **2.2.2 Mid-chain HFAs**

Mid-chain HFAs are common products of lipid oxidation, which is involved in a wide range of physiological processes.<sup>70, 138, 139, 37</sup> The oxidation of food lipids also commonly produces mid-chain HFAs.<sup>140, 141</sup> Specific lipid oxidation reactions can be either beneficial or detrimental to organisms<sup>142</sup> and mid-chain HFA contribute to this duality. In fact, the production of HFAs as chemically stable oxidation products contributes to the development of an adaptive response to subsequent oxidative stress.<sup>143</sup>

In animals, mid-chain HFAs of C20 and C18 have been thoroughly studied due to their close association with disease development and regulation, such as in nonalcoholic fatty liver disease (NAFLD)<sup>70</sup> and inflammatory diseases.<sup>139, 138, 144</sup> However, the specific bioactivities of each mid-chain-HFA species are diverse. For example, released 9- and 13-OH C18:2 endogenously contribute to the heat sensitivity of the TRPV1, the principle noxious heat (>43°C) receptor for the peripheral nervous system.<sup>138</sup> 9-OH C18:2 extracted from the folk

medicine plant *Typhonium blumei* shows anti-allergic activity.<sup>145</sup> The ester of 13-OH C18:2 also exhibits anti-inflammatory and pro-resolving properties.<sup>146</sup> Additionally, mid-chain HFAs have been observed as the metabolites of long-chain unsaturated FA from dietary supplements taken in clinical trials,<sup>147</sup> but their functions are yet to be fully elucidated.

For fungi, 8-HFA is an important compound involved in many activities in the fungal life cycle. (*R*)-8-hydroxy-*cis*-9,*cis*-12-octadecadienoic acid (8-OH C18:2) is the precocious-sexual-inducer ( $\psi$ ) B $\alpha$  factor, which contributes to the sexual development of *Aspergillus* spp.<sup>148</sup> The same compound is also involved in the inhibition against phycomycetous fungi,<sup>149</sup> regulation of conidia formation and mycotoxin production.<sup>150</sup> In the sclerotium of the phytopathogenic fungi *Claviceps purpurea*, a high portion of ricinoleic acid (12-OH C18:1) is usually accumulated in the peptide alkaloids producing strains.<sup>151, 152</sup> In fact, HFAs with -OH located in the middle of the chain are believed to play an important role in cross-kingdom signal communication among plants, animals and fungi.<sup>153</sup>

In plants, C16 and C18 HFA are the most common mid-chain HFAs. They play important roles in plant self-defense pathways, partly because HFAs have antimicrobial effects, especially targeting fungi.<sup>12, 13</sup> Similar to 2-HFA, their plant protection effect is distinct from their direct antimicrobial properties, due to their possible up-regulation of self-defense pathways against pathogens.<sup>12, 14</sup> In addition, plant materials can be a rich source for the extraction of HFA analogs. Oils from certain seeds may naturally accumulate a high portion of HFA, for example 9-OH C18:2 ( $\Delta$ 10*trans*, $\Delta$ 12*trans*) (dimorphecolic acid) from *Dimorphotheca sinuata*,<sup>154</sup> 13-OH C18:2 ( $\Delta$ 9*cis*, $\Delta$ 11*trans*) (coriolic acid) from *Coriaria nepalensis*,<sup>155</sup> 12-OH C18:1 ( $\Delta$ 9*cis*) (ricinoleic acid) from *Ricinus communis*<sup>61</sup> and 9-OH C18:1 ( $\Delta$ 12*cis*) from *Plantago ovate*.<sup>156</sup> Although their exact functions in these plants are not clear, some HFAs have established applications, for example, as antimicrobial agents,<sup>66</sup> food emulsifiers,<sup>157</sup> and industrial feedstocks.<sup>158</sup>



For bacteria, the hydration of unsaturated fatty acids into HFAs has been considered as a detoxification process against unsaturated fatty acids.<sup>159, 160, 17</sup> In some cases, this reaction is related to the virulence of pathogenic bacterial strains<sup>17</sup> and their competition with other species.<sup>15, 66</sup> Intriguingly, the production of 10- and 13-OH C18:1 by gut microbiota may contribute to their influence in lipid metabolism, and thus the health of the host.<sup>160</sup>

### 2.2.3 Omega-HFAs

Omega-OH ( $\omega$ -OH) FA, where the hydroxyl groups are close to the end of the hydrocarbon chain and remote from the carboxyl group, are usually found in protective structures, such as wool wax,<sup>161</sup> stratum corneum,<sup>162</sup> cell walls,<sup>163</sup> and plant cuticles.<sup>164</sup>

For plants,  $\omega$ -OH C16 or C18 HFA are components of the biopolymer cutin found in the plant cuticle, a hydrophobic structure that plays a critical role in plant self-defense.<sup>165, 164, 166</sup> Some plants accumulate  $\omega$ -HFA in their fatty acid profile; for example, *Mallotus philippinensis* seed oil<sup>167</sup> contains 50-60% of 18-OH C18:3, and can be used in industrial applications.<sup>168</sup>

In animal models, 20-HETE (20-OH C20:4) can reduce the change in cellular hyperpolarization and therefore act as an endogenous vasoconstrictor.<sup>169, 170</sup> It is also the inactivated metabolite of leukotriene, an inflammatory mediator.<sup>171</sup> It has been shown that  $\omega$ -OH C16:0 and C18:0 induced apoptosis in human melanoma cells.<sup>172</sup> One of the *N*-acylated derivatives of  $\omega$ -HFAs, lipokeratinogenoside, is characteristically found in mammalian epidermis.<sup>173</sup> (*O*-acyl)- $\omega$ -hydroxy-fatty acids with very long chains are found in highly specialized compartments such as sperm,<sup>174</sup> vernix caseosa,<sup>175</sup> amniotic fluid,<sup>176</sup> and especially in meibomian glands to maintain the tear film stability<sup>177</sup>.

#### 2.2.4 Di-HFAs and poly-HFAs

The presence of di- and poly-HFAs can be an important indicator of various physiological states. For example, an increased level of 11,12-diOH C20:4 in animals can be an indicator for nonalcoholic steatohepatitis.<sup>178</sup> The generation of these HFAs under specific stimuli may result in further processes that are necessary to maintain homeostasis, and these can be the inspiration for new treatments. For example, the production of 12,13-dihydroxy-9Z-octadecenoic acid (12,13-diOH C18:1) was increased in plasma of humans and mice after cold exposure, and this in turn promoted the metabolic activity of brown adipose tissue (BAT), a tissue responsible for heat production for mammals.<sup>179</sup> Injection of this di-HFA in mice increased cold tolerance; as a result of this finding 12,13-diOH C18:1 was proposed as a potential treatment for related metabolic disorders (*e.g.* obesity, diabetes, and hyperlipidemia).<sup>179</sup>

A significant amount of research has been performed on the docosahexaenoic acid (DHA)-, eicosapentaenoic acid (EPA)-, and arachidonic acid (ARA)-derived di- and tri-OH HFA, due to their close relationship with disease development, dietary supplementation and neural function.<sup>180</sup> The HFA metabolites of these very long chain fatty acids, such as protectins, maresins and resolvins, contribute to anti-aggregation and anti-inflammatory functions and thus to maintaining homeostasis in the hosts.<sup>63, 181</sup> In addition, the occurrence of di- or poly-HFAs can also be a quality indicator for food products.<sup>182</sup>

Other resources where readers can obtain more information on the biosynthesis, natural occurrence and functions of HFAs include but are not limited to: the enzymatic production of HFAs,<sup>39</sup> information on the natural distribution of HFAs in online resources Cyberlipid (<http://www.cyberlipid.org/fa/acid0005.htm>) and the PlantFA database (<https://plantfadb.org/>).

### 2.3 Pre-treatment before HFA analysis

In order to investigate the distribution of HFA species found in various biological contexts in an accurate and reproducible manner, methods to quantitatively extract HFAs are needed. Following extraction, separation methods such as between neutral and polar lipids, or between saponifiable lipids and non-saponifiables, are often performed in order to release and concentrate free HFAs. These sample treatments help to avoid interferences and to improve the final chromatographic separations and detection performance during analysis.

When extracting HFAs from a biological sample, it is highly recommended to spike the sample with known amounts of authentic standards (surrogate internal standard, SIS) and to validate the extraction method by confirming their recovery. A suitable SIS is required to be similar to the target analyte (a chemical analogue) but not to pre-exist in the samples. Hence a stable-isotope labeled form of HFA (*e.g.* a deuterated or  $^{13}\text{C}$  labeled analog) is an ideal internal standard for the analysis of HFAs.<sup>139, 183, 184</sup> For example, *d6-20-HETE*, *d8-5-HETE*, *d4-9-HODE* and *d11-14,15-diOH C20:3* have been used as surrogates for groups of HFAs.<sup>139, 183</sup> Alternatively, HFAs not commonly found in biological samples can be selected to be an SIS, such as odd-carbon-number HFA *10,11-diOH C19:0*.<sup>170</sup> SIS can and should also undergo the re-extraction steps mentioned below (*e.g.* after saponification or pre-analysis separation) to validate the method developed for specific analytical purpose, or more importantly, to compensate their recovery loss due to these re-extraction steps, as well as ion suppression in MS analysis.<sup>139</sup>

In some cases, during pre-treatments, target unsaturated HFAs may be susceptible to oxidation under the conditions applied. Therefore, antioxidants (*e.g.* butylated hydroxytoluene (BHT)), chelating agents, (*e.g.* ethylene diamine tetraacetic acid (EDTA)) and an inert dry gas atmosphere (*e.g.* nitrogen) have been used to protect these analytes.<sup>185,</sup>

Important general considerations for quantitative lipid extractions from organisms and tissues have been reviewed in detail;<sup>186</sup> industrial oil extraction has also been summarized.<sup>187</sup> It should be particularly noted that the diversity of lipids incorporating HFAs is reflected in the differences in their polarity, and therefore solvents of different polarity<sup>188, 189</sup> are required for their extraction. Because of this, although very non-polar solvents (*e.g.* hexanes) and versatile chlorinated solvents (*e.g.* chloroform and dichloromethane) are very useful to extract whole lipids, they can sometimes fail to efficiently extract HFA-rich oil.<sup>167, 168</sup> Thus, quantitative extraction of HFAs depends on the overall composition of an HFA-containing sample, and various solvents have been applied successfully, such as diethyl ether,<sup>167-168</sup> ethyl acetate,<sup>190</sup> chloroform-methanol-water mixtures (Folch method and Bligh and Dyer method),<sup>15, 191</sup> chloroform-isopropanol mixtures,<sup>192</sup> hexane-isopropanol mixtures<sup>193</sup> and ethyl acetate-hexane mixtures.<sup>194</sup> A hexane-isopropanol mixture was especially recommended as it is simple, convenient, versatile and it can be easily adjusted to a small volume.<sup>195</sup>

If the target analytes are free HFAs, they can be directly extracted and enriched using solid phase extraction (SPE) and eluted out with suitable solvents to eliminate interferences.<sup>183, 144</sup> For example, the extraction of HFA-containing mixtures was performed with Waters Oasis HLB (60 mg/30  $\mu$ m) SPE cartridge, eluted with ethyl acetate after conditioning.<sup>144</sup> In many cases, however, information on bound HFAs within a total lipid extract is required. One approach to this problem is to perform saponification of the lipid mixture using an alcoholic-aqueous solution of base, followed by acidification, to release the free fatty acid form of HFA.<sup>195, 196</sup> Alternatively transesterification in the presence of methoxide can be used to release HFA methyl esters prior to analysis.<sup>73, 197, 198</sup> Optimized protocols of saponification and transesterification, which allow bound fatty acids to be liberated for analysis by liquid chromatography (LC) or gas-chromatography (GC) methods with minimal degradation, can be found elsewhere.<sup>185, 199</sup>

After saponification, a non-polar solvent is used to remove non-saponifiable fraction. The water-soluble fraction is then pH-adjusted with acid so that HFAs are converted to their protonated forms and can then be extracted by a low-polarity solvent.<sup>200, 66</sup> By performing this step, most of the non-saponifiable non-polar components (e.g. sterol and non-polar pigment) and water-soluble components (e.g. saccharides and peptides) can be removed. Therefore, this post-saponification liquid-liquid separation is especially useful to clean up the interference compounds prior to HFA analysis. As an alternative, solid phase extraction (SPE) was also used to extract HFAs from saponified products as previously described.<sup>139</sup>

In the case of transesterification, the non-polar solvent is used to extract the mixture containing HFA methyl esters, followed by SPE clean-up and further derivatization prior to analysis if necessary.<sup>197</sup> A workflow was proposed to separate the HFA-containing oxidized FAME mixtures from other non-oxidized FAME, then to hydrogenate oxidized FAME in order to reduce the number of analytes and therefore simplify the quantitative results.<sup>74</sup>

When performing saponification before separation, information on the HFA linkage with other lipid components (glycerol, sterol, alcohol, etc; ester or other linkages) will be lost. Alternatively, pre-separation of lipid classes containing HFAs can be performed using SPE<sup>71</sup> or other methods<sup>201, 202, 203</sup> prior to saponification and further analysis.

More sophisticated analytical methods for intact HFA-containing lipids (*i.e.* without saponification) are also widely used.<sup>204</sup> For example, after oil extraction and SPE purification, long-chain fatty acid esters of HFAs (esterified to the hydroxyl side-chain) were directly analyzed by LC-MS/MS/MS.<sup>146</sup> The resulting fragmentation spectra indicate the position of the ester-linkage of the HFA and hence the location of the hydroxy group, as well as the ester type. Without saponification, separation of mono, di- and tri-acylglycerols containing HFAs was demonstrated using RP-HPLC-APCI-MS<sup>205</sup> and RP-HPLC-ESI-MS;<sup>206, 207</sup> some regio-specific separation was also shown to be possible.<sup>208</sup>

## 2.4 Conventional methods for hydroxy fatty acid analysis - GC based approaches

Since its development in the 1950s, GC has developed into a powerful tool that has been extensively used in the analysis of lipids.<sup>209</sup> It is especially well recognized as the most common method for profiling fatty acids, achieving high resolution separations with excellent sensitivity and reproducibility in both qualitative and quantitative analyses. In GC, which is also known as GLC (gas-liquid chromatography) compounds are separated based on their partition between the gas (mobile phase) and liquid phase (stationary phase) in the column. A wide range of detectors are available, with the flame ionization detector (FID) being the most widely used and universal in scope, with predictable response factors for the quantitative analysis of lipids, as described elsewhere.<sup>210, 211</sup>

For the study of HFA, GC coupled with mass spectrometry (GC-MS) is particularly useful and is the focus of this section. In addition to chromatographic separations it can provide molecular weight and fragmentation information that are essential to structural determination and permits the use of highly selective modes for HFA quantitation. GC and GC-MS based methods have made fundamental contributions to studies that have identified HFA distributions in diverse sources including microbes,<sup>212, 125</sup> animals<sup>213, 214</sup> and plants.<sup>156, 215</sup>

GC-MS is a mature technique with many well-established procedures for use in lipid analyses.<sup>216, 217</sup> A key consideration in the analyses of HFA in particular is the derivatization method, since the presence of a hydroxyl group along the fatty acyl chain profoundly affects both the chromatography and the fragmentation seen in electron ionization (EI) mass spectrometry. Here, a discussion of the derivatization methods used in HFA analysis is followed by some interpretation of the EI-MS spectra of HFAs and their derivatives.

### 2.4.1 Esterification (preparation of FAME)

Since fatty acids primarily occur bound within larger lipid entities (especially as triacylglycerides), as a prerequisite to GC-MS analysis they must first be converted into volatile, lower molecular weight derivatives. Fatty acid methyl ester (FAME) derivatives are the most commonly used, and these are applicable to HFA analyses.<sup>74, 218, 219</sup> Esterification agents can be broadly classified by means of the reaction conditions into acidic, neutral and basic.<sup>220</sup>

#### 2.4.1.1 Acid catalysed esterification/transesterification

Acid catalysed esterification/transesterification has been widely applied in FAME preparation and may follow hydrolysis to release bound fatty acids. Both Lewis acids (*e.g.* BCl<sub>3</sub>, BF<sub>3</sub>) and strong acids (*e.g.* HCl, H<sub>2</sub>SO<sub>4</sub>) in alcoholic solutions are widely used for acid esterification. For example, HFAs were esterified with 35% BF<sub>3</sub> in methanol at 100 °C for 2 min, with no observed side products.<sup>221</sup> Similarly, HFAs (10 mg) dissolved in 1 mL of methanol were mixed with 2 mL of 1% (v/v) H<sub>2</sub>SO<sub>4</sub> acid in methanol, and the reaction was performed at 50 °C for 2h.<sup>191, 211</sup> After the derivatization reaction, a re-extraction procedure is usually applied to clean up the sample prior to injection into the GC.<sup>191, 211</sup> There are reports that during acid catalysed esterification of HFAs, side reactions can occur, such as the methoxylation of the -OH group,<sup>222</sup> and the breakdown of methylation products if strong acid, high temperature or long reaction time are used.<sup>223, 154, 224</sup> Dehydration and double bond migration were also observed in GC analyses with certain HFA structures, such as with hydroxy-dienes (*e.g.* coriolic acid 13-OH C18:2 (Δ<sup>9,11</sup>) and dimorphecolic acid 9-OH C18:2 (Δ<sup>10,12</sup>)), and these result in ambiguities in FAME identification.<sup>225, 223, 154, 224</sup> Other structures, such as conjugated unsaturation, epoxy and cyclopropane rings are also vulnerable

to acid esterification.<sup>226</sup> Interestingly, acetylenic HFAs with the -OH group adjacent to conjugated unsaturation, as found in *Ongokea gore* (isano) oil, appeared to be resistant to acid catalyzed dehydration prior to GC analysis.<sup>226, 227</sup>

#### 2.4.1.2 Base catalysed transesterification

Although basic conditions cannot be used for the esterification of free HFAs, it is widely applied to the transesterification of bound HFAs. It is especially useful in lipid profiling since fatty acids occur mainly esterified within phospholipids, acylglycerols, sphingolipids or other lipid molecules. Base-catalysed transesterification can be used to obtain HFA methyl esters from their bound forms, even for acid-sensitive structures like those mentioned above, and particularly for HFAs with hydroxydiene structures. Using this method, methyl ester of coriolic acid (13-OH C18:2) and dimorphecolic acid (9-OH C18:2) were obtained and analyzed from the seed oils of *Coriaria nepalensis*<sup>155</sup> and *Dimorphotheca sinuata*<sup>154</sup> respectively. Application of these methods can also be valuable in investigations of oxidation products of plant oil, due to the common formation of acid-labile structures during lipid oxidation.<sup>197, 228</sup>

#### 2.4.1.3 Neutral esterification

If the FAME of acid-sensitive structures also cannot be obtained using basic catalysts (e.g. when they are originally in their free fatty acid form), diazomethane (CH<sub>2</sub>N<sub>2</sub>) is an alternative methylation agent. However, due to its unstable nature, precautions must be taken when using it. Practical procedures, such as the *in situ* preparation of diazomethane (commercial precursor “Diazald<sup>®</sup>”) using specialized apparatus,<sup>229, 230</sup> or reactions using diazomethane derivatives (trimethylsilyldiazomethane) under milder conditions,<sup>231</sup> have been developed.



For more reactive structures like hydroxydienes, hydroxyl groups also undergo partial methylation as a side reaction.<sup>223</sup> In spite of this, the method has been successfully used in the esterification of free labile HFA structures such as coriolic acid (13-OH C18:2),<sup>232, 233</sup> dimorphecolic acid (9-OH C18:2)<sup>223</sup> and fungal metabolites 8*R*-hydroxy-9*Z*,12*Z*-octadecadienoic acid (8-OH C18:2).<sup>234</sup> The methylation yield reach 96% for coriolic acid using the improved method of trimethylsilyldiazomethane.<sup>231</sup>

#### **2.4.2 Derivatisation methods used to locate HFA hydroxy groups**

After esterification or transesterification, the HFA hydroxy group typically requires further derivatization in order to be able to obtain useful information from GC-MS analysis. This is because of the possibly ambiguous mass spectra resulting from the side reactions at the high temperatures used in GC for separation.<sup>235</sup> At the same time, common derivatization reactions like acetylation may not protect the hydroxyl group during such conditions due to the potential for deacetylation processes, which lead to the loss of important structural information.<sup>235</sup> A solution to this problem is the further silylation of hydroxy groups of HFA methyl esters.

As part of the analysis of HFAs it is often beneficial to derivatize the hydroxy groups so that positional information is more likely to be obtained. In addition, a major advantage of such derivatization is to increase the  $m/z$  of the characteristic fragment ions, and therefore make the signals more distinguishable compared to other low MW signals. Also, since some derivatization of hydroxy groups can lead to abundant and structurally specific fragmentation patterns under EI-MS or tandem-MS (MS//MS), it can therefore provide useful fingerprint information for each HFA. Derivatization of the hydroxy group of HFA methyl ester can be useful for both qualitative and quantitative purposes.

One of the most common derivatization methods used is silylation, which converts hydroxyl groups into trimethylsilyl (TMS) ether derivatives (**Figure 2.1**)

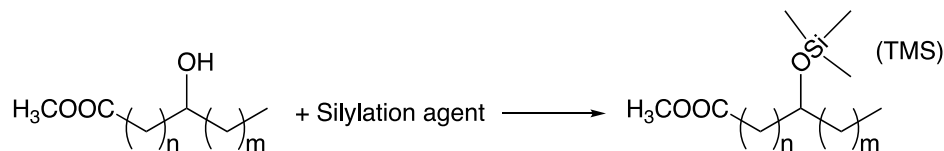


**Figure 2.1.** Silylation reaction

Silylation reagents are readily available and can be used with many established methods such as:

- 1) *N, O*-Bistrifluoroacetamide (BSTFA) as silylation agent with 1% trimethylsilyl chloride (TMCS) <sup>236</sup> catalyst, or pyridine acting both as solvent and catalyst (1:1 v/v pyridine/BSTFA), kept for 30 min at room temperature,<sup>197</sup>
- 2) A mixture of pyridine, BSTFA, hexamethyldisilazane (HMDS) and trimethylchlorosilane (TMCS), with a ratio of 0.2:1:2:1 (vol/vol) at 50 °C for 15 min,<sup>237</sup>
- 3) A commercially available mixture of *N, O*-Bis(trimethylsilyl)acetamide (BSA), TMCS and trimethylsilylimidazole (TMSI) with a ratio of 3:2:3,<sup>238</sup>

The literature cited above are examples of silylation specific to the analysis of HFAs, but other silylation methods have been summarized.<sup>239</sup> Optimization of specific reaction parameters, such as the reactivity of the silyl donor, temperature, time, solvent, *etc.* can be achieved with minimal side products <sup>240</sup> by monitoring the presence of a non-silylated HFA methyl ester as well as side products to indicate the extent of the silylation reaction.<sup>197</sup>

Converting HFAs first to FAME derivatives then further into to silyl derivatives is one of the main tools that has been used to analyze HFAs, <sup>234, 237, 238</sup> and to investigate the formation of lipid oxidation products including hydroxy- and peroxy-lipids. <sup>236, 197, 241</sup> Due to the useful

information that this method can provide, many EI spectra of silylated methyl esters of HFAs have been published and are very well summarized.<sup>242</sup> In **Table 2.1**, C18 fatty acids are used as an example to elucidate their EI fragmentation patterns. The following characteristic ions are often found in the EI-MS spectra of silylated HFA methyl esters:

- 1) **Molecular ion  $[M]^+$** : Molecular ions are not necessarily found in EI-MS spectra of HFAs since electron ionization induces extensive fragmentation. The presence or absence of an  $[M]^+$  ion is sometimes characteristic of a specific isomer. For example, the EI-MS spectrum of 18-OH C18:1 ( $\Delta^9$ ) exhibits a significant  $[M]^+$  signal in  $m/z$  384, while molecular ions are not observed in the spectra of other mono-OH C18:1 or 18-OH C18:0 analogs.
- 2)  **$[M-15]^+$** : A fragment ion formed due to the loss of a methyl group  $CH_3^\bullet$ , commonly seen for HFAs as the ion of highest  $m/z$  value, instead of  $[M]^+$ .
- 3)  **$[M-31]^+$** : A fragment ion formed due to the loss of a methoxy group  $OCH_3^\bullet$ .
- 4)  **$[M-47]^+$** : A fragment ion formed due to the loss of both a methyl group  $CH_3^\bullet$  and the loss of a methoxy group  $-OCH_3^\bullet$  plus  $H^\bullet$ .
- 5) **“ $\Delta$ -fragment ions”**: Formed due to the  $\alpha$ -cleavage between carbons at  $\Delta^n$  and  $\Delta^{n+1}$  (where  $\Delta^n$  is the position of  $-OSi(CH_3)_3$ ; these ions are formed with the retention of the methyl ester group): they are characteristic of a TMS-HFA methyl esters, with the exception of: (a)  $\omega$ -OH fatty acids, which have a TMS ether group located at the end of the fatty acid chain further from methylated carboxylic group; (b) 2-HFAs which give little or no response for the expected  $\alpha$ -cleavage ion between  $\Delta^2$  and  $\Delta^3$ ; and (c) some of the HFAs with an unsaturation located between  $\Delta^{n+1}$  and  $\Delta^{n+2}$ .
- 6) **“ $\omega$ -fragment ions”**: Formed due to the  $\alpha$ -cleavage between  $\Delta^n$  and  $\Delta^{n-1}$ ; these ions are also characteristic of TMS-HFA methyl ester EI spectra, with exceptions such as when

an unsaturation is located at the  $\alpha$ -carbon position relative to C–O–TMS close to the methylated carboxylic end (*i.e.* between  $\Delta^n$  and  $\Delta^{n-1}$  positions).

- 7) “**Migration ions**”: Formed via the migration of  $-\text{OSi}(\text{CH}_3)_3$  to the carboxylic carbon forming an ion as shown in **Figure 2.2**,<sup>243, 244</sup> where the  $-\text{OTMS}$  group is located at  $\Delta^n$ .<sup>243</sup> This even-numbered ion and the ion formed due the  $\alpha$ -cleavage between  $\Delta^n$  and  $\Delta^{n+1}$  differ in  $m/z$  by 29 (*i.e.* CHO), but the abundance of the migration ion varies with HFA structure.<sup>243, 244</sup> Di or tri-OH HFAs also show similar patterns. For example, in the spectrum of 9,10,18-OH C18:1( $\Delta$ 12), an ion at  $m/z$  361 is formed due to the  $\alpha$ -cleavage between  $\Delta$ 10 and  $\Delta$ 11; an ion at  $m/z$  332 is also formed due to the migration of  $-\text{OSi}(\text{CH}_3)_3$ . In some cases, however, one of this pair of ions may not be present, *e.g.* for 9,10-diOH C18:0 and 9,10,18-triOH C18:0; although  $m/z$  361 is not present, its migration ion  $m/z$  332 can be observed.

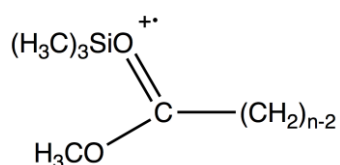


**Figure 2.2.** Migration ions

- 8) Other minor but commonly seen ions showed in EI-MS spectrum of TMS-HFA methyl ester derivatives include:
- [M-59]<sup>+</sup>**: The ion formed due to the loss of methylated carboxylic group  $[-\text{COOCH}_3]$ ; it is present in the mass spectrum of 2-HFAs with high abundance, likely due to  $\alpha$ -cleavage between  $\Delta$ 1 and  $\Delta$ 2.
  - [M-90]<sup>+</sup>**: The ion formed due to the loss of  $\text{HOSi}(\text{CH}_3)_3$ .
  - [73]<sup>+</sup>**: The ion formed due to  $\text{Si}(\text{CH}_3)_3$ .

Examples of characteristic MS spectra of TMS-FAME derivatives of 18-carbon HFAs are summarized in **Table 2.1**.

Pentafluorobenzyl ester-trimethyl silyl ether (PFB-TMS) derivatization can achieve comparable structural information to FAME-TMS analysis of HFAs and may also be able to provide molecular weight information in negative ion (electron capture) mode.<sup>245</sup>

Pyrrolidides of HFAs can also provide useful complementary information in GC-EI-MS analysis, especially for 2- or 3-HFAs since they allow  $\alpha$ -cleavage  $\Delta$ -fragment ions to be more clearly observed compared to their TMS-methyl ester derivatives.<sup>246, 247</sup>

### 2.4.3 Derivatization methods used to locate HFA unsaturation and other structural features

The derivatization methods described above primarily provide information on the HFAs' composition and hydroxyl group locations, but little information on the location of double bonds can be achieved. Therefore, additional methods are needed to achieve a more complete analysis of HFA structures by GC-MS. The use of 4,4-dimethyloxazoline (DMOX) derivatization (**Figure 2.3**) is commonly used method to locate double bond positions.<sup>248</sup>

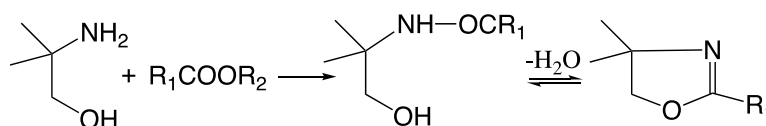


**Figure 2.3.** Reaction of DMOX derivatization

**Table 2.1.** Examples of characteristic MS spectrum ions of TMS-FAME of C18 HFAs

FAME-TMS	Compounds	MW	Characteristic EI spectral ions m/z								Ref.
			[M] <sup>+</sup>	[M-15] <sup>+</sup>	[M-31] <sup>+</sup>	[M-47] <sup>+</sup>	$\alpha$ -cleavage ions	$\alpha$ -cleavage ions-29 (TMSO migrant to -COOH)	$\omega$ -ion due to the $\alpha$ -cleavage near -OH	Other characteristic ions	
OH-C18:0	2-OH	386	386	371	/	/	/	/	327	343, 159, 129	242
	9-OH	386	/	371	/	339	259	/	229	115	197, 249
	10-OH	386	385 [M-1] <sup>+</sup>	371	355	339	273	244	215	169	197, 242
	13-OH	386	/	371	355	339	315	286	173	/	242
	15-OH	386	/	371	355	339	343	314	145	/	242
	17-OH	386	/	371	/	339	371	342	117	329	242
	18-OH	386	/	371	355	339	/	/	103	/	242
OH-C18:1	8-OH 9C=C	384	/	369	/	337	/	/	241	129	197
	9-OH 10C=C	384	/	369	/	337	/	/	227	129	197
	9-OH 12C=C	384	/	369	/	337	259	230	227	294,73	242
	10-OH 8C=C	384	/	369	/	337	271	/	/	149	197
	11-OH 9C=C	384	/	369	/	337	285	/	/	163	197
	12-OH 9C=C	384	/	369	/	337	299	270	187	73	197, 242
	18-OH 9C=C	384	384	369	353	337	/	/	103	262,159,75	242

(continued)

**Table 2.1. (Continued)**

FAME-TMS	Compounds	MW	Characteristic EI spectral ions m/z								Ref.
			[M] <sup>+</sup>	[M-15] <sup>+</sup>	[M-31] <sup>+</sup>	[M-47] <sup>+</sup>	α-cleavage ions	α-cleavage ions-29 (TMSO migrant to -COOH)	ω-ion due to the α-cleavage near -OH	Other characteristic ions	
OH-C18:2	8-OH 9,12 C=C	382	382	367	351	335	245	/	239	292, 284, 271, 261, 173, 149, 129, 121	234
	9-OH 10,12 C=C	382	382	367	/	/	/	/	225	143, 130, 311	197, 242
	12-OH 9,15 C=C	382	/	367	/	335	299	270	185	159, 117, 95	250
	13-OH 9,11 C=C	382	382	367	/	335	225	/	/	311	197
	15-OH 9,12 C=C	382	/	367	/	335	339	310	145	73	197
OH-C18:3	18-OH 9,11,13 C=C	380	380	365	349	333	/	/	/	290, 170, 91, 73	251
diOH-C18:0	9,10-diOH	474	/	/	443	/	259	332	/	215, 73	197
triOH-C18:0	9,10,18-triOH	562	/	547	532	/	259	332	303	243, 215	242
triOH-C18:1	9,10,18-triOH 12C=C	560	/	545	529	/	361, 259	332	301	147	242

Under EI conditions, DMOX fatty acid derivatives fragment at each position along the chain so the location of a single bond, double bond or a sidechain is indicated by the  $m/z$  differences between fragment ions. For example, comparing the spectra of 18-OH C18:0 with 18-OH C18:1 (Figure 2.4 A and B, spectra from <http://www.lipidhome.co.uk/><sup>242</sup>), it can be seen that the ions at  $m/z$  196 and 208 ( $m/z$  difference of 12) are associated with the presence of a double bond at the  $\Delta 9$  position. Similarly, in the DMOX spectrum of 15-OH C18:2 (Figure 2.4 C, spectra from <http://www.lipidhome.co.uk/><sup>242</sup>), the pairs of ions  $m/z$  196/208 and  $m/z$  236/248 indicate the double bonds at  $\Delta 9$  and  $\Delta 12$  positions. In this case the position of the hydroxyl group at  $\Delta 15$  position can also be seen clearly by the  $m/z$  276/306 fragment ion pair. Double bond positions have been successfully located by this method in other HFAs, such as 2-OH HFA<sup>252</sup> and ricinoleic acid (12-OH C18:1).<sup>253, 254</sup>

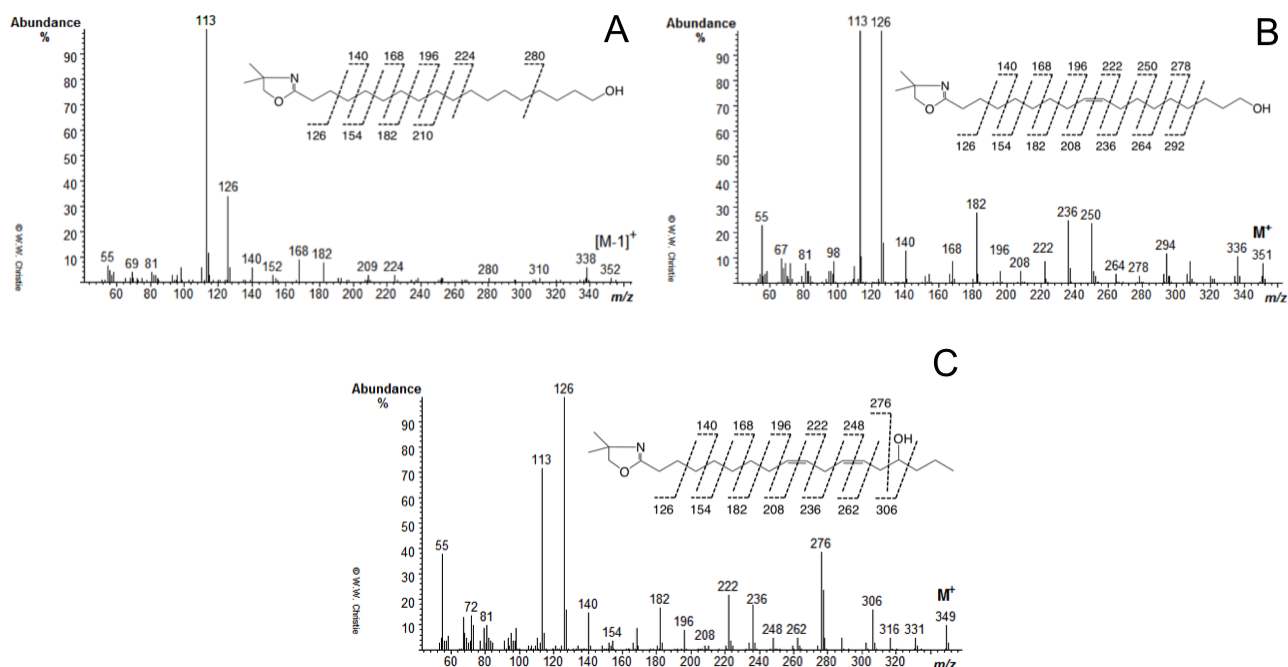


**Figure 2.4.** Examples of MS spectra of DMOX-18-OH HFAs of A) C18:0, B) C18:1, and C) C18:2. (Spectra from <http://www.lipidhome.co.uk/> are reprinted (adapted) with permission from Dr. William W. Christie. Copyright (2020) William W. Christie)<sup>242</sup>



Although GC-MS analysis of DMOX derivatized HFAs is a powerful tool for their structural elucidation, it does have limitations so the confirmation of assignments by other methods is still desirable. For example, a low abundance of HFAs may result in spectra that are too weak to allow unambiguous fragmentation patterns, since the ion intensity is divided between many fragment ion peaks in the EI spectra. Also, more complex or highly substituted HFA structures may also result in ambiguity in the interpretation of DMOX spectra of unknowns. Examples of this include, with conjugated HFAs, or where a side chain strongly directs the fragmentation, such as is in the case of silylated HFAs. An alternative to using DMOX derivatives that yields comparable double bond information is the use of 3-pyridylcarbinol derivatives.<sup>255</sup> The picolinyl esters of HFAs formed by this method results in a fragment ion pair with an  $m/z$  difference of 26 to indicate the position of double bond. As with other techniques leading to charge-remote fragmentation, the intensity of structurally informative ions is variable but the presence of these signals is highly useful for structural identification<sup>242</sup>.

Where information on double bond positions is hard to obtain directly from ion decomposition in EI, other derivatization methods have been used to convert double bonds into structures that can be easily identified. For example, double bonds were converted into diol structures by OsO<sub>4</sub> oxidation and therefore the resulting structures could be analyzed as poly-HFA.<sup>256</sup> Finally, it should be noted that achieving separation of *cis/trans* isomers of unsaturated HFA relies on the selectivity of the GC column.<sup>257</sup> In addition, typically, identification of *cis/trans* isomers of fatty acids must be obtained by comparison to standard compounds or *via* assumptions about the relative elution order of these isomers, as discussed elsewhere.<sup>258, 259</sup>

The carbon atom carrying the hydroxy group in HFAs is a chiral center (except in the case

of  $\omega$ -1 HFAs). Although it is known that certain biological functions of HFAs may be closely related to their chirality,<sup>83, 88, 260</sup> conventional GC analysis cannot separate these enantiomers directly. One approach is to use chiral derivatization methods, such as Mosher's reagents<sup>83, 261</sup> or methoxy (*S*)- phenylethylamide derivatives of HFAs.<sup>262, 129</sup> These result in different GC elution times for derivatized chiral HFA stereoisomers. Chiral GC columns, such as those using peptide derivatives or cyclodextrin as stationary phases<sup>263</sup> have also been developed and there are a few report of their application to HFA.<sup>264</sup>

## **2.5 Current methods for HFA analysis - LC/MS approaches**

Although GC-based methods are the most common approaches, they require the analytes to be volatile as well as thermally stable. This nature of GC provides additional challenge to the analysis of HFAs, especially in the context of the lipid oxidation products of diverse biological or chemical processes, requiring suitable derivatisation strategies to modify non-volatile HFAs. Derivatisation processes may result in unwanted side reactions that are difficult to identify in complex mixtures of HFAs and other oxygenated lipids. In contrast, in liquid chromatography (LC), analytes with diverse solubility and heat stabilities can be analyzed without derivatization, and so provide a good alternative to GC-based methods.

Analogous to GC, LC separation is based on the different affinities of analytes between two phases (the mobile and stationary phases, which are liquid and solid/solid-support material respectively). The LC separation depends on the type of stationary phase chosen, which may be based on separation principles such as absorption, partition, ion exchange and molecular exclusion.

### 2.5.1 Choices of LC mobile phase and stationary phase

LC columns containing non-polar stationary phases, such as C<sub>8</sub> and C<sub>18</sub>, can achieve separation of HFAs according to their chain lengths, degrees of unsaturation and number of hydroxy groups (see **Figure 2.5**).<sup>144</sup>

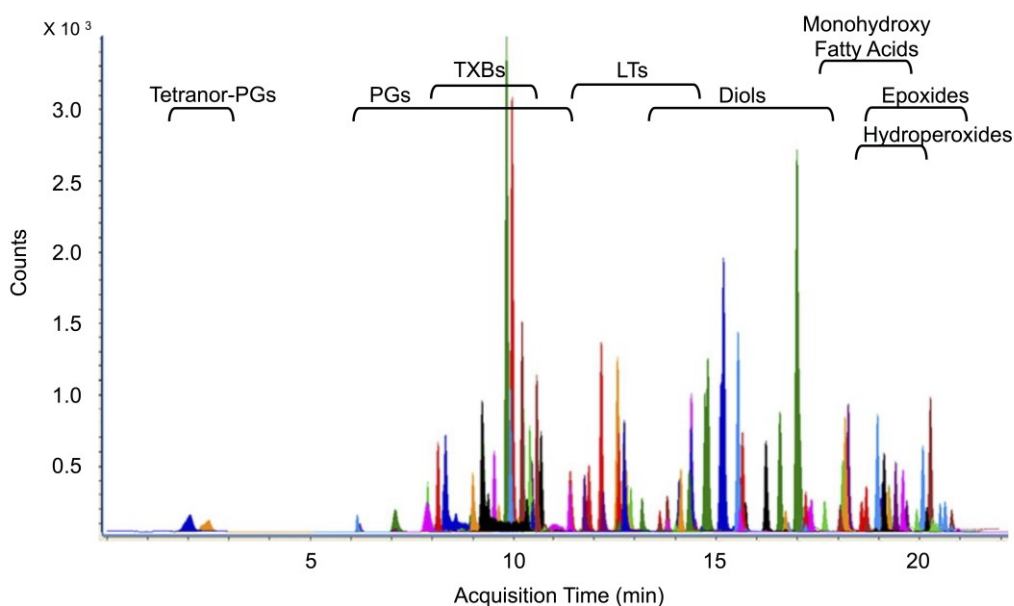


**Figure 2.5.** LC-MS/MS-MRM analysis of oxylipins performed on a triple quadrupole MS (tri-, di- and mono-OH HFAs were eluted out at ~9-20min. Different colors imply different MRM transitions; LT-leukotrienes; TXB-thromboxanes; PG-prostaglandins.) (Figure is reprinted (adapted) from “Strassburg, K.; Huijbrechts, A. M. L.; Kortekaas, K. A.; Lindeman, J. H.; Pedersen, T. L.; Dane, A.; Berger, R.; Brenkman, A.; Hankemeier, T.; van Duynhoven, J.; Kalkhoven, E.; Newman, J. W.; Vreeken, R. J. Quantitative profiling of oxylipins through comprehensive LC-MS/MS analysis: application in cardiac surgery. *Anal. Bioanal. Chem.* 2012, 404, 1413-1426.”<sup>144</sup> under the terms of Creative Commons Attribution 2.0 International License (<https://creativecommons.org/licenses/by/2.0>))

However, overlapping peaks are still likely in complex mixtures containing many different HFAs, including isomers. LC separation performance can be enhanced by strategies that improve peaks shapes and thus resolution, such as:

- 1) Weak organic acids, *e.g.* formic or acetic acid are commonly added<sup>265,266</sup> in small concentration (0.025-1%) to reduce dissociation (maintain protonation) of fatty acids and achieve better peak shapes. However, acidic conditions may compromise the sensitivity of MS, as ionization of –COOH to form anions may be suppressed.<sup>267</sup> Therefore in some cases, methods such as post-column addition of a basic solution<sup>268</sup> has been applied to improve the compromised MS sensitivity (LOQ at femtogram level).<sup>267</sup> Most commonly, multiple reaction monitoring (MRM), the most sensitive and specific type of LC-MS/MS analysis, is used for fatty acids analysis.<sup>269</sup> In this way, LC-MS can achieve satisfactory separation and detection of HFAs and other oxygenated fatty acids, without the need to perform further derivatization.<sup>144, 139</sup>

- 2) Although isocratic HPLC-MRM can be used to analyze HFA isomers,<sup>270</sup> a gradient of mobile phases (from high to low hydrophilicity) is usually applied to reduce the peak widths.<sup>195, 144</sup>

In reversed-phase HPLC, for a given stationary phase, the elution order may be altered by the composition of mobile phase.<sup>271</sup> Successful examples of HPLC separations of HFAs are shown in **Table 2.2** and **2.3**, with a summary of their ion transitions, retention time and LC method. From these studies, the elution order of HFAs separated by reversed-phase HPLC can be summarized with the following features:

- 1) For HFAs with the same carbon chain length, HFAs with more C=C double bonds have higher hydrophilicity, which result in shorter retention time in reversed phase HPLC compared to their analogues. For example, 15*S*-hydroxy-8*Z*,11*Z*,13*E*-eicosatrienoic acid (15-OH C20:3), 15*S*-hydroxy-5*Z*,8*Z*,11*Z*,13*E*-eicosatetraenoic acid (15-OH C20:4) and 15*S*-

hydroxy-5*Z*,8*Z*,11*Z*,13*E*,17*Z*-eicosapentaenoic acid (15-OH C20:5) elute at 19.41 min, 18.58 min and 17.28 min, respectively.<sup>144</sup>

2) With all other structural features being identical, HFAs with fewer -OH groups have longer retention times. For example, 5*S*-hydroxy-6*E*,8*Z*,11*Z*,14*Z*-eicosatetraenoic acid (5-OH C20:4), 5*S*,15*S*-dihydroxy-6*E*,8*Z*,11*Z*,13*E*-eicosatetraenoic acid (5,15-OH C20:4) and 5*S*,6*R*,15*S*-trihydroxy-7*E*,9*E*,11*Z*,13*E*-eicosatetraenoic acid (5,6,15-OH C20:4) have the retention of 11.06 min, 9.2 min and 6.78min, respectively.<sup>272</sup>

3) With the same number and similar position of -OH or unsaturated groups, the longer the chain length, the longer the retention time the analytes have. For example, 12*S*-hydroxy-5*Z*,8*E*,10*E*-heptadecatrienoic acid (12-OH C17:3) elutes at 15.73 min, which is earlier than 12*S*-hydroxy-5*Z*,8*Z*,10*E*,14*Z*-eicosatetraenoic acid (12-OH C20:4) with retention time of 19.24 min.<sup>144</sup>

4) In some cases, the elution order of positional isomers (identical chain length, number of -OH groups and C=C double bonds) can vary systematically. For example, among 6 different mono-OH HETE (mono-hydroxy-eicosatetraenoic acid, mono-OH C20:4) isomers (5-HETE, 9-HETE, 8-HETE, 12-HETE, 11-HETE, 15-HETE and 20-HETE), the one with -OH at the position closer to -COOH elutes later, although there is little separation between 8 and 9-HETE, as well as between 11 and 12-HETE. This pattern can also be found among the 3 mono-OH C20:5 isomers, and among 2 mono-OH C18:2 isomers. Little separation is observed between isomers 9-OH C18:2 and 13-OH C18:2, though the retention of the former is also slightly longer the later.

These elution patterns indicate that slight difference in molecular structures can result in significantly different retention of HFA in LC-MS analyses, making this a suitable technique for HFA identification in the context of biological samples such as brain, liver and plasma for animals,<sup>270</sup> or seed oil for plants.<sup>139</sup>

**Table 2.2.** Ion transitions and retention times for HFAs in LC-MS/MS analyses

Full name	Short form	Q1	Q3	Retention Time		Retention time 3 <sup>272</sup> (min)
		( <i>m/z</i> )	( <i>m/z</i> )	1 <sup>144</sup> (min)	2 <sup>272</sup> (min)	
9 <i>S</i> ,12 <i>S</i> ,13 <i>S</i> -trihydroxy-10 <i>E</i> -octadecenoic acid	9,12,13-OH C18:1	329.2	211.2	9.83	/	/
9,10,13-trihydroxy-11-octadecenoic acid	9,10,13-OH C18:1	329.2	171.1	9.96	/	/
5 <i>S</i> ,6 <i>R</i> ,15 <i>S</i> -trihydroxy-7 <i>E</i> ,9 <i>E</i> ,11 <i>Z</i> ,13 <i>E</i> -eicosatetraenoic acid	5,6,15-OH C20:4	351.2	115.0	/	6.78	8.58
(+/-)-12,13-dihydroxy-9 <i>Z</i> ,15 <i>Z</i> -octadecadienoic acid	12,13-OH C18:2	311.2	293.0	13.62	/	/
12,13-dihydroxy-9 <i>Z</i> -octadecenoic acid-(d4)	12,13-OH C18:1-(d4)	317.3	185.2	14.73	/	/
12,13-dihydroxy-9 <i>Z</i> -octadecenoic acid	12,13-OH C18:1	313.2	183.2	14.80	/	/
9,10-dihydroxy-12 <i>Z</i> -octadecenoic acid-(d4)	9,10-OH C18:1-(d4)	317.3	203.2	15.12	/	/
9,10-dihydroxy-12 <i>Z</i> -octadecenoic acid	9,10-OH C18:1	313.2	201.1	15.18	/	/
8 <i>S</i> ,15 <i>S</i> -dihydroxy-5 <i>Z</i> ,9 <i>E</i> ,11 <i>Z</i> ,13 <i>E</i> -eicosatetraenoic acid	8,15-OH C20:4	335.2	235.2	13.62	/	/
(+/-)-17,18-dihydroxy-5 <i>Z</i> ,8 <i>Z</i> ,11 <i>Z</i> ,14 <i>Z</i> -eicosatetraenoic acid	17,18-OH C20:4	335.2	247.2	14.01	/	/
5 <i>S</i> ,15 <i>S</i> -dihydroxy-6 <i>E</i> ,8 <i>Z</i> ,11 <i>Z</i> ,13 <i>E</i> -eicosatetraenoic acid	5,15-OH C20:4	335.2	115.2	14.06	9.20	11.03
(+/-)-14,15-dihydroxy-5 <i>Z</i> ,8 <i>Z</i> ,11 <i>Z</i> ,17 <i>Z</i> -eicosatetraenoic acid	14,15-OH C20:4	335.2	207.1	14.49	/	/
5 <i>S</i> ,6 <i>S</i> -dihydroxy-7 <i>E</i> ,9 <i>E</i> ,11 <i>Z</i> ,14 <i>Z</i> -eicosatetraenoic acid	5,6-OH C20:4	335.2	115.1	17.20	10.20	13.80

(continued)

**Table 2.2.** (continued)

Full name	Short form	Q1 ( <i>m/z</i> )	Q3 ( <i>m/z</i> )	Retention Time 1 <sup>144</sup> (min)	Retention Time 2 <sup>272</sup> (min)	Retention time 3 <sup>272</sup> (min)
8,9-dihydroxy-5 <i>Z</i> ,11 <i>Z</i> ,14 <i>Z</i> -eicosatrienoic acid	8,9-OH C20:3	337.2	127.0	16.71	9.99	13.40
14,15-dihydroxy-5 <i>Z</i> ,8 <i>Z</i> ,11 <i>Z</i> -eicosatrienoic acid-(d11)	14,15-OH C20:3-(d11)	348.3	207.1	15.54	/	/
14,15-dihydroxy-5 <i>Z</i> ,8 <i>Z</i> ,11 <i>Z</i> -eicosatrienoic acid	14,15-OH C20:3	337.2	207.2	15.65	9.67	12.70
11,12-dihydroxy-5 <i>Z</i> ,8 <i>Z</i> ,14 <i>Z</i> -eicosatrienoic acid	11,12-OH C20:3	337.2	167.2	16.23	9.84	13.01
5,6-dihydroxy-8 <i>Z</i> ,11 <i>Z</i> ,14 <i>Z</i> -eicosatrienoic acid	5,6-OH C20:3	337.2	145.1	17.34	/	/
10 <i>S</i> ,17 <i>S</i> -dihydroxy-4 <i>Z</i> ,7 <i>Z</i> ,11 <i>E</i> ,13 <i>Z</i> ,15 <i>E</i> ,19 <i>Z</i> -docosahexaenoic acid	10,17-OH C22:6	359.2	153.2	14.13	/	/
(+/-)-19,20-dihydroxy-4 <i>Z</i> ,7 <i>Z</i> ,10 <i>Z</i> ,13 <i>Z</i> ,16 <i>Z</i> -docosapentaenoic acid	19,20-OH C22:5	361.2	273.3	15.60	/	/
12 <i>S</i> -hydroxy-5 <i>Z</i> ,8 <i>E</i> ,10 <i>E</i> -heptadecatrienoic acid	12-OH C17:3	279.2	179.2	15.73	/	/
9 <i>S</i> -hydroxy-10 <i>E</i> ,12 <i>Z</i> ,15 <i>Z</i> -octadecatrienoic acid	9-OH C18:3	293.2	171.1	16.57	/	/
13 <i>S</i> -hydroxy-9 <i>Z</i> ,11 <i>E</i> -octadecadienoic acid	13-OH C18:2	295.2	195.2	18.12	/	/
9 <i>S</i> -hydroxy-10 <i>E</i> ,12 <i>Z</i> -octadecadienoic acid-(d4)	9-OH C18:2-(d4)	299.2	172.1	18.18	/	/
9-hydroxy-10 <i>E</i> ,12 <i>Z</i> -octadecadienoic acid	9-OH C18:2	295.2	171.1	18.25	/	/
15 <i>S</i> -hydroxy-5 <i>Z</i> ,8 <i>Z</i> ,11 <i>Z</i> ,13 <i>E</i> ,17 <i>Z</i> -eicosapentaenoic acid	15-OH C20:5	317.2	219.2	17.28	10.25	14.04

(continued)

**Table 2.2.** (continued)

Full name	Short form	Q1	Q3	Retention Time	Retention Time	Retention time
		( <i>m/z</i> )	( <i>m/z</i> )	1 <sup>144</sup> (min)	2 <sup>272</sup> (min)	3 <sup>272</sup> (min)
12 <i>S</i> -hydroxy-5 <i>Z</i> ,8 <i>Z</i> ,10 <i>E</i> ,14 <i>Z</i> ,17 <i>Z</i> -eicosapentaenoic acid	12-OH C20:5	317.2	179.1	17.67	/	/
5 <i>S</i> -hydroxy-6 <i>E</i> ,8 <i>Z</i> ,11 <i>Z</i> ,14 <i>Z</i> ,17 <i>Z</i> -eicosapentaenoic acid	5-OH C20:5	317.2	115.1	18.05	/	/
20-hydroxy-5 <i>Z</i> ,8 <i>Z</i> ,11 <i>Z</i> ,14 <i>Z</i> -eicosatetraenoic acid-(d6)	20-OH C20:4-(d6)	325.3	279.2	17.15	/	/
20-hydroxy-5 <i>Z</i> ,8 <i>Z</i> ,11 <i>Z</i> ,14 <i>Z</i> -eicosatetraenoic acid	20-OH C20:4	319.2	289.2	17.20	/	/
15 <i>S</i> -hydroxy-5 <i>Z</i> ,8 <i>Z</i> ,11 <i>Z</i> ,13 <i>E</i> -eicosatetraenoic acid	15-OH C20:4	319.2	219.2	18.58	10.45	14.33
11-hydroxy-5 <i>Z</i> ,8 <i>Z</i> ,11 <i>E</i> ,14 <i>Z</i> -eicosatetraenoic acid	11-OH C20:4	319.2	167.1	18.97	10.62	14.83
12 <i>S</i> -hydroxy-5 <i>Z</i> ,8 <i>Z</i> ,10 <i>E</i> ,14 <i>Z</i> -eicosatetraenoic acid-(d8)	12-OH C20:4-(d8)	327.3	184.2	19.13	10.70	14.80
12 <i>S</i> -hydroxy-5 <i>Z</i> ,8 <i>Z</i> ,10 <i>E</i> ,14 <i>Z</i> -eicosatetraenoic acid	12-OH C20:4	319.2	179.2	19.24	10.70	14.77
8 <i>S</i> -hydroxy-5 <i>Z</i> ,9 <i>E</i> ,11 <i>Z</i> ,14 <i>Z</i> -eicosatetraenoic acid	8-OH C20:4	319.2	155.1	19.25	10.76	14.86
9-hydroxy-5 <i>Z</i> ,7 <i>E</i> ,11 <i>Z</i> ,14 <i>Z</i> -eicosatetraenoic acid	9-OH C20:4	319.2	167.1	19.47	/	/
5 <i>S</i> -hydroxy-6 <i>E</i> ,8 <i>Z</i> ,11 <i>Z</i> ,14 <i>Z</i> -eicosatetraenoic acid-(d8)	5-OH C20:4-(d8)	327.3	116.1	19.59	/	/
5 <i>S</i> -hydroxy-6 <i>E</i> ,8 <i>Z</i> ,11 <i>Z</i> ,14 <i>Z</i> -eicosatetraenoic acid	5-OH C20:4	319.2	115.1	19.69	11.06	15.36
15 <i>S</i> -hydroxy-8 <i>Z</i> ,11 <i>Z</i> ,13 <i>E</i> -eicosatrienoic acid	15-OH C20:3	321.2	221.2	19.41	/	/
(+/-)-17-hydroxy-4 <i>Z</i> ,7 <i>Z</i> ,10 <i>Z</i> ,13 <i>Z</i> ,15 <i>E</i> ,19 <i>Z</i> -docosaheptaenoic acid	17-OH C22:6	343.2	281.3	18.71	/	/



**Table 2.3.** Examples of LC methods used in the analysis of HFAs

	Method 1 <sup>144</sup>		Method 2 <sup>272</sup>		Method 3 <sup>272</sup>	
LC column	Ascentis Express C18 (2.1mm × 150 mm, 2.7 µm) at 40 °C		Grace Vydac C18 (2.1mm × 250mm, 5 µm) at 35°C		Grace Vydac C18 (2.1mm × 250mm, 5 µm) at 35°C	
LC flow rate	0.35 mL/min		0.3 mL/min		0.3 mL/min	
LC mobile phase A	Water with 0.1% acetic acid		Water/acetonitrile mixture (63:37) with 0.02% formic acid		Water/acetonitrile mixture (72:28) with 0.1% acetic acid	
LC mobile phase B	Acetonitrile/isopropano l mixture (9:1)		Acetonitrile/isopropanol mixture (1:1)		Acetonitrile/isopropan ol mixture (4:6)	
LC gradient	Tim (min)	% B	Tim (min)	% B	Tim (min)	% B
	0	15	0.0	0	0.0	0
	3.5	33	6.0	20	22.0	85
	5.5	38	6.5	55	23.0	85
	7	42	11.0	72	23.5	0
	9	48	16.0	72	25.0	0
	15	65				
	17	75				
	18.5	85				
	19.5	95				
	21	15				
	26	15				
Sample loading	5 µL, 2 nM up to 558 nM in 8 levels		5 µL, 0.2 ng/ul in water/ethanol mixture (1:1)		10 µL, 1 ng/ul in ethanol	

Ultra performance LC (UPLC) systems, which employ columns with smaller particle sizes and operate at higher pressures than conventional LC, have also been used for HFA analyses.<sup>139</sup> UPLC separations result in similar elution patterns, but much faster analysis with equivalent or better peak resolution.

Reversed-phase LC only has a finite capacity to separate the HFA positional isomers with the same molecular formula (identical chain lengths, degrees of unsaturation and number of –OH groups).<sup>195</sup> In LC-MS/MS where MRM mode is available, this problem can be partly overcome through monitoring positional isomers by means of their characteristic ion transitions (Q1 -> Q3). However, while using other detectors, a more complete separation of HFA isomers by LC is still required.

Better separations of HFA positional isomers can be achieved by normal-phase HPLC. For example, using a polar YMC PVA-Sil stationary phase, HFA isomers of 10-hydroxy-12-octadecenoic acid and 13-hydroxy-9-octadecenoic acid are well separated (**Figure 2.6**).<sup>15, 191</sup>

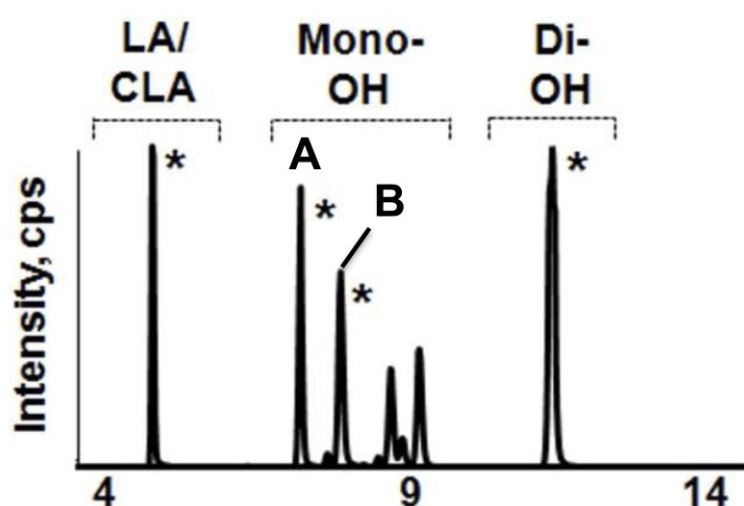


**Figure 2.6.** Normal-phase LC-MS extracted ions chromatogram of crude lipid extract from *Lactobacillus plantarum*. Reprinted (adapted) with permission from “Black, B. A.; Sun, C. X.; Zhao, Y. Y.; Gänzle, M. G.; Curtis, J. M. Antifungal lipids produced by Lactobacilli and their structural identification by normal phase LC/atmospheric pressure photoionization-MS/MS. *J. Agr. Food Chem.* **2013**, *61*, 5338-5346.”<sup>191</sup> Copyright (2013) American Chemical Society.

(Targeted ion range of non-, mono- and di-OH C18; Peak A) and B) represented 13-hydroxy-9-octadecenoic acid (7.8min) and 10-hydroxy-12-octadecenoic acid (8.4min), respectively.<sup>191</sup> The separation used a YMC PVA-Sil column and a 0% to 30% gradient of isopropanol in hexane with the addition of 0.2% acetic acid.)

Silver ion chromatography is another type of LC separation that can provide additional information on the *cis/trans* isomerization of carbon-carbon double bonds due to the stronger interactions between  $\text{Ag}^+$  ions with *cis* double bonds compared to *trans* isomers. Most commonly, lipids are converted to low-polarity methyl ester derivatives, which also allow for separation of isomers of a single fatty acyl chain only, as opposed to the more complicated situation in a triacylglyceride.<sup>273</sup> Generally, *cis*-forms of unsaturated fatty acids have stronger retention compared to *trans*-isomers; retention times also decrease with increasing chain length, and increase with increasing numbers of double bonds and the distance between double bonds (the conjugated double bond has the least retention in poly-unsaturated system).<sup>273</sup> For example, the *cis* and *trans* geometric isomers of 10-hydroxy-12-octadecenoic acid FAME can be well separated as shown in **Figure 2.7**.

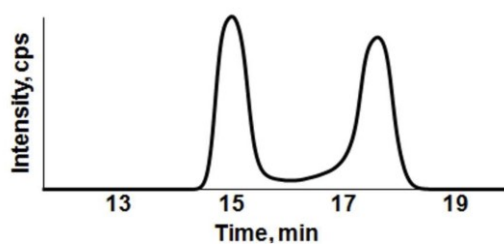


**Figure 2.7.** Silver ion chromatography-MS extracted ion chromatogram of the characteristics ions ( $[\text{M}+\text{H}-\text{H}_2\text{O}]^+$ ,  $m/z$  295.2) of the FAME derivatives of 10-hydroxy-12-octadecenoic fatty acids extracted from *Lactobacillus hammesii* fermentation products.<sup>191</sup> The *trans* isomer (at 15.0 min) elutes ahead of the *cis* isomer (at 17.6 min). Reprinted (adapted) with permission

from “Black, B. A.; Sun, C. X.; Zhao, Y. Y.; Gänzle, M. G.; Curtis, J. M. Antifungal lipids produced by Lactobacilli and their structural identification by normal phase LC/atmospheric pressure photoionization-MS/MS. *J. Agr. Food Chem.* **2013**, *61*, 5338-5346.”<sup>191</sup> Copyright (2013) American Chemical Society.

Similar to GC analysis, separation of compounds based on their chirality can be achieved by (1) chiral derivatization and the use of a non-chiral column (*e.g.* (+)- $\alpha$ -methoxy- $\alpha$ -trifluoromethylphenylacetic acid esters<sup>274</sup>), and 2) the use of a chiral column without derivatization.<sup>275</sup> The elution order of (*R*)- and (*S*)- isomer varies with the specific analyte.<sup>276</sup> For example, when a Chiralcel OB-H (250  $\times$  4.6 mm, 5 $\mu$ m, Daicel) (normal phase) column was used, the (*R*)-isomer eluted earlier in the case of 13-OH:2 methyl ester, while the opposite was shown for 9-OH C18:2 methyl ester.<sup>276</sup> In another example, when a Chiralcel OD-RH (150 mm  $\times$  4.6 mm, 5 $\mu$ m, Daicel) was used at 0 °C, all of the (*R*)-HFAs (including 5-OH C20:4, 12-OH C20:4, 15-OH C20:4 and 13-OH C18:2) eluted earlier compared to their (*S*)-isomers.<sup>275</sup> Hence, positive identifications mostly rely on comparisons to the retention times of authentic standards.<sup>88, 218</sup> The combination of derivatization method (*e.g.* 3, 5-dinitrophenyl urethane derivatives) and a chiral HPLC column were also used to separate the chiral 2- and 3-HFA with various chain lengths.<sup>127, 277</sup>

### 2.5.2 Interpretation of mass spectra of HFAs

The EI-MS method is more likely to results in more characteristic HFA fragmentation patterns generated *in source*, as described above. In contrast, in the commercial ionization sources that are coupled to LC (*e.g.* electrospray ionization (ESI), atmospheric pressure chemical ionization (APCI) and atmospheric pressure photo ionization (APPI)), the ionization processes result in much lower energy uptakes by analyte molecules, and hence

less fragmentation. ESI can be applied in a wide range of analytes with diverse polarity and molecular weight, and thus more studies on HFAs have been done using this technique.<sup>278, 279</sup> However, although APCI and APPI are restricted to a more limited range of analytes (relatively low molecular weights and lower polarities), these methods still provide excellent sensitivity and selectivity for certain applications, including HFA.<sup>280, 191, 281, 282, 283</sup> As with other fatty acids, LC-MS analysis of HFAs is usually performed in negative ion mode since carboxylic acids readily deprotonate to form gaseous anions  $[M-H]^-$ .

In order to generate structure-related fragment ions, collision-induced dissociation (CID) with a neutral gas molecule (nitrogen, for example) is applied to selected parent (precursor) ions in a tandem mass spectrometer.<sup>284</sup> The general ion decomposition mechanisms for HFA are well summarized elsewhere.<sup>97, 285</sup> The major product ions of HFAs observed in MS/MS spectra in addition to the molecular ion  $[M-H]^-$  usually include:

- (1) Fragment ions formed due to the loss of water  $[M-H-H_2O]^-$ .
- (2) For unsaturated HFAs, fragment ions formed due the loss of  $CO_2$ , including  $[M-H-H_2O-CO_2]^-$ , and the ions formed due to  $\alpha$ -cleavage at  $-C-C-$  bonds adjacent to a hydroxyl group followed by the loss of  $CO_2$ . For saturated HFAs, the ions  $[M-H-H_2-CO_2]^-$  are observed instead.
- (3) Fragment ions produced due to  $\alpha$ -cleavage at  $-C-C-$  bonds adjacent to a hydroxyl group. These ions can be formed as a result of either the charge directed or charge remote mechanisms.<sup>97, 285, 286</sup>
- (4) As the number of double bonds in HFAs increases, so too does the resulting product ion complexity.<sup>97</sup> This can be illustrated by comparing the MS/MS spectra of 15-OH C20:3, 15-OH C20:4 and 15-OH C20:5, as shown in **Figure 2.8**. It is clear that the product ion complexity greatly increases with the number of double bonds, due to double bond

migrations prior to fragmentation.<sup>97, 285</sup> In another example, homolytic bond cleavage of the =C-O- of 3-hydroxy-1,5-hexadiene structure<sup>285</sup> in a polyunsaturated HFA can lead to the formation of a radical anion known as an oxy-Cope reaction product<sup>286</sup> ( $m/z$  208 for 12-HETE and 8-HETE).<sup>97, 285</sup> However, in order to observe significant signals of this radical anion product, a delocalized structure (such as 5-hydroxy-1,3,7-octatriene) is required. The complexity of the fragmentation spectra is also increased by the number of –OH groups in HFAs. Multiple and competing fragmentation mechanisms have been reported for the cases of poly-OH unsaturated HFAs.<sup>285</sup>

Although structure-related fragmentation spectra generated by ESI-MS/MS are not always straightforward to interpret, their product ions are very characteristic to the analytes. Hence, MRM experiments that monitor both the parent/precursor ion (Q1) and its characteristic fragmentation product ions (Q3) as an ion transition (Q1 → Q3), along with its retention time, are usually very specific to an individual HFA compound. Therefore, even without a complete resolution of two peaks in chromatogram, robust qualitative and quantitative methods can be achieved. For the purpose of identification, online resources of HFA mass spectral databases, like LIPID MAPS (<http://www.lipidmaps.org>)<sup>501</sup> can be very helpful. Characteristic ions found in the MS/MS spectra of HFAs studied are summarized in **Table 2.4**.

Through measurement of exact molecular mass of an HFA (to identify its elemental composition) along with its fragmentation pattern, it is possible to predict the number of double bonds as well as the approximate location of double bonds (*e.g.* on which side of the –OH group). With this information, combined with the LC retention time compared to known standards, the identification of an HFA can be made. However, this can still be challenging for the identification of an unknown HFA since MS/MS alone may not, for example, provide

enough information on the exact locations of double bonds. In this case, the help of other types of analyses, or additional types of HFA derivatization need to be attempted.

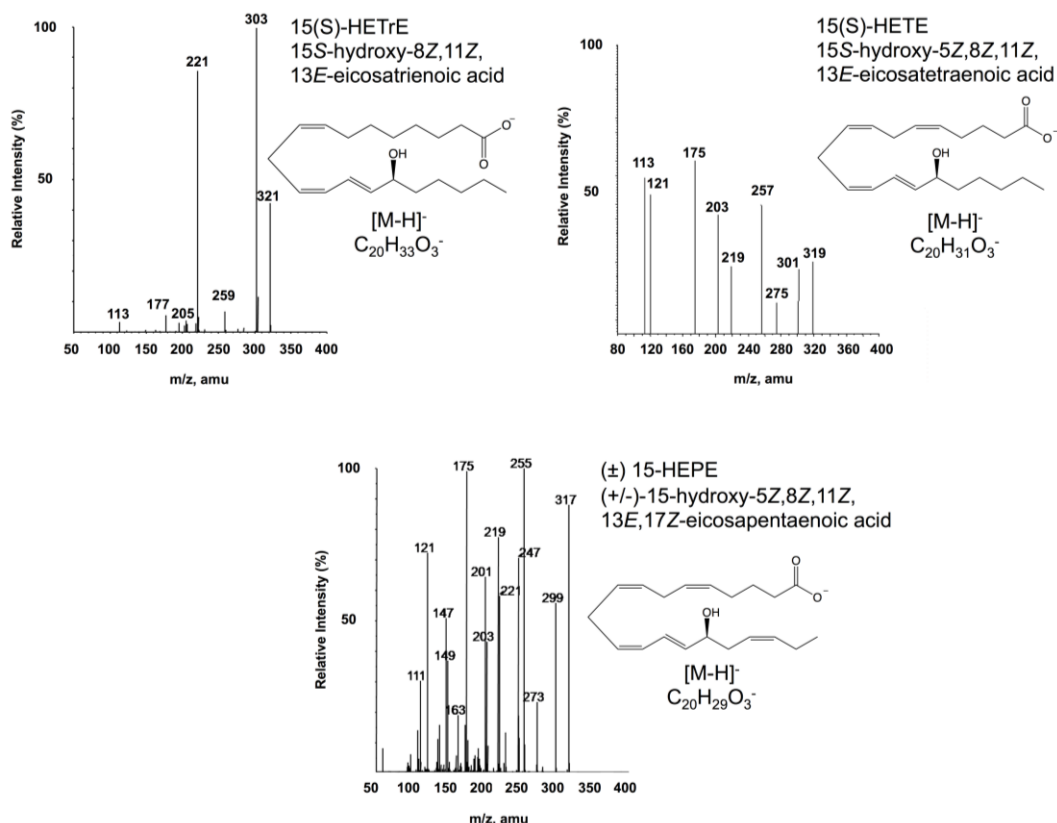


**Figure 2.8.** Negative ion MS/MS spectra of 15-OH C20 analogues

(Figures are reprinted (adapted) from “Sud, M.; Fahy, E.; Cotter, D.; Brown, A.; Dennis, A. E.; Glass, K. C.; Merrill, H. A.; Murphy, C. J. R.; Raetz, R. H. C.; Russell, W. D.; Subramaniam, S. LMSD: LIPID MAPS structure database, *Nucleic Acids Res.*, 2006, 35, D527–D532.”<sup>272</sup> and “The LIPID MAPS Lipidomics Gateway. <http://www.lipidmaps.org/> (accessed February 4th, 2020).”<sup>501</sup> with permission from LIPID MAPS)

**Table 2.4.** Characteristic product ions in the negative ion MS/MS spectra of HFAs

HFA	Characteristic ions						Ref.
	[M-H] <sup>-</sup>	[M-H <sub>2</sub> O] <sup>-</sup>	[M-H-CO <sub>2</sub> -H <sub>2</sub> ] <sup>-</sup>	Others			
15-OH C15:0	257	239	211	/			284
2-OH C16:0	271	253	225	/			284
3-OH C16:0	271	/	225	59 [C <sub>2</sub> H <sub>3</sub> O <sub>2</sub> ] <sup>-</sup>			284
	[M-H] <sup>-</sup>	[M-H-H <sub>2</sub> O] <sup>-</sup>	[M-H-H <sub>2</sub> O-CO <sub>2</sub> ] <sup>-</sup>	α-cleavage of - OH	[M-H-H <sub>2</sub> O- CO <sub>2</sub> -28] <sup>-</sup>	Others	
10-OH C18:1	297	279	/	185	/	/	<sup>191</sup> (using APPI)
13-OH C18:1	297	279	/	197	/	179, 113, 99	<sup>191</sup> (using APPI)
12-OH C18:1	297	279	/	183	/	/	286
9-OH C18:2	295	277	/	171	/	/	286
13-OH C18:2	295	277	/	195	/	/	286
12-OH C17:3	279	261	217	179	189	/	286

(continued)



**Table 2.4.** (continued)

HFA	Characteristic ions						Ref.
	[M-H] <sup>-</sup>	[M-H-H <sub>2</sub> O] <sup>-</sup>	[M-H-H <sub>2</sub> O-CO <sub>2</sub> ] <sup>-</sup>	α-cleavage of - OH	[M-H-H <sub>2</sub> O- CO <sub>2</sub> -28] <sup>-</sup>	Others	
2-OH C18:3	293	275	/	247	/	191, 153, 139, 125, (110, 97, 84, 71)	109, 287
13-OH C18:3	293	275	231	193	/	/	286
13-OH C18:3	293	275	/	223, 195	247	224*	286
15-OH C20:3	321	303	259	221	/	205, 117, 113	272
5-OH C20:4	319	301	257	203, 115	/	59	286
8-OH C20:4	319	301	257	127, 155, 163	/	192*	286
9-OH C20:4	319	301	257	167, 139, 151	229	168*, 123 [167-CO <sub>2</sub> ] <sup>-</sup> , 179, 69, 59	286
11-OH C20:4	319	301	/	167, 195	/	152*, 149 [167-H <sub>2</sub> O] <sup>-</sup> , 59	286
12-OH C20:4	319	301	257	207, 179	/	208*	286
15-OH C20:4	319	301	257	219	/	275, 203, 175 [219-CO <sub>2</sub> ] <sup>-</sup> , 121, 113, 59	286
15-OH C20:5	317	299	255	219	/	273, 247, 221, 203, 201, 175, 163, 149, 147, 121, 111	272

(continued)

\*: ions formed by homolytic fragmentation via oxy-Cope rearrangement

**Table 2.4.** (continued)

HFA	Characteristic ions							Ref.
	[M-H] <sup>-</sup>	[M-H-H <sub>2</sub> O] <sup>-</sup>	[M-H-2(H <sub>2</sub> O)] <sup>-</sup>	[M-H-H <sub>2</sub> O-CO <sub>2</sub> ] <sup>-</sup>	[M-H-2(H <sub>2</sub> O)-CO <sub>2</sub> ] <sup>-</sup>	α-cleavage of -OH	Others	
10,13-OH C18:0	315	297	279	/	/	243, 185, 127, 99	168, 141, 113	<sup>191</sup> (using APPI)
5,6-OH C20:3	337	319	301	275	257	191, 145, 115	163, 101, 71	285, 272
8,9-OH C20:3	337	319	301	275	257	(209), 185, 155, 151, 127	141, 123, 111, 73	285, 272
11,12-OH C20:3	337	319	(301)	(275)	(257)	(225), 197, 169, 167	207, 149, 73	285, 272
14,15-OH C20:3	337	319	301	(275)	257	237, 207, 129, 99	163, 113	285, 272
5,6-OH C20:4	335	(317)	/	273 (271)	/	219, (189), (145), 115	163, 59	285, 272
5,12-OH C20:4	335	317	/	273	/	195	203, 181, 151, 129, 123, 109, 71, 59	285
5,15-OH C20:4	335	317	/	273	/	(235), 201, 115	255, 173, 59	285, 272
8,15-OH C20:4	335	317	/	273	/	235, 208, 179, 155, 127	221, 190, 163, 113	285
5,6,15-OH C20:4	351	333	/	289	271	235, 115	217, 135, 59	285
5,14,15-OH C20:4	351	333	315	/	271	251, 221, 115	233, 201, 191, 181, 165, 155, 139, 129, 107, 83, 69, 59	285

### 2.5.3 Online-derivatization for LC-MS analysis of HFA

Since it is often difficult to fractionate and collect individual HFA compounds due to the low amounts available and the complexity of HFA mixtures, another strategy is required. Thus, post-separation (column) derivatization is highly desirable instead of pre-separation to acquire a targeted signal.

Online ozonolysis has been used to identify the double bond position of HFAs. The mechanism of ozonolysis of unsaturated fatty acids is shown in **Figure 2.9** (left). Briefly,  $O_3$  reacts with the double bond to form primary ozonide (1,2,3-trioxolane). This product will then break down into aldehyde and Criegee intermediate, which will reversibly convert to secondary ozonide.<sup>288, 289</sup> It has been used in the double bond identification in HFA (10-OH-12-octadecenoic acid), as shown in **Figure 2.9** (right).<sup>191</sup> The HFA undergoes dehydration to form an additional double bond, but this side reaction is likely to happen after ozonolysis due to the observed absence of ozonized products at the dehydrated positions. However, the presence of aldehyde ions formed due to the cleavage of the HFA double bond can provide a clear indication about the position and the number of the double bonds.<sup>289</sup>

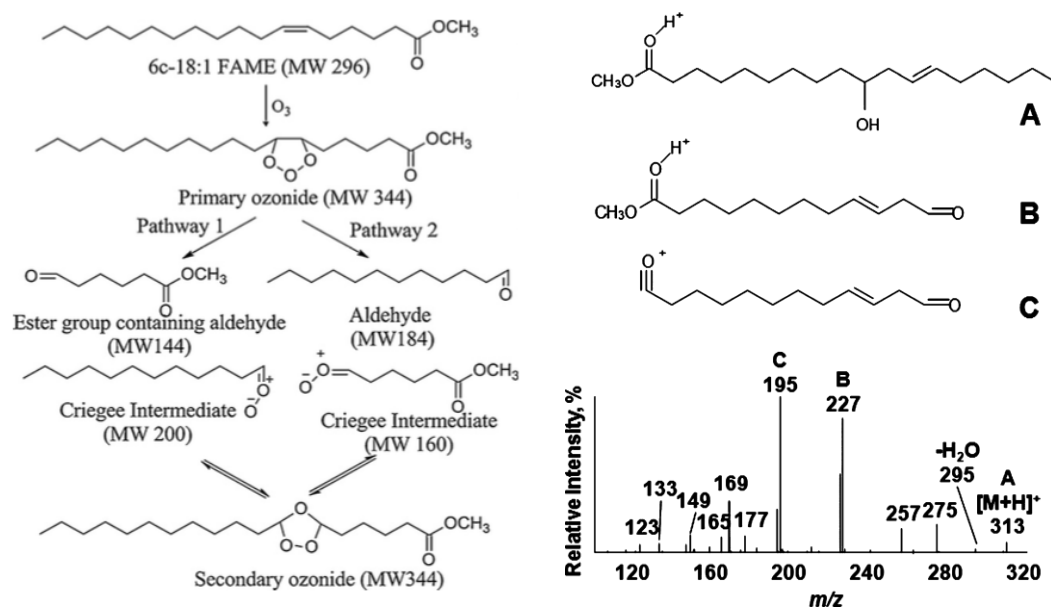


**Figure 2.9.** Ozonolysis mechanism for an unsaturated FAME (left) and ozonolysis-APPI-MS spectrum and proposed fragmentation ion structures of FAME of 10-hydroxy-octadecenoic acid (right): (A) molecule ions  $[M + H]^+$   $m/z$  313; (B) fragment ion  $m/z$  227; and (C) fragment ion  $m/z$  195.

(The left figure was reprinted from “Sun, C. X.; Zhao, Y. Y.; Curtis, J. M. The direct determination of double bond positions in lipid mixtures by liquid chromatography/in-line ozonolysis/mass spectrometry. *Anal. Chim. Acta*, 2013, 762, 68-75.”<sup>289</sup>, Copyright (2012), with permission from Elsevier.)

(The right figure was reprinted (adapted) with permission from “Black, B. A.; Sun, C. X.; Zhao, Y. Y.; Gänzle, M. G.; Curtis, J. M. Antifungal lipids produced by Lactobacilli and their structural identification by normal phase LC/atmospheric pressure photoionization-MS/MS. *J. Agr. Food Chem.* **2013**, 61, 5338-5346.”<sup>191</sup> Copyright (2013) American Chemical Society.)

Combining silver ion chromatography with ozonolysis has been shown to provide a

convenient method to both separate *cis/trans* isomers and at the same time identify the double bond positions.<sup>289,290</sup> Online ozonolysis has also been used with bound lipids (e.g. phospholipids),<sup>291</sup> which further expand the scope of this approach. Another novel post-column but pre-ionization derivatization approach that has been reported involves the photochemical Paterno-Büchi reaction with acetone to assist the CID process in the production of fragmentation to identify the double bond positions.<sup>292</sup> In this method, acetone reacts with double bonds and form an oxetane adduct. In the following CID process, isopropenyl carboxylate anions are formed from the fragmentation of oxetane, and it can be observed in the MS/MS spectrum, locating the double bond positions. However, the use of this technique specifically for HFAs hasn't been reported, and more studies are required.

## **2.6 Summary for the analysis of hydroxy fatty acids, outlook on lipidomics and beyond**

The methods described above can and have been used to advance knowledge of the structures, distribution and the biological significance of HFAs. Other technologies such as NMR and FTIR are also useful to determinate the structure of isolated HFA fractions, but are outside the scope of this chapter. However, no single method provides a comprehensive picture of the detailed structures and distributions of HFAs in an efficient manner. Therefore, it can be seen that the continued development of analytical methods remains important, especially in the context of lipidomics, which aims to provide a global investigation of all lipid populations, requiring both reliable identification and quantification. Lipidomic methods, including both extraction and analyses, that are sufficiently sophisticated to provide full structural identification and quantitation of HFA in a single experiment, do not yet exist although there are excellent combinations of methods used in lipidomics.<sup>293</sup> For HFAs, lipidomics can find widespread application in understanding, and manipulating biological or

chemical processes ranging from food spoilage to disease development.

Previous lipidomics methods have demonstrated good accuracy, precision and reproducibility in a short amount of time (<30 min).<sup>139, 144, 294</sup> In order to further increase the time-efficiency of analysis, MS-based shotgun lipidomics analysis has also been used in oxygenated lipids.<sup>295</sup> Online-sample purification method coupled with LC-MS was developed for HFA-contained lipid, which reduced the labor-consuming sample preparation and further increased the sensitivity of detection.<sup>296</sup> Also, simple techniques for online derivatization of compounds have been developed to achieve additional useful structural information.<sup>297</sup> These targeted analyses greatly benefit from the availability of authentic standards. Overall, such methods have proved very useful, but many applications covering the full range of HFA-containing lipids are yet to be fully explored.

Ideally, analytical methods will progress into providing higher information content within a shorter analysis time, to allow for more sophisticated, non-targeted analyses. However, in reality, this is a difficult task. For example, for HFA isomers that only differ in their double bond positions, their *cis/trans* isomerization, or by their chirality may co-elute in common LC experiments, at the same time as having identical MS/MS spectra. Without the ability to identify such closely similar isomers, a more delicate understanding of the structure-function relationships of HFAs cannot be achieved.

In conclusion, progress in the analysis of HFA-containing lipids has empowered the systematic investigation of the roles of these lipids. In the context of lipidomics analyses, the development of efficient and reliable global analytical methods providing confirmative qualitative and quantitative information still remains a highly desirable goal.

## Chapter 3. Characterization of linoleate 10-hydratase of *Lactobacillus plantarum* and novel antifungal metabolites

### 3.1 Introduction

Antifungal metabolites of lactic acid bacteria have potential for applications as antifungal preservatives in cereal products, and in silage.<sup>24, 298</sup> Several hydroxy fatty acids have antifungal activity<sup>299, 300</sup> and antifungal 3-hydroxy fatty acids of C<sub>10</sub> to C<sub>14</sub> chain lengths are formed by *Lactobacillus plantarum* MiLAB 14.<sup>129</sup> *Lactobacillus hammesii* accumulates 10-HOE, an antifungal compound that increased the mold-free shelf life of bread.<sup>15, 191</sup> The biosynthesis of antifungal hydroxy fatty acids and the application of hydroxy fatty acids in food are dependent on knowledge of enzymes involved in microbial fatty acid-hydroxylation.<sup>39</sup>

Linoleate hydratase (LAH) activity was first characterized in *Streptococcus pyogenes*; the hydratase was previously described as myosin cross-reactive antigen.<sup>301</sup> The FAD containing LAH in *S. pyogenes* hydrates the *cis*-9 and *cis*-12 double bonds of C<sub>16</sub> and C<sub>18</sub> fatty acids to produce 10-hydroxy and 10,13-dihydroxy fatty acids.<sup>17</sup> Remarkably, the LAHs of bifidobacteria, lactobacilli and *Nocardia spp.* exclusively hydrate *cis*-9 double bond.<sup>302, 303, 304</sup> The crystal structure of the LAH from *Lactobacillus acidophilus* provided the structural basis for the selective substrate recognition of linoleate 10-hydratase.<sup>305</sup> A second LAH in *L. acidophilus* hydrates the *cis*-12 double bond to produce 13-hydroxy fatty acid.<sup>306, 307</sup>

The physiological and ecological function of LAHs have been investigated. The LAH/myosin-cross reactive antigen of *S. pyogenes* mediated adherence to human keratinocytes; LAH was also suggested to detoxify linoleic acid by conversion to a hydroxyl-product with lower antibacterial activity.<sup>17</sup> Similarly, a *L. acidophilus* mutant with truncated

LAH exhibited a decreased adherence to intestinal epithelial cells, and was more sensitive to stresses.<sup>308</sup> Heterologous expression of a LAH of *Bifidobacterium breve* in *Lactococcus lactis* increased resistance to heat and solvent stresses.<sup>303</sup> Linoleate 10-hydratase is predicted to be a membrane-associated protein with one trans-membrane helix,<sup>301, 303</sup> and hydration of linoleic acid occurs in the cell periphery.<sup>309</sup> However, the effect of linoleic acid hydratase on properties of cell membranes and the cell surface have not been demonstrated. Moreover, 10-HOE has antifungal activity<sup>15</sup> but a corresponding activity of alternative hydration products of fatty acids remains unknown.

This study aimed to characterize linoleic acid hydratases in *L. plantarum*, *Lactobacillus reuteri*, *L. hammesii*, and *Lactobacillus spicheri*. Strain selection included strains which produce only 10-HOE and strains that produce 10-HOE and 13-HOE.<sup>15</sup> Four enzymes were characterized after heterologous expression in *Escherichia coli*. The physiological function of the linoleate 10-hydratase of *L. plantarum* was studied in more detail by comparison of the ethanol resistance and cell surface properties of *L. plantarum* TMW1.460 and its linoleate 10-hydratase deficient mutant *L. plantarum* TMW1.460  $\Delta lah$ . The antifungal activity of 13-HOE was compared to the activities of other hydroxy fatty acids.

## **3.2 Materials and methods**

### **3.2.1 Bacterial strains and fermentation**

*Lactobacillus reuteri* LTH2584, *L. plantarum* TMW1.460, *L. hammesii* DSM16381, *L. spicheri* Lp38 and *Lactobacillus sanfranciscensis* ATCC 27651 were anaerobically cultivated at 37 °C (*L. reuteri*) or 30 °C (all other strains) in modified De Man Rogosa Sharpe (mMRS) medium containing 0.1% Tween 80 (mMRS-Tween 80).<sup>49</sup> mMRS-Tween 20 was prepared by replacing Tween 80 with an equal weight of Tween 20. *E. coli* DH5 $\alpha$  (New England Biolabs)



served as a host for plasmids in the cloning procedures, and *E. coli* BL21 Star (DE3) (ThermoFisher Scientific) was used for protein overexpression. *E. coli* strains were cultivated in Luria–Bertani (LB) medium (BD, Mississauga, CA, USA) with agitation at 200 rpm and 37 °C. Antibiotic-resistant *E. coli* carrying plasmid pET-28a(+), pUC19 or pJRS233 were cultured in media containing 50 mg/L kanamycin, 50 mg/L ampicillin, or 500 mg/L erythromycin, respectively. Erythromycin-resistant *L. plantarum* was grown in presence of 5 mg/L erythromycin. *Aspergillus niger* FUA5001 and *Penicillium roqueforti* FUA5005 were grown at 25°C for 72 h on malt extract agar.

Linoleic acid metabolism of lactobacilli was analyzed after incubation in mMRS-Tween80 broth supplied with 5% inoculum and 4 g/L linoleic acid anaerobically for 4 days. Lipids were isolated by addition of one volume of 85:15 (vol/vol) chloroform-methanol to cultures prior to incubation 4°C overnight; cultures were then extracted twice with additional two volumes of chloroform–methanol (85:15, vol/vol). The organic solvent was evaporated under reduced pressure and the dry residue stored at –20 °C under nitrogen.

### **3.2.2 DNA manipulations**

Genomic DNA was isolated using the Blood & Tissue Kit (Qiagen, Hilden, Germany). Plasmid DNA from *E. coli* was extracted with a QIAprep Spin Miniprep kit (Qiagen). PCR primers used in this study were synthesized by Integrated DNA Technologies (San Diego, CA, USA). The Taq DNA polymerase was purchased from TaKaRa Bio (Shiga, Japan). T4 DNA ligase and restriction enzymes were obtained from Thermo Scientific (Mississauga, CA, USA). PCR products were purified by using the DNA gel extraction kit (Qiagen). DNA sequencing was performed by Macrogen (Rockville, MD, USA).

### 3.2.3 Sequence and phylogenetic analysis of linoleate hydratases in lactobacilli

Genes of putative LAHs in *L. spicheri* Lp38, *L. reuteri* LTH2584 and *L. plantarum* TMW1.460 were amplified with primers that are specific to LAHs in genome-sequenced strains of these species (**Table 3.1**). To identify the LAH in *L. hammesii*, *lah* sequences from the closely related *L. spicheri* and *L. brevis* were aligned and specific primers targeting conserved sequences upstream and downstream of *lah* coding sequences were designed (**Table 3.1**). The four *lah* genes were sequenced by service of Macrogen (Rockville, MD, USA).

The phylogenetic analysis of LAHs included the type strains of the 24 groups of the genus *Lactobacillus sensu lato*<sup>310</sup> and the genera *Weissella*, *Leuconostoc*, and *Oenococcus*. Sequences of biochemically characterized linoleate 10-hydratase and linoleate 13-hydratase from *Lactobacillus* spp., *Bifidobacterium* spp. and *Streptococcus* spp. were included in the phylogenetic analysis.<sup>17, 303, 304, 306</sup> Protein sequences of LAH were retrieved from GenBank (<http://www.ncbi.nlm.nih.gov>), using NCBI BLAST analysis with organism specific search. Protein phylogenetic tree was built in MEGA7.

### 3.2.4 Cloning and heterologous expression of linoleate hydratases of lactobacilli

Coding regions of the four *lah* were amplified from genomic DNA of the respective strains with primers listed in **Table 3.1**. Amplicons were purified and cloned into pGEM-T Easy vector (Promega, Madison, WI, USA). The *lah* fragments in recombinant pGEM-T vectors were digested with restriction endonucleases (**Table 3.1**), purified and ligated into expression vector pET-28a(+) (Novagen, Toronto, Ontario, Canada), yielding the respective constructs pET28a/LAH for each strain. Recombinant plasmids were introduced into chemically competent *E. coli* BL21 Star (DE3) (Thermo Fisher Scientific) and transformants

were plated on LB agar containing 50 mg/L kanamycin. The gene cloning was verified by PCR amplification and sequencing.

Four recombinant *E. coli* BL21 (DE3) strains were grown to an optical density (OD) at 600 nm of 0.6. Protein expression was induced by the addition of isopropyl- $\beta$ -D-thiogalactopyranoside (IPTG) to a final concentration of 1.0 mM, followed by incubation for 4 h and harvesting of cells by centrifugation at 4°C.

**Table 3.1.** Primers used in this study

Primers (forward (F); reverse (R))	Sequence (5'-3')	Restriction site*
DSM16381 sequencing, F1	5'-TACGGAGGTGTTTTTGGATGGT-3'	—
DSM16381 sequencing, R1	5'-CGTAAATTCATAAATCATTGGTGCATGTA-3'	—
DSM16381 sequencing, F2	5'-TACATGCACCAAATGATTTATGAATTTACG-3'	—
DSM16381 sequencing, R2	5'-TACTTCGTCTTAGGTGACCA-3'	—
LTH2584 cloning, F	5'-CGCC <u>CATATG</u> TACTATTCAAACGGAAATTATG-3'	NdeI
LTH2584 cloning, R	5'-ATTTGCGGCCGCTTAAAGTAAATGTTGTTCTTCCATT-3'	NotI
TMW1.460 cloning, F	5'-CCGGAATTCATGGTTAAAAGTAAAGCAATTATGA-3'	EcoRI
TMW1.460 cloning, R	5'-ATTTGCGGCCGCTTAAACAAACATCTTCTTAGTTGC-3'	NotI
DSM16381 cloning, F	5'-CGCGGATCCATGGTTAAAACAAAAGCAGTAATG-3'	BamHI
DSM16381 cloning, R	5'-CCCA <u>AGCT</u> TTTAGCTAAACATCCGCTTCGTTGC-3'	HindIII
Lp38 cloning, F	5'-CCGGAATTCATGGTTAAGACAAAAGCTGTAATG-3'	EcoRI
Lp38 cloning, R	5'-ATAGTTTAGCGGCCGCTTAACTAAACATTTCTTCGTTGCC-3'	NotI
<i>lah</i> -upstream A, F	5'-AACTGCAGGCCTAAAACGAGCTAAACGAC-3'	PstI
<i>lah</i> -upstream A, R	5'-ACATGCATGCCCGGCACCAATCATAATTGCTTTAC-3'	SphI
<i>lah</i> -downstream B, F	5'-ACATGCATGCAAGAAGATGTTTGATTAATTTAAA-3'	SphI
<i>lah</i> -downstream B, R	5'-CCCA <u>AGCT</u> TATGAAAAAATTAACATCAGTCG-3'	HindIII

\* restriction sites are underlined.

### 3.2.5 Purification of linoleate hydratases

Overexpressed LAHs were present mainly as inclusion bodies. Solubilization and refolding of inclusion bodies were carried out with the protein refolding kit (Novagen) according to the manufacturer's instructions. The refolded proteins were concentrated by using a 10 KDa Amicon Ultra-15 centrifugal filter Unit (Millipore, Germany).

After concentration, the His-tagged LAHs were purified by Ni-NTA spin columns (Qiagen). The purified LAHs were finally dialyzed against 50 mM 4-morpholineethanesulfonic acid (MES) buffer (pH 6.1) (Sigma-Aldrich) overnight at 4 °C. The purified enzymes were assessed by SDS-PAGE and staining with Coomassie blue. FAD was added to the purified enzymes at a final concentration of 0.2 mM and incubated at 4 °C for 24 h.<sup>311</sup>

### 3.2.6 Enzymatic activity assay and fatty acid analysis

To determine the enzymatic activity, 4.5 mg linoleic acid and 25 µg purified LAH were incubated in 1 ml of 50 mM MES buffer (pH 6.1) containing 50 mM NaCl, 2% ethanol and 10% glycerol at 25 °C for 3 h. Fatty acids were extracted following the procedure described above. The organic phase of the extracts was collected and analyzed with LC-APPI-MS as described.<sup>191,</sup>

15

### 3.2.7 Construction of *L. plantarum* TMW1.460Δ*lah* by double-crossover mutagenesis

Gene disruption of *lah* in *L. plantarum* TMW1.460 was achieved by an in-frame, unmarked deletion.<sup>312</sup> The approximately 900bp 5'-flanking regions (fragment A) and 1000bp 3'-flanking regions (fragment B) of *lah* were amplified by PCR with primers listed in **Table 3.1**. The

fragment A was digested with PstI, SphI, and fragment B was digested with SphI, HindIII. The resulting fragments were purified and sequentially ligated into vector pUC19 to generate pUC19/AB. The AB fragment in pUC19/AB was confirmed by sequencing, and sub-cloned into the PstI and HindIII restriction sites of pJRS233 to create pJRS233/ $\Delta$ lah. Recombinant plasmids were transformed into electrocompetent *L. plantarum* TMW1.460 at 12.5 kV/cm, 25  $\mu$ F and 200  $\Omega$ . The cells were grown in mMRS-Tween80 broth containing 5 mg/l erythromycin at 42-44 °C for 80 generations to select for single-crossover mutants. Several colonies were isolated, cultured in mMRS-Tween80 broth for approximately 100 generations, and plated on mMRS-Tween80 agar at 30 °C. The colonies were replica plated on mMRS-Tween80-erythromycin agar to identify erythromycin-sensitive double-crossover mutants. Gene replacement was confirmed by PCR amplification and sequencing. The phenotype was determined by LC-APPI-MS analysis of culture supernatant of *L. plantarum* TMW1.460 $\Delta$ lah grown in mMRS-Tween80 supplemented with 4 g/L linoleic acid.

### **3.2.8 Determination of ethanol resistance**

Ethanol tolerance of *L. plantarum* TMW1.460 and TMW1.460 $\Delta$ lah was carried out with strains grown in mMRS-Tween 80, or mMRS-Tween 20. Ethanol was added as indicated and media were sterilized by filtration after addition of ethanol. Stationary phase cells were harvested by centrifugation and resuspended in the same volume of mMRS-Tween 80 or -Tween 20 containing 20% ethanol. A 100 $\mu$ l aliquot of cell suspension was analyzed as untreated control. The samples were incubated in 30 °C and aliquots were removed in 1.5 h intervals and serially diluted in 0.85% NaCl. The appropriate dilutions were surface plated in duplicate on respective

mMRS-Tween80 or -Tween20 agar and incubated at 30 °C for 24 h. Ethanol resistance was determined in three independent experiments.

### 3.2.9 Determination of the membrane fluidity under ethanol stress

To investigate the membrane fluidity, Laurdan (6-dodecanoyl-2-dimethylaminonaphthalene) (Thermo Fisher Scientific) was employed to measure generalized polarization (GP) value. *L. plantarum* TMW1.460 and TMW1.460 $\Delta$ lah were cultivated at 30°C for 20 h in mMRS-Tween80 or mMRS-Tween 20. The membrane fluidity of the cells influenced by ethanol at the concentration ranging from 0% to 16% was assessed as described.<sup>313</sup> The effect was determined in three independent experiments.

### 3.2.10 Physicochemical properties of cells surface

Cell surface hydrophobicity was assessed by quantification of microbial adhesion to solvents (MATS).<sup>314</sup> Solvents used were: chloroform (polar and electron acceptor) and tetradecane (non-polar), ethyl acetate (polar and electron donor) and octane (nonpolar). The MATS is based on the comparison between microbial cell affinity to a polar and nonpolar solvent within a couple that pose similar van der Waals surface tension components.

*L. plantarum* TMW1.460 and TMW1.460 $\Delta$ lah were grown in mMRS-Tween 20, or mMRS without Tween but supplemented with 1 g/L oleic acid or linoleic acid. Cells were harvested by centrifugation, washed twice and resuspended in 150 mM NaCl to a final cell concentration of 10<sup>8</sup> CFU/ml. A 1 ml aliquot was removed as untreated control (A<sub>0</sub>). A 2.4 ml aliquot of cell suspension was mixed with 0.4 ml of solvent by vortexing for 60 s, respectively. The emulsified

mixture was allowed to stand for 20 min to ensure the complete separation of the two phases. A sample (1 ml) was carefully taken from the aqueous phase (A). The optical cell density of sample  $A_0$  and A was measured at 600 nm. The microbial adhesion percentage to each solvent was calculated with the equation: percent affinity= $100 \times [1 - (A/A_0)]$ . Each measurement was determined in three independent experiments.

### **3.2.11 Extraction and purification of 13-HOE and 10-HOE**

Extraction and purification of 13-HOE and 10-HOE was based on a protocol developed for 10-HOE.<sup>15</sup> Fermentation of *L. hammesii* or *L. plantarum* TMW1.460 $\Delta$ lah in mMRS-Tween 80 with 4g/L linoleic acid was conducted for production of 10-HOE or 13-HOE, respectively. The crude extraction of cellular lipids was performed as described above. Subsequently, the purification of 10-HOE or 13-HOE was based on a protocol described previously.<sup>15</sup> The fermentation of *L. hammesii* or *L. plantarum* TMW1.460 $\Delta$ lah in mMRS-Tween 80 with 4g/L linoleic acid and the crude extraction of fatty acid mixtures were performed as described above. For further purification, 25 mg of sample dissolved in chloroform was applied to a 500-mg Sep-Pak silica cartridge (Waters Ltd., Mississauga, ON, Canada) previously equilibrated with 6 ml chloroform. The cartridge was successively washed with the following gradient of isopropanol in chloroform: 35 ml of chloroform, followed by 18 ml of 1, 5, 10, and 50% (vol/vol) isopropanol in chloroform. Eluates were collected and concentrated to dryness under nitrogen. The dry residues were dissolved in chloroform for analysis by LC-APPI-MS to identity of the product, and the removal of contaminating lipids.

### 3.2.12 Determination of the antimicrobial activity of fatty acids

The minimum inhibitory concentration (MIC) was determined to assess the toxicity of linoleic acid to lactobacilli, and to determine the antifungal activity of 10-HOE, 13-HOE, coriolic acid, ricinoleic acid and linoleic acid. Lipids dissolved in ethanol were serially diluted twofold in mMRS-Tween80 using 96-well microtiter plates. Ethanol in the samples was evaporated under a sterile laminar flow hood before inoculation with indicator strains. Stationary phase cells of lactobacilli were harvested by centrifugation, washed twice in mMRS-Tween80 and diluted to approximately  $10^7$  CFU/ml in the same medium. The plates were incubated at 30 °C.

For evaluation of the antifungal activity, lipids diluted with serial twofold dilutions. Conidiospores of *A. niger* and *P. roqueforti* were prepared as reported.<sup>15</sup> The plate was inoculated with *A. niger* as an indicator organism and incubated at 25 °C for 2 days, while the plate inoculated with *P. roqueforti* was incubated for 3 days. Fungal growth without addition of lipids served as the positive control and media alone as the negative control. The MIC was defined as the lowest concentration of lipids that inhibited the growth of fungi when growth was visible in the positive control. MIC values were determined by six independent experiments.

### 3.2.13 Statistical analysis

Data analysis was conducted with R 3.1.2 (R Core Team, 2014). Significant differences in the assessment of cell survival and membrane fluidity under ethanol stress were determined by one-way analysis (ANOVA). Significance was assessed at a 5% probability of error ( $P < 0.05$ ).



### 3.2.14 Accession numbers

The sequences of linoleate 10-hydratase in *L. reuteri*, *L. plantarum*, *L. hammesii* and *L. spicheri* were deposited in GenBank with accession numbers KX827285, KX827286, KX827287, KX827288, respectively.

## 3.3 Results

### 3.3.1 Identification of the products of linoleate conversion by lactobacilli

The products of linoleic acid conversion by five lactobacilli were analyzed by negative ion LC/APPI-MS/MS (**Table 3.2**). MS/MS spectra of the products confirmed the position of hydroxyl groups (**Figure 3.1**).<sup>191</sup> The strains of lactobacilli differed in with respect to their conversion of linoleic acid to hydroxy fatty acids (**Table 3.2**). *L. reuteri*, *L. hammesii* and *L. spicheri* produced 10-HOE only, while *L. plantarum* produced 10-HOE, 13-HOE and 10,13-dihydroxy octadecanoic acid. *L. plantarum* TMW1.460 $\Delta$ *lah* produced 13-HOE but not 10-HOE or 10,13-dihydroxy octadecanoic acid, demonstrating that their formation by *L. plantarum* TMW1.460 is attributable to a dedicated linoleate 13-hydratase acting on linoleic acid and 10-HOE, respectively. *L. sanfranciscensis* did not convert linoleic acid.

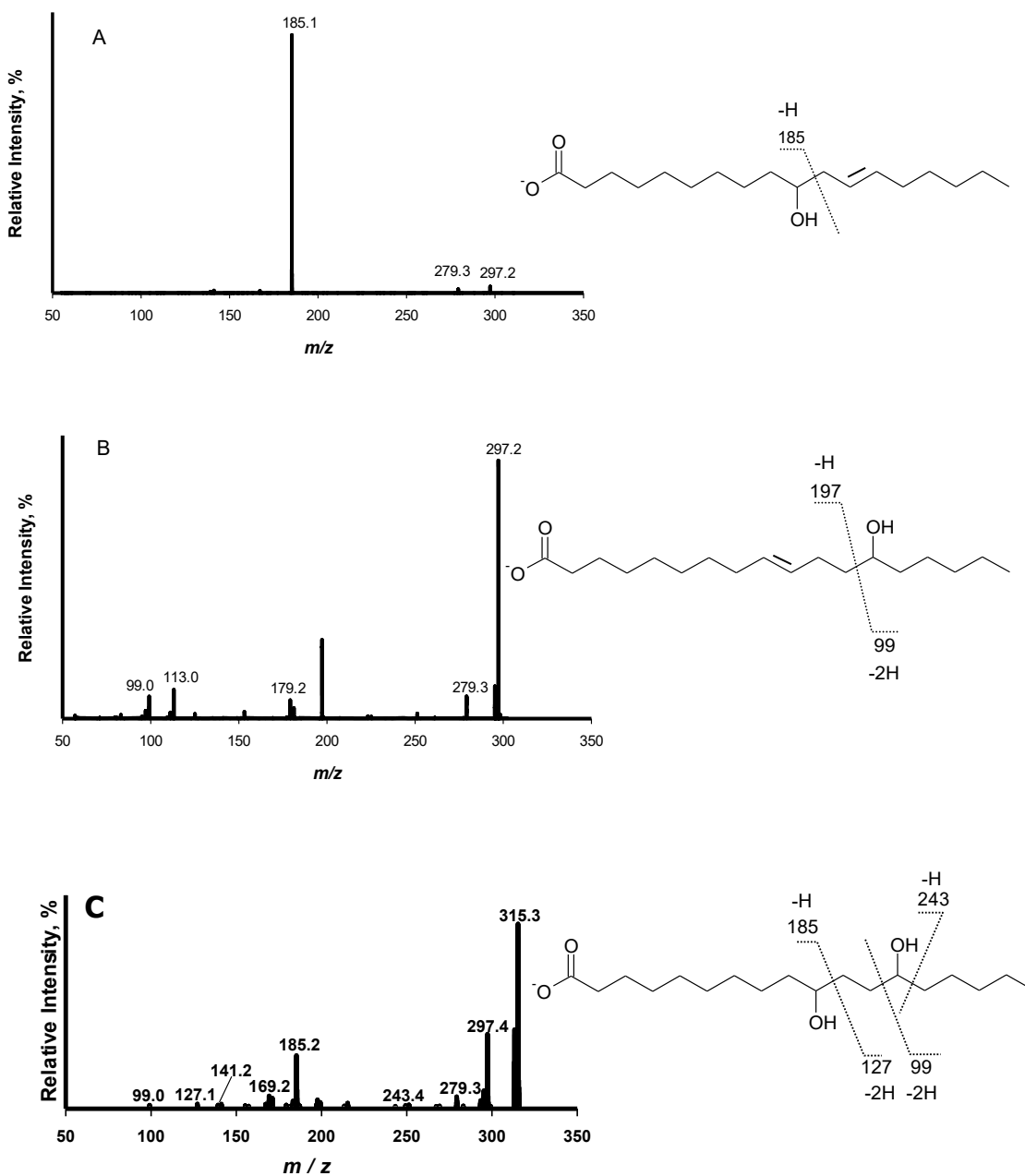


**Figure 3.1.** Fragmentation pattern and APPI-MS/MS spectra of hydroxy fatty acids produced when linoleic acid was used as substrate. (A) Mass spectrum of 10-hydroxy-12-octadecenoic acid; (B) mass spectrum of 13-hydroxy-9-octadecenoic acid; (C) mass spectrum of 10,13-dihydroxy octadecanoic acid.

**Table 3.2.** Comparison of products obtained from strain fermentation and enzymatic reaction with linoleic acid as substrate

Strain	Products of fermentation	Products of LAH	Fragmentation ions ( <i>m/z</i> )
<i>L. reuteri</i> LTH2584	10-HOE <sup>a)</sup>	10-HOE	297[M-H] <sup>-</sup> , 185
<i>L. hammesii</i> DSM16381	10-HOE	10-HOE	297[M-H] <sup>-</sup> , 185
<i>L. spicheri</i> LS38	10-HOE	10-HOE	297 [M-H] <sup>-</sup> , 185
	10-HOE,		297 [M-H] <sup>-</sup> , 185
<i>L. plantarum</i> TMW1.460	13-HOE <sup>a)</sup> and 10,13-HOA <sup>a)</sup>	10-HOE	297 [M-H] <sup>-</sup> , 99, 197 315 [M-H] <sup>-</sup> , 99, 127, 185, 243
<i>L. plantarum</i> TMW1.460 $\Delta$ lah	13-HOE	---	297 [M-H] <sup>-</sup> , 99, 197
<i>L. sanfranciscensis</i> ATCC 27651	No products	No products	---

<sup>a)</sup> 10-HOE, 10-hydroxy-12-octadecenoic acid; 13-HOE, 13-hydroxy-9-octadecenoic acid; 10,13-HOA, 10,13-dihydroxy octadecanoic acid

### 3.3.2 Phylogenetic analysis of linoleate hydratase

Phylogenetic relationships of putative LAHs from lactobacilli were compared to the corresponding enzymes of the 24 type strains in the genus *Lactobacillus*, and type strains from the genera *Pediococcus*, *Weissella*, *Leuconostoc*, and *Oenococcus* (**Figure 3.2**). All four hydratases from lactobacilli that were investigated in this study belonged to myosin cross reactive antigen family. *L. sanfranciscensis* harbored no LAH. The topology of the protein tree

did not conform to the evolutionary relationship of the organisms.<sup>310</sup> The tree displayed two clusters but the two clusters do not differentiate between linoleate 10-hydratases and linoleate 13-hydratases (**Figure 3.2**).

### 3.3.3 Characterization of linoleate 10-hydratase

Sequence analysis did not distinguish 10-hydratases from 13-hydratases, and therefore, LAHs from four strains of lactobacilli were characterized biochemically after heterologous expression in *E. coli* and purification by affinity chromatography. A single band was observed by SDS-PAGE analysis after purification of the four enzymes (**Figure 3.3**); this band was absent in crude cellular extracts of *E. coli* strains prior to induction (data not shown). The genes from *L. reuteri*, *L. plantarum*, *L. hammesii* and *L. spicheri* encoded a protein of 590, 564, 564, 564 amino acids, respectively, matching the size of the major band observed by SDS-PAGE analysis (**Figure 3.3**). The addition of cofactor FAD to apoenzyme was essential for activity. LC-APPI-MS analysis revealed that all four recombinant proteins produced 10-HOE from linoleic acid, as demonstrated by the fragment ion at  $m/z$  185.1 in the MS/MS spectra (**Table 3.2**). Hence, all four recombinant proteins were shown to be 10-hydratases. The substrate specificity of the linoleate 10-hydratase of *L. plantarum* TMW1.460 confirmed that formation of 13-HOE and 10,13-dihydroxy octadecanoic acid by this strain is likely attributable to a second and dedicated linoleate 13-hydratase.

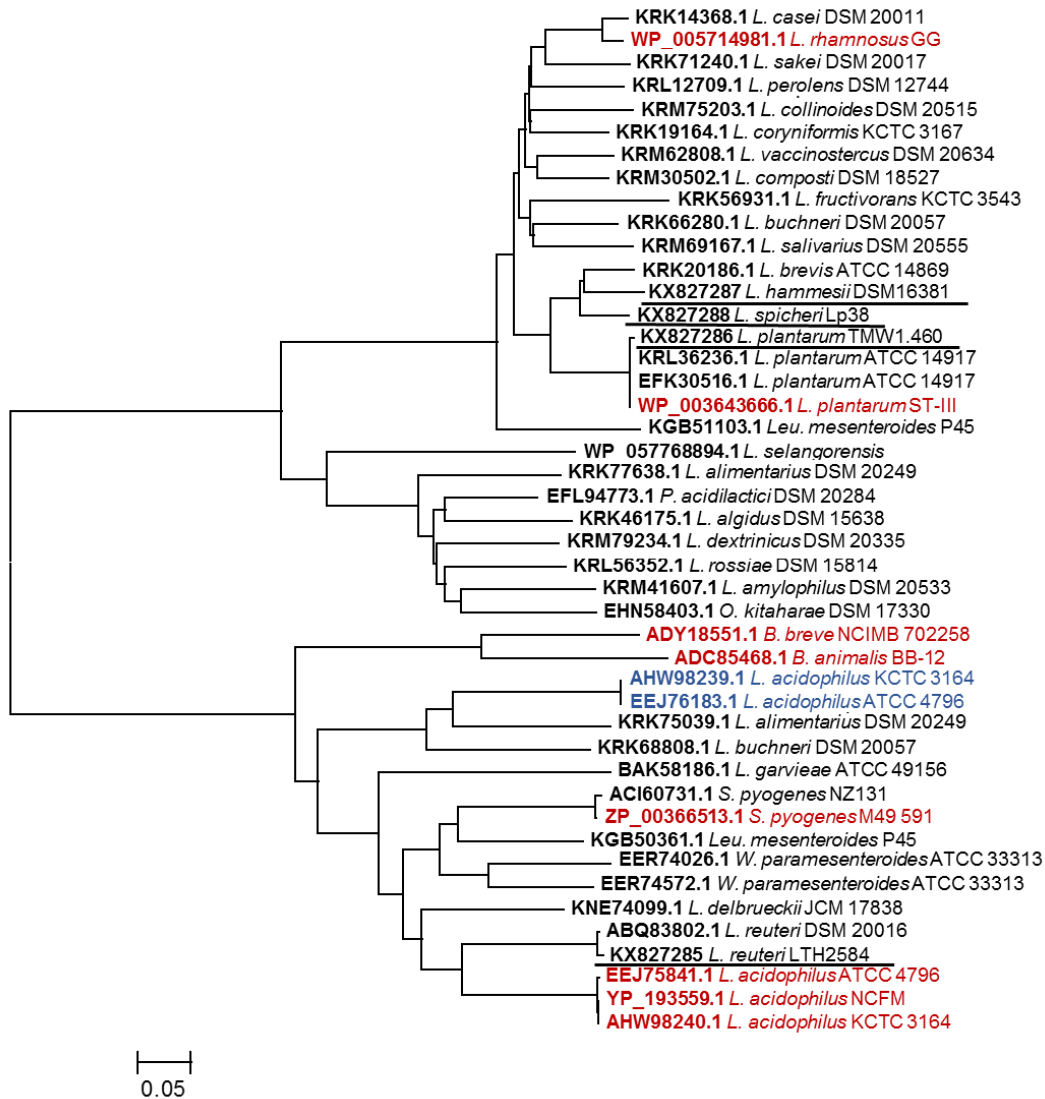


**Figure 3.2.** Phylogenetic tree of linoleate hydratases (LAHs). The evolutionary relationships are shown with scale bar line, which represents an evolutionary distance of 0.05. Linoleate 10-hydratases reported in the literature are highlighted in red, linoleate 13-hydratases are highlighted in blue, linoleate 10-hydratases that were characterized in this study are underlined.

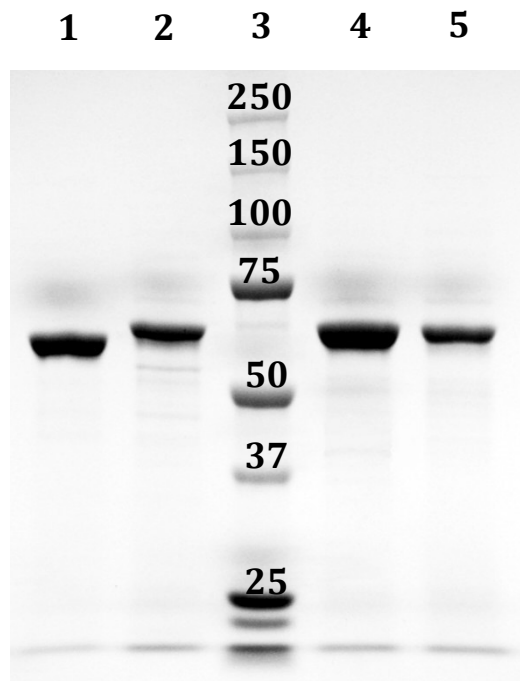


**Figure 3.3.** SDS-PAGE analysis of purified LAHs expressed from respective recombinant *Escherichia coli* BL21 (DE3) cells. Lane 1, LAH of *Lactobacillus reuteri*; lane 2, LAH of *Lactobacillus plantarum*; lane 3, molecular mass marker proteins (250, 150, 100, 75, 50, 37 and 25 kDa); lane 4, LAH of *Lactobacillus hammesii*; lane 5, LAH of *Lactobacillus spicheri*.

### 3.3.4 Most lactobacilli require oleic acid or linoleic acid for growth

Tween 80 is a derivative of oleate and a component of mMRS.<sup>315,316</sup> mMRS-Tween20 did not support the growth of *L. reuteri*, *L. hammesii* and *L. sanfranciscensis* but did support the growth of *L. plantarum* and its  $\Delta 10\text{-lah}$  mutant (data not shown). However, unsaturated fatty acids (UFAs) may also exhibit antibacterial activity.<sup>317</sup> Therefore, the MICs of oleic and linoleic acid to lactobacilli including *L. plantarum* TMW1.460 $\Delta\text{lah}$  were assessed. The MICs of oleic and linoleic acids were > 8 g/L for all strains, which indicates a high tolerance towards oleic and linoleic acid. *L. sanfranciscensis* showed less tolerance and its growth was inhibited by 1 g/L oleic acid and 0.5 g/L linoleic acid.

### 3.3.5 The effect of *lah* on stress tolerance in *L. plantarum*

To investigate the effect of hydroxy fatty acids or 10-LAH itself on ethanol resistance, the survival of *L. plantarum* TMW1.460 and TMW1.460 $\Delta\text{lah}$  was assessed in mMRS-Tween80 and mMRS-Tween20 containing 20% ethanol. The ethanol tolerance of *L. plantarum* TMW1.460 and TMW1.460 $\Delta 10\text{-lah}$  did not differ (**Figure 3.4**). However, the presence of Tween 80 in the growth medium enhanced bacterial survival, especially for *L. plantarum* TMW1.460 (**Figure 3.4**).

### 3.3.6 The effect of *lah* on ethanol-dependent membrane fluidity in *L. plantarum*

The ethanol-dependent membrane phase behavior of strains grown in mMRS-Tween80 or - Tween 20 was analyzed (**Figure 3.5**). The GP values decreased with increasing ethanol concentration, indicating that ethanol increased the fluidity of the membrane. The response of the

membrane fluidity of *L. plantarum* TMW1.460 and TMW1.460 $\Delta$ *lah* to ethanol was similar. Tween 80 supplemented medium induced a more fluid membrane in both strains.

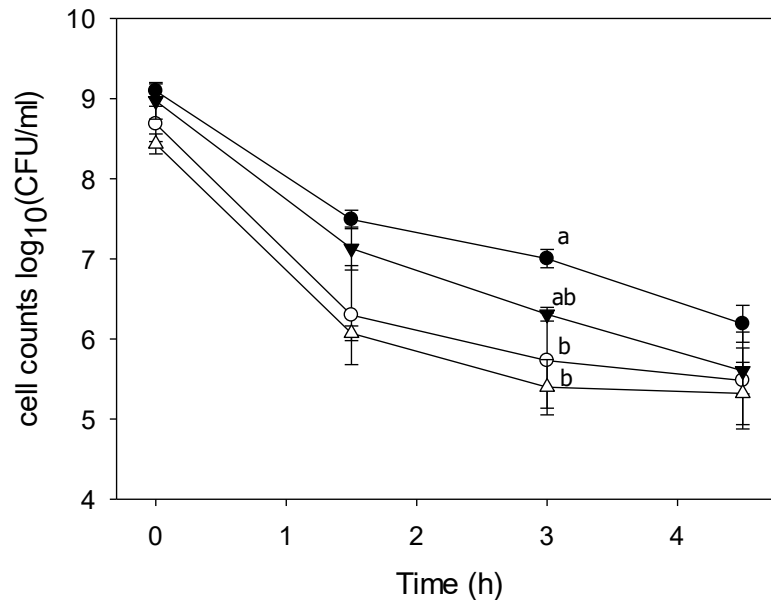


**Figure 3.4.** Survival of *L. plantarum* and its *lah* deficient derivative under 20% ethanol treatment. *L. plantarum* TMW1.460 was incubated in mMRS-Tween80 (closed circles) or mMRS-Tween20 (open circles); *L. plantarum* TMW1.460 $\Delta$ *lah* was grown in mMRS-Tween80 (closed triangle) or mMRS-Tween 20 (open triangle) during treatment. Values obtained at the same treatment time that do not share common superscripts are significantly different ( $P < 0.05$ ). Data represent means  $\pm$  standard deviations of three independent experiments with duplicate determinations of cell counts.



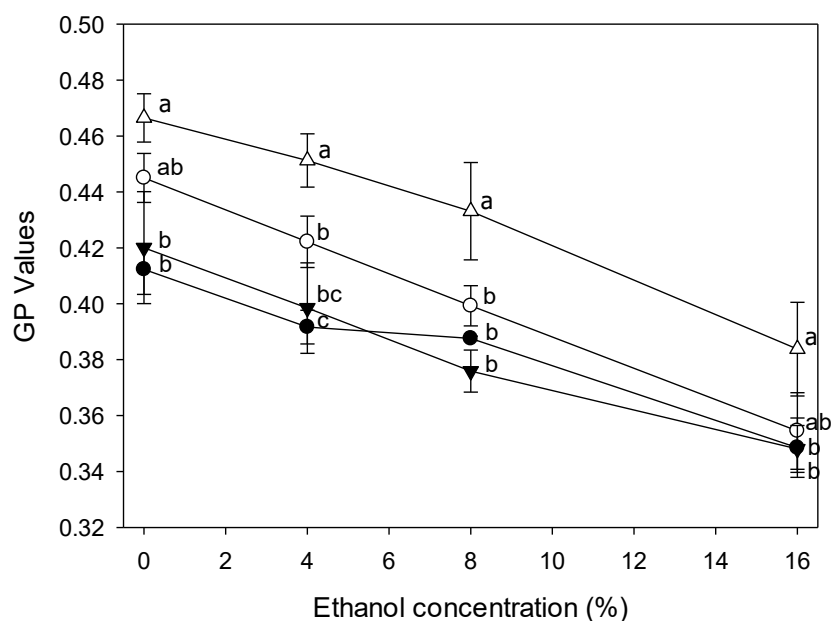


**Figure 3.5.** General polarization (GP) values of *L. plantarum* and its  $\Delta lah$  derivative stained with Laurdan under ethanol stress. *L. plantarum* TMW1.460 was cultivated in mMRS-Tween80 (closed circles) or mMRS-Tween 20 (open circles) prior to staining; *L. plantarum* TMW1.460 $\Delta lah$  strain was cultivated in mMRS-Tween80 (closed triangle) or mMRS-Tween 20 (open triangle) prior to staining. Values obtained at the same treatment time that do not share common superscripts are significantly different ( $P < 0.05$ ). Data represent means  $\pm$  standard deviations of three independent experiments with duplicate determinations of cell counts.

### 3.3.7 Influence of *lah* on cell surface properties in *L. plantarum*

The MATS of *L. plantarum* TMW1.460 and TMW1.460 $\Delta$ *lah* cultivated in mMRS-Tween20, or mMRS-Tween20 supplemented with oleic or linoleic acid are shown in **Figure 3.6**. The deletion of *lah* modified the properties of the cell surface. The adhesion of *L. plantarum* TMW1.460 $\Delta$ *lah* was more solvent-dependent when compared to the wild-type strain and the affinity of cells to the four solvents was generally higher for  $\Delta$ *lah* mutant than for wild-type strain. Similar trends were noted with strains grown in mMRS with different supplements, suggesting that the differences between wild-type and mutant strains are attributable to other functions of 10-LAH, not the oleic/linoleic acid-derived product of this enzyme. Similar behavior was observed when strains cultivated in Tween 80 (Data not shown).

In this study, both wild-type and mutant strains exhibited low affinity for tetradecane and octane (non-polar solvents), indicating that the cell surface of both strains was hydrophilic rather than hydrophobic. To determine the effect of deletion of 10-*lah* on the Lewis electron donor/electron acceptor property, the bacterial affinity to chloroform and ethyl acetate between different strains were also compared (Figure 3.6). *L. plantarum* wild-type strain showed similar adhesion ability to chloroform and ethyl acetate. However, regardless of the different supplement in medium, the adhesion of the mutant strain was always higher to chloroform (electron acceptor and acidic solvent) than to ethyl acetate (electron donor and basic solvent).

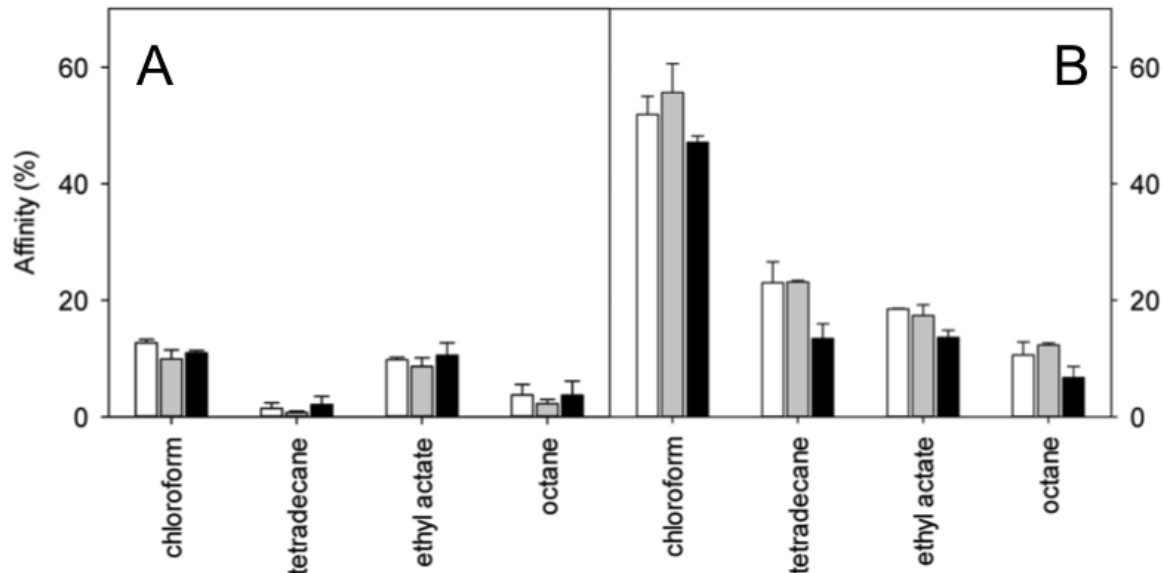


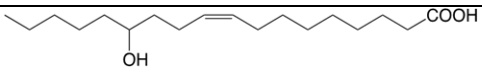
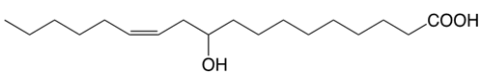
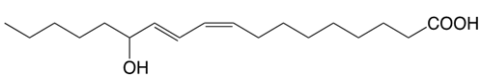
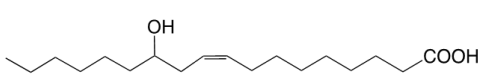
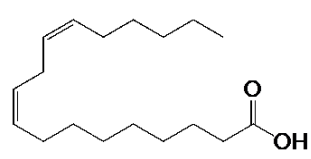
**Figure 3.6.** Effect of 10-*lah* on cell surface properties of *L. plantarum* grown in different media. Cell surface hydrophobicity was measured using the MATS method. (A) *L. plantarum* TMW1.460; (B) *L. plantarum* TMW1.460Δ*lah*. White bar indicates % affinity to solvents when cells were grown in mMRS -Tween 20; gray bar indicated in mMRS (Tween 20) supplemented with 1 g/L oleic acid; black bar indicated in mMRS (Tween 20) supplemented with 1 g/L linoleic acid. Data represent means ± standard deviations of three independent experiments.

### 3.3.8 Antifungal properties of purified hydroxy fatty acids

13-HOE and 10-HOE were purified from organic extracts of cultures of *L. plantarum* TMW1.460Δ*lah* and *L. hammesii*, respectively, when 4 g/L linoleic acid was used as substrate. The major impurity detected in the organic phase was linoleic acid; other more oxidized forms of hydroxy C<sub>18</sub> fatty acids were also present. The compounds were purified by silica solid phase microextraction and analyzed by LC-APPI-MS/MS. 10-HOE or 13-HOE were

eluted in the 1% isopropanol fraction and a single peak was observed in the LC-APPI-MS/MS chromatogram after purification. The antifungal activity of purified 13-HOE and 10-HOE against *A. niger* and *P. roqueforti* is shown in **Table 3.3** and compared to reference lipids differing in the number and position of hydroxyl groups or double bonds. Both coriolic acid and ricinoleic acid were active against all fungi indicators with MICs between 0.26 and 0.29. Linoleic acid showed the lowest antifungal activity.

**Table 3.3.** Minimum inhibitory concentrations (MICs) of hydroxy fatty acids extracted from cultures of *L. hammesii* and *L. plantarum* TMW1.460 $\Delta$ lah and reference fatty acids (n=3)

Structure	Compound	MIC (g/L)	
		<i>A. niger</i>	<i>P. roqueforti</i>
	13-HOE	0.25±0.00	0.38±0.14
	10-HOE	0.42±0.13	0.38±0.14
	Coriolic acid	0.26±0.09	0.26±0.09
	Ricinoleic acid	0.29±0.10	0.29±0.10
	Linoleic acid	4.00±0.00	5.33±2.07

### 3.4 Discussion

Linoleate hydratases are highly conserved in both Gram-positive and Gram-negative bacteria.<sup>17</sup> Our study revealed that 10-LAH and 13-LAH, or enzymes that produce both 10-HOE and 13-HOE are not distinguished by phylogenetic and sequence analysis. All hydratases from lactobacilli examined in this study were determined as 10-LAH, however, they are distributed in two different clusters which also contain 13-LAH. Moreover, the topology of the protein tree disagreed with the evolutionary relationship of the organisms,<sup>310</sup> indicating that LAHs are accessory proteins.<sup>318</sup>

Linoleate 10-hydratase is a FAD-containing enzyme and exhibits flavin-like UV absorbance.<sup>303</sup> FAD cofactor is bound to the conserved FAD binding motif of 10-LAH and stabilizes the active conformation of the enzyme but it is not directly involved in catalysis.<sup>17, 304</sup> The non-covalently bound FAD is easily lost in the purification process.<sup>305</sup> This study confirmed that 10-LAH is a FAD-dependent enzyme<sup>311</sup> and demonstrated that purification of active 10-LAH from inclusion bodies required addition of FAD. Different from the LAH of *S. pyogenes*, which catalyzes formation of 10-HOE and 13-HOE,<sup>17</sup> the 10-LAH characterized in this study formed exclusively 10-HOE from linoleate. The comparison of products formed by *L. plantarum* TMW1.460, the 10-LAH deficient mutant of this strain, and the 10-LAH of this strain strongly suggest that 13-HOE and 10,13-dihydroxy octadecanoic acid formation by this strain is attributable to a linoleate 13-hydratase that was recently characterized in *L. acidophilus*.<sup>307</sup>

Unsaturated fatty acids are essential for growth of many LAB<sup>315, 316</sup> but high concentrations may inhibit growth of LAB.<sup>319</sup> In contrast, in the present work oleic and linoleic acids stimulated growth of *L. reuteri*, *L. hammesii* and *L. sanfranciscensis*. The bacteriostatic and bactericidal activities exerted by UFAs against lactobacilli is strain dependent;<sup>320</sup> the observation that the

LAH-negative *L. sanfranciscensis* was the only strain that was inhibited by oleic and linoleic acids suggests that LAH contributes to these strain-specific differences.

Oleic acid modulated membrane fluidity and influenced the ethanol tolerance of *L. plantarum* TMW1.460 and TMW1.460 $\Delta$ *lah*. Consistent with our results, addition of Tween 80 to the growth medium increased viability of *Oenococcus oeni* in wine<sup>319</sup> and supplementation of UFAs to *Saccharomyces cerevisiae* protected against stress.<sup>321</sup> However, we observed no difference in ethanol resistance between *L. plantarum* TMW1.460 and TMW1.460 $\Delta$ *lah*. The protective effect of 10-LAH that was previously observed in exponential phase bifidobacteria may relate to the presence of the enzyme rather than its oleic/linoleic acid-derived products.<sup>303, 322</sup>

The physiochemical properties of cell surface play a critical role in adhesion of pathogens and probiotics to intestinal surfaces. An evaluation of surface properties is achieved by determination of MATS.<sup>323, 324</sup> Both *L. plantarum* wild-type and *lah* mutant strains displayed a hydrophilic surface character with weak adhesion to non-polar solvents. Similar results were obtained in other *Lactobacillus* spp. and *Lactococcus* spp.<sup>325, 326, 327</sup> The hydrophobicity of the cell surface changed when the bacteria were cultivated in medium with addition of UFAs,<sup>314, 328</sup> which was not observed in our study. Bacteria grown in mMRS medium with or without different supplement exhibited similar affinity to solvents. However, *lah* deficiency resulted in a fundamental change in the profile of solvent affinity. Compared with wild-type strain, *L. plantarum* TMW1.460 $\Delta$ *lah* presented more basic and electron-donating properties. The bacteria with basic character are considered to possess COO<sup>-</sup> and HSO<sub>3</sub><sup>-</sup> chemical groups on their cell surface.<sup>325</sup> *Lactobacillus casei* BL83, BL208 and BL229 also displayed low cell adhesion that was associated with their basic surface property.<sup>329</sup> Indeed, the deletion of 10-LAH was involved in the reduced adherence to human keratinocytes by *S. pyogenes* and to human intestinal

epithelial cells by *L. acidophilus*.<sup>308, 17</sup> In our study, 10-LAH mediated differences in cell surface properties may explain the changed cell adhesion to human cells in the previous reports.

Linoleic acid possesses antifungal activity against the plant pathogenic fungi, especially for *Crinipellis pernicioso* at the concentration of 100  $\mu$ M.<sup>330</sup> In our study, linoleic acid was less active against *A. niger* and *P. roqueforti*, fungi that are commonly found in cereals and cereal products.<sup>129, 331</sup> Remarkably, the MIC of 13-HOE was approximately 15 times lower than that of linoleic acid. Therefore, 13-HOE may be as suitable as 10-HOE as an antifungal agent in foods.<sup>15</sup> The antifungal activity of hydroxy fatty acids is likely related to their partitioning into lipid bilayers, thus increasing membrane permeability.<sup>129</sup> The MICs of 13-HOE, 10-HOE along with coriolic acid and ricinoleic acid were all comparable, suggesting that all unsaturated monohydroxy fatty acids of C<sub>18</sub> varying in their hydroxyl group position or degree of unsaturation exert antifungal property. Similar inhibition activities of *Aspergillus* and *Penicillium spp.* were detected among 9- and 13-hydroxy of C<sub>18</sub> UFA analogs of plant oxylipins.<sup>12</sup> In contrast, dihydroxy saturated C<sub>18</sub> fatty acids do not display antifungal activity.<sup>15</sup>

In conclusion, our study revealed that the differentiation of accessory proteins between 10-LAH and 13-LAH cannot be achieved by phylogenetic analysis. Thus, the linoleate hydratases from lactobacilli were characterized by heterologous expression and identified as FAD-dependent 10-LAH. Generation of a 10-LAH deficient mutant of *L. plantarum* demonstrated that 13-HOE, generated by a different and dedicated hydratase, is a novel antifungal hydroxy fatty acid. The most prominent physiological difference of the 10-LAH deficient mutant and the wild-type strain was the altered surface hydrophobicity of the bacterial cells. *L. plantarum* is part of the phyllosphere of many plants<sup>332</sup> and oxylipins are an important component of the plant

defense against pathogens.<sup>12</sup> It is possible that the lipid-converting properties of LAHs and their influence on cell surface properties are components of host-microbe interactions.



## Chapter 4. High-speed counter-current chromatography (HSCCC) purification of antifungal hydroxy unsaturated fatty acids from plant-seed oil and *Lactobacillus* cultures

### 4.1 Introduction

Pathogenic and spoilage fungi present enormous challenges to agriculture.<sup>24, 26</sup> Spoilage fungi, such as *Aspergillus clavatus* and *Mucor plumbeus*, and phytopathogenic fungi, such as *Leptosphaeria maculans* and *Pyrenophora teres* f. *teres*, affect the yield or quality of agricultural products.<sup>21, 333</sup> Mycotoxin-producing fungi, such as *Aspergillus flavus* and *Aspergillus parasiticus*, are a safety concern in food and feed.<sup>21</sup> Increased virulence or resistance of spoilage or pathogenic fungi toward common fungicides,<sup>26</sup> poor hygiene practices,<sup>334</sup> the abusive use of chemically synthesized fungicides,<sup>335</sup> and climate change<sup>25</sup> impede the control of fungi in the food supply and necessitate the development of an alternative or complementary fungicides.

Unsaturated fatty acids (UFAs) and hydroxy unsaturated fatty acids (HUFA) include compounds with antifungal activity.<sup>36, 13</sup> Their antifungal activities have been reported to relate to specific structural attributes,<sup>13, 15</sup> but structure-function relationships have not been sufficiently explored. Moreover, the antifungal activity of individual HUFA has been evaluated only with few indicator organisms. Coriolic acid, (*R*)-13-hydroxy-9(*Z*),11(*E*)-octadecadienoic acid or 13-OH C18:2), was first extracted and characterized in its methyl ester form.<sup>155</sup> In wheat dough, coriolic acid is generated through lipoxygenase activity, followed by reduction by low-molecular-weight thiols.<sup>15, 336</sup> Coriolic acid extends the mold-free shelf life of wheat bread;<sup>15</sup> lipid oxidation and thiol-exchange reactions are additionally linked to bread volume and flavor.<sup>336</sup> In plants and mushrooms, coriolic acid contributes to the defense against phytopathogens.<sup>12, 337, 338</sup> However, the inhibitory spectrum of coriolic acid is unknown, as is the range of HUFA structures showing

comparable antifungal activity. In order to further understand the influence of the molecular structure on the antifungal activities and the other biological roles of HUFA, an effective method for the production of specific HUFA is required.

Coriolic acid was previously obtained by extraction from hydrolyzed plants-seed oil,<sup>73</sup> by chemical synthesis,<sup>339</sup> by enzymatic conversion from unsaturated fatty acids (UFA),<sup>340</sup> and from recombinant bacteria.<sup>341</sup> *Lactobacillus* spp. expressing linoleate hydratases convert linoleic acid to the antifungal 10-hydroxy-12-octadecenoic acid (10-OH C18:1) or 13-hydroxy-9-octadecenoic acid (13-OH C18:1).<sup>15, 191</sup> Coriolic acid inhibited the growth of phytopathogenic blast fungus, *Magnaporthe grisea*,<sup>342</sup> of *Phytophthora parasitica*; and of *Cladosporium herbarum* at low effective dose.<sup>12</sup> However, the amounts of HUFA that were obtained in previous studies did not allow determination of the inhibitory spectrum or potential application.<sup>15, 343</sup>

High-speed counter-current chromatography (HSCCC) has been used to purify antimicrobial compounds in sufficient quantities for the determination of the inhibitory spectra and mode of action of natural antimicrobial compounds.<sup>60</sup> HSCCC employs the partition of analytes into two immiscible liquids.<sup>344</sup> It has a high sample-loading capacity and high recoveries of the target analytes.<sup>344, 59, 144</sup> HSCCC separated fatty acid esters from fish oil, but the separation methods for fatty acids differing in their degree of unsaturation required different solvent systems,<sup>345, 346, 347</sup> and HSCCC solvent systems have not been optimized for the separation of HUFA. It was therefore the aim of this study to develop HSCCC as a purification method for HUFA and to obtain purified HUFA in sufficient amounts to investigate their inhibitory spectrum with mycelial fungi, conidiospores, and yeasts. Coriolic acid, 10-OH C18:1, and 13-OH C18:1, were extracted from plants or microbial cultures and purified by HSCCC, and their purity and molecular structures

were characterized by liquid chromatography coupled with tandem mass spectrometry (LC-MS/MS).

## 4.2 Materials and methods

### 4.2.1 Chemicals and reagents

HPLC-grade solvents hexane, ethyl acetate, methanol, water, acetonitrile, chloroform and Optima grade acetic acid were purchased from Fisher Scientific (Ottawa, Canada). Fatty acid standards including tetradecanoic (myristic) acid, hexadecanoic (palmitic) acid, 9-*cis*-octadecenoic (oleic) acid, 12-hydroxy-9-*cis*-octadecenoic (ricinoleic) acid, 9-*cis*,12-*cis*-octadecadienoic (linoleic) acid, octadecanoic (stearic) acid, 9-*cis*,12-*cis*,15-*cis* octadecatrienoic (alpha linolenic) acid with purity >99% were purchased from Nu-Chek Prep, Inc (Elysian, MN, USA). Microbiological media were purchased from Fisher Scientific.

### 4.2.2 Microbial strains and culture conditions

*L. hammesii* DSM16381<sup>348</sup> and *L. plantarum* TMW1.460 $\Delta$ *lah*<sup>343</sup> were cultured on modified De Man Rogosa Sharpe (mMRS) medium for 24 h at 30 °C. Microbial conversion of linoleic acid to HUFA was achieved by subculturing the strains with a 5% (v/v) inoculum in mMRS broth containing 4 g/L linoleic acid, followed by an anaerobic incubation for 4 days at ambient temperature.<sup>15</sup>

*Aspergillus niger* FUA5001, *Mucor plumbeus* FUA5003, *Penicillium roqueforti* FUA5004, *Aspergillus clavatus* FUA5005, and *Aspergillus brasiliensis* ATCC16404 were cultivated on malt extract agar (MEA) at 25 °C for 7 days in darkness to harvest spores as described.<sup>49</sup> Briefly, spores

were freshly harvested from agar plates by adding 10mL of physiological solution (0.9% sodium chloride and 0.1% tween 80) and harvesting of fungal biomass with a sterile inoculum loop. The spore suspension was filtered to eliminate mycelial cells, and the spores were counted with a hemocytometer (Fein-Optik, Jena, Germany).<sup>51</sup> The spore counts were adjusted to  $10^4$  cfu/mL by dilution with mMRS broth. *A. niger* FUA5001 and *P. roqueforti* FUA5005 were also cultured on MEA for 2 days, and their mycelia, the white, thread-like edges of the colonies, were harvested by picking them with 1mL pipet tips prior to the MIC test.

The following yeasts were used in the MIC assays: *Zygosaccharomyces* spp. FUA4034, *Candida albicans* ATCC10231, *Candida humilis* FUA4001, *Saccharomyces cerevisiae* FUA4011, *Torulospora delbrueckii* FUA4023, *Wickerhamomyces anomalus* FUA4024, *Saccharomyces unisporus* FUA4027, *Candida valida* FUA4030, *Pichia membranefaciens* FUA4031, and *Pichia orientalis* FUA4032. *Zygosaccharomyces* spp. FUA4034 were cultivated on Potato Dextrose (PD) agar for 2 days; the other yeasts were cultivated on yeast-extract peptone dextrose (YPD) agar. To prepare inocula for the MIC assays, single colonies were picked and grown to the stationary phase in PD or YDP broth for 2 days at 30 °C. The optical densities of the yeast cultures at 600 nm was related to the cell count by counting with a hemocytometer, and the inocula of the yeasts were adjusted to  $10^4$  cell/mL by dilution to the corresponding optical density.

#### **4.2.3 Extraction of fatty acid mixtures from *Coriaria nepalensis* Wall. seed oil and from cultures of *L. plantarum* TMW1.460Alah and *L. hammesii* DSM16381**

The extraction from powdered seeds of *Coriaria nepalensis* Wall. seeds (XinTai Seed Production and Wholesale Co. Jiangsu, China) was performed with hexane. For small-scale extraction, approximately 5 g of powdered seeds were used with 200 mL of boiling hexane in a

Soxhlet extractor. After a 6 h extraction, the solvent was evaporated under reduced pressure. For large-scale production, 300 g of powdered *C. nepalensis* seeds were boiled in 2 L round-bottom bottle with 600 mL of hexane, refluxed for 6 h, and separated from the solvent, and the solvent in the extract was evaporated. The oil was stored at -20 °C with nitrogen.

Saponification of *Coriaria* seed oil was performed as described with minor modifications.<sup>200</sup> In brief, 5 g of *C. nepalensis* seed oil was dissolved in 50 mL 10% KOH in ethanol and refluxed at 70 °C for 4 h at a stirring speed of 200 rpm. After the reaction, 50 mL of water was added, and the ethanol was mostly evaporated under reduced pressure. The nonsaponifiable lipids in the aqueous fraction were extracted by adding 100 mL of hexane; this extraction was repeated three times. The remaining aqueous phase was then acidified with 12% (v/v) HCl, and the fatty acids were extracted three times with 100 mL of hexane. The hexane fractions were combined and washed with distilled water until a pH of approximately 5 was achieved. The final hexane extract was dried in rotary evaporator under reduced pressure.

The extraction of fatty-acid mixtures from cultures of the *Lactobacillus* spp. was performed as described.<sup>343, 349</sup> In brief, 250 mL of culture was adjusted to a pH of 2, and the fatty-acid mixtures were extracted with 250 mL of chloroform-methanol (85:15%, v/v); the extraction was repeated three times. Extracts in the lower phase were combined and evaporated to dryness under vacuum.

#### **4.2.4 LC-MS and MS/MS analyses of fatty acids**

The fatty acids were dissolved in methanol to a concentration of 50 mg/L and analyzed using reversed-phase liquid chromatography coupled with negative-ion electrospray-ionization tandem mass spectrometry (LC-ESI-MS/MS) and normal-phase liquid chromatography coupled with negative-ion atmospheric-pressure-photoionization tandem mass spectrometry (LC-APPI-

MS/MS). The fatty acids were separated using an Ascentis Express C8 column (15 cm × 2.1 mm, 3 μm; Sigma, St. Louis, MO) at 25 °C using Agilent 1200 series LC system (Agilent Technologies, Palo Alto, CA). The samples (5 μL) were injected at 15 °C and eluted at 0.25 mL/min with a gradient of (A) water with 10 mM ammonium acetate and 0.2% acetic acid and (B) 98:2% acetonitrile-water with 10 mM ammonium acetate and 0.2% acetic acid. The gradient was 70 to 100% B in 23 min, which was followed by re-equilibration to 70% B, with a total run time of 30 min.

Negative-ion ESI-MS was performed on a 3200 QTRAP triple-quadrupole mass spectrometer (AB SCIEX, Concord, ON) coupled with a turbospray electrospray-ionization ion source. AB SCIEX Analyst 1.4.2 software was used for data acquisition and processing. Full-scan mode was used to identify fatty acids, and multiple-reaction-monitoring (MRM) mode was used for the quantitation of fatty acids. Nitrogen was used as the curtain gas, nebulizing gas and drying gas. The conditions of ion source and mass spectrometer were used as follow: The full-scan mass range was from  $m/z$  100-1000 at a frequency of 1 scan/s. GS1, GS2, and the curtain gas were set at 40, 60 and 25 arbitrary units, respectively. The declustering potential (DP), ion spray voltage, and ion-source temperature were set at -60 V, -4500 V, and 450 °C. The collision energy (CE), collision-cell entrance potential (CEP), and collision-cell exit potential (CXP) were -36 V, -20 V and -1 V. The dwell time was 40 ms. The MS transitions and retention times of fatty acids analyzed by LC/ESI-MS in multiple-reaction-monitoring (MRM) mode are listed in **Table 4.1**. The calibration curves were generated from dilution series of pure standards. Because no commercial external standards were available for coriolic acid, 13-OH C18:1 and 10-OH C18:1, the purity of the HSCCC-purified coriolic acid was verified by LC-MS and LC-UV and by NMR analysis, provided as service of the NMR facility of the Department of Chemistry at the University of Alberta (**Figure**

**4.1-4.3).** This purified fraction was used as an external standard for quantitation of coriolic acid. The calibration curve established with ricinoleic acid was used to quantify its isomers, 13-OH C18:1 and 10-OH C18:1 in the following LC-APPI-MS/MS analysis.

**Table 4.1.** MS transition and retention time of fatty acids in LC/ESI-MS/MS-MRM quantitative analysis

Compound	MS transitions (amu) Q1/Q3	Retention time (min)
Coriolic acid	295.2/277.2	5.2
13-OH C18:1	297.2/197.1	6.2
10-OH C18:1	297.2/185.1	6.2
Ricinoleic acid	297.2/183.1	6.2
Linolenic acid	277.2/277.2	11.9
Myristic acid	227.2/227.2	12.3
Linoleic acid	279.2/279.2	14.9
Palmitic acid	255.2/255.2	17.2
Oleic acid	281.2/281.2	18.4
Stearic acid	283.2/283.2	22.2
Heptadecanoic acid	269.2/269.2	19.8

Normal-phase LC-APPI-MS/MS was performed to confirm the molecular structures and concentrations of fatty acids, as described in a previous study with minor modifications.<sup>191 343</sup> Briefly, 2µL of 50 ppm fragmented fatty acids dissolved in hexane were separated on a PVA-Sil column (Waters Ltd, Mississauga, Canada) at 25 °C with mobile phase comprised of (A) 0.2% acetic acid in hexane and (B) 0.2% acetic acid in isopropanol. The gradient was as follow: 99% A

at 0 min, 70% A at 20 min, and 99% A at 20.1 min, with total run time of 27 min. Fatty acids were detected by APPI-MS/MS on a QStar Elite hybrid orthogonal Q-TOF mass spectrometer equipped with a PhotoSpray source (Applied Biosystems/MDS Sciex, Concord, ON). The following parameters were used: nebulizer gas, 65; auxiliary gas, 10; curtain gas, 25; ionspray voltage, -1300 V; source temperature, 325 °C; declustering potential (DP), -35 V; focusing potential (FP), -130 V; and DP2, -13V. In addition to a total-ion scan of  $m/z$  50-1000, a product-ion scan ( $m/z$  50-700) of  $m/z$  295.2 was also performed in the fragmented *Coriaria* sample, and a product-ion scan ( $m/z$  50-700) of  $m/z$  297.2 was done for the two fragmented samples from *Lactobacillus* fermentation. The data were analyzed using Analyst QS 2.0.

#### 4.2.5 Measurement of partition-coefficient ( $K$ ) values

The solvent system for HSCCC separation was optimized by measuring the partition coefficient ( $K$ ) as described by Ito with modifications.<sup>59</sup> The sample or standard was dissolved in approximately 10 mL of the respective solvent system and mixed, and the upper and lower phases were separated. After the addition of 5 mg/L of a C17:0 fatty acid as the internal standard, the fatty acids in the upper and lower phases were quantified by MRM-mode LC-ESI-MS/MS analysis. The results were recorded as the average of duplicate measurements. The partition coefficients,  $K$ , of the compounds of interest was calculated as:

$$K = \frac{\text{Peak area}_{\text{Upper phase}}}{\text{Peak area}_{\text{Lower phase}}}$$



#### 4.2.6 Purification of fatty acids by high-speed counter-current chromatography (HSCCC)

A TBE-300B HSCCC system was used to purify mono-HUFA. The system was configured with a Model 501 PrimeLine solvent delivery module (Analytical Scientific Instruments, El Sobrante, CA), a multilayer coiled column with 260 mL column capacity ( $\beta=0.5-0.8$ ) and 1.9 mm i.d. tubing (Tauto Biotech, Shanghai, China), a VUV-24 Visacon UV-Vis detector (Reflect Scientific Inc., Orem, UT), and a CHF 122SC fraction collector (Avantec Toyo Kaisha Ltd., Tokyo, Japan).<sup>191, 60</sup> The 2 L solvent system was equilibrated after mixing and settling; and the upper phase was used as the stationary phase, and the lower phase was used as the mobile phase. The HSCCC column was filled with the stationary phase and rotated at 1000 rpm, which was followed by the introduction of the mobile phase at a constant flow rate of 3 ml/min. The column was equilibrated until the elution of the mobile phase was constant. Samples (200 mg of *Coriaria* oil extract or 250 mg of an extract from a *Lactobacillus* cultures) were dissolved in 5 mL of the upper phase and 5 mL of the lower phase and injected in the column. The elution of coriolic acid from *Coriaria* seed oil or of the mono-OH C18:2 fatty acids eluted before mono-OH C18:1 from the fermentations was monitored at a wavelength of 242 nm. The fractions were collected every 3 minutes, and the composition of each fraction was analyzed by ESI-MS/MS flow injection. The fractions containing the mono-HUFA of interest without interference compounds were combined, evaporated to dryness under vacuum, and then freeze-dried to eliminate water. The identity of each purified mono-HUFA was confirmed by LC-MS/MS as described above.

#### 4.2.7 Minimum-inhibitory-concentration (MIC) assay

The antifungal activities of the fatty-acid standards and fatty acids after purification by HSCCC were determined by a critical dilution assay.<sup>51</sup> The fatty acids were dissolved in 100% ethanol to

concentrations of 42.7 g/L for mono-HUFA and 85.3 g/L of oleic acid and linoleic acid. A solution of calcium propionate (21.3 g/L in 50% ethanol) was used for comparison. For each experiment, 100  $\mu$ L of the fatty-acid stock solution was mixed with 100  $\mu$ L of mMRS both (for the conidiospores and sporangiospore) or YPD or PD broth (for the yeasts) in 96-well microtiter plate, followed by a series of 2-fold dilutions with the respective growth medium. The ethanol was evaporated by placing microtiter plates without a lid in a laminar flow hood until 50  $\mu$ L of ethanol placed in an empty well of the same plate was completely evaporated. The wells were inoculated with  $10^4$ cfu/mL spores or vegetative cells of the indicator organism or with mycelia picked from the thread-like edge of colonies. The controls contained inocula, but ethanol was used instead of the fatty-acid stock solutions. The growth was observed visually; the minimum inhibitor concentration (MIC) was recorded 1 day after growth was visible in the absence of inhibitors. The MICs were reported as the minimum concentration of fatty-acid analytes that inhibited the growth of fungal strains tested. The MIC values were determined in three independent experiments using replicate preparations of the conidiospores.

## 4.3 Results

### 4.3.1 Identification and quantification of fatty acids in *Coriaria* seed oil and in the lipids extracted from *Lactobacillus* cultures

To compare the abundance of mono-HUFA from different sources, the hydroxy fatty acids in seed oil and in the lipid extracts of the microbial cultures were quantified by LC-MS/MS (**Table 4.2**). The MS/MS fragmentation pattern of coriolic acid included molecular ion  $[M-H]^-$  at  $m/z$  295.2259, and the characteristic fragmentation ions of  $m/z$  277.2162  $[M-H-H_2O]^-$ , 195.1393  $[C_{12}H_{19}O_2]^-$ , and 113.0971  $[C_7H_{13}O]^-$ .<sup>350</sup> These distinctive fragments were monitored in

quantitative LC-MS/MS-MRM experiments. The MS/MS fragmentations of 10-OH C18:1 and 13-OH C18:1 were consistent with prior reports<sup>343</sup>. The characteristic fragment ions of 10-OH C18:1 and 13-OH C18:1 were observed at  $m/z$  185.1 [ $C_{10}H_{17}O_3$ ]<sup>-</sup> and at  $m/z$  197.2 [ $C_{12}H_{21}O_2$ ]<sup>-</sup>, respectively, resulting from the  $\alpha$ -cleavage of hydroxy group at carbon-10 and -13, respectively (**Figure 4.4**).<sup>191</sup>

The exact stereoisomerism of coriolic acid from *Coriaria* seed oil was proposed to be (*R*)-13-hydroxy-*cis*-9,*trans*-11-octadecadienoic acid;<sup>155</sup> this configuration differs from coriolic acid produced by soy lipoxygenase and from reduction of the peroxide.<sup>351</sup> We confirmed the *cis/trans* configuration of this structure using NMR analysis. The structural features of coriolic acid as revealed by the NMR spectra (**Figure 4.1-4.3**) matched the published NMR data on coriolic acid, all reprinted (adapted) with permission from “Ding, L.; Peschel, G.; Hertweck, C. Biosynthesis of archetypal plant self-defensive oxylipins by an endophytic fungus residing in *Mangrove Embryos*. *ChemBioChem* 2012, 13, 2661-2664.” Copyright (2012) John Wiley and Sons (WILEY-VCH Verlag GmbH & Co. KGaA, Weinheim).<sup>350</sup>

**Table 4.2.** Fatty acid content (% w/w) in lipid extracts from *C. nepalensis* seed oil and lipids extracted from *L. hammesii* and *L. plantarum* TMW1.460 $\Delta$ lah cultures.

Lipid samples	Fatty acids*							
	RA	CA	LA	PA	SA	OA	10-OH C18:1	13-OH C18:1
<i>Coriaria</i> oil	0.89±0.02	66.7±3.4	10.6±0.2	1.78±0.30	2.68±0.04	4.67±0.33	NF	NF
<i>L. hammesii</i> extract	NF	6.24±0.00	67.3±22.2	NF	NF	0.67±0.08	12.3±2.2**	NF
<i>L. plantarum</i> TMW1.460 $\Delta$ lah extract	NF	1.71±0.08	72.5±16.6	NF	NF	0.64±0.10	NF	4.06±0.35 **

\*RA=ricinoleic acid; CA=coriolic acid; LA=linoleic acid; PA=palmitic acid; SA=stearic acid; OA=oleic acid; 10-OH C18:1=10-hydroxy-12-octadecenoic acid; 13-OH C18:1=13-hydroxy-9-octadecenoic acid; NF=not found;

\*\* : Semi-quantitation using isomer standard of ricinoleic acid in full scan mode in LC/APPI-MSMS due to lack of standard.

\*\*\*: Values are presented as means ( $n=2$ )  $\pm$  standard deviation.

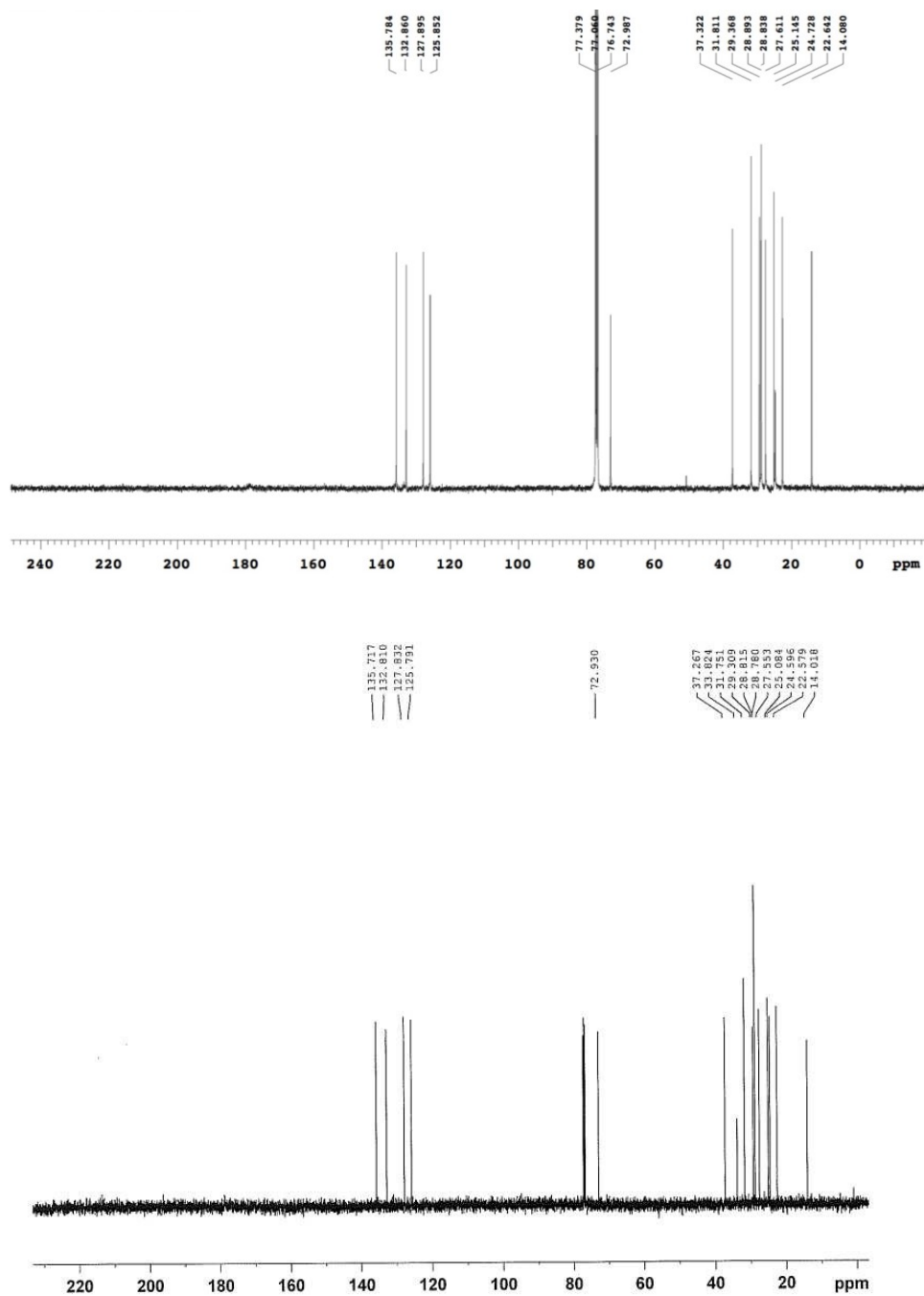


**Figure 4.1.**  $^{13}\text{C}$  NMR spectrum of purified HUFA from *Coriaria nepalensis* seed oil (400MHz,  $\text{CDCl}_3$ ) (upper) compared to the according spectrum published previously (125MHz,  $\text{CDCl}_3$ ) (lower) (adapted from Ref. <sup>350</sup>, Copyright (2012) John Wiley and Sons).



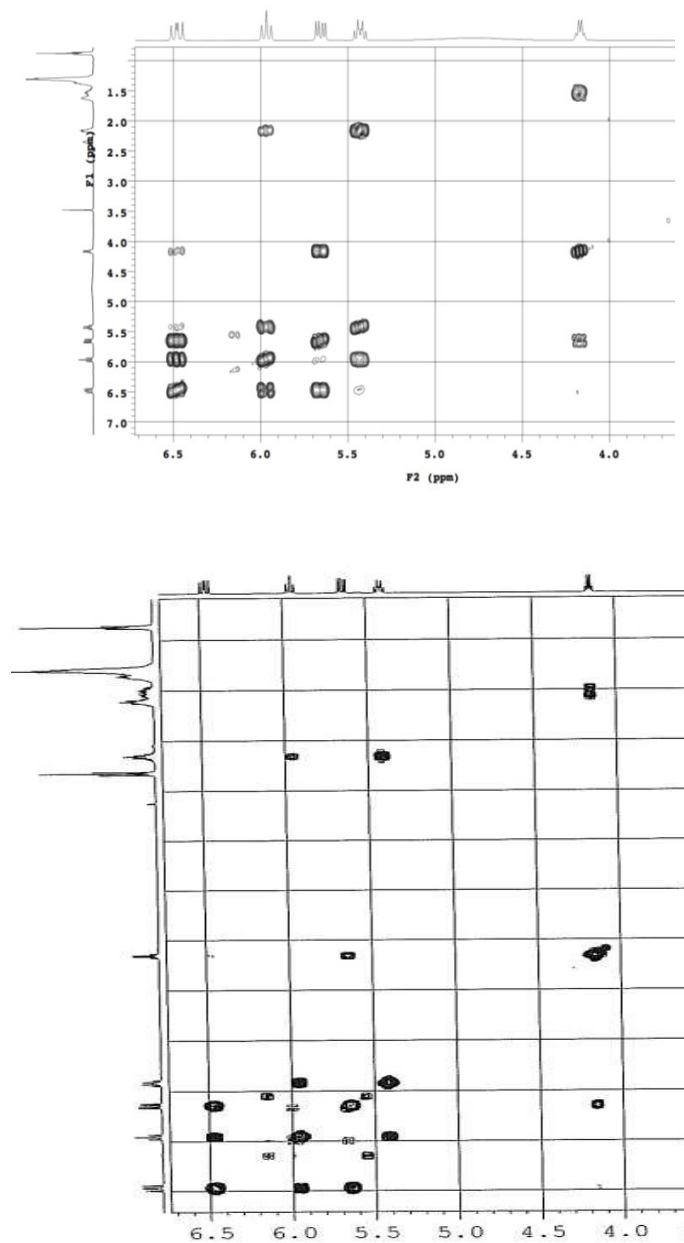


**Figure 4.3.** COSY analysis of purified HUFA from *Coriaria nepalensis* seed oil (400MHz, CDCl<sub>3</sub>) (upper) compared to the according spectrum published in a previous literature (lower) 500MHz, CDCl<sub>3</sub>) (adapted from Ref. <sup>350</sup>, Copyright (2012) John Wiley and Sons).

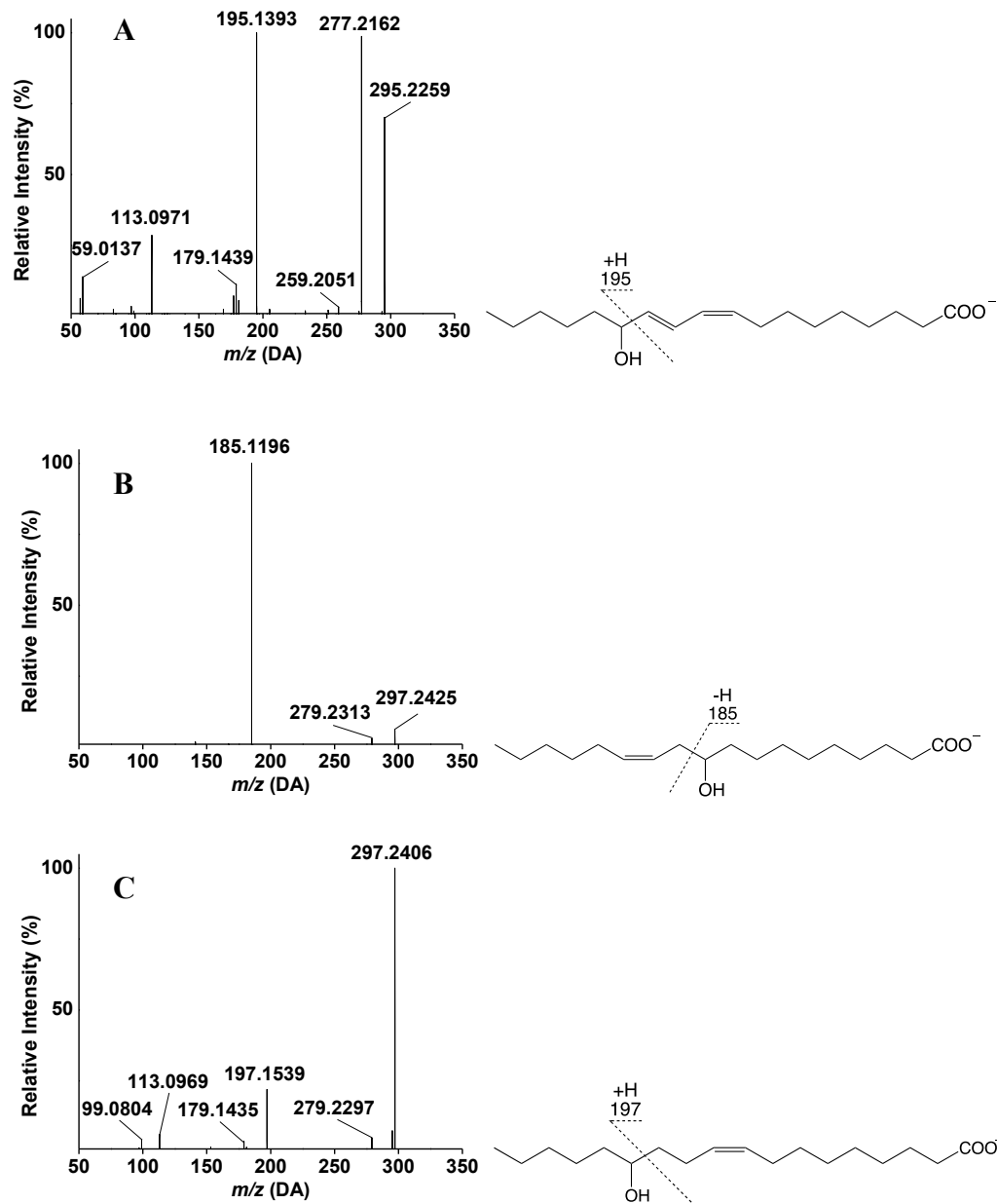


**Figure 4.4.** Negative-mode LC-APPI-MS/MS fragmentation spectra of antifungal fatty acids purified via HSCCC. **(A)** coriolic acid. **(B)** 10-hydroxy-12-octadecenoic acid (10-OH C18:1). **(C)** 13-hydroxy-9-octadecenoic acid (13-OH C18:1). The inserts indicate molecular structure and proposed fragmentation pattern.



The linoleate hydratases of lactobacilli were reported to produce (*S*)-13-OH-*cis*-9-octadecenoic acid from linoleic acid.<sup>307</sup> *L. hammesii* converted linoleic acid into a mixture of the *cis* and *trans* isomers of 10-OH C18:1;<sup>15</sup> however, the *S* configuration of 10-OH C18:1 from *L. hammesii* has not been confirmed. Likewise, the configuration of 13-OH C18:1 produced by *L. plantarum* TMW1.460 remains unknown. Because our data on the antifungal activity of coriolic acid demonstrates that the *R*- and *S*-isomers of HUFA have equivalent antifungal activities, the configuration of the HUFA from lactobacilli was not further investigated.

Coriolic acid accounted for 67% of the fatty acids in *Coriaria* seed oil, consistent with prior reports.<sup>73, 200</sup> The lipids extracted from cultures of *L. hammesii* and *L. plantarum* TMW1.460 $\Delta$ lah consisted of the fermentation products 10-OH C18:1 and 13-OH C18:1, linoleic acid, and traces of oleic acid.<sup>343</sup> In both cases, isomers of coriolic acid were also present, likely resulting from the auto-oxidation of linoleic acid. The yield of 13-OH C18:1 from *L. plantarum* TMW1.460 $\Delta$ lah was lower than the yield of 10-OH C18:1 from *L. hammesii*. This observation indicates that the 13-linoleate hydratase in *L. plantarum* TMW1.460 $\Delta$ lah is less active than the 10-OH hydratase in *L. hammesii*.

#### **4.3.2 Optimization of HSCCC solvent systems and preparative separation of HUFA by HSCCC**

To purify the antifungal mono-HUFA fatty acids by HSCCC, the solvent system was optimized to achieve a partition coefficient (*K*) in the range of  $0.5 \leq K \leq 2.0$  for analytes of interest. In addition, the separation factor  $\alpha = K_1/K_2$  was considered if two compounds were present in the same sample. The solvent systems were chosen to obtain an  $\alpha = K_1/K_2$  of  $> 1.5$ .<sup>59, 352</sup> Twelve solvent systems were evaluated (**Table 4.3**) and hexane-ethyl acetate-methanol-water (HEMW, 5:1.5:3:2, v/v/v/v) was

chosen on the basis of the partition coefficient and separation factor. The partition coefficient  $K_{\text{coriolic acid}}$  was 1.5 and the separation factor  $\frac{K_{\text{coriolic acid}}}{K_{\text{ricinoleic acid}}}$  was 1.5. This solvent system resulted in an elution time for coriolic acid of 147 min. A faster elution of coriolic acid of 112 min was achieved with hexane-ethyl acetate-methanol-water (HEMW, 3.5:1.5:3.5:2, v/v/v/v) but the partition and separation coefficients were reduced to  $K_{\text{coriolic acid}}=0.9$  and  $\frac{K_{\text{coriolic acid}}}{K_{\text{ricinoleic acid}}}=1.3$ . Using this solvent system, adequate separation between the HSCCC peaks of coriolic acid and ricinoleic acid was achieved, such that the majority of coriolic acid could be collected in pure fractions (**Figure 4.5**). Both solvent systems resulted in consistent retention times (data not shown), each with >70% retention of the stationary phase after the equilibrium of the HSCCC system. A sample loading of  $202.60 \pm 2.08$  mg of saponified fatty acids from *Coriaria* oil per HSCCC run yielded  $115.32 \pm 6.04$  mg of purified coriolic acid; this corresponded to a purification yield of  $56.9 \pm 2.5\%$  and an average recovery of coriolic acid of 85% in the pure fractions. The molecular structure and purity of fatty acids were confirmed by LC-APPI-MS/MS (**Figure 4.4 and 4.6**). After purification, all fatty acids eluted as single peak without contamination and were detected by LC-APPI-MS/MS analysis (**Figure 4.6**).

**Table 4.3.** Partition coefficients (*K*) of the target components in different hexane-ethyl acetate-methanol-water (HEMW) solvent system

	HEMW System (v/v)	Partition coefficient ( <i>K</i> ) value						
		CA	RA	MA	LA	PA	OA	SA
1	5:6:5:6	15.3	19.9	48.6	86.2	76.3	113.0	81.4
2	1:1:1:1	9.8	11.1	71.0	107.6	113.8	142.6	158.4
3	3:2:3:2	2.1	2.4	21.2	34.5	38.8	48.0	58.7
4	5:1.5:3:2	1.5	2.3	29.8	49.0	62.9	70.7	100.0
5	4:1.5:3:2	1.6	2.3	29.8	45.7	48.1	64.9	76.0
6	3.5:1.5:3:2	1.7	2.3	26.7	43.5	45.7	62.4	73.8
7	5:2:5:2	0.5	0.5	9.5	12.8	18.8	21.9	30.5
8	3:2:3.5:1.5	0.8	0.9	8.9	13.8	17.4	19.7	26.0
9	3.5:1.5:3.5:1.5	0.6	0.7	9.7	14.5	19.5	22.9	31.1
10	3.5:2:3.5:1.5	0.7	0.9	9.4	13.2	18.1	19.8	28.0
11	3.5:2:3.5:2	1.1	1.4	18.3	28.2	31.4	37.4	54.1
12	3.5:1.5:3.5:2	0.9	1.1	15.7	27.1	38.9	47.4	62.5

\*RA=ricinoleic acid; CA=coriolic acid; LA=linoleic acid; PA=palmitic acid; SA=stearic acid; OA=oleic acid; 10-OH C18:1= 10-hydroxy-12-octadecenoic acid; 13-OH C18:1= 13-hydroxy-9-octadecenoic acid.

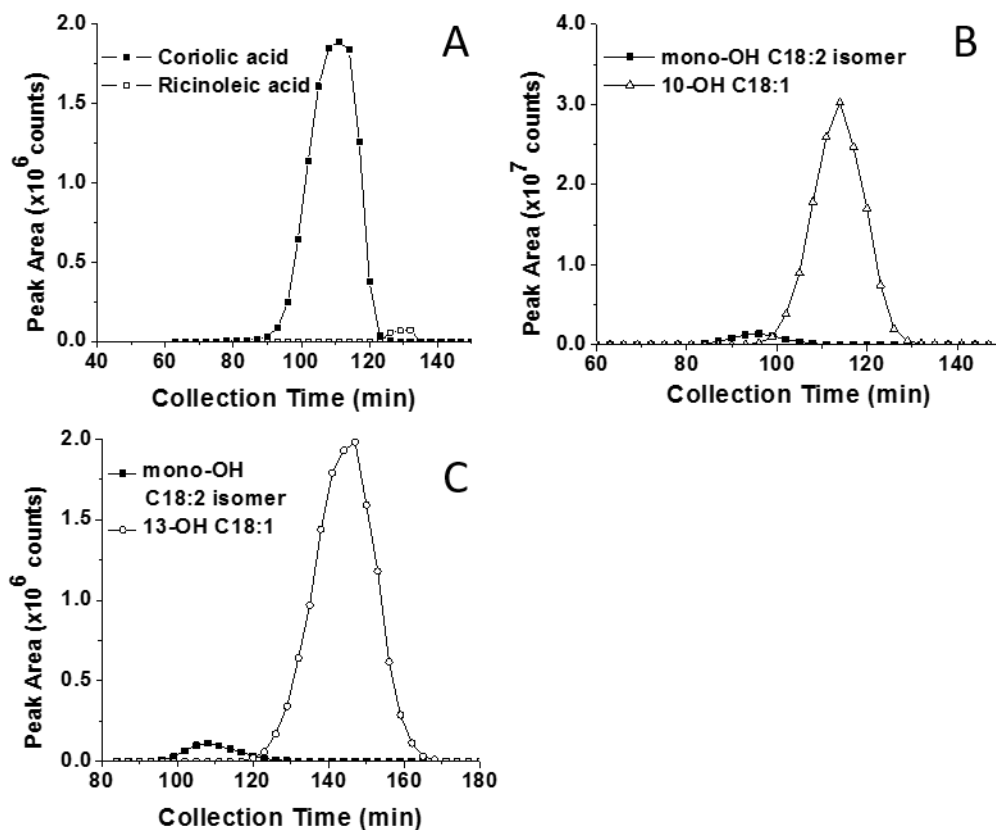


**Figure 4.5.** ESI-MS/MS flow injection analysis of HSCCC purification fractions collected during HSCCC purification using solvent system of HEMWat (3.5:1.5:3.5:2, v/v/v/v). Panel A, fractionation of hydrolyzed *Coriaria* seed oil. Panel B, fractionation of lipids extracted from cultures of *L. hammessi*. Panel C. fractionation of lipids extracted from *L. plantarum* TMW1.460 $\Delta$ lah. The compositions of peaks of analytes of interest were monitored by different ion transition, i.e., coriolic acid and mono-OH C18:2 isomer (Q1/Q3=295.2/197.2), ricinoleic acid (Q1/Q3=297.2/183.1), 10-OH C18:1 (Q1/Q3=297.2/185.1) and 13-OH C18:1 (Q1/Q3=297.2/197.1).

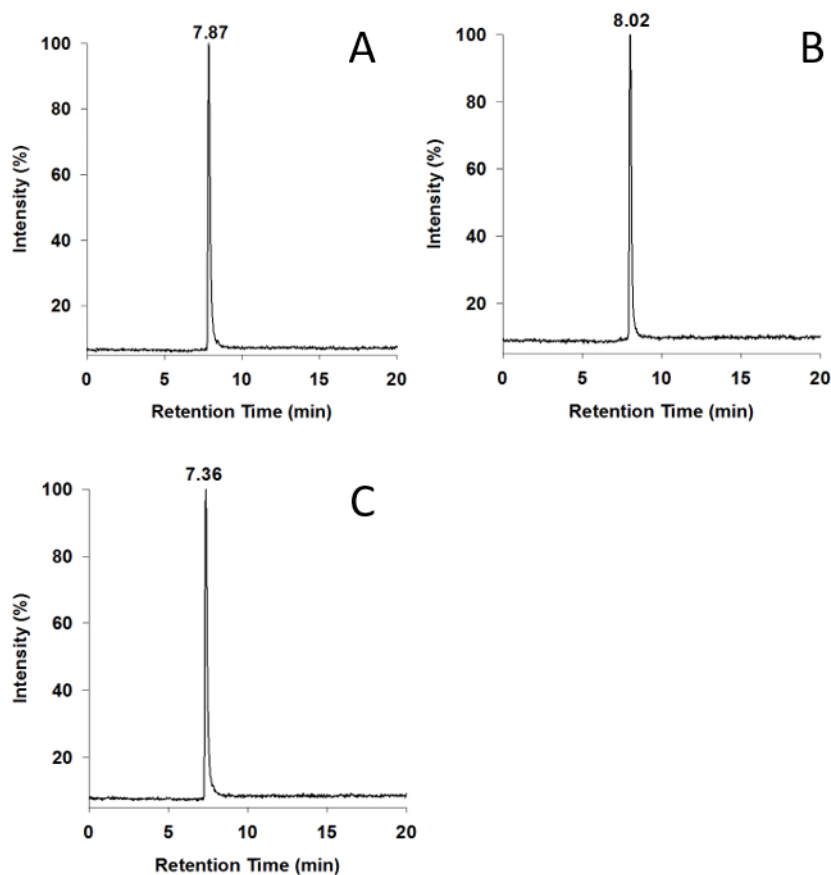


**Figure 4.6.** Negative-mode LC-APPI-MS total ion chromatogram (TIC) of antifungal fatty acids purified via HSCCC. Panel A. coriolic acid; Panel B. 10-OH C18:1 (10-hydroxy-12-octadecenoic acid); Panel C. 13-OH C18:1 (13-hydroxy-9-octadecenoic acid).

### 4.3.3 Antifungal activity of mono-HUFA and other UFA

HSCCC purification provided sufficient amounts of coriolic acid to test its antifungal activity against a broad spectrum of organisms. The antifungal spectrum of coriolic acid was compared with those of the two other major fatty acids in *Coriaria* seed oil, that is, linoleic acid and oleic acid, to ascertain the role of the hydroxy group on antifungal activity (**Table 4.4**). Conidiospores

and sporangiospores are asexual propagules produced by filamentous fungi.<sup>353</sup> Conidiospores from *Aspergillus* spp. and *P. roqueforti* as well as sporangiospores from *M. plumbeus* were sensitive to coriolic acid, with MICs  $\leq 1$  g/L. The MIC of linoleic acid and oleic acid against spores were higher than those of coriolic acid (**Table 4.4**). Similarly, fungal mycelia were sensitive to coriolic acid but not to oleic and linoleic acids. In contrast to the mycelia fungi, all yeasts tested in this assay were resistant to coriolic acid (**Table 4.4**). This implies that the presence of hydroxyl groups contributes highly to the specific structure-function relationships of fatty acids in the inhibition of foodborne spoilage or pathogenic fungi.

To determine whether the structure of monohydroxy unsaturated fatty acids determines their antifungal activity, the MIC of coriolic acid, ricinoleic acid, 10-OH C18:1, and 13-OH C18:1 was determined with two indicator strains (**Table 4.5**). Regardless of their degrees of unsaturation or the position of the carbon double bonds and hydroxy groups, the HUFA had similar inhibition effect against the two filamentous fungi tested.

**Table 4.4.** Minimum inhibitory concentration (MIC) of coriolic acid against food spoilage and pathogenic fungi compared to linoleic acid and oleic acid. Data are shown as means  $\pm$  standard deviation of triplicate independent experiments.

Strains		MIC of fatty acids (g/L)		
		Coriolic acid	Linoleic acid	Oleic acid
Conidiospores	<i>A. niger</i>	0.29 $\pm$ 0.07	3.67 $\pm$ 1.53	$\geq$ 8
	<i>P. roqueforti</i>	0.33 $\pm$ 0.14	3.33 $\pm$ 1.15	$\geq$ 8
	<i>A. brasiliensis</i>	0.42 $\pm$ 0.14	3.33 $\pm$ 1.15	$\geq$ 8
	<i>A. clavatus</i>	0.38 $\pm$ 0.13	6.67 $\pm$ 2.31	$\geq$ 8
Sporangiospores	<i>M. plumbeus</i>	0.67 $\pm$ 0.29	3.33 $\pm$ 1.15	$\geq$ 8
Mycelia	<i>A. niger</i>	0.07 $\pm$ 0.05	6.00 $\pm$ 3.46	$\geq$ 8
	<i>P. roqueforti</i>	0.27 $\pm$ 0.22	6.67 $\pm$ 2.31	$\geq$ 8
Yeasts	<i>C. albicans</i>	$\geq$ 8	$\geq$ 8	$\geq$ 8
	<i>C. humilis</i>	$\geq$ 8	6.67 $\pm$ 2.31	$\geq$ 8
	<i>S. cerevisiae</i>	$\geq$ 8	$\geq$ 8	$\geq$ 8
	<i>T. delbrueckii</i>	$\geq$ 8	$\geq$ 8	$\geq$ 8
	<i>W. anomalus</i>	4.00 $\pm$ 0.00	$\geq$ 8	$\geq$ 8
	<i>S. unisporus</i>	$\geq$ 8	$\geq$ 8	$\geq$ 8
	<i>C. valida</i>	$\geq$ 8	4.00 $\pm$ 0.00	$\geq$ 8
	<i>P. membranaefaciens</i>	$\geq$ 8	6.67 $\pm$ 2.31	$\geq$ 8
	<i>P. orientalis</i>	$\geq$ 8	$\geq$ 8	$\geq$ 8
<i>Zygosaccharomyces</i>	5.33 $\pm$ 2.31	$\geq$ 8	$\geq$ 8	

**Table 4.5.** Minimum inhibitory concentration (MIC) comparison of four mono-hydroxy fatty acids against *A. niger* and *P. roqueforti*. Data represent means  $\pm$  standard deviation of triplicate independent experiments.

Strains	MIC of HUFA (g/L)			
	Coriolic acid	Ricinoleic acid	10-OH C18:1	13-OH C18:1
<i>A. niger</i>	0.29 $\pm$ 0.07	0.33 $\pm$ 0.14	0.50 $\pm$ 0.00	0.42 $\pm$ 0.14
<i>P. roqueforti</i>	0.33 $\pm$ 0.14	0.42 $\pm$ 0.14	0.42 $\pm$ 0.14	0.42 $\pm$ 0.14

#### 4.4 Discussion

This work developed HSCCC as an efficient method for preparative purification of antifungal mono-HUFA from *Coriaria* seed oil and *Lactobacillus* cultures. The amounts of purified compounds obtained by HSCCC were sufficient to investigate the antifungal spectrum of mono-HUFA with a panel of 15 indicator strains. Remarkably, mycelial fungi were sensitive to HUFA, but yeasts were highly resistant.

To purify the target HUFA and avoid interference from other compounds in the original samples, HSCCC was used as an efficient purification method. HSCCC purified fatty acids from diverse matrixes without derivatization or combination with other separation technologies. The separation factors,  $\alpha$ , between fatty acids of interest in this study and their closest elution interferences indicated good separation efficiency.<sup>59</sup> The analytes were obtained in sufficient amounts to allow the screening of their inhibitory spectrum against a wide range of indicator organisms.

The antifungal activity of HUFA was suggested to be specific for target fungi.<sup>13, 12</sup> This study therefore compared the activities of HUFA against mycelial fungi to their activities against yeasts.



Yeast strains included baker's yeast, *S. cerevisiae*; yeasts involved in traditional food fermentations, *C. humilis*, *T. delbrueckii*, *W. anomalus*, and *S. unisporus*; the spoilage yeasts *C. valida*, *P. membranefaciens*, *P. orientalis*, and *Zygosaccharomyces*, and the pathogenic *C. albicans*. Coriolic acid was active against asexual spores and mycelia of filamentous fungi but inactive against yeasts. HUFA are thus unlikely to inhibit food spoilage caused by yeasts but can be applied as effective antifungal agents in fermented foods that require the growth and activity of yeasts.<sup>41</sup> In contrast, medium-chain hydroxy fatty acids from *L. plantarum* inhibited yeasts more actively than it did filamentous fungi.<sup>129</sup> This may be explained by the diversity in the chemical compositions of the membranes of different fungi<sup>354</sup> and differences in the interactions of medium-chain and long-chain fatty acids with fungal membranes.

The comparison of different antifungal HUFA also allowed for the inference of the structural requirements of their antifungal activity. The antifungal activity of HUFA depended on the presence of hydroxy groups in the middle of the carbon chain,<sup>13, 15, 12</sup> and varied with the number<sup>355, 299</sup> and position<sup>12</sup> of the hydroxy groups. Unsaturation was critical to the antifungal activity of long-chain HUFA<sup>15, 342</sup> but not for the middle-chain HUFA.<sup>129</sup> The position of the double bond<sup>12</sup> and chirality<sup>337, 339, 342</sup> were reported to have only minor impacts on the antifungal activity. Our data also support the conclusion that HUFA with *R* and *S* configurations have equivalent activities. The activity of (*R*)-13-OH-*cis*-9,*trans*-11-coriolic acid extracted from *Coriaria* seed oil against *A. niger* and *P. roqueforti* (this study) was comparable to the activity of coriolic acid generated from soybean lipoxygenase.<sup>15, 343</sup> Soy lipoxygenase generates the *S*-isomer of coriolic acid (98% (*S*)-13-OH-*cis*-9,*trans*-11).<sup>351</sup> The MIC data are in general agreement with prior studies;<sup>15, 343</sup> however, we observed a higher activity for ricinoleic acid than that in previous reports.<sup>15</sup> This discrepancy with prior reports warrants further comparisons of the activities of ricinoleic acid and coriolic acid

with larger panels of indicator strains. The present study additionally demonstrates that hydroxy groups are essential for the antifungal activities of fatty acids. Moreover, all HUFA with hydroxy groups in the center of the acyl chains exhibited comparable antifungal activities.

The mechanism of antifungal HUFA has been explained by their detergent-like interactions with cell membranes,<sup>13, 354</sup> and hence differences in fungal resistance of HUFA may relate to variations in membrane composition. However, the antifungal activity of HUFA may also relate to other aspects of fungal physiology. For example, (*R*)-8-hydroxy-*cis*-9,*cis*-12-octadecadienoic acid (8-OH C18:2), an isomer of coriolic acid, is a precocious-sexual-inducer ( $\psi$ ) Ba factor that regulates the sexual development of *Aspergillus* spp.<sup>148</sup> The same compound has antifungal activity against phycomycetous fungi.<sup>149</sup> This compound was also associated with the regulation of conidia formation and the production of fumonisins by *Fusarium verticillioides*.<sup>150</sup> Those roles of HUFA in fungal physiology and ecology indicate that their modes of action may be species-specific. The HSCCC protocol, as developed in this study to allow the milligram- to gram-scale purification of HUFA, will facilitate future research on their modes of action.

Foodborne fungi may develop resistances to commonly used antifungal agents, including organic acids and their salts.<sup>356</sup> HUFA are present in foods with a tradition of safe use<sup>15, 191, 357</sup> and were used as antifungal agents in food. Their activity in preventing fungal spoilage of bread was comparable to conventional preservatives.<sup>15</sup> The resistance of yeasts restricts the use of HUFA to foods in which spoilage yeasts, such as *Zygosaccharomyces bailii*, *Pichia* spp., and *Candida* spp. are not relevant.<sup>358</sup> Conversely, their specific inhibitory spectrum allows their use in fermented foods (e.g. bread) in which the inhibition of CO<sub>2</sub> and flavor formation by *S. cerevisiae* or sourdough yeasts would compromise food quality.<sup>15</sup> Their use may also prevent phytopathogenic fungi in plant production. In plants, UFA and their oxygenated derivatives not

only act as antifungal agents but also are critical in signaling self-defense responses.<sup>12, 359, 360</sup> The present study extended the range of the potential uses of HUFA to food preservation and plant protection.

In conclusion, an efficient HSCCC-based method of purifying useful quantities of antifungal fatty acids has been established and has enabled investigations of the biological functions of HUFA. A comparison of species-specific antifungal abilities among coriolic acid, linoleic acid, oleic acid, and two monohydroxy C18:1 fatty acids provided insights into the structure-function relationships of antifungal fatty acids. It confirmed the contribution of hydroxy groups to the antifungal abilities of fatty acids. In addition, it has demonstrated that the potential applications of antifungal fatty acids should be further explored for prolonging food shelf life and controlling plant diseases, both of which directly relate to significant economic losses and health concerns worldwide.

## **Chapter 5. An investigation into the relationship between the structures of monohydroxy unsaturated fatty acids and their antifungal activities**

### **5.1 Introduction**

Fungal food spoilage contributes substantially to the 1.3 billion tons of annual global food lost or wasted at the retail or household levels,<sup>19, 20</sup> and the associated allergens and mycotoxin production additionally constitute food safety risks.<sup>21</sup> Furthermore, the populations of spoilage fungi which are threats to food safety and food security, may undergo changes due to increasingly complex food value chains,<sup>24</sup> and due to climate change.<sup>25</sup>

Common perishable or processed foods that are susceptible to fungal spoilage include in some types of fruits, vegetables, bread, cereals, nuts and refrigerated foods with longer storage lives.<sup>20, 21</sup> Currently used preservatives, such as propionic acid or sorbic acid, impact food flavor and may be incompatible with the food industry's efforts to offer "clean-label" products.<sup>33, 34</sup> Thus, it is of interest to explore alternative strategies for inhibiting fungal growth on agricultural commodities and food.

Natural plant defenses against pathogens provide a potential source of antifungal compounds for use in food since they often involve the production of defense compounds against such phytopathogens.<sup>12, 361</sup> In addition, bacterial symbionts can also be sources of defense compounds.<sup>362</sup> It is known that hydroxy-unsaturated fatty acids (HUFA) contribute to plant defenses against fungi.<sup>12, 35, 36, 37</sup> Both plants and bacteria can produce antifungal HUFA that have potential applications in food.<sup>15</sup> However, their role in microbial ecology and their antifungal activity in food are poorly documented.

The antifungal activity of HUFA has been shown to be related to the number of double bonds<sup>15</sup> and the number and the position of hydroxy groups.<sup>12, 355</sup> Additionally, different fungal species show different sensitivity toward HUFA; notably, yeasts show high resistance compared to filamentous fungi.<sup>66</sup> However, the reported structure function relationships are mainly limited to HUFA with hydroxylation at the  $\Delta 2$ -,  $\Delta 9$ -, and  $\Delta 13$ -positions, and to phytopathogens as indicator organisms.<sup>12</sup> The inhibitory spectrum against food fermentation and food spoilage organisms is largely unexplored and the mechanisms of resistance of individual yeasts or fungi have not yet been explained.

Plant oxylipins are only produced in small quantities during plant defense activities,<sup>35, 37</sup> and so are difficult to extract in sufficient quantities for investigation of their antifungal properties. In contrast, some plants seed oils contain high amount of HUFA,<sup>40, 38</sup> which can be fractionated for further study, for instance using high speed counter chromatography (HSCCC).<sup>66</sup> In addition, *Lactobacillus* species convert linoleic acid into 10-hydroxy-12 octadecenoic acid and 13-hydroxy-9-octadecenoic acid.<sup>343</sup> These sources can provide diverse HUFA analogues that can be used in studies of the HUFA structure-function relationships.

It has been proposed that the partition of HUFA into fungal membranes alters membrane fluidity, which provides the mode of action.<sup>13, 363, 354</sup> However, how this mechanism relates to the species-specific fungal resistance to HUFA<sup>12, 66</sup> is not well understood. Fungal sensitivity towards the membrane active fatty acid *cis*-9-heptadecenoic acid (C17:1) was accompanied by a lower fungal sterol content, which is an important membrane-fluidity modifier.<sup>354</sup> It remains unknown however, whether membrane composition, and particularly the distribution of sterols in fungal membranes, also relate to fungal resistance to HUFA.

To address these gaps in knowledge, this study aimed to obtain better understanding of the effect of HUFA structure on their antifungal activities, and on their interaction with fungal membranes. In order to do this, information on plant seed oils containing C18 mono-HUFA was retrieved from the PlantFAdb database,<sup>17</sup> which connects fatty acid structures with the plant species in which they have been found. After the plant seed oils were extracted, saponification and purification of HUFA fractions were performed by HSCCC. In addition, HUFA were also obtained through bacterial fermentation. The purified HUFA were characterized by LC-MS/MS and their antifungal activities against food-related yeasts and molds were determined. The relationship between the inhibitory spectrum of HUFA and their interaction with fungal membranes was assayed by determination of the membrane fluidity and the sterol content of fungi.

## 5.2 Materials and methods

### 5.2.1 Chemical materials

Plant seeds were purchased from the following sources: *Thymus vulgaris* L. (French Thymus) seeds were purchased from Richters Herbs (Goodwood, ON, Canada); *Dimorphotheca sinuata* DC. (African Daisy Seeds) seeds were obtained from High Country Gardens (Shelburne, VT, US) and *Mallotus philippensis* (Lam.) Muell. Arg. were obtained from Rarepalmseeds.com (München, Germany). *Coriaria nepalensis* Wall. seeds were purchased from XinTai Seed Production and Wholesale Company (Jiangsu, China).

ACS-grade hexane, ethyl acetate and methanol were purchased from Sigma-Aldrich (St. Louis, MO). Deionized ultra-filtered water was obtained from Fisher Scientific (Ottawa, Ontario, Canada). Laurdan (6-dodecanoyl-2-dimethylaminonaphthalene) was purchased from Thermo Scientific (Burlington, ON, Canada). Oleic acid and ricinoleic acid (purity > 99%) were obtained

from Nu-Chek Prep, Inc. (Elysian, MN). Microbiological media were obtained from Fisher Scientific.

### 5.2.2 Microbial strains and culture conditions

The filamentous fungi *Aspergillus niger* FUA5001 and *Penicillium roqueforti* FUA5004 were grown on malt extract agar (MEA) at 25 °C for 7 days; the yeasts *Pichia membranaefaciens* FUA4031, *Candida valida* FUA4030, *Candida albicans* ATCC10231, and *Saccharomyces cerevisiae* FUA4011 were cultured in yeast extract-peptone-dextrose (YPD) broth at 30 °C for 2 days and prepared for MIC test as previously reported.<sup>66</sup>

### 5.2.3 Extraction and saponification of oils from plant seeds rich in HUFA

In order to investigate the structure-function relationship of HUFA, mono-HUFA with various molecular structures were obtained via extraction and saponification of plant seed oil rich in HUFA. The distribution information of mono-HUFA in plant materials was obtained from PlantFAdb database (<https://plantfadb.org/>)<sup>40</sup> (Table 5.1). The extraction and saponification of plants seed oil followed the protocols for the production of coriolic acid from *Coriaria nepalensis* Wall. seed.<sup>66</sup> Briefly, 5g of plant seeds (*C. nepalensis*, *D. sinuata*, *M. philippensis* or *T. vulgaris*) were finely ground with liquid nitrogen respectively, and their total lipid fractions were then extracted using a Soxhlet extractor. Oils of *C. nepalensis*, *D. sinuata* and *T. vulgaris* were each extracted with 200mL hexane, 450rpm for 6 hours. For *Mallotus philippensis*, the same extraction conditions were applied except that petroleum ether (6h) and diethyl ether (6h) were used to extract this oil subsequently,<sup>167</sup> instead of using hexane. Then every 1g of extracted oil was saponified with 10mL

0.1g/mL ethanolic KOH solution at 70 °C, 450rpm, followed by the extraction of free fatty acid mixture described previously.<sup>66</sup>

#### 5.2.4 Purification and analysis of HUFA

A solvent system was developed for the high-speed counter-current chromatography (HSCCC) purification of individual HUFA. The partition coefficient ( $K$  value) of various hexane/ethyl acetate/methanol/water solvent systems was tested for each of the HUFA-containing saponified plant oils with modifications to optimize the separation for each analyte.<sup>66</sup> Briefly, a 100 g/L stock solution of saponified oil in methanol was prepared, a 50  $\mu$ L aliquot of which was added into 5 mL of a solvent system consist of hexane, ethyl acetate, methanol and water. Then, 200  $\mu$ L aliquots of both the upper phase and the lower phase were put into separate 2mL HPLC vials, each of which dried under nitrogen and re-dissolved with 1mL methanol. For each compound, the peak area from LC-ESI-MS/MS analysis in the MRM mode was recorded (as explained below) and a partition coefficient ( $K$  value) was calculated using the formula  $K = A_{upper}/A_{lower}$ , where  $A_{upper}$  and  $A_{lower}$  stands for the peak area of an analyte in the upper and lower phases, respectively.

Saponified plant oil (200mg) was then separated via HSCCC (TBE-300B HSCCC system, Tauto Biotech, Shanghai, China) with the selected solvent system using the published protocols.<sup>66</sup> Briefly, approximately 2L of the selected solvent systems were made in separation funnel and equilibrated overnight. The upper and lower phases were then separately collected. The upper phase (stationary phase) was first pumped (PrimeLine solvent delivery module, Analytical Scientific Instruments, El Sobrante, CA) in the system to fill up the HSCCC column (260 mL,  $\beta = 0.5$ – $0.8$ , 1.9 mm i.d. tubing). Following that, the mobile phase (lower phase) was pumped into the HSCCC column at 3mL/min with the column rotating (1000 rpm). Once the mobile phase started



constantly eluting out from the outlet, 200-250 mg of a saponified oil sample dissolved in 5mL of each of the 2 phases was injected into the HSCCC system. Fractions from the outlet were then collected every 3 min (CHF 122SC fraction collector, AvanteC Toyo Kaisha Ltd., Tokyo, Japan).

Each HSCCC fraction was then analyzed by flow-injection (FIA)-ESI-MS/MS analysis.<sup>66</sup> The specific ion transitions of various HUFA analogues used to monitor the elution of HUFA in the purification process are given in **Table 5.1**. This allowed identification of the fractions, which contained the target HUFA; these were collected, combined, dried, re-dissolved and analyzed for purity by LC-APPI-MS/MS.

In order to quantify HUFA in the saponified oil samples, and to measure the *K* value for HUFA partitioned between immiscible phases, LC-ESI-MS/MS was used in the MRM mode using the ion transitions indicated in **Table 5.1**.<sup>66</sup> Each sample (2  $\mu$ L) was separated on the Ascentis Express C8 column (15 cm  $\times$  2.1 mm, 3  $\mu$ m; Sigma, St. Louis, MO) at 25  $^{\circ}$ C within an Agilent 1200 series LC system (Agilent Technologies, Palo Alto, CA). The fatty acids were eluted at a flow rate of 0.25 mL/min with a gradient of mobile phases (A) water with 10 mM ammonium acetate and 0.2% acetic acid and (B) 98% acetonitrile with 10 mM ammonium acetate and 0.2% acetic acid. The gradient was 70 to 100% B in 23 min, followed by re-equilibration to 70% B, with a total run time of 30 min. A 3200 QTRAP triple-quadrupole mass spectrometer (AB SCIEX, Concord, ON) coupled with a turbospray electrospray-ionization ion source was used to perform negative-ion ESI-MS/MS. GS1, GS2, and the curtain gas were nitrogen and set at 40, 60, and 25 arbitrary units, respectively. The ion-spray voltage, ion-source temperature and dwell time were set at  $-4500$  V,  $450$   $^{\circ}$ C and 40 ms respectively. The declustering potential (DP), collision energy (CE), collision-cell entrance potential (CEP) and collision-cell exit potential (CXP) were specific for each target compound: for coriolic acid, DP  $-45.00$ , EP  $-7.00$ , CEP  $-18.00$ , CE  $-26.00$ , CXP  $-2.00$ ; for

dimorphecolic acid, DP -60.00, EP -12.00, CEP -20.00, CE -36.00, CXP -1.00; for kamlolenic acid, DP -60.00, EP -12.00, CEP -22.50, CE 36.00, CXP -1.00; for 2-hydroxy oleic acid, DP -50.00, EP -7.00, CEP -14, CE -28.00, CXP 0.00.

Data acquisition and processing was performed using AB SCIEX Analyst 1.4.2 software. To analyze the HSCCC fractions using FIA-ESI-MS/MS, the same method was used except the gradient was kept at the starting point for 2 min, followed by a gradient of 70 to 100% B in 23 min and re-equilibration to 70% B, with a total run time of 32 min.

To analyze the purified fractions by normal-phase LC-APPI-MS/MS,<sup>66</sup> 2  $\mu$ L of samples (50ppm in hexane) were separated by PVA-Sil column (Waters Ltd., Mississauga, ON) at 25 °C with gradient consist of (A) 0.2% acetic acid in hexane and (B) 0.2% acetic acid in isopropanol: 99% A at 0 min, 70% A at 20 min, and 99% A at 20.1 min (total run time 27min). APPI-MS/MS detection was performed using a QStar Elite hybrid orthogonal Q-TOF mass spectrometer equipped with a PhotoSpray source (Applied Biosystems/MDS Sciex, Concord, ON). The nebulizer gas, auxiliary gas, curtain gas, ionspray voltage, source temperature, declustering potential (DP), focusing potential (FP), and DP2 were set to 65, 10, 25, -1300 V, 325 °C, -35 V, -130 V and -13 V, respectively. MS full scan was obtained over the range of m/z 50–1000; for MS/MS, a product-ion scan at m/z 50–700 of the according molecular ion [M-H]<sup>-</sup> was also performed to characterize the purified HUFA. The data were analyzed using Analyst QS 2.0.

### 5.2.5 Antifungal test of hydroxy fatty acids

The collected purified HUFA was applied to challenge the growth of food-related fungi, including one human pathogenic yeast, *Candida albicans*, two spoilage yeasts, *Pichia membranaefaciens* and *Candida valida*, two filamentous fungi, *Aspergillus niger* and *Penicillium*

*roqueforti* and one food fermenting yeast, *Saccharomyces cerevisiae*. The minimum inhibitory concentration (MIC) of HUFA against these fungal strains was tested using a critical dilution assay.<sup>66</sup>

### 5.2.6 Extraction and GC-MS quantitation of fungal sterols

To determine the content of sterol, a representative membrane fluidity modulator, the fungi tissues were first prepared as follow: sub-culture was kept at 25 °C (filamentous fungi at mMRS broth) or 30 °C (yeasts at YPD broth) at 150 rpm for 3 days. The fungi tissues were then washed through centrifugation and rinsing with physiological water twice and sterile distilled water once before freeze-drying. Non-saponifiable components of fungal tissues were then extracted as described<sup>364</sup> with some modifications: 20 g of ground lyophilized tissues of fungi were weighed, followed by the addition of the internal standard (12.5 µL of 1.25 g/L 5 $\alpha$ -Cholestane in hexane). Later, 37.5 µL of pyrogallol solution (0.5% in ethanol, w/v), 25 µl potassium hydroxide solution (60%, w/w), 37.5 µL ethanol and 100 µL water were added into the sample. After vortexing, saponification was performed at 90 °C, 30 min. The reaction mixture was the cooled down, followed by the addition of 100 µL of water and 400 µL hexane. After vortexing and centrifugation, the upper phase of the mixture was collected, and the lower aqueous phase was re-extracted with another 400 µL of hexane twice. The hexane extracts were combined and dried under nitrogen. In order to silylate the –OH in the fungal sterol for improved GC separation,<sup>365</sup> mixture of BSA+TMCS+TMSI, 3:2:3 (Sylon BTZ) Kit (Supelco Inc., Bellefonte, PA, USA) (20 µL) and anhydrous pyridine (20 µL) were added in to the extracted non-saponifiable fractions and kept 60 °C, 15 min. Hexane (210 µL) was added into the reaction mixture. The mixture was first injected

neat into GC-MS for qualitative analysis, then a 1:4 (v/v) dilution in hexane was used in quantitative analysis.

The GC-MS analysis was performed on a 6890N GC system coupled with 5975B mass spectrometry in electron ionization mode. A column capillary column (30.0 m × 320.00 µm × 0.25 µm) was used. Helium was the carrier gas. Injection temperature was 290 °C and the solvent delay time set at 1.80 min. Split mode was used and the split ratio was set to 12.5:1, with injection volume 1.00 µL. The oven temperature was set at 245 °C initially with initial hold of 0.50 min, then increased to 265 °C at a rate of 2.00 °C/min, followed by a ramp to 290 °C at a rate of 3.60 °C/min, and final hold of 10.00 min. The total run time was 27.64 min. An MS scan range of *m/z* 50-1000 was applied.

### **5.2.7 Measurement of fungal membrane fluidity using Laurdan assay**

The fluorescent probe Laurdan was applied in the spectroscopic measurement of the fluidity changes of fungal membrane, as described previously with some modifications.<sup>66 366</sup> Briefly, 3-day fungal sub-culture was harvested via centrifugation and washed with 30 mL physiological water twice. Washed fungal tissue (10 mg) was weighed then 300 µL saline (9 g/L NaCl and 1 g/L Tween 80) was then added to re-suspend the fungal tissue. Laurdan solution (2 mM in ethanol) were added to the fungal tissue suspensions to a final concentration of 80 µM; they were then incubated in the dark for 3 hours at 25 °C. After incubation, fungal tissues were washed twice with saline (9 g/L NaCl and 1 g/L Tween 80) and re-suspended in saline with/without treatment of fatty acid (4 g/L) for 30 min (25 °C). The fluorescent intensity of treated sample at emission wavelength from 400 nm to 600 nm was recorded with excitation wavelength of 360 nm. Generalized polarization (GP) was calculated as  $GP = (I_{440} - I_{490}) / (I_{440} + I_{490})$ , where  $I_{440}$  and  $I_{490}$  were the

fluorescent intensity at the wavelength of 440 nm and 490 nm respectively.

### 5.2.8 Statistical analysis

A significant difference test (Tukey's) was performed on SPSS Statistics Software. Significant differences were determined at a confidence level of P values of 0.05.

## 5.3 Results

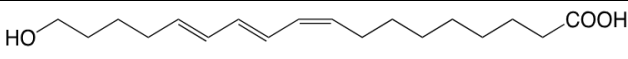
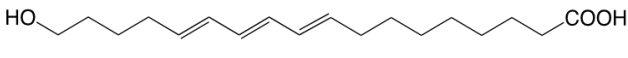
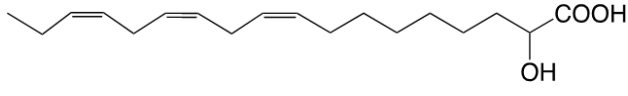
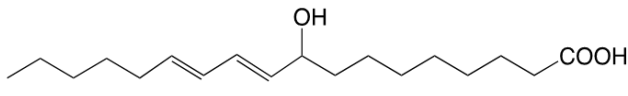
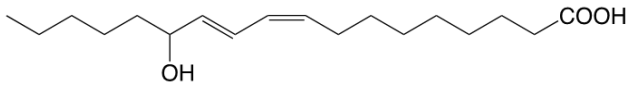
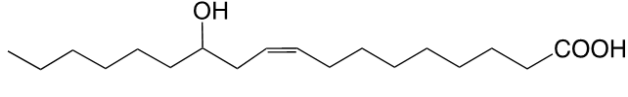
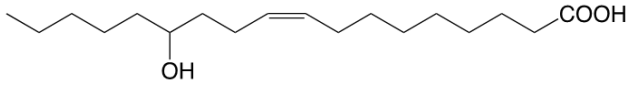
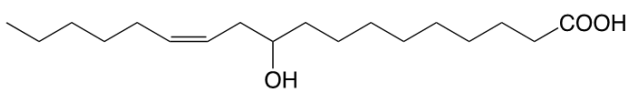
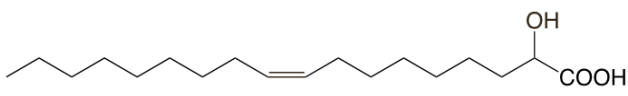
### 5.3.1 Extraction, HSCCC purification, and identification of antifungal HUFA from plant seed oil.

Sources of HUFA that cover a range of structural characteristics were identified using the PlantFAdB database (<https://plantfadb.org>).<sup>40</sup> Of the plants containing hydroxylated C18 fatty acids, those shown in **Table 5.1** were commercially available in seed form, as an oil extract or in free fatty acid form. In addition, **Table 5.1** includes hydroxylated fatty acids produced by the bacteria *L. hammesii* and *L. plantarum* TMW1.460 $\Delta$ lah.<sup>66</sup> The oil yield (g oil / g seed) from the seeds of *Coriaria nepalensis*, *Dimorphotheca sinuata*, *Thymus vulgaris* and *Mallotus philippensis* was 67%,<sup>66</sup> 22%, 32% and 34%, respectively, which is similar to previous studies.<sup>367, 105, 167, 66</sup>

After saponification and conversion to free fatty acids, HUFA were purified by HSCCC. The hexane/ethyl acetate/methanol/water system with ratio of 7:3:7:4 (v/v/v/v) was selected for the *Dimorphotheca sinuata* fatty acids due to the anticipated similarity in the partition behavior of the conjugated hydroxy diene isomers, dimorphecolic acid (9-OH C18:2) and coriolic acid (13-OH C18:2). Suitable solvent systems were selected based on the partition coefficient criterion of  $0.4 \leq K \leq 2.5$ ,<sup>66</sup> for fatty acids extracted from both *Thymus* and *Mallotus*. The *K* values of fatty acids

present in these oils in various solvent systems were measured as **Table 5.2** and **Table 5.3**. For the separation of 2-OH C18:3, the solvent system 7:3:7:3 with a *K* value 0.96 for HUFA was chosen; for separation of 18-OH C18:3, the solvent system 6:4:6:4, providing a *K* value 0.79 for the analyte, was chosen. Fractions containing the analyte (**Figure 5.1**) were combined. The combined fractions were then analyzed by LC-MS/MS to confirm their identities (**Figure 5.2**), and to determine their purities.

**Table 5.1** HUFA analogues extracted from plant oils and *Lactobacillus* fermentation, or purchased, and their LC-MS/MS (multiple reaction monitoring, MRM) ion transitions, which were for construction of HSCCC chromatogram and the measurement of *K* value

HUFA	Molecular structures	Sources	Q <sub>1</sub> (m/z)	Q <sub>3</sub> (m/z)
Kamlolenic acid (18-OH C18:3) 168	 or 	<i>Mallotus philippensis</i>	293.2	263.2
2-OH linolenic acid (2-OH C18:3)		<i>Thymus vulgaris</i>	293.4	191.3
Dimorphecolic acid (9-OH C18:2)		<i>Dimorphotheca sinuata</i>	295.2	171.1
Coriolic acid (13-OH C18:2)		<i>Coriaria nepalensis</i>	295.2	195.1
Ricinoleic acid (12-OH C18:1)		Castor bean oil	297.2	183.1
13-OH C18:1		<i>Lactobacillus plantarum</i> TMW1.460Δ <i>lah</i>	297.2	197.1
10-OH C18:1		<i>Lactobacillus hammesii</i>	297.2	185.1
2-Hydroxy oleic acid (2-OH C18:1)		Commercial standard	297.6	251.4

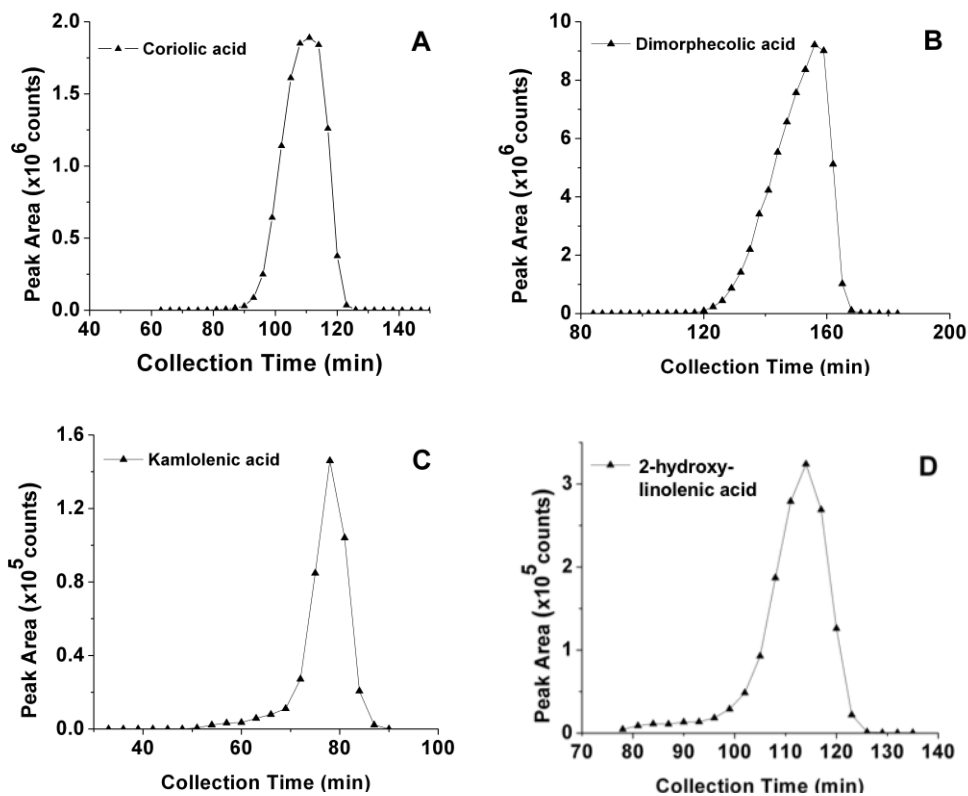
**Table 5.2** Partition coefficient (*K* value) of 2-OH linoleic acid in the hexane/ethyl acetate/methanol/water (HEMWat) systems with different solvent ratios. Fatty acids, C16:0, C17:0, C18:0, C18:1, C18:2, C18:3, 2-OH C18:1, 2-OH C18:3 were measurement with LC-MS/MS (MRM) with the following ion transition: 255.2/255.2, 269.2/269.2, 283.2/283.2, 281.2/281.2, 279.2/279.2, 277.2/277.2, 297.2/251.2, 293.4/191.3.

HEMWat System Ratio (v/v/v/v)	C16:0	C17:0	C18:0	C18:1	C18:2	C18:3	2-OH C18:1	2-OH C18:3
9:1:9:1	2.29	2.75	>=3	2.48	1.72	1.22	<0.5	<0.5
8:2:8:2	>=3	>=3	>=3	>=3	>=3	3.00	0.79	<0.5
7:3:7:3	>=3	>=3	>=3	>=3	>=3	>=3	2.66	0.96
7:3:7:4	>=3	>=3	>=3	>=3	>=3	>=3	>=3	1.67
7:3:6:4	>=3	>=3	>=3	>=3	>=3	>=3	>=3	2.29
7:3:5:5	>=3	>=3	>=3	>=3	>=3	>=3	>=3	>=3

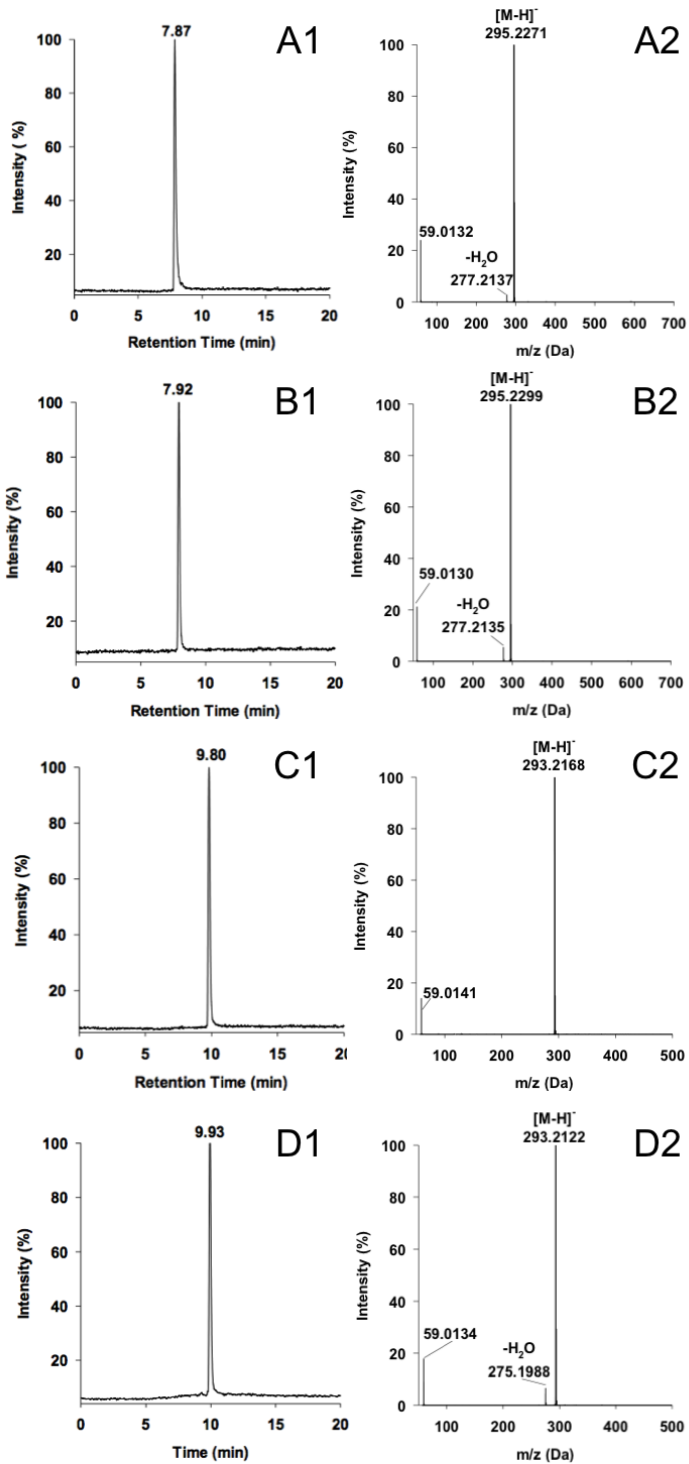


**Table 5.3** Partition coefficient (*K*) of kamlolenic acid in hexane-ethyl acetate-methanol-water (HEMWat) systems with different solvent ratios. Fatty acids, beside the fatty acid mentioned above, 13-OH C18:2, mono-OH C18:0 and 18-OH C18:3 were monitored with the following ion transition and retention time: 295.2/195.1 (5.14 min), 299.2/299.2 (7.83 min), and 293.2/263.2 (3.71 min).

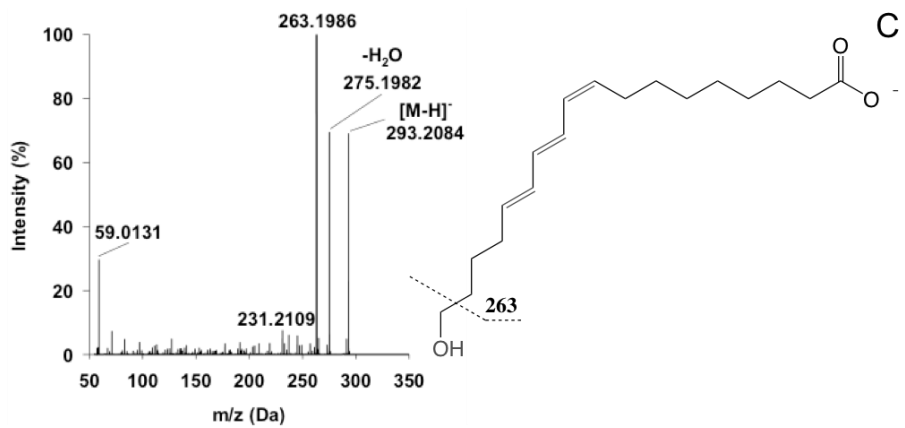
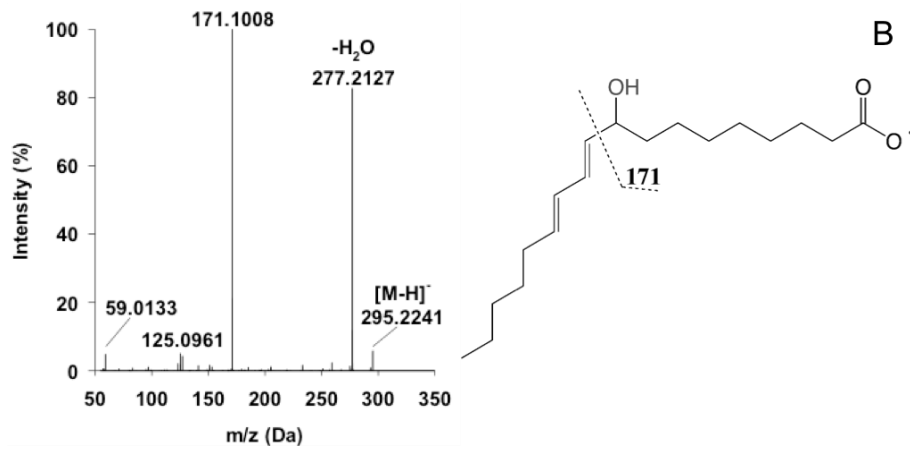
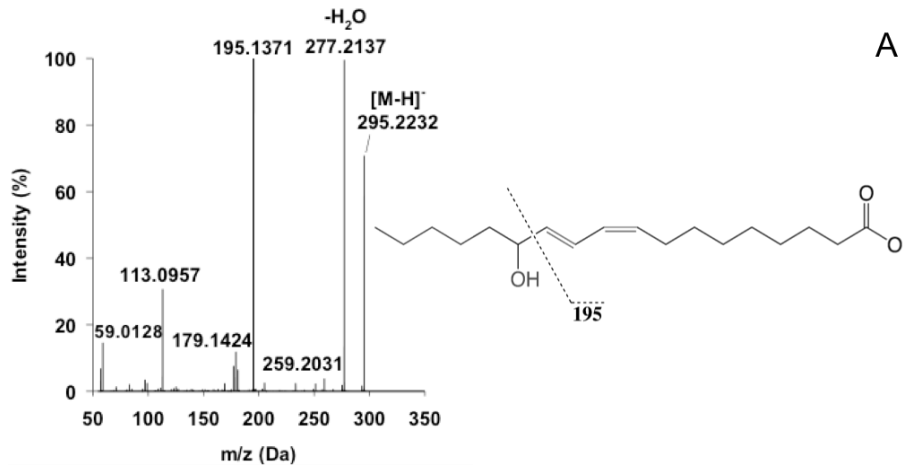
HEMWat							13-OH	Mono-OH	18-OH
System Ratio	C16:0	C17:0	C18:0	C18:1	C18:2	C18:3	C18:2	C18:0	C18:3
(v/v/v/v)									
7:3:7:3	>=3	>=3	>=3	>=3	>=3	>=3	<0.5	0.70	<0.5
7:3:7:4	>=3	>=3	>=3	>=3	>=3	>=3	1.29	1.46	<0.5
7:3:6:4	>=3	>=3	>=3	>=3	>=3	>=3	1.91	2.20	0.65
6:4:6:4	>=3	>=3	>=3	>=3	>=3	>=3	1.95	2.68	0.79
7:3:5:5	>=3	>=3	>=3	>=3	>=3	>=3	>=3	>=3	2.31



**Figure 5.1.** HSCCC chromatogram of saponified seed oil from various oil sources: (A) coriolic acid (13-hydroxy-9,11-octadecadienoic acid) from *Coriaria nepalensis* seed oil; (B) dimorphecolic acid (9-hydroxy-10,12-octadecadienoic acid) from *Dimorphothecha sinuata* seed oil; (C) kamlolenic acid (18-hydroxy-9,11,13-octadecatrienoic acid) from *Mallotus philippensis* seed oil; (D) 2-hydroxy-linolenic acid (2-hydroxy-9,12,15-octadecatrienoic acid) from *Thymus vulgaris* seed oil.



**Figure 5.2.** LC-APPI-MS total ion chromatograms (1), and APPI-MS spectra (2) of ionized purified hydroxyl fatty acids (A) coriolic acid; (B) dimorphecolic acid; (C) kamlolenic acid; and (D) 2-hydroxy-linolenic acid



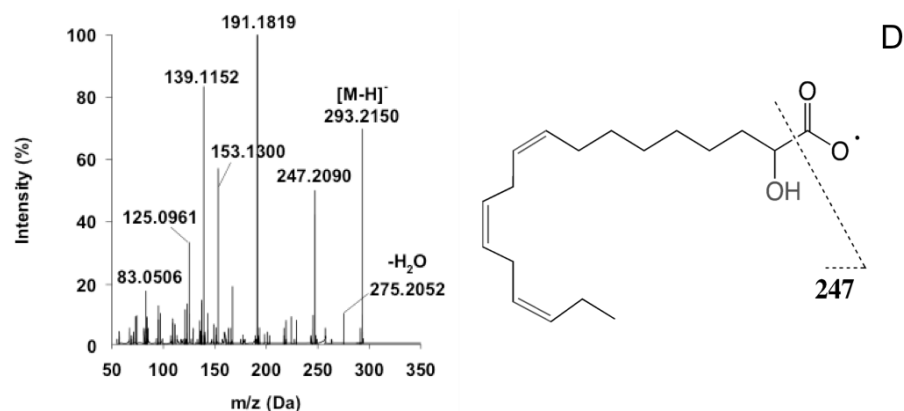


**Figure 5.3.** APPI-MS/MS spectra of  $[M-H]^-$  ion and molecular structure of ionized purified hydroxyl fatty acids (A) coriolic acid; (B) dimorphecolic acid; (C) kamlolenic acid; and (D) 2-hydroxy-linolenic acid

In the LC-APPI-MS total ion current chromatograms, single peaks were observed in the purified fractions (**Figure 5.2 - A1, B1, C1 and D1**). The fragment ions seen in the LC-MS/MS spectra of these purified fractions (**Figure 5.3**) were consistent with those reported in previous literature: A) 13-OH C18:2 ( $m/z$  295.2322  $[M-H]^-$ , 277.2137  $[M-H-H_2O]^-$ , and 195.1371 [ $\alpha$ -cleavage of 13-OH group]),<sup>66, 284, 286</sup> B) 9-OH C18:2 ( $m/z$  295.2241  $[M-H]^-$ , 277.2127  $[M-H-H_2O]^-$ , and 171.1008 [ $\alpha$ -cleavage of 9-OH group]);<sup>284, 286</sup> and D) 2-OH C18:3 ( $m/z$  293.2150  $[M-H]^-$ , 275.2052  $[M-H-H_2O]^-$ , 247.2090 [ $\alpha$ -cleavage of 2-OH group], 191.1819 and 139.1152).<sup>368, 287</sup> However, no LC-MS/MS data was found for kamlolenic acid 18-OH C18:3 ( $m/z$  293.2084, 275.1982, 263.1986) (**Figure 5.3C**), but the observed fragmentation matched the expected interpretation for HUFA of  $[M-H]^-$ ,  $[M-H-H_2O]^-$  and [ $\alpha$ -cleavage of 18-OH group], respectively.

### 5.3.2 Antifungal activity of HUFA

In order to relate the antifungal properties to the molecular structures of HUFA, the antifungal activity of purified HUFA were determined against 6 food-related fungi (**Table 5.4**). Mono- and diunsaturated fatty acids with hydroxylation at position 9, 10, 12 and 13 exhibited a similar antifungal activity; their MIC against *A. niger* and *P. roqueforti* ranged from 0.23-0.50 g/L. Unsaturated fatty acids with hydroxylation at position 2 or 18 exhibited a lower antifungal activity and the MICs against *A. niger* and *P. roqueforti* were 1.2 g/L or higher. Yeasts were resistant to all of the HUFA tested; only 2-OH C18:3 displayed weak inhibitory activity against yeasts with MICs in the range of 1 – 5 g/L.

**Table 5.4** Minimum inhibitory concentrations of various hydroxyl fatty acids against filamentous fungi. Results are presented as means  $\pm$  standard deviation of triplicate independent experiments.

Fatty acids	Minimum inhibitory concentrations (g/L)					
	<i>Aspergillus niger</i>	<i>Penicillium roqueforti</i>	<i>Candida albicans</i>	<i>Saccharomyces cerevisiae</i>	<i>Candida valida</i>	<i>Pichia membranaefaciens</i>
13-OH C18:2	0.33 $\pm$ 0.07	0.33 $\pm$ 0.14	$\geq$ 8	$\geq$ 8	$\geq$ 8	$\geq$ 8
9-OH C18:2	0.23 $\pm$ 0.03	0.33 $\pm$ 0.14	$\geq$ 8	$\geq$ 8	$\geq$ 8	$\geq$ 8
13-OH C18:1	0.42 $\pm$ 0.14*	0.42 $\pm$ 0.14*	$\geq$ 8	$\geq$ 8	$\geq$ 8	$\geq$ 8
12-OH C18:1	0.38 $\pm$ 0.13	0.33 $\pm$ 0.14	$\geq$ 8	$\geq$ 8	$\geq$ 8	$\geq$ 8
10-OH C18:1	0.50 $\pm$ 0.00*	0.42 $\pm$ 0.14*	$\geq$ 8	$\geq$ 8	$\geq$ 8	$\geq$ 8
18-OH C18:3	1.17 $\pm$ 0.29	$\geq$ 8	$\geq$ 8	$\geq$ 8	$\geq$ 8	$\geq$ 8
2-OH C18:3	1.50 $\pm$ 0.29	2.33 $\pm$ 1.53	3.00 $\pm$ 1.73	3.00 $\pm$ 1.73	2.00 $\pm$ 0.00	1.00 $\pm$ 0.00
2-OH C18:1	1.50 $\pm$ 0.87	2.67 $\pm$ 1.15	$\geq$ 8	$\geq$ 8	$\geq$ 8	0.83 $\pm$ 0.29

\*data from Chapter 4.

### 5.3.3 Effect of HUFA on the fluidity of fungal membranes monitored by Laurdan

In order to evaluate the effect of HUFA treatment on the fluidity of fungal membranes in presence or absence of HUFA, General Polarization (GP) values were measured by Laurdan assay. A decrease of GP indicates the transition of a membrane from the gel-phase to a liquid-crystalline (liquid disorder)-phase, and thus an increase in membrane polarity.<sup>369</sup>

In order to validate this Laurdan method, we first used it to monitor the fungal membrane fluidity change after addition of ethanol, due to its known effect on membrane fluidity in *S. cerevisiae*.<sup>370</sup> In the controls without ethanol, the GP value decreased in the order *A. niger* > *S. cerevisiae* > *P. roqueforti* and was thus not related to the resistance of the organisms to HUFA. The GP value of all three organisms decreased with increasing ethanol concentrations, indicating an increased fluidity of the membrane (**Figure 5.4 Upper figure**). The impact of the antifungal ricinoleic acid on GP values of *S. cerevisiae* and *P. roqueforti* was not different from oleic acid, which has no antifungal activity, further indicating that membrane fluidity as measured by the GP is not related to the resistance to hydroxyl fatty acids (**Figure 5.4 Lower figure**).



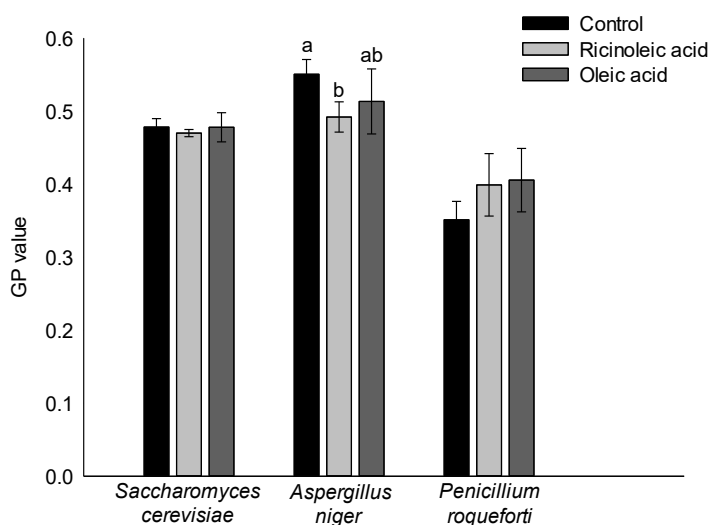
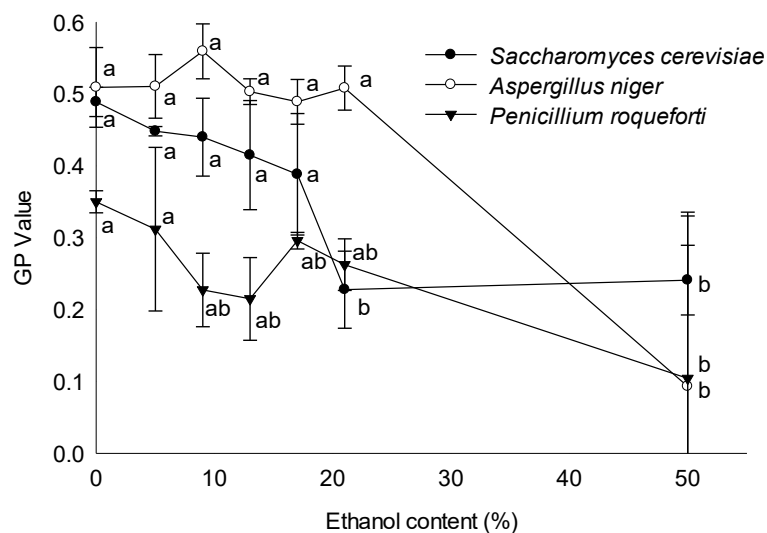


**Figure 5.4.** Upper figure) Fungal membrane fluidity change in different concentration of ethanol, monitored by GP value using Laurdan assay; Lower figure) The measurement of fungal cell membrane fluidity of *Saccharomyces cerevisiae*, *Aspergillus niger* and *Penicillium roqueforti* under fatty acid (ricinoleic and oleic acid) or negative control treatment. Generalized polarization  $GP = (I_{440} - I_{490}) / (I_{440} + I_{490})$ , where  $I_{440}$  and  $I_{490}$  stood for fluorescent intensity under wavelengths of 440 nm and 490 nm, respectively.

### 5.3.4 Comparison of the sterol level in HUFA-resistant and HUFA-sensitive fungi

Sterols are known to play a role in the maintenance of membrane fluidity,<sup>371,372</sup> and sterol levels have previously been associated with fungal sensitivity towards an antifungal fatty acids produced by *Pseudozyma flocculosa*.<sup>354</sup> Here, ergosterol was quantified by GC/MS<sup>365</sup> in order to investigate whether the sterol content of the fungal tissues relates to fungal sensitivity to HUFA. Ergosterol is the main constituent of membrane sterols in all samples tested, accounting for more than 85% of the total peak area of possible sterol peaks in the GC-MS chromatograms. The highest sterol content was identified in *W. anomalus* (**Figure 5.5 Left figure**); mycelial fungi had a low ergosterol content. *C. albicans* was the only yeast with an ergosterol content of less than 4 mg/g in fungal biomass (**Figure 5.5 Left figure**). A plot of the HUFA MIC values against the measured sterol content of fungal biomass revealed a clear distinction between yeasts and mycelial fungi. Yeasts can be seen to have high MIC values and high ergosterol contents, with the exception of *C. albicans*, which has a low ergosterol contents. In contrast, all of the mycelial fungi tested were found to have low MIC values and low sterol contents (**Figure 5.5 Right figure**).

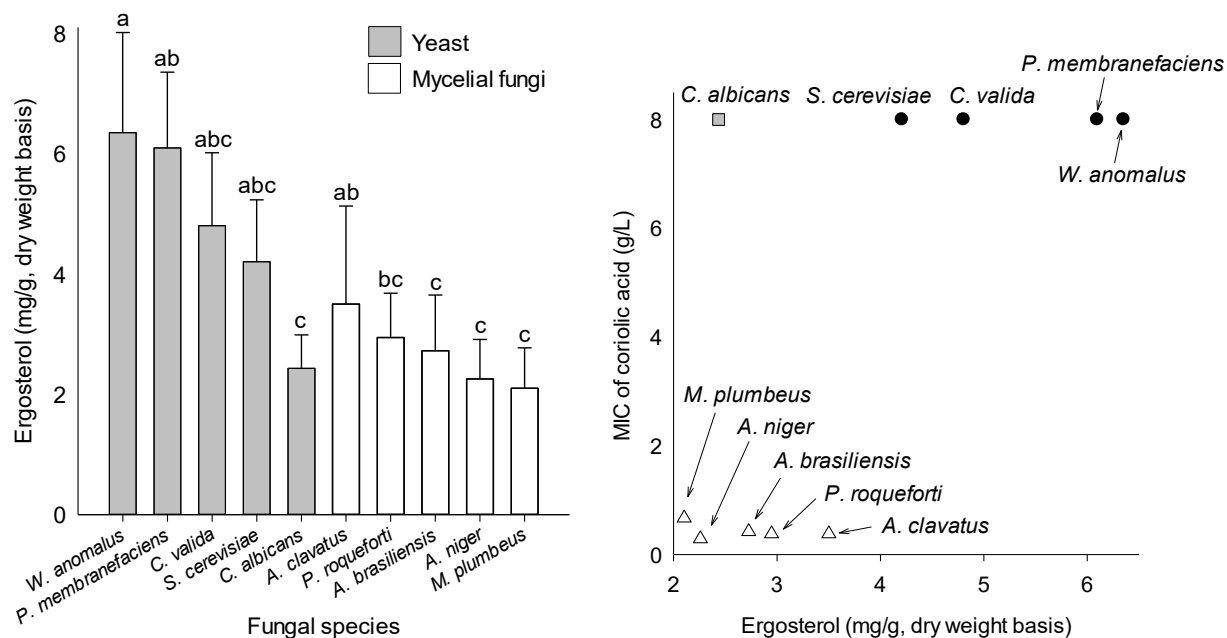


**Figure 5.5.** Left figure) GC-MS quantitation of ergosterol extracted from food-related fungi (dry weight basis); Right figure) relationship between fungal ergosterol content and fungal MIC of coriolic acid. The abbreviation of fungi species represented the following strains: *Candida valida*, *Pichia membranefaciens*, *Saccharomyces cerevisiae*, *Candida albicans*, *Wickerhamomyces anomalus*, *Penicillium roqueforti*, *Aspergillus brasiliensis*, *Mucor plumbeus*, *Aspergillus niger*, and *Aspergillus clavatus*. The outlier (grey □: *C.a*) was determined using Cook's distance >0.4 in SPSS software.

## 5.4 Discussion

In the present study, HUFA from plant seed oils were identified in the PlantFAdB database, extracted, purified and then tested against food-related fungi. The antifungal properties of mono-OH HUFA were found to depend on their specific structure, with most activity when their hydroxyl

groups are located in the middle (C9-C13) of the C18 HUFA chain. Studies on their mode of action suggested that HUFA are membrane active, and that fungal resistance to HUFA relates to the sterol content of the fungi biomass.

Previous studies have indicated antifungal properties of HUFA,<sup>12, 13</sup> especially 13-OH C18:2,<sup>35</sup> 9-OH C18:2<sup>36</sup> and 2-OH C18:3<sup>37</sup> but provided only limited information on structure-function relationship.<sup>12</sup> This lack of knowledge is linked to the small quantities of HUFA that were available in past studies. The present study focused on plant seed oils that contain high amounts of HUFA which, in combination with an efficient purification technique, enabled additional observations on the structure-function relationship of HUFA. Long-chain saturated hydroxy fatty acids exhibit no antifungal activity,<sup>15</sup> possibly due to their high hydrophobicity and low solubility.<sup>13</sup> The present study showed that unsaturated HUFA with hydroxylation at the C9-C13 position of the C18 chain exhibited comparable antifungal activity while their 2- and 18-OH analogues were less active. This might be attributed to differences in the dissociation constants between fatty acids ( $pK_A$ ),<sup>363</sup> and/or their different interactions with fungal cellular membrane,<sup>13, 371, 354</sup> including the translocation across the cell membrane.<sup>373</sup> The -OH position will also alter the monolayer packing properties of HUFA when these integrate into phospholipid bilayers.<sup>374</sup> In contrast to other HUFA analogues, 2-OH C18:3 showed a broad spectrum of weak inhibition against all of the species tested (MIC  $\geq$  1g/L). This may indicate that different HUFA have different modes of antifungal action.

Due to the diversity of possible fungal strains, it is useful to understand the structure-function relationships of HUFA targeting food-related fungi. The observed differences in antifungal activity between HUFA containing different hydroxylation patterns, and the difference between the resistance to HUFA antifungal activity of yeasts compared to filamentous fungi, help to expand on prior knowledge obtained with coriolic acid.<sup>66</sup> Similar to the food spoilage fungi *A. niger* and

*P. roqueforti*, phyto-pathogenic filamentous fungi like *Botrytis cinerea* and *Cladosporium herbarum* exhibited similar specificity to HUFA structures. Specifically, the latter fungi were highly inhibited by 9-OH and 13-OH C18:2 or C18:3 HUFA, but not 2-OH C18:3 or C18:1.<sup>12</sup> Some previous studies have also indicated the sensitivity of phyto-pathogenic fungi to HUFA structures. For example, for HUFA with –OH in the center of the 13-OH C18:3 fatty acid chain and chemotaxonomic, the isomer 13(*S*)-hydroxy-9(*Z*),11(*E*),15(*Z*)-octadecatrienoic acid) inhibited *B. cinerea* and *C. herbarum* at a concentration of 0.03 g/L, while another isomer 13(*S*)-Hydroxy-6(*Z*),9(*Z*),11(*E*)-octadecatrienoic acid, was not active.<sup>12</sup> In addition, other filamentous fungi like *Alternaria brassicicola*, *Fusarium oxysporum*, and *Rhizopus sp.* were resistant to any of the HUFA tested, at a concentration of around 0.03g/L.<sup>12, 36</sup> In a study targeting the phytopathogenic fungi *Leptosphaeria maculans* and *Alternaria brassicae*, 0.3 g/L of 13-OH C18:3 HUFA, but not 13-OH C18:2 (coriolic acid) inhibited growth of hyphae,<sup>355</sup> 0.3 g/L of coriolic acid inhibited the spore germination of *Leptosphaeria maculans* in certain growth conditions.<sup>355</sup> The underlying explanation of this diversity in sensitivity of fungi to HUFA may relate to specific resistance mechanisms of phytopathogens.

The delay of cell growth and inhibition of germ sporulation caused by antifungal fatty acids has been related to their partition into fungal membranes and the associated increase in membrane fluidity.<sup>13, 363, 354</sup> Partitioning of both HUFA and their non-OH counterparts into membranes is rapid without assistance of membrane protein,<sup>363, 375</sup> and thus does not explain differences in their antifungal activities.<sup>66, 343</sup> The present study documented that GP values of fungal membranes were similar after treatments with HUFA and non-hydroxylated fatty acids, so it is concluded that there is no specific impact of HUFA on the overall membrane fluidity and hence this does not explain differences in fungal resistance. It is still possible, however, that HUFA target specific regions of

the fungal membrane without changing the overall membrane fluidity. Similarly, it has been reported that ricinoleic acid and oleic acid exhibited different effects on membrane disorder but show the same effect on phase transition in a dimyristoylphosphatidylcholine (DMPC) lipid membrane model.<sup>62</sup> Furthermore, intracellular fatty acid binding proteins (FABP) in the cytosol, in the presence of phospholipid bilayers, exhibited binding preference towards HUFA (13-OH C18:2) over their non-OH FA precursors; in addition, liver FABP, in the presence of vesicles, specifically showed higher efficiency while binding 13-OH C18:2 compared to intestinal FABP.<sup>375</sup> These different characteristics may at least partially contribute to the antifungal activity of HUFA compared to their non-OH counterparts. Clearly, more studies are needed to investigate the interaction between HUFA and fungal membranes in order to explain the observed structure-function differences.

Fungal membrane lipid compositions, including phospholipids, unsaturated fatty acids and sterols, have been associated with their sensitivity towards antifungal fatty acids.<sup>371, 354</sup> In particular, sterols maintain the structure of the membrane during stress<sup>354, 372</sup> and their content is altered in fungi that alternate between unicellular and a mycelial/pseudo-mycelial state.<sup>376, 377</sup> Ergosterol is the major sterol in fungal membranes and thus representative of the total sterol content. For example, >90% of sterol was ergosterol in *C. albicans* ATCC 10231.<sup>378</sup> In the present study, the minor sterols were not quantified because they had a very low abundance (data not shown).

In this study, we observed that yeasts were resistant to HUFA and tended to have high sterol content, while mycelial fungi were sensitive to HUFA and had a lower sterol content. Previous research indicated that *S. cerevisiae* had higher sterol content compared to *A. niger* and some of the *Penicillium* spp.<sup>379</sup> It was also observed that the yeast strain *Pseudozyma rugulosa* had higher

sterol content compared to other mycelial fungi tested, and showed higher resistance towards antifungal fatty acids.<sup>354</sup> However, one exception was also observed here, i.e. a pathogenic fungi *C. albicans*, a HUFA-resistant strain with a sterol content that was comparable to or lower than that of HUFA-sensitive mycelial fungi. Data obtained in the present study by GC/MS confirmed the prior data on *A. niger*, *Penicillium spp.*, and *C. albicans* that was obtained by the Liebermann-Burchard reaction.<sup>380, 379</sup> *C. albicans* alters the sterol content of its membrane to adjust its cellular morphology.<sup>376</sup> In addition, the sterol profile of membranes of *C. albicans* is also modified in response to antifungal compounds.<sup>381</sup> Therefore, HUFA-resistant species may employ different stress responses under HUFA treatment; these will require further investigation into the membrane composition changes. Other studies will be necessary to investigate the specific function of the fungal sterol of HUFA-resistant strains, and to explore the potential of synergistically combining sterol biosynthesis-targeted antifungals and HUFA.

Other than being antifungal compounds, the production of HUFA has been closely related to a board spectrum of biological functions, such as signaling,<sup>14, 63</sup> virulence,<sup>17</sup> and response mechanisms towards biotic stresses.<sup>14, 12</sup> In particular, 2-OH C18:3 has been classified as phytoalexin due to its *in vivo* production in plant associated with phytopathogenic fungal infection.<sup>37</sup> In addition, it exhibited a tissue-protective effect against phytopathogenic bacterial infection,<sup>108</sup> but this protective effect wasn't attributed to its direct bacteriostatic or bactericidal effects.<sup>108, 12</sup> This suggests that 2-OH C18:3 may be associated with other plant defense and/or signaling mechanisms.<sup>368</sup> The dual functions of HUFA as direct antifungals and plant signal molecules may lead to further applications in antifungal plant protection.<sup>12, 14</sup> The general methods used in this study to source, extract and purify diverse HUFA species could be beneficial in an expanded investigation of the diverse bioactivities of HUFA.

In conclusion, the present study has identified specific plant seed oils as a source of antifungal hydroxy unsaturated fatty acids, and showed the distinguishable antifungal properties of HUFA with hydroxyl groups located towards the center of the fatty acid chain, at about the C9-C13 positions, compared to those with hydroxyl groups near either terminus, at C2 or C18 positions. The HUFA with –OH in C9-C13 position inhibited the growth of food spoilage mycelial fungi *P. roqueforti* and *A. niger*, but it allowed the growth of the yeasts tested. In contrast, 2-OH linoleic acid (2-OH C18:3) showed minor inhibition against both mycelial fungi and yeasts. HUFA-resistant strains tended to possess a higher sterol content than in HUFA-sensitive. The present study made use of HSCCC for purification of HUFA; since this is a scalable technique it could be used in developing HUFA-based antifungal methods for food and agricultural applications, as well as in further studies of their antifungal properties. Plant derived HUFA have the potential for being used to inhibit mycelial spoilage fungi in food, whilst the growth of yeasts is not affected. Although the resistance of yeasts prevents applications of HUFA in food where spoilage by yeasts is of concern, at the same time it enables applications in foods where yeasts are used for desired fermentations. The use of HUFA in plant protection to inhibit fungi and to enhance plant immunity remains to be explored.



## Chapter 6. Exploiting synergies of sourdough and antifungal organic acids to delay fungal spoilage of bread

### 6.1 Introduction

Fungal spoilage is a key limiting factor for the shelf life of bread and causes considerable economic losses. Bakery products are easily colonized by fungal conidiospores from diverse genera including *Aspergillus*, *Cladosporium*, *Endomyces*, *Penicillium*, and *Rhizopus*.<sup>382</sup> Conidiospores of filamentous fungi are ubiquitous in the biosphere and are dispersed by air unless contamination is controlled by clean room technology.<sup>383</sup> The water activity and pH of bread support growth of mycelial fungi on bread that is stored at ambient temperature.<sup>49,384</sup> Refrigeration delays fungal growth but also accelerates starch retrogradation and bread staling.<sup>385</sup>

UV light and pulsed light technology reduce spore contamination of bread but find only limited commercial application.<sup>386</sup> Chemical preservatives are more commonly used to extend the shelf life of bread. Ethanol vapors delay germination of fungal spores,<sup>387</sup> calcium propionate and sorbic acid are widely used as preservatives in pre-packed and sliced bread.<sup>386</sup> However, the use of preservatives conflicts the aim to develop “clean label” products that avoid the use of additional chemicals.<sup>388,389</sup>

Lactic acid bacteria are used in baking applications as leavening agents, to achieve dough acidification, or to improve specific quality attributes of bread,<sup>390,391</sup> Lactic acid bacteria produce metabolites with antifungal activity; however, their antifungal metabolites are uncharacterized, unproven in food, or negatively impact bread flavour.<sup>392, 15, 393</sup> Acetic acid produced in primary carbohydrate metabolism has antifungal activity but also impacts flavour and texture of bread.<sup>394, 395, 396</sup> The levels of acetic acid produced in sourdough fermentations are readily adjusted by

addition of pentoses, or by addition of sucrose as electron acceptor in heterofermentative metabolism.<sup>397</sup> Co-fermentation of *L. diolivorans* and *L. buchneri* produced propionic acid in the sourdough; however, propionic acid also impacts bread flavour when added at effective concentrations.<sup>49</sup> 3-Phenyllactic acid and cyclic dipeptides have antifungal activity *in vitro* but their contribution to the inhibition of fungal growth on bread remains unproven<sup>54, 398, 52, 392</sup> Hydroxylated unsaturated fatty acids have antifungal activity in bread but their accumulation to active concentrations in sourdough remains to be demonstrated.<sup>15, 66</sup> *In situ* preservative effects of lactic acid bacteria have often been attributed to synergistic activities of uncharacterized compounds.<sup>392 57</sup>

Plant-derived antifungal compounds support the antifungal activity of bacterial metabolites. For example, hop extract was recently demonstrated to be an effective antifungal ingredient in bread making,<sup>399</sup> compounds with antifungal activity isolated from legume flours (*Pisum sativum*, *Phaseolus vulgaris*) were also successfully employed to extend the mould-free shelf life of wheat bread.<sup>400, 401</sup> Flaxseeds have a high oil content with a high proportion of linoleic acid, a substrate for enzymatic or microbial conversion to hydroxy-fatty acids.<sup>15</sup> The microbial and enzymatic conversion products of free linoleic acid, 10-hydroxy-12-octadecenoic and coriolic acids, respectively, have similar antifungal activity.<sup>15, 66</sup>

The use of multiple antifungal metabolites to exploit synergies improves the antifungal effect of sourdough while minimizing the impact of organic acid on bread flavour.<sup>49, 402</sup> However, synergistic effects of different antifungal metabolites have not been systematically assessed by comparison of the correlation of *in vitro* MIC and *in situ* preservative effects.<sup>392</sup> This study therefore aimed to compare the minimum inhibitory concentration of antifungal compounds to their antifungal effect in bread. Antifungal compounds were assessed in bread produced with

straight dough process, and in sourdough bread. Wheat sourdoughs were compared to flaxseed sourdoughs.

## **6.2 Materials and methods**

### **6.2.1 Strains and growth conditions**

*Lactobacillus hammesii* DSM16381 from French sourdough<sup>403</sup> and *Lactobacillus plantarum* C264 and *Lactobacillus brevis* C186 from maize bran<sup>404</sup> were cultivated on modified MRS (mMRS) medium<sup>15</sup> 30 °C. Representative of common fungal spoilage of bread, *Aspergillus niger* FUA5001 and *Penicillium roqueforti* FUA5005, were used as target strains for the antifungal assay. *P. roqueforti* is an isolate from mouldy bread with high resistance to antifungal interventions.<sup>49</sup> Fungal strains were cultivated on malt extract agar medium at 25 °C for 72 h, and spores were collected by adding physiological solution (0.85% NaCl, 0.01 % Tween80). After filtration with Whatman N.1 filter paper, the suspensions were stored at -20° C until further use. Spore suspensions were diluted to proper spore density ( $10^2$  or  $10^4$  spores/mL) counted with hemocytometer (Fein-Optik, Jena, Germany).

### **6.2.2 Antifungal activity assay**

Minimum inhibitory concentrations (MIC) were determined with serial 2-fold dilutions of ricinoleic acid, 3-phenyllactic acid, acetic acid, calcium propionate and sorbic acid (Merck, Darmstadt, Germany) in 96-well microtiter plates.<sup>51</sup> In the MIC assays, the pH was controlled at pH 4.5 by adjustment of the pH of the medium and the stock solutions of antifungal compounds. Microtiter plates were inoculated with mMRS broth containing  $10^4$  spores/ mL of *A. niger* or *P.*

*roqueforti* and incubated at 25 °C for 5 days. The MIC was determined as the lowest concentration of compound inhibiting the mould growth. Ethanol, which was used as solvent for ricinoleic acid, was removed by evaporation under a laminar flow hood before the addition of the fungal spores.

A checkerboard procedure<sup>405</sup> was carried out to determine the combined inhibitory activity of two compounds. The plates were inoculated and incubated at 25 °C for 5 days. The MIC was determined as the lowest concentration of the two compounds inhibiting the mould growth. Experiments were performed in triplicate.

### 6.2.3 Sourdough fermentation and bread preparation

*L. hammesii*, *L. plantarum* and *L. brevis* were used to prepare sourdough bread. Cells from an overnight culture in mMRS medium were washed twice and suspended in sterile tap water to a concentration of 10<sup>8</sup> CFU/mL. Sourdough was prepared by mixing white wheat flour or flaxseed flour, sterile tap water, and culture in a ratio of 2:1:1 (wt/wt/wt). The dough was fermented at 30 °C for 24 h. Samples were taken at time 0 and after 24 hours for determination of cell counts and pH values, and for quantification of organic acids. Colony morphology and uniformity were used to verify the identity of fermentation microbiota with the inoculum. Cell counts for the three strains reached 10<sup>9</sup>-10<sup>10</sup> CFU/g after 24 h.

Bread formulations shown in **Tables 6.1** and **6.2**. Sourdough bread was prepared with 10% addition of sourdough. Bread with chemical preservatives was prepared with different concentrations according to MIC results. Bread making procedure was described.<sup>15</sup> After baking, the breads were cooled to 20 °C on racks for 120 min, and samples were taken for challenge test, pH determination, and quantification of organic acids.

The same protocol was used in the bread experiments to investigate the antifungal effect of the combination of *L. hammesii* sourdough and ricinoleic acid, with minor modifications. Sourdough was fermented for 2 days and breads were produced from 50 g flour, *i.e.* all the ingredients were used in the same proportion shown in **Table 6.1** and **6.2**, but half of the amount. Bread was hand-kneaded for extra 3 min after mechanical mixing. The second proofing was 85 min. Bread experiment groups include control without addition of sourdough or ricinoleic acid (control); *L. hammesii* fermented sourdough bread with addition 2% linoleic acid during sourdough fermentation, *L. hammesii* sourdough bread with addition of 0.03%, 0.08% and 0.15% ricinoleic acid added at the bread stage, respectively.

#### **6.2.4 Bread challenge test against *P. roqueforti* and *A. niger***

Mould challenge test was conducted as described.<sup>15</sup> Bread samples were sliced in 25-mm thick slices and inoculated with a suspension containing  $10^2$  spores/mL. The spore suspensions were sprayed on each corner of the slice and in the middle, delivering 90  $\mu$ L of suspension or about 10 spores on each spot. The inoculated slices were placed into plastic bags with filter tips ensure aerobic conditions. Slices were incubated for 12 d at 20 °C and monitored every 12 h. The last day before visible mycelial growth was recorded as mould-free shelf life. The effect of chemical preservatives or sourdough fermentation or the combination of the two was determined in triplicate independent experiments (triplicate sourdough fermentation and baking). Statistical analysis was done with Tukey's test with Graphpad Software or SPSS Statistics Software. Significant differences were reported at a confidence level of *P* values of 0.05.

**Table 6.1.** Ingredients in bread formulation with chemical preservatives and their combinations.

Ingredients (g)	Control	Ca-propionate	Phenyllactate	Sorbic acid	Ricinoleic acid	Acetic acid	Ca-propionate + acetic acid	Sorbic acid + acetic acid
Wheat flour	100	100	100	100	100	100	100	100
Water	60	60	60	60	60	60	60	60
Yeast	2	2	2	2	2	2	2	2
Salt	2	2	2	2	2	2	2	2
Canola oil	2	2	2	2	2	2	2	2
Calcium propionate	-	0.25	-	-	-	-	0.058	-
3-Phenyllactate	-	-	0.42	-	-	-	-	0.002
Sorbic acid	-	-	-	0.01	-	-	-	-
Ricinoleic acid	-	-	-	-	0.5	-	-	-
Lactic acid	-	-	-	-	-	0.18	-	-
Acetic acid	-	-	-	-	-	0.25	0.037	0.037

**Table 6.2.** Ingredients of sourdough bread. Wheat or flaxseed sourdoughs were fermented with *L. hammesii*, *L. plantarum* or *L. brevis*. 10% of the experimental sourdough was added to bread dough.

Ingred. (g)	Non-fermented control		Sourdough ( <i>L. brevis</i> , <i>L. hammesii</i> or <i>L. plantarum</i> )					<i>L. hammesii</i> wheat sourdough			<i>L. hammesii</i> flaxseed sourdough					
	Wheat	Flax	Wheat	Flax	Wheat + sucrose	Flax + sucrose	Prop. <sup>1)</sup>	Sorbic acid	Linoleic acid	Ricinoleic acid		Linoleic acid	Ricinoleic acid			
Wheat	100	90	90	90	90	90	90	90	90	90	90	90	90	90	90	90
Flaxseed		10														
Water	60	60	50	50	50	50	50	50	50	50	50	50	50	50	50	50
Yeast	2	2	2	2	2	2	2	2	2	2	2	2	2	2	2	2
Salt	2	2	2	2	2	2	2	2	2	2	2	2	2	2	2	2
Canola oil	2	2	2	2	2	2	2	2	2	2	2	2	2	2	2	2
Prop.							0.058									
Sorb.								0.002								
Ricinol.										0.037	0.075	0.15		0.037	0.075	0.15
Linol.									2				2			
Sucrose <sup>2)</sup>					0.8	0.8										
Sourd <sup>3)</sup>			20	20	20	20	20	20	20	20	20	20	20	20	20	20

<sup>1)</sup> Prop. = Ca propionate; sorb. = sorbic acid; ricinol. = ricinoleic acid; linol. = linoleic acid.

<sup>2)</sup> Sucrose was added to the sourdough.

<sup>3)</sup> Sourdough, prepared with 10 g water and 10 g flaxseed flour or wheat flour and sucrose as indicated.

### 6.2.5 Quantification of acetic acid with high performance liquid chromatography (HPLC)

Acetic acid was determined by HPLC with an Aminex HPX-87 column (300 mm × 7.8 mm, Biorad, USA) at a temperature of 80 °C and a flow rate of 0.4 mL/min with 5 mM H<sub>2</sub>SO<sub>4</sub> as the eluent. The injection volume was 10 µL. A refractive index detector and UV detector (210 nm) were used for detection. For sample preparations, 2 g of bread was diluted with 10 mL of MilliQ water and incubated for 3 h at 80 °C. After centrifugation, 7% perchloric acid were added and the solution incubated at 4 °C overnight. Precipitated protein was removed by centrifugation. The samples were filtered before injection in the column.

## 6.3 Results

### 6.3.1 MIC of preservatives and combination effects

The individual MIC for each of the five compounds was tested *in vitro* against the two indicator strains *A. niger* and *P. roqueforti* at pH of 4.5. Sorbic acid was the strongest inhibitor ( $0.4 \pm 0.1$  and  $0.2 \pm 0.0$  mM for *A. niger* and *P. roqueforti*, respectively), followed by propionic acid ( $1.3 \pm 0.2$  and  $12.0 \pm 0.0$  mM), ricinoleic acid ( $1.7 \pm 0.0$  and  $3.5 \pm 0.0$  mM) and acetic acid ( $8.2 \pm 3.4$  and  $25.0 \pm 5.5$  mM). 3-Phenyllactic acid was the weakest inhibitor with MIC values of  $30 \pm 10$  and  $50 \pm 0$  mM against *A. niger* and *P. roqueforti*. Synergistic activities of acetic acid with other inhibitors were determined with checkerboard assays. Acetic acid exhibited additive activity with calcium propionate, sorbic acid and ricinoleic acid (**Figure 6.1**). MIC values of calcium propionate and acetic acid combination were lower than the individual MICs, respectively, with  $0.6 + 6.2$  mM against *A. niger* and  $3.1 + 6.2$  mM against *P. roqueforti* (**Figure 6.1**). The combination of sorbic



acid and acetic acid was active at 0.2 + 3.1 mM against *A. niger* and 0.2 + 6.2 mM against *P. roqueforti* (Figure 6.1).

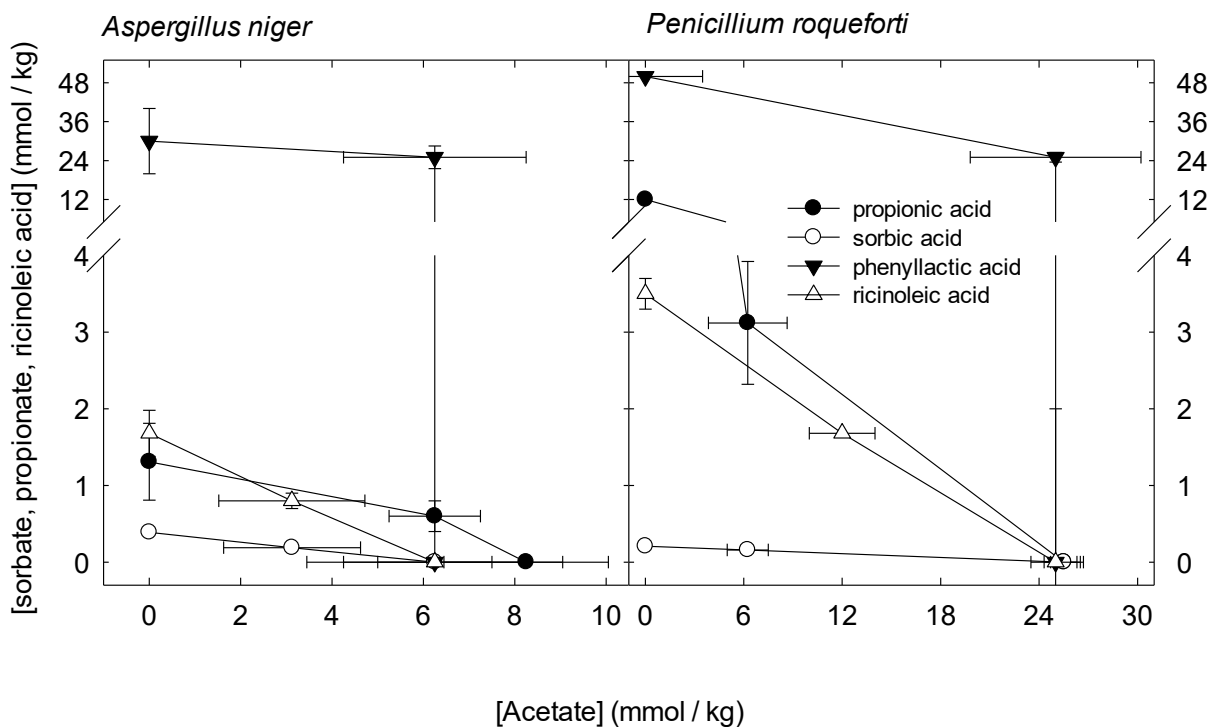


**Figure 6.1.** Minimum inhibitory concentration of acetic acid in combination with sorbic acid, propionic acid, phenyllactic acid, or ricinoleic acid. The minimum inhibitory concentrations were evaluated at a pH of 4.50. The results are shown as means  $\pm$  standard deviations of three independent experiments.

### 6.3.2 Antifungal effect of organic acids addition to bread

The organic acids were used in baking trials; compounds or combination of compounds were added to bread at levels matching commercial practice (propionate, sorbate) or at the level matching the *in vitro* MIC (all other compounds and combination treatments). Bread was challenged by inoculation with *A. niger* or *P. roqueforti* and stored until visible mycelial growth,

or for 12 days. The results are shown in **Table 6.3**. With the exception of ricinoleic acid, the results obtained *in vitro* are comparable with the data obtained *in situ*. 3-Phenyllactic acid, the weakest inhibitor *in vitro*, showed no antifungal effect *in situ* when added at a level corresponding to 20 mmol / kg bread (**Table 6.3**). Acetate, calcium propionate and sorbic acid significantly extended the mould-free shelf life of bread; sorbic acid and acetic acid extended the shelf life by 5-6 days. Acetic acid extended the shelf life of bread by 3 days ( $p < 0.05$ ) in combination with propionic acid; acetic acid in combination with sorbic acid extended the shelf life only by two days ( $P < 0.1$ ) relative to the control (**Table 6.3**).

To determine whether the antifungal effects relate to the pH, the pH of breads is also shown **Table 6.3**. The pH of control bread was 5.5. Addition of acetic acid and phenyllactic acid reduced the pH to values below 4.5 while other organic acids had no major effect on the pH.

**Table 6.3.** Effect of preservatives alone or in combination on the mould-free shelf life of bread.

Preservatives were added as indicated in **Table 6.1** to match their MIC *in vitro*. Data are shown as means  $\pm$  standard deviations of three independent experiments. Values in the same row that do not share a common superscript differ significantly ( $p < 0.05$ ).

Additive	Control	3-PLA	Ricinoleic acid	Acetic acid	Prop.	Sorb.	Prop. + acetic	Sorb. + acetic
pH	5.4 $\pm$ 0.1 <sup>a</sup>	4.4 $\pm$ 0.0 <sup>b</sup>	5.3 $\pm$ 0.0 <sup>a</sup>	4.4 $\pm$ 0.0 <sup>b</sup>	5.4 $\pm$ 0.0 <sup>a</sup>	5.1 $\pm$ 0.1 <sup>a</sup>	4.8 $\pm$ 0.7 <sup>ab</sup>	4.9 $\pm$ 0.5 <sup>ab</sup>
Indicator	Bread mould-free shelf life (d)							
<i>A. niger</i>	3.6 $\pm$ 1.1 <sup>b</sup>	5.3 $\pm$ 0.5 <sup>b</sup>	4.3 $\pm$ 1.1 <sup>b</sup>	9.7 $\pm$ 0.5 <sup>a</sup>	8.3 $\pm$ 1.1 <sup>a</sup>	10.0 $\pm$ 1 <sup>a</sup>	8.5 $\pm$ 0.7 <sup>a</sup>	6.0 $\pm$ 0.0 <sup>ab</sup>
<i>P. roqueforti</i>	4.3 $\pm$ 0.1 <sup>b</sup>	5.0 $\pm$ 1.0 <sup>b</sup>	4.7 $\pm$ 1.1 <sup>b</sup>	9.3 $\pm$ 0.5 <sup>a</sup>	8.0 $\pm$ 1.0 <sup>a</sup>	9.0 $\pm$ 0.7 <sup>b</sup>	7.5 $\pm$ 0.3 <sup>ab</sup>	6.5 $\pm$ 0.7 <sup>ab</sup>

PLA = 3 phenyllactic acid; Prop. = Ca propionate; sorb. = sorbic acid

### 6.3.3 Antifungal effect of sourdough addition to bread

The effect of sourdough alone or in combination with preservatives on the mould-free shelf life was also assessed in challenge studies with *P. roqueforti* and *A. niger*. A first series of sourdoughs was prepared with wheat flour, fermented with *L. plantarum*, or *L. brevis* or *L. hammesii*. Use of wheat sourdough fermented with these three lactobacilli moderately but significantly extended the shelf life of bread challenged with *A. niger* but was ineffective against *P. roqueforti* (**Table 6.4**). The acetic acid concentrations in breads produced with *L. hammesii*, *L. plantarum* and *L. brevis* sourdoughs were 12.6  $\pm$  3.4, 13.2  $\pm$  4.7 and 16.2  $\pm$  2.3 mmol/kg, respectively.

**Table 6.4.** Effect of sourdough on the pH and the mould-free shelf life of bread. The sourdough was fermented with *L. hammesii*, *L. plantarum* or *L. brevis*, with or without addition of 4% sucrose; *L. hammesii* sourdough was combined with calcium propionate (3.1 mM) or sorbic acid (0.16 mM). The challenge test was with two indicator strains. Data are shown as means  $\pm$  standard deviations of three independent experiments. Values obtained for different breads with the same indicator strain differ significantly if they do not share a common superscript ( $p < 0.05$ ).

	Not fermented	<i>L. hammesii</i>	<i>L. plantarum</i>	<i>L. brevis</i>	<i>L. hammesii</i> + propionate	<i>L. hammesii</i> + sorbic acid	<i>L. hammesii</i> + sucrose	<i>L. plantarum</i> + sucrose	<i>L. brevis</i> + sucrose
<i>A. niger</i>									
Wheat	3.0 $\pm$ 0.6 <sup>c</sup>	4.8 $\pm$ 0.3 <sup>b</sup>	4.3 $\pm$ 0.6 <sup>b</sup>	4.7 $\pm$ 0.6 <sup>b</sup>	10.5 $\pm$ 0.7 <sup>a</sup>	7.0 $\pm$ 1.4 <sup>a</sup>	5.5 $\pm$ 0.7 <sup>b</sup>	5.0 $\pm$ 0.0 <sup>b</sup>	9.0 $\pm$ 0.0 <sup>a</sup>
Flaxseed	3.0 $\pm$ 0.0 <sup>c</sup>	5.0 $\pm$ 0.6 <sup>b</sup>	3.6 $\pm$ 0.6 <sup>c</sup>	3.7 $\pm$ 0.6 <sup>c</sup>	n.d.	n.d.	6.5 $\pm$ 0.0 <sup>b</sup>	5.0 $\pm$ 0.0 <sup>b</sup>	9.0 $\pm$ 0.0 <sup>a</sup>
<i>P. roqueforti</i>									
Wheat	5.3 $\pm$ 0.6 <sup>b</sup>	5.3 $\pm$ 0.6 <sup>b</sup>	5.0 $\pm$ 0.0 <sup>b</sup>	5.0 $\pm$ 0.0 <sup>b</sup>	8.3 $\pm$ 0.3 <sup>a</sup>	5.5 $\pm$ 0.7 <sup>b</sup>	6.5 $\pm$ 0.7 <sup>ab</sup>	5.5 $\pm$ 0.7 <sup>b</sup>	8.5 $\pm$ 0.7 <sup>a</sup>
Flaxseed	3.3 $\pm$ 0.6 <sup>c</sup>	5.0 $\pm$ 0.0 <sup>b</sup>	3.6 $\pm$ 0.6 <sup>c</sup>	4.3 $\pm$ 0.6 <sup>c</sup>	n.d.	n.d.	6.5 $\pm$ 0.7 <sup>ab</sup>	5.5 $\pm$ 0.7 <sup>b</sup>	8.5 $\pm$ 0.0 <sup>a</sup>
pH									
Wheat	5.4 $\pm$ 0.6 <sup>a</sup>	4.3 $\pm$ 0.1	4.3 $\pm$ 0.1	4.3 $\pm$ 0.0	4.2 $\pm$ 0.2	4.1 $\pm$ 0.2	4.5 $\pm$ 0.3	4.3 $\pm$ 0.1	4.6 $\pm$ 0.2
Flaxseed	5.3 $\pm$ 0.1 <sup>a</sup>	4.6 $\pm$ 0.1	4.5 $\pm$ 0.1	4.5 $\pm$ 0.6	n.d.	n.d.	4.4 $\pm$ 0.0	4.3 $\pm$ 0.0	4.3 $\pm$ 0.1

n.d., not determined.

The use of flaxseed sourdough in baking reduced the shelf life of bread except for sourdoughs fermented with *L. hammesii*. The acetate concentrations in bread produced with flaxseed sourdoughs fermented with *L. hammesii*, *L. plantarum* and *L. brevis* were  $33.8 \pm 4.4$ ,  $17.8 \pm 6.3$  and  $23.8 \pm 3.8$  mmol/kg of bread, respectively, which was substantially higher than acetate concentrations obtained with wheat sourdoughs.

Addition of calcium propionate (3.1 mM) to *L. hammesii* sourdough bread prolonged the shelf life of wheat bread challenged with *P. roqueforti* and *A. niger*; the combination of *L. hammesii* sourdough with addition of sorbic acid (0.2 mM) extended the shelf life of bread challenged with *A. niger* but not with *P. roqueforti*.

To additionally evaluate the effect of acetic acid concentrations, wheat or flaxseed sourdoughs were fermented with addition of 4% sucrose. Remarkably, the addition of sucrose to sourdough did not increase the concentration of acetic acid in bread relative to the bread without sucrose addition (data not shown). The mould-free shelf life of bread nevertheless increased, particularly for *L. brevis* sourdoughs, which increased the shelf life to 8.5 and 9 days for bread challenged with *P. roqueforti* and *A. niger*, respectively. A similar shelf-life was only obtained with the addition of propionate or sorbate.

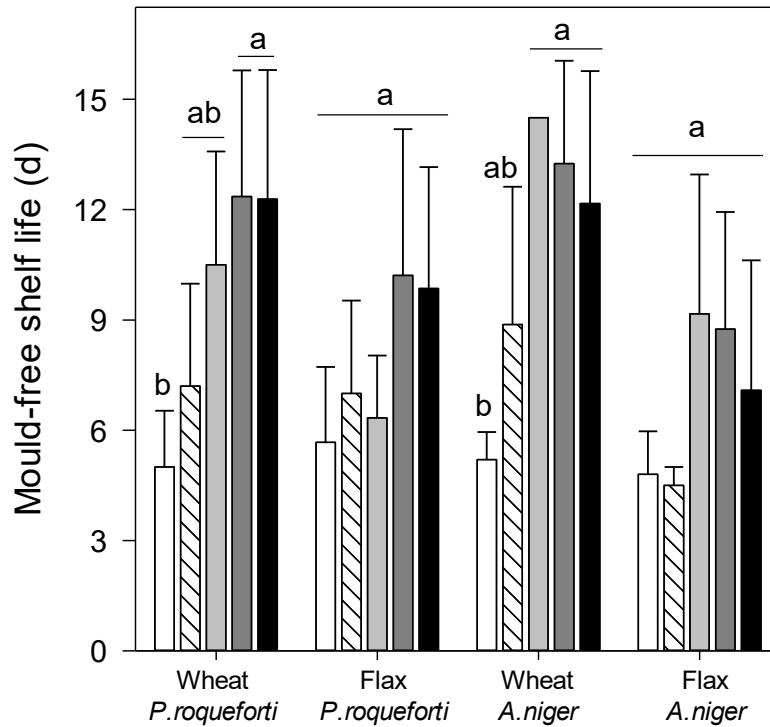


**Figure 6.2.** Effect of sourdough in combination with ricinoleic acid on the mould-free shelf life of bread. Control bread was produced without addition of sourdough (white bars); *L. hammesii*-fermented sourdough bread was produced with addition of 2% linoleic acid during sourdough fermentation (white hatched bars); or with addition of 0.03% (gray bars), 0.08% (dark gray bars) or 0.15% ricinoleic acid (black bars) added at the bread stage. Experiments were done with wheat sourdough or flaxseed sourdough as indicated and *Penicillium roqueforti* and *Aspergillus niger* were used as challenge organisms. Data are shown as mean  $\pm$  standard deviations of seven independent experiments. Values produced with the same sourdough and challenged with the same organism differ ( $p < 0.05$ ) if they do not share a common superscript.

Ricinoleic acid inhibited fungal growth *in vitro* (**Figure 6.1**) but did not delay fungal growth when added as sole preservative to bread (**Table 6.3**). To determine its activity in combination with *L. hammesii* sourdough, 0.03% to 0.15% ricinoleic acid, corresponding to 1 to 5 mM, were added to bread produced with *L. hammesii* wheat and flaxseed sourdoughs. Sourdough fermented with addition of 2% linoleic acid, the substrate for formation of the antifungal 10-hydroxy-12-octadecenoic acid by *L. hammesii*, was additionally evaluated. Addition of 0.08 or 0.15% ricinoleic acid increased the shelf life of wheat bread challenged with *A. niger* or *P. roqueforti* to >12 days (**Figure 6.2**); addition of 0.03% ricinoleic acid was effective only against *A. niger*. Addition of linoleic acid to sourdoughs fermented with *L. hammesii* did not delay fungal growth (**Figure 6.2**). An extension of the shelf life by sourdough in combination with ricinoleic acid was not observed in wheat bread with flaxseed sourdough; the increase of the average shelf life was less than experimental error (**Figure 6.2**).

#### 6.4 Discussion

Bread is subject to rapid deterioration after baking. Fungal spoilage is one of the main causes of bread spoilage. Moreover, formation of mycotoxins production by filamentous fungi represents a health risk.<sup>406</sup> *P. roqueforti*, one of the challenge strains used in this study, is highly resistant to biological or chemical preservation; this organism also often occurs as spoilage agent in bread.<sup>392</sup> An inoculum of 100-1000 spores per slice of bread<sup>399, 407, 49</sup> is substantially higher than the environmental contamination in industry practice. Environmental mould contamination is difficult to control and to reproduce, however, studies on the mould-free shelf life of bread consistently demonstrate that spoilage by environmental contaminants is substantially slower and more readily controlled by preservatives when compared to bread challenged with *Penicillium* spp.<sup>408, 384, 15</sup>

Challenge studies with *P. roqueforti* therefore represent a worst case scenario but nevertheless allow comparative assessment of different sourdoughs or additives.

We compared the *in vitro* MIC of antifungal bacterial metabolites and preservatives. Phenyllactic acid has the weakest antifungal activity. Inhibition of fungal growth at pH 4.5 was observed only at concentrations exceeding 30 mmol/L, corresponding to 5 g/L.<sup>58,407</sup> During growth in sourdough, lactobacilli produce phenyllactate from phenylalanine, however, the concentration of phenyllactate in sourdough remains below 0.2 mmol / kg or < 1% of the MIC.<sup>58, 54, 52</sup> The combination of different organic acids displays additive rather than synergistic activity when adjusting for the pH; therefore, phenyllactate is not likely to make a contribution to inhibition of fungal growth in bread.

Propionic acid, sorbic acid, ricinoleic acid and acetic acid displayed antifungal activity in the range of 1 – 24 mmol / L and the *in situ* activity matched the *in vitro* activity when assayed at the same pH. The pH plays a key role for the activity of weak organic acids.<sup>409</sup> Undissociated acids penetrate the fungal membrane and acidify the cytoplasm, leading to cell death.<sup>410</sup> The pKa of ricinoleic acid is estimated at 4.74; acetic acid, sorbic acid, and propionic acid have a pKa of 4.75, 4.76, and 4.90, respectively. Their activity in sourdough bread with pH < 5.0 is thus much higher than their activity in yeast-leavened bread with a pH of 5.5. Indeed, ricinoleic acid was ineffective in bread with a pH of 5.5 but displayed antifungal activity in sourdough bread. Sourdough fermentation thus has a double role in preservation as it accumulates antifungal organic acids and reduces the pH, thus increasing their antifungal activity. Of note, the Joint Food and Agriculture Organization/World Health Organization Expert Committee on Food Additives established an acceptable daily intake of castor oil, the primary source of ricinoleic acid, of 0.7 mg/kg body



weight.<sup>411</sup> However, ricinoleic acid is approved for use in food and the acceptable daily intake of ricinoleic acid was estimated to be much higher, 2.4 g per person and day.<sup>412</sup>

Lactic acid bacteria produce multiple metabolites with *in vitro* activity against fungal spores, including organic acids, cyclic dipeptides, and long-chain hydroxyl fatty acids.<sup>392, 15, 395</sup> The present study identified acetic acid as the most relevant antifungal compound produced by lactic acid bacteria, as it is readily accumulated to concentrations matching the MIC against fungal spores. Acetate formation by heterofermentative lactic acid bacteria can be adjusted by addition of sucrose, providing fructose to allow regeneration of co-factors and increased acetate formation in heterofermentative metabolism.<sup>413, 397</sup> Addition of acetic acid to bread delays fungal spoilage;<sup>394</sup> however, excess levels of acetic acid also result in an unacceptable flavour<sup>414</sup> and interfere with development of the gluten network in wheat baking.<sup>396</sup> Acetic acid in concentrations of 10–30 mmol/kg has a beneficial impact on bread flavour;<sup>414</sup> the current study demonstrates that this range of acetic acid concentration also substantially contributes to the mould-free storage life of bread.

The combination of acetate with other antifungal compounds reduces or prevents the adverse impact of individual organic acids on bread flavour. Proof of concept was provided by prior studies using sourdough containing propionic and acetic acids,<sup>49</sup> or using sourdough in combination with propionate.<sup>402</sup> We extended prior observations by demonstrating additive activity of sourdough or acetic acid with propionic acid, ricinoleic acid and sorbic acid. The antifungal effect of acetic acid in combination with other antifungal organic acids is attributable to the additive antifungal activity of organic acids (**Tables 7.3 and 7.4**). In combination with acetic acid or sourdough, the propionate or sorbate concentration required for shelf life extension of wheat sourdough bread was reduced 7-fold when compared to the amount required for preservation of straight dough bread. Remarkably, ricinoleic acid was effective only in combination with sourdough.

The additive activity of *L. hammesii* sourdough and ricinoleic acid, an unsaturated hydroxy-fatty acid present in castor oil, was further explored by adding different levels of ricinoleic acid to bread produced with *L. hammesii* sourdough. The antifungal activity of ricinoleic acid is comparable to other unsaturated hydroxy fatty acids including coriolic acid and 10-hydroxy-12-octadecenoic acid, which are produced by enzymatic or microbial conversion of linoleic acid in sourdough.<sup>15,66</sup> The addition of 0.15% coriolic acid to bread also significantly increased the mould-free shelf life of bread.<sup>15</sup> Our study demonstrates that a combination of sourdough and ricinoleic acid displayed a similar antifungal performance at a ricinoleic acid concentration of 0.08%.

Sucrose addition to sourdough did not substantially increase the acetate concentration in bread. The availability of substrates for co-factor regeneration in wheat sourdough supports formation of 10-20 mmol/g acetate in wheat sourdough; the acetate concentration can be increased by addition of sucrose.<sup>415</sup> With a sourdough addition of 10%-30%, the carry-over of acetic acid from sourdough accounts for only 2-6 mmol/g and most of the acetic acid that is present in bread, 10-20 mmol/g, was produced after the final mixing in the bread dough where sucrose levels were not different. Heterofermentative lactobacilli produce acetate rather than ethanol as long as electron acceptors are available.<sup>415, 413</sup> In artisanal and industrial practice, the sourdough addition to bread dough ranges from as little as 3% for high acidity, long time fermented type II sourdoughs to >30% for metabolically active type I sourdoughs with a relatively high pH and low acidity.<sup>416, 417, 418</sup> Independent on the level of addition, however, antifungal compounds present in sourdough are diluted three-fold to >10-fold. Sourdoughs that are propagated in bakeries typically are fermented to warrant a high metabolic activity of lactobacilli in bread dough,<sup>417, 419</sup> however, a substantial proportion of industrial sourdough products does not warrant metabolic activity of sourdough microbiota in bread dough.<sup>416, 418</sup> In brief, the impact of sourdough on the mould-free shelf life of

bread necessitates metabolic activity of sourdough microbiota during proofing and hence depends strongly on the sourdough technology employed.

Replacement of wheat with other substrates for sourdough fermentation and/or baking significantly impacts the mould-free shelf life of bread.<sup>58,408</sup> Different substrates support formation of different levels of organic acids<sup>408</sup> and are a potential source of plant bioactives with antifungal activity.<sup>397</sup> We explored the use of flaxseed sourdough; flaxseed is rich in linoleic acid<sup>420</sup> and may support the enzymatic or microbial formation of antifungal hydroxy fatty acids from linoleic acid. In addition, flaxseed offers health benefits in relation to cardiovascular diseases that are derived from its high fibre content and the content of  $\omega$ -3 fatty acids.<sup>421, 422, 423</sup> Fungal growth on bread produced with flaxseed or flaxseed sourdoughs was equal or faster when compared to the wheat counterparts. Bread produced with flaxseed sourdoughs contained higher levels of acetate than the corresponding wheat breads; however, flaxseed also contains mucilage with high water binding capacity.<sup>424</sup> Hydrocolloids may increase the water activity of bread and hence accelerate fungal spoilage. Our data suggest that linoleic acid bound in triglycerides does not support formation of the antifungal 10-hydroxy-12-octadecaenoic acid by *L. hammesii* in flaxseed sourdoughs. Bacterial hydration of free unsaturated fatty acids is a mechanism of detoxification<sup>17</sup> and past studies aiming to convert plant oil to bioactive lipids by lactic acid bacteria employed lipase to achieve hydrolysis of triglycerides.<sup>425</sup>

In conclusion, we demonstrate that the *in vitro* MIC of bacterial metabolites and preservatives matches the *in situ* antifungal effect. We also demonstrated that the accumulation of antifungal metabolites in sourdough is a difficult proposition - because sourdough is used at a dosage of only 10 to 20%, antifungal metabolites are relevant only if they are produced in bread dough, or if the concentration of antifungal metabolites in sourdough exceeds the MIC by a factor of at least 5-10.

Acetic acid is the most significant antifungal metabolite of lactobacilli, mainly because it is rapidly produced during mixing and proofing of the bread dough and is thus present in bread at concentrations close to the MIC. Irrespective of the presence of antifungal metabolites, however, the use of sourdough greatly enhances the activity of weak organic acids through the reduction of pH, and allows to exploit additive antifungal activities of different organic acids. We have demonstrated additive activity of sourdough use with sorbic acid, propionic acid, and ricinoleic acid. In addition, the study provides a conceptual template for the exploration of synergistic or additive effects of sourdough with other antifungal additives or ingredients.

## Chapter 7. Identification and quantitation of fatty acids in fermented sausage samples

### 7.1 Introduction

Lipid profile, including lipid content and fatty acid composition plays a critical role in the quality of meat products,<sup>426, 427</sup> including fermented meats.<sup>428</sup> While impacting the susceptibility towards lipid oxidation, lipid profile also impact protein oxidation and thus the formation of carbonyl compounds.<sup>428</sup> These oxidation reactions can strongly influence the shelf life, nutritional value, and the development of taste, color, odor and texture in meat products.<sup>429, 430, 431</sup> During fermentation, free fatty acids are released from triglycerides.<sup>432, 433</sup> Volatile fatty acids with less than 6 carbon atoms are flavor compounds (sour-like sensation);<sup>46, 434</sup> long chain fatty acids, especially unsaturated fatty acids are not only flavor contributor of “Oleogustus” taste<sup>434</sup> (for example, oleic acid has a taste threshold of less than 1 g / kg),<sup>435</sup> but also precursors for oxidation to potent flavor volatiles.<sup>436, 437, 438, 439</sup> Endogenous lipases are a major factor in controlling the hydrolysis of bound lipids into free fatty acids during sausage ripening;<sup>432, 433</sup> fatty acids are then converted into other products via non-enzymatic oxidation and microbial enzymatic reactions.<sup>439, 440, 441</sup>

Microbial conversion of fatty acids generates oxygenated derivatives of fatty acids<sup>39</sup> that provide additional functions in food. For example, the conversion of linoleic acid to mono-hydroxy fatty acids by *L. hammesii* in sourdough extended the mold-free shelf life of bread.<sup>191</sup> *L. sakei*, which is commonly used as starter culture in fermented meats, also possesses fatty acid hydratase<sup>442</sup> but the production of hydroxy fatty acids (HFAs) has not been described in meat fermentations.<sup>443</sup> Hydroxy fatty acids have antifungal activity,<sup>343</sup> in addition, they are precursors for odor-active lactones.<sup>444</sup> The hydroxy fatty acid coriolic acid (13-OH C18:2) has a bitter taste

with a threshold of about  $\sim 2 \text{ g / L}$ .<sup>445, 357</sup> These functions of HFA as antifungals<sup>343</sup> or flavor contributors are dependent on the specific HFA structure as well as the antagonistic, additive or synergistic interaction with other compounds in the food matrix. It is therefore important to characterize HFA structures and concentrations, in order to attribute them to specific functions, and thus manipulate them in the pursuit of desirable food qualities.

While the relevance of oxylipins for taste and preserving activity has been demonstrated in cereal products including oats and bread,<sup>357, 15</sup> their formation in meat products, which typically have a much higher lipid content, is poorly documented. Linking microbial metabolism to biochemical conversion in meat fermentation requires controlled sausage models that exclude interference of spontaneous microbiota.<sup>446, 447, 448</sup> The profile of free fatty acid in fermented meats has been documented only in sausage models without aseptic control, and thus include a contribution of uncharacterized background microbiota.<sup>449, 450, 451, 452, 453</sup> In addition, past studies have quantified lipolytic activity *via* the equivalent weight percentage of oleic acid produced,<sup>454, 455</sup> rather than to investigate fatty acid metabolisms through quantifying the production of various fatty acid and oxylipin species. Oxylipins were identified in meat products,<sup>456, 457</sup> but knowledge of the impact of starter cultures on the production of these oxylipins in fermented meats, as well as their function in meat products, are scarce.

This study aims to investigate how starter cultures impact the quality of fermented meat products *via* the possible production of HFA. We have used samples from a beef sausage model that was developed to achieve a well-controlled aseptic environment, with non-detectable microbiota within the 20-day ripening stage.<sup>458</sup> Novel HFAs were extracted from the meat matrix and purified by high-speed count-current chromatography (HSCCC) in order to elucidate their structures by a combination of LC-MS/MS and GC-MS methods. HSCCC methods were

previously developed to separate HFA from bread<sup>191</sup> and plants;<sup>66</sup> these solvents systems need to be optimized for the separation of the specific HFA structures found in meat products. In addition, LC-MS/MS method was validated for the quantitation of fatty acid in modeled beef sausages, including an aseptic negative control and sausages fermented with strains isolated from industrial sausage cultures, including *Lactobacillus sakei*-fermented sausage and sausage co-fermented with *Lactobacillus sakei* and *Staphylococcus carnosus*. These samples were analyzed to compare the effect of starter culture on the fatty acid composition of sausage.

## 7.2 Materials and methods

### 7.2.1 Chemical and reagents

Optima<sup>®</sup> LC/MS-grade solvents, including acetonitrile, acetic acid and water, molecular-biology-grade isopropanol and HPLC-grade reagents, including ammonium acetate, hexane and isopropanol were purchased from Fisher Scientific (Ottawa, Canada); ACS-grade methanol was obtained from Sigma-Aldrich (Oakville, Canada).

Fatty acid standards, including tetradecanoic (myristic, C14:0) acid, hexadecanoic (palmitic, C16:0) acid, 12 hydroxy-9-*cis*-octadecenoic (ricinoleic, 12-OH C18:1) acid, 9-octadecenoic (oleic, C18:1) acid, 9-*cis*,12-*cis* octadecadienoic (linoleic, C18:2) acid, octadecanoic (stearic, C18:0) acid, 9-*cis*,12-*cis*,15-*cis* octadecatrienoic (alpha linolenic, C18:3) acid, heptadecanoic (C17:0) acid, 9-tetradecenoic (myristoleic, C14:1) acid, 9-hexadecenoic (palmitoleic, C16:1) acid and 12-hydroxy stearic acid (12-OH C18:1) with purity >99% were obtained from Nu-Chek Prep, Inc (Elysian, MN, USA). 9,10-dihydroxy stearic acid was obtained from Pfaltz & Bauer (Waterbury, USA).

2-Hydroxyoleic acid (2-OH OA, sodium salt, purity >99%) was purchased from Avanti Polar Lipids, Inc (Alabaster, USA). The free acid form of 2-hydroxyoleic acid was obtained by dissolving approximately 140mg 2-OH OA sodium salt in 10mL pure water, adding 1mL 4M HCl to adjust pH, extracting free fatty acid with 10mL hexane for three times, combining the hexane fractions and removing the hexane under nitrogen.

13-Hydroxy-9-*cis*,11-*trans*-octadecadienoic acid (coriolic, 13-OH C18:2) acid was purified from *Coriaria nepalensis* seed oil using high-speed counter-current chromatography (HSCCC) and its purity was confirmed by the single peak observed both in LC-APPI-MS and LC-ESI-MS.<sup>66</sup>

### 7.2.2 Preparation of beef sausage fermentation

Samples were obtained from fermented beef sausages described by Tang et al.<sup>458</sup> Briefly, *L. sakei* FUA 3009, *L. sakei* FUA 3549 and *S. carnosus* FUA2133 were isolated from commercial meat starter cultures. The sub-culture of *L. sakei* was cultivated in MRS media at 30 °C anaerobically for 16 h, and sub-culture of *S. carnosus* was grown in MRS at 37 °C, 200rpm. Starter culture inoculation was performed with the strains sub-cultured twice, followed by centrifugation, washing, and re-suspension. For *L. sakei* fermentation, 10mL of FUA 3009 was used; for fermentation of *L. sakei* and *S. carnosus*, 5mL of each of FUA 3549 and FUA 2133 were combined. The cell count of inoculum was controlled to obtain ~9 log (cfu/mL) for *Lactobacillus* and ~8log (cfu/mL) for *S. carnosus*. For the aseptic control, 10mL of antibiotics solution containing 100mg/L each of chloramphenicol, ampicillin and erythromycin was used instead. For the following procedures, a laminar flow biosafety cabinet was used for handling of meat and sausage batters, and 70% ethanol was used to sterilize product contact surfaces and utensils. Sausage batter was made with the following ingredients (expressed as w/w %): 86%



ground beef, 3.66 % NaCl, 0.01% NaNO<sub>2</sub>, 0.3% glucose, 0.03% sodium ascorbate and 10 % bacterial inoculum for the bacterial fermentation groups, or 10% antibiotics solution for the aseptic control.

In preparation of the sausages, a exterior fat, intramuscular fat and connective tissues were removed from a bottom round of beef with a sterile knife, and the cuts were vacuum-packaged and frozen at -20 °C. Frozen lean beef was defrosted at 4 °C overnight and a seasoned beef batter was prepared by mincing the meat with dry ingredients using a food processor. The batter was portioned, packaged and frozen at -20 °C again. The batter was portioned, packaged and then frozen at -20 °C again. To prepare the beef sausages, the seasoned beef batter was thawed at 4 °C overnight and mixed with inoculum or antibiotics. This beef batter was then homogenized by a stomacher, stuffed into dialysis tubing (32mm\*3.3mL\*5cm) with plastic closures at refrigeration temperature, and the outside was sprayed with 20% (w/v) potassium sorbate solution. The sausages were then incubated at 20 °C at a relative humidity of 90% (controlled using saturated barium chloride solution) for 3 days, and then incubated at 18 °C and relative humidity of 83% (controlled with 2.9 mol/kg NaCl solution) for an additional 17 days. Observation of a uniform colony morphology in the cell counting agar plate (MRS agar of pH 5.5 was used for lactobacilli and mannitol salt agar was used for staphylococci) of inoculated samples was used to confirm the identity of fermentation microbiota with the inoculum.<sup>458</sup> Cell count of un-inoculated seasoned beef was found to be below the detection limit. Sausage samples were then freeze-dried, powdered using mortar and pestle, and stored at -20 °C before analysis.

Sausages with different fermentation methods (negative control, *Lactobacillus sakei* and *L. sakei* + *Staphylococcus carnosus*) were sampled at fermentation times of 0, 3 and 20 days (labeled

as D0, D3 and D20, respectively). Three biological repeats were performed for each type of sausage at each time point.

### **7.2.3 Extraction of fatty acids from sausage sample**

Fatty acids were extracted from sausage samples by mixing of 0.1 g homogenized sausage sample with 5 mL isopropanol and vortexing for 30 s. Solids were removed by centrifugation at 5000 rpm for 5 min and the supernatant was collected. Solids were additionally extracted 3 times by vortexing with 3mL isopropanol<sup>15</sup> and additionally 3 times with 3 mL hexane/isopropanol (3:2, v/v).<sup>459</sup> Organic supernatants were combined and dried under nitrogen. The extraction recovery was then confirmed in the method development section.

### **7.2.4 HPLC-MS and MS/MS analysis of fatty acids**

#### **7.2.4.1 Quantitation of major free fatty acids in sausage samples**

Free fatty acid extracted from 0.1 g of homogenized sausage sample were re-dissolved in 1 mL methanol, and diluted 1:20 (v/v) with addition of ricinoleic acid as internal standard to a concentration of 5 mg/L. The diluted samples were then analyzed by reversed-phase liquid chromatography coupled with negative-ion electrospray ionization-tandem mass spectrometry (LC-ESI-MS/MS).

For absolute quantitation of the major free fatty acids, the diluted samples (2  $\mu$ L) were injected to Agilent 1200 series LC system comprised of a binary pump and auto-sampler (Agilent Technologies, Palo Alto, CA, USA). Fatty acids were separated on an Ascentis Express C8 column (15 cm $\times$ 2.1 mm, 2.7  $\mu$ m in particle size) (Sigma, St. Louis, MO) at room

temperature, using a 0.25 mL/min flow of mobile phase comprised of water with 10 mM ammonium acetate and 0.2% acetic acid (**A**) and 98% acetonitrile and 2% of water with 10 mM ammonium acetate and 0.2% acetic acid (**B**). The gradient was as follows: 0-23 min 70% to 100% **B**, followed by re-equilibration to 70% **B**. Total run time was 30 min.

Negative-ion ESI-MS/MS was operated on a 3200 QTRAP triple-quadrupole mass spectrometer coupled with a TurboIonSpray electrospray ionization ion source (AB SCIEX, Concord, ON, Canada).

For the identification of fatty acids, each targeted ion (**Table 7.1**) was extracted and retention times was compared against authentic fatty acid standards in both full scan mode and multiple reaction monitoring (MRM) mode; MRM mode was then used for the quantitation of fatty acids, with parameters listed in **Table 7.1**.

Nitrogen was used as the curtain gas, nebulizing gas and drying gas. The conditions of the ion source and mass spectrometer used were as follows: mass range  $m/z$  100-1000, scan rate of 1 scan/sec, GS1 40, GS2 60, curtain gas 25, declustering potential (DP) -60 V, ion spray voltage -4500 V, ion source temperature 450 °C, collision energy (CE) 36 V, collision cell entrance potential (CEP) -20 V and collision cell exit potential (CXP) -1 V. A dwell time of 40 ms was used in MRM experiments.

#### **7.2.4.2 Relative quantitation of potential 2-hydroxy fatty acid in sausage samples**

For the relative quantification of 2-OH fatty acids in sausage samples, due to their low abundance in the extracts, instead of diluting sample as described in section **2.4.1** above, a 40 $\mu$ L aliquot of each extract was dried under nitrogen and re-dissolved in 50 $\mu$ L methanol containing the

internal standard (ricinoleic acid) at a concentration of 5 mg/L. LC-MS was performed as described above (section 2.4.1) with two modifications: 1) replacing acetic acid and ammonium acetate by formic acid and ammonium formate, respectively, at the same concentrations; 2) in addition, another MRM transitions were added as shown in **Table 7.1** (decorated with “\*”), and parameters for each ion transition, including declustering potential (DP), entrance potential (EP), collision energy (CE), collision cell entrance potential (CEP) and collision cell exit potential (CXP) were optimized for possible hydroxy fatty acids containing the characteristic pattern of fragmentation ions of  $[M-H]^-$  and  $[M-H-46]^-$  using one of the sample of 3549-D20.

Calibration curves were generated from dilution series of pure standards. Data acquisition and processing was operated through AB SCIEX Analyst 1.4.2. software.

### **7.2.5 Optimization of HSCCC solvent system and enrichment of HFAs from sausage sample using HSCCC**

*K* value determination and HSCCC procedures were similar to that described in a previous study.<sup>66</sup> After optimization, 2L of the selected solvent system composed of hexane-ethyl acetate-methanol-water was prepared, and the two immiscible phases were mixed, settled, separated, and sonicated. The upper phase was used as stationary phase and pumped into the system before rotation of the column. After the column was filled with the upper phase, the column was rotated at 1000 rpm, and the mobile (lower) phase was introduced at 3 ml/min. Once the mobile phase eluted continuously from the column, a 10mL sample (600uL of the extracted sample dried and re-dissolved in 5mL upper phase and 5mL lower phase) was then injected into the column. The fractions were collected every 1min. These fractions were monitored by flow injection analysis

(FIA)-ESI-MS/MS-MRM. Fractions that have the same composition were combined, dried, further derivatized and analyzed.

#### **7.2.6 Methylation, silylation and GC-MS analysis of fatty acids.**

CCC-enriched fractions were dried under nitrogen and 0.4mL of 15% boron trifluoride in methanol (Sigma) was added to the samples. After vortexing, the reaction was carried out at 100°C for 7min. The mixture was cooled down to room temperature, and 0.8mL of hexane and 0.8mL water were both added into the mixture. After mixing and settling, the hexane layer was collected and another portion of 0.8mL of hexane was added to repeat the extraction. The hexane extracts containing fatty acid methyl esters (FAME) were combined and dried under nitrogen, then re-dissolved in 100 µL of hexane, prior to the direct GC-MS analysis of FAME, or further reaction to silylate the hydroxy group of FAME.

In order to silylate the hydroxyl groups in any HFAs which are present, BSA+TMCS+TMSI reagents (Sigma-Aldrich Canada, Oakville, Canada) (10µL) and anhydrous pyridine (10µL) were added into the FAME sample described above , and the mixture was kept at room temperature for 15min. Then, hexane (80 µL) was added into the reaction mixture, prior to GC-MS analysis.

The EI-GC-MS analysis was performed on a 7890A GC system coupled with 5975C mass spectrometry with triple-axis detector (Agilent Technologies). A splitless injection volume of 1.0 µL was used. Derivatized fatty acids were separated using a mid-polarity column DB-17 (30 m, 0.25 mm, 0.25 µm) (Agilent). The injection temperature was 250°C. The oven temperature was initially kept at 50°C for 2min, then increased to 250°C at a rate of 20°C/min and held for 10min (a total run time 22min). The mass spectrometer operated over a mass range of  $m/z$  50-700.

## 7.3 Results

### 7.3.1 Identification of hydroxy fatty acids in beef sausages fermented with *L. sakei*, or *L. sakei* and *S. carnosus*.

In order to test the hypothesis that *L. sakei* or the combination of *L. sakei* and *S. carnosus* produce HFAs in meat, LC-MS analyses were performed to search for the presence of HFAs.

LC-APPI-MS/MS was used to determine whether mono-hydroxy derivatives of C18 fatty acids that are produced by *Lactobacillus* spp.<sup>39, 191</sup> are present in the sausage samples. To do this, product ion scans of the ions of  $m/z$  297.2, which correspond to mono-hydroxy C18:1 fatty acids were performed. Comparing the LC-APPI-MS/MS traces for C18:1  $m/z$  297.2 (**Figure 7.1A**) it was found that the abundance of mono-HFA was much greater for samples fermented with both *L. sakei* and *S. carnosus*. Comparison of the MS/MS spectra of the main peaks in the chromatogram (labelled as peaks a, b, c, d and e in **Figure 7.1A**) reveals that the compound represented by peak a (**Figure 7.1 A**) is specific to the fermentation of *L. sakei* and *S. carnosus*, giving an intense fragment ion of  $[M-H -46]^-$ . In contrast, peaks b and d, and peak c and e have similar MS/MS spectra that are distinct from that of peak a. The similarity between the chromatograms and the MS/MS spectrum of the two major peaks for the negative control and *L. sakei*-fermented sausage suggests that mono-OH C18:1 in *L. sakei*-fermented sausage is likely to be formed by lipid peroxidation, followed by reduction of the peroxide to the hydroxide (as is the case for the negative control).

**Table 7.1.** MRM transition and optimized parameters for fatty acid standards

Compounds	Q1 Mass	Q3 Mass	DP (volts)	EP (volts)	CEP (volts)	CE (volts)	CXP (volts)	Retention time (min)
Ricinoleic acid	297.2	183.1	-50	-6.5	-14	-30	0	5.9
9,10-di OH stearic acid	315.3	171.1	-60	-8.5	-16	-36	0	3.8
Coriolic acid	295.2	195.1	-45	-7	-18	-26	-2	5.0
Linoleic acid	279.2	279.2	-45	-10.5	-14	-16	-2	14.2
Heptadecanoic acid	269.3	269.3	-45	-6	-12	-14	-2	19.0
Myristic acid	227.1	227.1	-50	-10.5	-12	-14	-2	11.7
Palmitic acid	255.2	255.2	-55	-8.5	-14	-16	-2	16.5
Stearic acid	283.3	283.3	-50	-11.5	-14	-16	-2	21.4
Oleic acid	281.3	281.3	-55	-7.5	-14	-14	-2	17.6
Linolenic acid	277.2	277.2	-40	-8.5	-18	-12	-2	11.3
2-OH oleic acid	297.2	251.2	-60	-6.5	-14	-28	-2	9.4
Myristoleic acid	225.2	225.2	-40	-7.5	-12	-16	0	8.6
Palmitoleic acid	253.2	253.2	-50	-4.5	-14	-12	-2	12.9
12-OH stearic acid	299.2	299.2	-55	-12	-14	-14	-2	7.5
Hypothetical hydroxy C14:0	243.2	197.2	-60	-8	-14	-26	0	7.0*
Hypothetical hydroxy C16:1	269.2	223.2	-65	-7	-14	-26	0	7.9*
Hypothetical hydroxy C18:2	295.2	249.2	-65	-8.5	-14	-26	-2	9.0*
Hypothetical hydroxy C16:0	271.2	225.2	-65	-7	-12	-28	-2	10.5*
Hypothetical hydroxy C18:1	297.2	251.2	-65	-8	-14	-30	-2	11.5*
Hypothetical hydroxy C18:0	299.2	253.2	-65	-8	-14	-30	-2	13.8 and 14.4*

\*: Retention time obtained using the method in section of “7.2.4.2 relative quantitation of potential 2-hydroxy fatty acid in sausage samples”

\* Abbreviation: declustering potential (DP), entrance potential (EP), collision energy (CE), collision cell entrance potential (CEP) and collision cell exit potential (CXP)

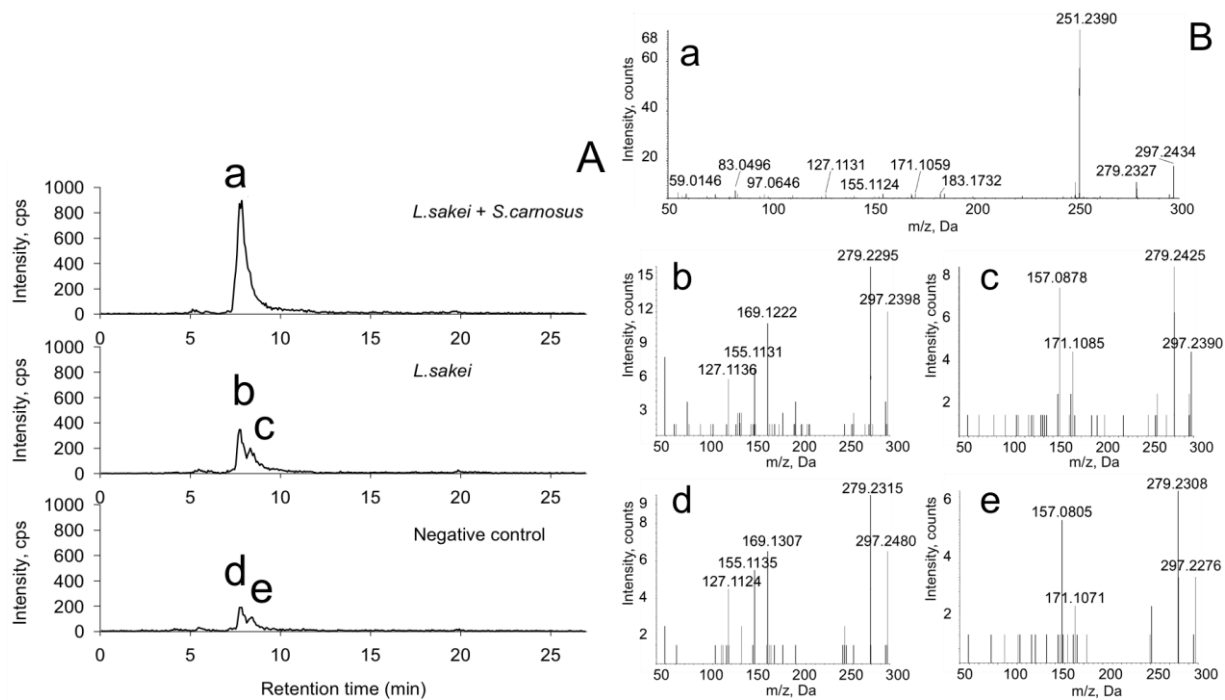


**Figure 7.1.** A) LC-APPI-MS Extracted ion chromatogram (XIC) of  $m/z$  297 of sausage lipid in negative control, or sausage lipid fermented by *Lactobacillus sakei* and *L. sakei* + *S. carnosus*; 5 peaks observed in the chromatogram are label as peak a-e; B) LC-APPI-MSMS spectra of precursor ion of  $m/z$  297 of peak a-e in A, respectively.



In the case of fermentation with *L. sakei* and *S. carnosus*, a unique HFA isomer is formed, likely as a result of a microbial enzyme (**Figure 7.1A** peak a). Similar HFAs unique to this fermentation were also observed in the product ion scan of ion  $m/z$  299.2 and 295.2, which represent mono-OH C18:0 and mono-OH C18:2 (not shown). The major ions in the MS/MS spectra of these three mono-HFA  $[M-H]^-$  ions from the LC-MS/MS chromatograms all include the fragment ions  $[M-H-46]^-$ , i.e.  $m/z$  299.260 $\rightarrow$ 253.256, 297.243 $\rightarrow$ 251.239, 295.229 $\rightarrow$ 249.222. This fragmentation  $[M-H]^- \rightarrow [M-H-46]^-$  is common for the MS/MS spectra of hydroxy fatty acids (HFAs), ascribed to a mechanism of charge directed loss of CO<sub>2</sub> and loss of H<sub>2</sub>, as reported.<sup>460 284</sup> The presence of hydroxy fatty acids with carbon number of C2-C22 and 0-3 double bonds was then explored by LC- MRM analysis using the  $[M-H]^- \rightarrow [M-H-46]^-$  transition for each possible HFA (**Figure 7.1B** and **Table 7.1**). Seven peaks were detected, and their LC-ESI-MS/MS-MRM parameters were recorded (**Table 7.1**). Among them, the two major peaks represented the hypothetical structures of hydroxy C16:0 and C18:1 fatty acid, respectively.

In order to confirm the structures of these HFAs, other techniques are required that are more specific to the location of hydroxyl groups and double bonds. To this end, it was necessary to purify the observed HFAs, which was achieved using HSCCC. The solvent system used initially consisted of the widely used hexane-ethyl acetate-methanol-water (HEMWat),<sup>59</sup> in this case at ratios of 7-3-7-3 and 8-2-8-2 (v/v/v/v). With these solvent mixtures, the partition coefficients (K) of the six hypothetical HFAs, (i.e. OH-C14:0, OH-C16:1, OH-C18:2, OH-C16:0, OH-C18:1 and -OH-C18:0) between upper and lower phases, were in the range of 0.1-0.4. This is outside of the range that would be considered suitable for separating these compounds.<sup>461</sup> The addition of 0.1% of acetic acid (v/v, of the total volume of the solvent system) improved the  $K$  values of these 6

compounds to the range of 1.4-8.0 for the 7-3-7-3 solvent system, but were still not suitable due to the very strong retention of the target compounds within the solvent system.<sup>461</sup> Finally, *K* values of 0.4, 0.5, 0.6, 0.8, 1.0, 2.0 were obtained (for OH-C14:0, OH-C16:1, OH-C18:2, OH-C16:0, OH-C18:1 and -OH-C18:0 respectively) using an 8-2-8-2 HEMWat solvent system.

The separation of six hypothetical HFAs was then attempted using this solvent system. To do this, the HSCCC fractions were monitored using flow injection analysis (FIA)-ESI-MS/MS (**Figure 7.2A**, where the signal of each hypothetical HFA was monitored). Good separation of the six hypothetical HFAs was achieved, as seen in **Figure 7.2 A**. In addition, LC-ESI-MS/MS analysis was used to confirm the purity of the fractions collected, which was performed by generating total ion chromatograms (TIC) of 44 MRM transitions of  $[M-H]^-$  and  $[M-H-46]^-$  that represent possible C2-C22 hydroxy fatty acids with 0-3 double bonds (**Figure 7.2B**). Using the same TIC analysis, 7 peaks were observed in the chromatogram before separation (**Figure 7.2B-a**) while mostly single peaks were observed in the chromatograms of separated fractions (**Figure 7.2B-b-g**).

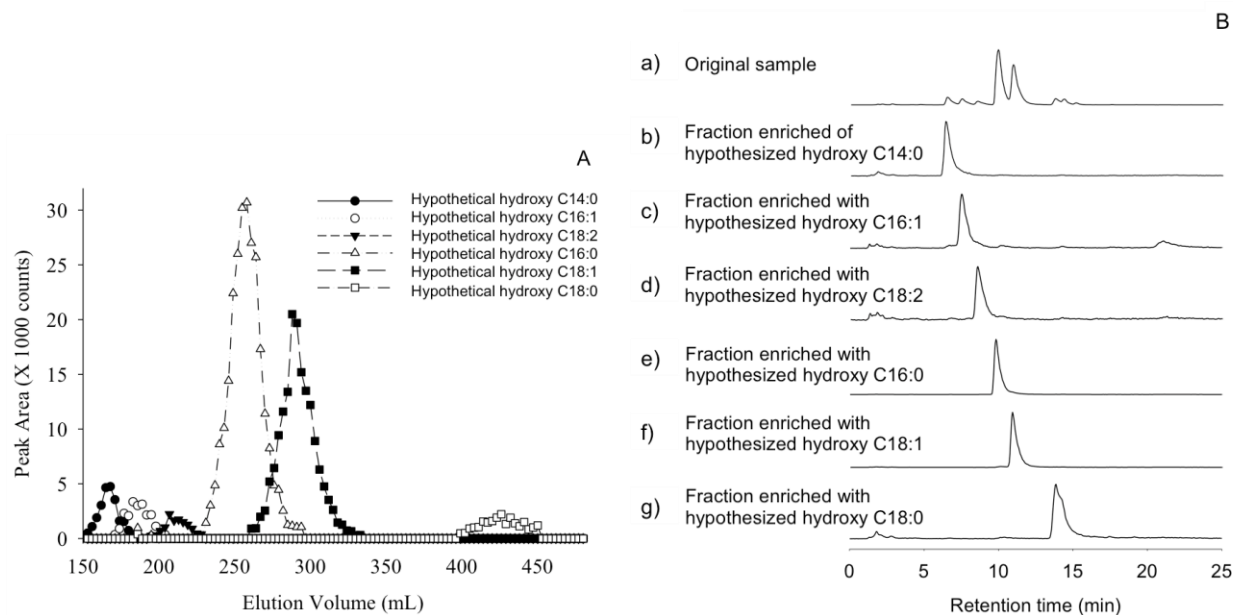


**Figure 7.2. A)** HSCCC chromatogram of hypothetical hydroxy fatty acids from sausages.

Fractions were analyzed by FIA-ESI-MRM (TIC) of the fractions collected during HSCCC separation. HSCCC employed the solvent system of HEMW (4:1:4:1, v/v/v/v) with 0.1% acetic acid addition. **B)** HSCCC separation of hypothesized HFAs, monitored by LC-ESI-MSMS-MRM experiment. a) was analysis of original samples before separation and b)-g) were of different fractions collected from separation that was enriched with 6 individual hypothetical hydroxy fatty acids.

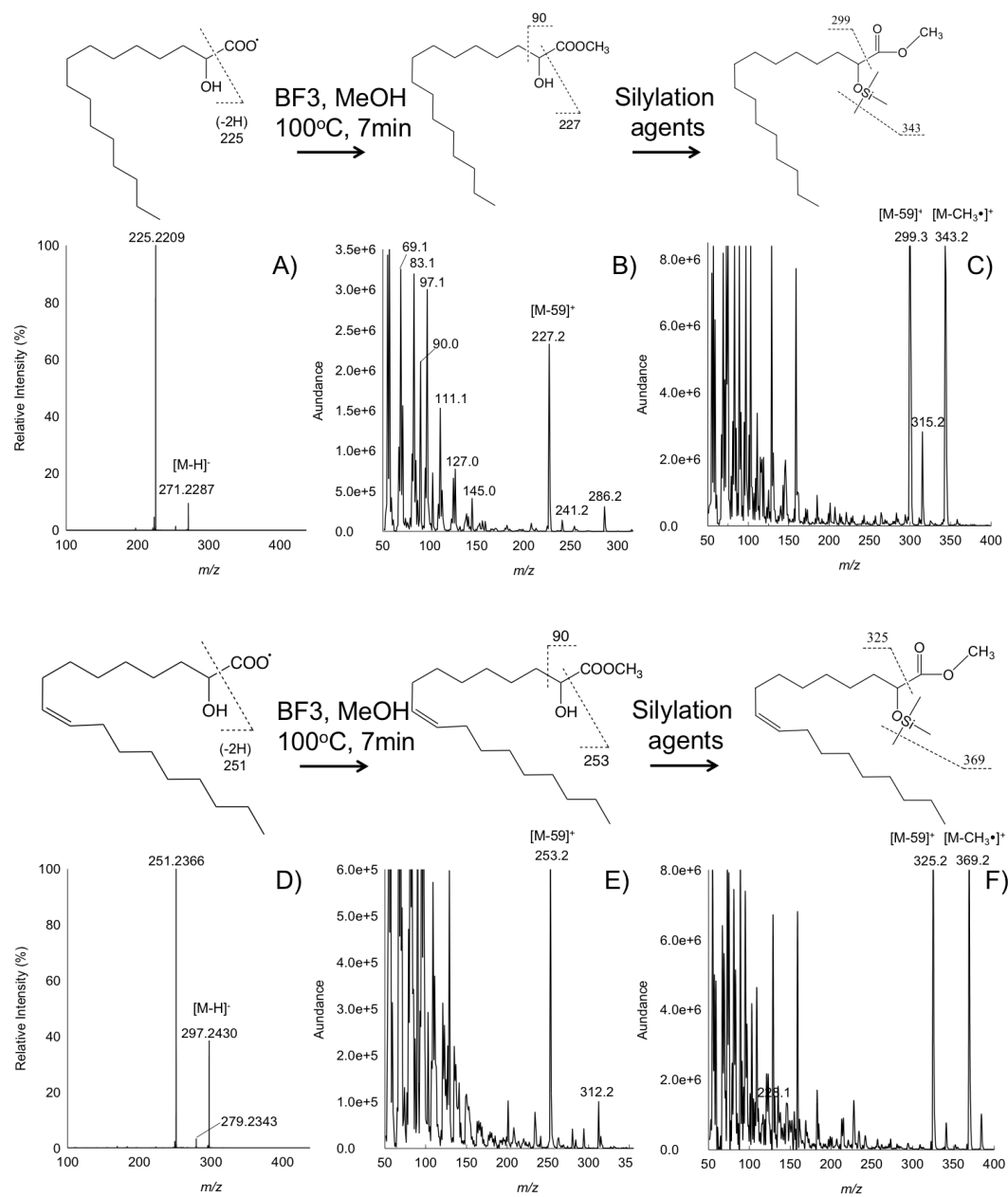


**Figure 7.3.** A) ESI-MS spectrum of hypothesized 2-OH C16:0 enriched fraction; B) EI-MS spectrum of hypothesized 2-OH C16:0 FAME structure; C) EI-MS spectrum of hypothesized silylated 2-OH C16:0 FAME structure; D) ESI-MS spectrum of hypothesized 2-OH C18:1; E) EI-MS spectrum of hypothesized 2-OH C18:1 FAME structure; F) EI-MS spectrum of hypothesized silylated 2-OH C18:1 FAME structure.

To characterize the two major hydroxy fatty acids shown in **Figure 7.2**, which is hypothesized to be 2-OH C16:0 and 2-OH C18:1, ESI-MS analysis, and methylation and silylation, followed by GC-MS analysis were performed. The ESI-MS spectrum of the enriched fractions of the two structures confirmed the characteristic ion combination of  $[M-H]^-$  and  $[M-H-46]^-$  (**Figure 7.3A and D**). In GC-MS analysis, the mass spectra of methylated fractions matched the corresponding spectra of the standard in the NIST library (The NIST Mass Spectral Search Program for the NIST/EPA/NIH Mass Spectral Library Version 2.0 f, build Jul 23 2008) (**Figure 7.3B**) and prior reports which also indicate the presence of major fragmentation adjacent to the position of the hydroxyl group. For example,  $[M-59]^-$  ion of  $m/z$  337 and molecular ion of  $m/z$  396 was detected in FAME of 2-hydroxy-tetracos-15-enoate (2-OH C24:1).<sup>242</sup> As indicated in **Figure 7.3B and 7.3E**, these ions at  $m/z$  227 and 253 respectively, suggest that both HFAs are likely hydroxylated at the  $\Delta^2$  position. Furthermore, the corresponding trimethylsilyl ether derivatives of these hydroxy-FAME (**Figure 7.3C and 7.3F**), show fragment ions at  $m/z$  299 and 325 that are consistent with the assignment of  $\Delta^2$  hydroxyl groups, arising through loss of the methyl ester group as indicated. This fragmentation is consistent with literature reports of trimethylsilyl ether derivatives of methylated 2-hydroxy fatty acids,<sup>242</sup> which also matched NIST reference spectra and literature data,<sup>242 462</sup> Taken together, the ESI-MS/MS data on  $[M-H]^-$  ions and GC/EI data on the FAME and TMS-FAME derivatives confirm the identity of 2-OH C16:0 and 2-OH C18:1. As further proof, the GC-MS retention time and the characteristic fragment ions of FAME or TMS-FAME derivatives of an authentic standard of 2-OH C18:1n9 (FAME derivative's retention time was 14.396 min, and the one of FAME-TMS was 14.184 min) directly compared to those of the 2-OH C18:1 fraction (**Figure 7.3 D-F**) to confirm its structure.

The characteristic ions of methylated and silylated-methylated derivatives of 2-OH C16:0 and 2-OH C18:1 are listed in **Table 7.2**.

**Table 7.2.** GC-MS information of methylated (FAME) or methylated and silylated (TMS) hydroxy fatty acids.

Structure	Methylated FA		Methylated and silylated FA	
	Rt (min)	Characteristic ions	Rt (min)	Characteristic ions
2OHC16:0	12.910	286.2, 227.2	12.851	358.2, 343.2, 299.2
2OHC18:1	14.382	312.2, 253.2	14.169	384.2, 369.2, 325.2

### 7.3.2 Validation of analytical method for the analysis of fatty acids in sausage model

To ensure a reliable method for the fatty acid profiles in different sausage, the LC-MS/MS-MRM method was validated for the analysis of fatty acids in the sausage model. The linear range, accuracy, precision and extraction recovery were established for 13 free fatty acids. The  $R^2$ -values of the calibration curves were 0.9973 or higher over the linear ranges indicated (**Table 7.3**). The accuracy and precision of each calibration curve were confirmed with the three data points selected throughout the linear range for each fatty acid (**Table 7.4**). The accuracy of measuring fatty acids at low, medium and high concentrations within the were in the range of 92.3-115.3%, 96.5-108.2%, and 93-109.7%, while the coefficient of variation ranged from 3.5-14.9%, 1.3-15% and 7.6-15.3% respectively. The extraction efficiency was measured (**Table 7.5**) by spiking each fatty acid at levels of 0.75 and 7.5ppm in the original sausage sample resulting in measured recoveries of 97-

115% and 102-114%. In conclusion, the LC-MS/MS-MRM method provided a reliable quantitation of fatty acids and hydroxy fatty acids in the sausage model.

**Table 7.3.** Linear range of major fatty acids

Compounds	Calibration Curve		R <sup>2</sup> value	Tested linear dynamic range (ppm)	S/N of LOQ (ppm) *
	y=ax+b				
	a	b			
9,10-di OH stearic acid	0.00607	0.00000	0.9999	0.250 - 7.500	11.8
Coriolic acid	0.04770	-0.00035	0.9997	0.025 - 7.500	10.2
Linoleic acid	0.31900	-0.00335	0.9989	0.075 - 7.500	10.7
Heptadecanoic acid	0.25100	-0.00984	0.9980	0.100 - 5.000	10.9
Myristic acid	0.12900	-0.01460	0.9992	0.250 - 7.500	10.3
Palmitic acid	0.21700	0.00251	0.9973	0.500 - 7.500	10.3
Stearic acid	0.23000	-0.00969	0.9999	0.750 - 7.500	11.1
Oleic acid	0.33800	-0.00837	0.9991	0.100 - 7.500	10.2
Linolenic acid	0.22200	-0.00189	0.9989	0.100 - 7.500	11.9
2-OH oleic acid	0.13600	-0.00057	0.9991	0.050 - 0.750	11.4
Myristoleic acid	0.13400	-0.02300	0.9996	0.250 - 7.500	19.6
Palmitoleic acid	0.27700	-0.01840	0.9991	0.250 - 7.500	13.3
12-OH stearic acid	0.39800	0.00515	0.9993	0.075 - 7.500	11

\*: S/N: signal to noise ratio; LOQ: limit of quantitation

**Table 7.4.** Accuracy and precision (matrix effect) (triplicates)

Compounds	QC-low		QC-medium		QC-high	
	Accuracy	Precision	Accuracy	Precision	Accuracy	Precision
	(%)	(RSD, %)	(%)	(RSD, %)	(%)	(RSD, %)
315.3 / 171.1	102.4	6.5	102.1	7.8	98.5	13.3
295.2 / 195.1	100.8	14.0	101.8	12.1	97.9	15.3
279.2 / 279.2	106.4	14.9	106.4	13.2	106.0	11.3
269.3 / 269.3	98.7	8.2	103.6	8.4	100.1	12.6
227.1 / 227.1	104.3	9.4	107.7	8.2	108.3	7.6
255.2 / 255.2	101.2	11.4	107.8	1.3	102.7	9.5
283.3 / 283.3	115.3	3.5	108.2	2.9	99.9	9.0
281.3 / 281.3	97.4	11.4	102.2	5.7	101.4	14.5
277.2 / 277.2	103.2	11.9	105.3	10.5	102.7	11.5
297.2 / 251.2	92.3	12.0	96.5	6.7	93.0	14.2
225.2 / 225.2	100.5	6.4	106.6	4.5	109.7	10.0
253.2 / 253.2	97.5	8.5	102.9	4.4	103.7	9.1
299.2 / 299.2	103.5	10.9	100.4	15.0	97.2	13.4



**Table 7.5.** Extraction recovery (duplicates)

Compounds (nM)	Spiked concentration (ppm)		Non	Measured concentration (ppm)		Extraction recovery (%)	
	Low	High		Low	High	Low	High
	315.3 / 171.1	0.75		7.5	0.000	0.730	7.970
295.2 / 195.1	0.75	7.5	0.024	0.834	8.175	108	109
279.2 / 279.2	0.75	7.5	0.388	1.230	8.425	112	107
269.3 / 269.3	0.75	7.5	0.063	0.896	8.185	111	108
227.1 / 227.1	0.75	7.5	0.109	0.923	8.645	109	114
255.2 / 255.2	0.75	7.5	2.000	2.735	9.720	98	103
283.3 / 283.3	0.75	7.5	1.360	2.125	8.990	102	102
281.3 / 281.3	0.75	7.5	1.660	2.475	9.470	109	104
277.2 / 277.2	0.75	7.5	0.039	0.886	8.075	113	107
297.2 / 251.2	0.75	7.5	0.000	0.863	7.615	115	102
225.2 / 225.2	0.75	7.5	0.025	0.815	8.405	105	112
253.2 / 253.2	0.75	7.5	0.330	1.150	8.205	109	105
299.2 / 299.2	0.75	7.5	0.000	0.856	8.225	114	110

### 7.3.3 Comparison of fatty acid composition among different fermentation beef sausages

To elucidate the effect of endogenous lipolytic activity and the lipolytic activity of starter cultures in the sausage model, the fatty acid composition of the 3 different sausage treatments were compared. The concentration of saturated fatty acids, mono-unsaturated fatty acids (C14:1, C16:1 and C18:1) and total fatty acids varied with time but was not different between samples fermented with different cultures (**Table 7.6**). In contrast, the accumulation of di or poly-unsaturated fatty acids (C18:2 and C18:3) and the production of OH-fatty acids depended on both the starter culture and time (**Table 7.6**). In particular, mono-OH C18:0 accumulated in all samples fermented with *L. sakei*, while production of 2-OH C18:1 and other 2-HFA was observed only in samples that also contained *S. carnosus*. Coriolic acid (13-OH C18:2) was present in all samples including the negative control but at a significantly higher level in sausage fermented with *L. sakei* only (**Table 7.6**).

**Table 7.6.** Concentration of free fatty acids in sausages fermented with different starter cultures

Free fatty acids (mg/100g DM)	Time (days)	Aseptic control	<i>L. sakei</i>	<i>L. sakei</i> and <i>S. carnosus</i>
Saturated fatty acids	0	90±14 B	120±40 B	69±23 C
	3	130±7.0 B	90±43 B	110±4.4 B
	20	220±0.77 A	240±7.3 A	190±15 A
C14:1 (Myristoleic acid)	0	2.1±1.1	2.3±1.2	2.3±1.2
	3	3.4±0.14	2.3±1.2	2.4±1.2
	20	4.8±0.20	4.5±0.31	5.2±0.90
C16:1 (Palmitoleic acid)	0	4.0±0.67 B	5.6±0.49 B	3.6±0.11 B
	3	7.1±0.25 B	4.2±2.0 B	6.5±0.71 B
	20	17±0.79 A	16±1.1 A	11±1.8 A
C18:1 (Oleic acid)	0	31±6.2 B	46±5.6 B	25±1.5 B
	3	63±4.8B	37±19 B	53±7.4 B
	20	160±14 A	150±8.3 A	104±16 A
C18:2 (Linoleic acid)	0	9.0±2.3 B	11±0.56 B	7.1±0.33
	3	14±1.1 B	8.4±3.9 B	12±3.1
	20	39±4.7 A	34±3.0 A	19±5.5
C18:3 (Linolenic acid)	0	0.57±0.29 B	0.94±0.17	0.90±0.10
	3	1.3±0.14 B	0.78±0.36	1.3±0.11
	20	3.0±0.29 A	1.9±0.36	1.2±0.38
Mono-OH C18:0	0	0±0	0±0	0±0
	3	0±0	0±0	0±0
	20	0±0	0.60±0.12	1.5±0.43
2-OH C18:1 (2-OH oleic acid)	0	0±0	0±0	0±0
	3	0±0	0±0	0±0
	20	0±0	0±0	12±3.4
13-OH C18:2 (coriolic acid)	0	0.41±0.054	0.67±0.11 B	0.28±0.025
	3	0.58±0.12	0.29±0.24 B	0.34±0.053
	20	0.99±0.17 Y	1.9±0.22 A,X	0.57±0.047 Y
Total FA	0	140±25 B	190±13 B	110±2.3 B
	3	220±72 B	140±68 B	190±18 B
	20	450±44 A	440±16 A	440±43 A

Data represent means ± standard error of mean of triplicate independent fermentations. Superscripts A, B, C denote significant differences ( $P < 0.05$ ) among concentrations of the same fatty acid in dry sausages with same strain over time. Superscripts X, Y, Z denote significant differences ( $P < 0.05$ ) among concentrations of the same fatty acid with different starter cultures at the same time. Superscripts are not indicated if values were not significantly different.

## 7.4 Discussion

In this study, non-derivatized fatty acid and hydroxy fatty acids were quantified in a model beef sausage that was incubated aseptically, fermented with *L. sakei*, or with *L. sakei* and *S. carnosus*. The results expand upon prior knowledge of the quantification of hydroxy fatty acids in food, especially in meat products, by analysis of sausage models that employed fermentations with pure strains that were compared to an aseptic control prepared with an absence of interferences from uncontrolled background microbiota.

We observed that the accumulation of saturated, mono-hydroxy and total fatty acids mainly depended on the fermentation time, but not on the starter cultures. Thus, the starter culture of *L. sakei* or *L. sakei* + *S. carnosus* did not accelerate the accumulation of these fatty acids. This agrees with a previous observation that during fermentation, free fatty acids are mainly released by endogenous lipases.<sup>432, 433</sup> Although *Staphylococcus* express lipases,<sup>463, 464</sup> their activities are very low at in the pH range of 5.0 – 5.5, which is typical for fermented sausages<sup>464, 465, 458, 464</sup> Lipases of *Lactobacillus* spp. are intracellular and also inhibited at pH < 6.<sup>466, 467, 465</sup> The microbial lipolytic enzymes become relevant in meat products when fungal lipases are involved in surface ripening.<sup>468, 469</sup>

Distinct from the overall lipid accumulation, linoleic acid (C18:2) accumulated in the control fermentation and *L. sakei*-fermented sausage, but not significantly in the fermentation with *L. sakei* and *S. carnosus*. Linolenic (C18:3) acid accumulated in the aseptic control fermentation but not in the fermentation with *L. sakei* or with *L. sakei* and *S. carnosus*. These differences indicate microbial conversion of these fatty acids. The production of hydroxy fatty acids, including 13-OH C18:2, 2-hydroxy fatty acids and a monohydroxy C18:0, were also found to be specific to the

starter culture. This data suggests that unsaturated fatty acids like C18:2 and C18:3 may contribute to the production of these hydroxy fatty acids.

*L. sakei* produces hydrogen peroxide during sausage ripening.<sup>470, 471, 472</sup> *L. sakei* possesses the *katA* gene,<sup>473</sup> which encodes heme-dependent catalase.<sup>471, 474</sup> However, the activity of *L. sakei* to accumulate reactive oxygen species (ROS) such as superoxide radical ( $O_2^-$ ) and  $H_2O_2$  is strain-specific.<sup>475, 476</sup> Therefore, *L. sakei* may accumulate ROS, enhance lipid oxidation.<sup>470, 471, 472</sup> This is consistent with the increased accumulation of coriolic acid in *L. sakei* fermentation, which supports the formation of primary lipid oxidation products like fatty acid hydroperoxides. These oxidation products may then undergo reduction into hydroxide derivatives,<sup>349</sup> which are more chemically stable forms,<sup>37</sup> by the reductive agents in meat such as glutathione (GSH)<sup>477</sup> and cysteine.<sup>478</sup> In comparison, superoxide dismutase (SOD) and catalase produced by *Staphylococcus* spp. efficiently removes reactive oxygen species and so prevents lipid oxidation.<sup>479, 480, 481</sup> This agrees with the observation here that sausage co-fermented with *L. sakei* and *S. carnosus* didn't accumulate coriolic acid, as the one with *L. sakei* only did.

The mono-OH C18:0 produced by *Lactobacillus sakei* is likely to be 10-OH C18:0.<sup>442</sup> This hydroxy fatty acid is produced by 10-linoleate hydratase from oleic acid. The 10-linoleate hydratase gene in the genome of *L. sakei* is 79% identical to the 10-linoleate hydratase of *L. plantarum*, which converts linoleic and oleic acids to 10-OH C18:1 and 10-OH C18:0, respectively; it is also 31% identical to the 13-linoleate hydratase of *L. plantarum*, which converts linoleic acid to 13-OH C18:1.<sup>191, 343</sup> The production of 10-OH C18:0, instead of its C18:1 analogues is supported by the higher abundance of oleic acid (C18:1) compared to linoleic acid (C18:2) in the model beef sausages. As a comparison, the mono-OH C18:1 is dominantly produced from the *Lactobacillus*-fermented sourdough,<sup>15</sup> where the substrate is the wheat flour containing substantially more

linoleic acid (58%) than oleic acid (20%).<sup>482</sup> In both matrixes, microbial conversion of unsaturated fatty acids is initiated by the release of free fatty acids from triacylglycerol, mainly due to the endogenous lipase from cereals and meat, respectively.<sup>483, 33, 17, 484</sup> Therefore, the enzymatic conversion of unsaturated fatty acid into their oxygenated fatty acid not only depends on the microbial enzyme, but also the conversion substrate made available from the matrixes. Saturated hydroxy fatty acids lack antifungal activity,<sup>15</sup> but more studies need to be done to investigate the exact isomers present, and to elucidate the overall metabolism of fatty acids in fermented sausage by starter cultures.

We also observed the unique presence of 2-hydroxy fatty acid in the sausage co-fermented by *L.sakei* and *S. carnosus*. 2-Hydroxy fatty acids are present in Gram-negative bacteria as lipopolysaccharides (Lipid A),<sup>485</sup> or produced by Gram-positive bacteria including *Bacillus subtilis*.<sup>88</sup> The bacterial enzyme responsible for the synthesis of 2-HFA is the  $\alpha$ -hydroxylase activity of cytochrome P450 enzyme, which converts C12-C18 saturated fatty acid and arachidonic acid into 2 or 3-HFA.<sup>486, 39</sup> The  $\alpha$ -hydroxylase encoded in the genome of *Bacillus subtilis* (WP\_061419180.1) was used as query sequence to identify related enzymes in staphylococci, however, no significant hits were identified. Alternatively, collaboration of multiple enzymes in producing 2-HFA has also been documented,<sup>37</sup> and therefore the collaboration of *S. carnosus* and *L. sakei* in producing 2-HFA remains a possibility. Furthermore, 2-HFA can be found in animal sources with close association with sphingolipids<sup>487</sup> and neural system.<sup>488</sup> *S. carnosus* may have the lipolytic capacity on these polar lipids, but it also requires further study to validate this possibility. Derivatives of 3-hydroxy fatty acids are produced via incomplete beta-oxidation by *S. carnosus*.<sup>489</sup> The production of these hydroxy fatty acid acyl CoA has been linked to the production of aroma compounds like methyl ketones,<sup>489</sup> but free 3-hydroxy fatty acids were not observed here.

The characterization and quantitation of HFA supports the explanation of their potential functions in fermented meat products, which are usually specific to their structures and concentrations. For example, to achieve antifungal activities, MIC of  $1.50\pm 0.87\text{g/L}$  and  $2.67\pm 1.15\text{g/L}$  of 2-OH C18:1 are required to inhibit the growth of fungi *Aspergillus niger* and *Penicillium roqueforti* in mMRS media (Chapter 5), and  $0.03\text{g/L}$  ( $100\mu\text{M}$ ) is needed to exhibit minor antifungal activity against phyto-pathogen *Fusarium oxysporum*.<sup>12</sup> Likewise, the highest concentration of coriolic acid of in the sausage tested,  $1.9\pm 0.22\text{ mg/100g}$  ( $0.019\pm 0.0022\text{g/L}$ ) was still lower than the min MIC of  $0.3\text{g/L}$ .<sup>66</sup> Other hydroxy fatty acids detected in the sausage sample are mainly saturated hydroxy fatty acids that have no antifungal activity.<sup>15</sup> These analytical results for HFA in sausage indicate that the concentration of antifungal HFAs is too low to inhibit surface ripening cultures that are used as ripening agent in fermented meat products.<sup>490, 491, 492</sup>

Hydroxy fatty acids may serve as flavor/aroma compounds or their precursors. Coriolic acid has a bitter threshold of  $7.6\text{-}8.5\ \mu\text{mol/mL}$  ( $2.25\ \text{g/L}\text{-}2.52\ \text{g/L}$ ),<sup>445</sup> which is higher than the content reported here in the sausage model, as well as higher than the effective antifungal concentration used in a bread model.<sup>15</sup> In contrast, its monoglyceride form has lower threshold for bitter taste ( $1.1\text{-}2.2\ \mu\text{mol/mL}$ ) and its hydroperoxy analogues has no bitter flavor at  $14\ \mu\text{mol/mL}$ .<sup>445</sup> In addition, the bitter taste threshold ( $0.75\ \text{g/L}$ ) of a mixture of 9-OH C18:2 and 13-OH C18:2 was measured in water suspended oat flour, but it was measured with the co-presence of  $0.062\ \text{g/L}$  of tri-hydroxy fatty acids.<sup>357</sup> This indicates possible synergetic/additive effect of different flavor compounds. In addition, hydroxy fatty acids, including coriolic acid and 10-OH C18:0 may serve as precursors for lactone production, through beta-oxidation and lactonization with the involvement of yeasts and filamentous fungi,<sup>444, 493</sup> and therefore contribute critically to the taste/aroma profile of fermentation products. The strong aroma of dry-cured from *S. carnosus*

fermented sausage has been related to methyl ketones, which is produced by the 3-hydroxyfatty acid-related incomplete beta-oxidation.<sup>494</sup> However, with the limited aroma/flavor data available on other hydroxy fatty acid structures or concentrations, the impact of 2-OH fatty acids found in the fermented beef sausage, remains speculative.

Other than antimicrobial and flavor properties, the hydroxy fatty acids may also exert additional bioactivities. Coriolic acid down-regulates the peroxisome proliferator-activated receptor that promotes colonic tumorigenesis at the  $\mu\text{M}$  level,<sup>495</sup> which is lower than the highest amount of coriolic acid detected in sausage in this study. 2-OH C18:1 is also known to be an anticancer agent, but its inhibition on the proliferation of cancer cells and the development of tumor volume requires a concentration of 0.023 g/L-0.1 g/L.<sup>78, 75, 496, 76</sup> The beef sausage co-fermented with *L. sakei* and *S. carnosus* for 20 days accumulated  $0.12 \pm 0.034$  g/L of 2-OH C18:1 and similar levels of 2-OH C16:0, so this may provide sources of 2-OH fatty acids with active concentration for specific functions. As a comparison of the 2-HFA analogue, 2-OH C18:3, is non-antibacterial *in vitro*, but its production can be stimulated by infection to exert a tissue-protective effect against bacterial infection symptom in plant *in vivo*. Therefore, the functions of HFA need to be studied with a comprehensive consideration of other potential antagonistic, additive or synergistic components in the matrixes.

The sausage model and the analytical and separation technique used here are suitable tools for future investigation of the functions of minor bioactive lipids in different contexts. Elucidation of the microbial metabolites that contribute to specific characteristics of fermented foods will enable production of safe, controllable, long-lasting, and tasteful products.



## Chapter 8. General discussion and conclusions

### 8.1 Advancement in the analysis, separation and development of structure-function relationship of HUFA

Lipids are well known as a basic component of membrane structure. Beyond that, they are increasingly being recognized for their important roles in signal transduction in plants, animals and microbes.<sup>497</sup> They are also being recognized as important biomarkers for disease diagnosis or therapeutic targets for treatments.<sup>497, 178, 138, 144, 498</sup> In food, they not only act as energy sources but also are essential nutrients and functional compounds; they and their metabolites are critical in contributing to smell and taste, producing specific textures and delivering essential water-insoluble nutrients.<sup>499</sup> The presence of lipids and these functions of lipids critically influence how foods are accepted, tasted and perceived.<sup>500</sup> Knowledge on the structures and functions of lipid is gained thanks to the development and advancement of separation<sup>11</sup> and analytical<sup>2</sup> techniques for lipids.<sup>500</sup> Despite these advances, due to the high degree of structure diversity that exists within the lipidome, a lot is still to be discovered. In particular, establishing specific structure-function relationships for lipids is challenging, because it requires a readily available combination of extraction and synthetic methods, analytical and preparative separation techniques, detection techniques, and bioassays. Using combinations of these methods to elucidate structure-function relationships is essential in order to better understand and predict lipid functions, and potential applications from a knowledge of lipid structures.

In order to remove the knowledge gaps concerning antifungal hydroxy fatty acids, it is necessary to develop both reliable analytical methods and efficient preparative ones. Recently, LC-MS based analytical methods have been developed for HUFA.<sup>501, 285, 286, 270, 139, 144</sup> These new

methods are important advances on the conventional TLC-based methods which have limited resolution. Additionally, these methods also improve on GC-MS methods that require HUFA derivatization.<sup>2</sup> However, MS and MS/MS parameters for various HUFA still need to be developed and the validation of analytical methods needed to be performed in new matrices. In this thesis, LC-APPI-MS/MS was used to characterize HUFA molecules, and consequently provides APPI-MS/MS spectra of HUFA that have not been reported before. Also, LC-ESI-MS/MS methods for the quantitation of hydroxy fatty acids were developed and validated for a food matrix, fermented beef sausage. Due to the presence of closely similar isomers, the development of MS and MS/MS detection are, in many cases, necessary to distinguish different HUFA because the commonly used reversed-phase LC separation alone cannot.<sup>144, 272</sup> The development of these methods expands the choice of analytical tools for HUFA.

A notable advance in preparative separation was achieved using the liquid-liquid chromatographic technique HSCCC, which was applied to the isolation of various HUFA structures. In particular, HSCCC protocols were developed for the purification of hydroxy fatty acids found in 2 *Lactobacillus* fermentation extracts, 4 saponified plant seed oils and a fermented sausage model. These experiments used solvent systems consisting of hexane/ethyl acetate/methanol/water (HEMWat)/acetic acid mixtures, in proportions which were adjusted according to the polarities of the HUFA. Separation of these hydroxy fatty acids from impurities, such as non-hydroxy fatty acids, was achieved. These HSCCC separations allow for hundreds of milligrams of sample loading per run, and therefore facilitates studies of structure-function relationships for these purified HUFA. In an additional experiment, the advantages of using HSCCC to separate bioactive lipids were demonstrated by the separation of 6 closely similar ganglioside analogues, which only slightly differ in the arrangement or composition of their

saccharide moieties, or in the composition of their ceramides. Compared to HSCCC, commonly used semi-preparative LC methods have a much more limited ability to fractionate comparably high sample loadings in order to isolate purified fractions of closely similar analogues within a reasonable time.<sup>502</sup> HSCCC is thus a powerful alternative separation technique that is versatile, efficient, and resulted in scalable separations of closely similar lipid analogues,<sup>503, 504, 502, 346, 505</sup> which are essential for studies of lipid functions.

A notable relationship was established in this work between the structures of HUFA and their antifungal properties. HUFA with a hydroxyl group located in the middle of the C18 chain (C9-C13 position) are active antifungal against molds, while HUFAs with hydroxy group at the end of the chain (2- or 18-OH) are inactive; their activity against molds is well distinguished from their non-hydroxylated analogues, like oleic and linoleic acid. This relationship associates the activity of HUFA to a structural characteristic, which unifies this observation for the food spoilage fungi studied in this work with previously investigated HUFA activity against phytopathogenic fungi.<sup>12</sup> At the same time, the HUFA that are active against molds were found not to be active against yeast. This relationship associates fungal sensitivity to HUFA with fungal morphologies. This suggests the anti-mold application for HUFA and its possible association with the lipid-related difference between filamentous fungi and yeasts. Furthermore, the yeast morphologies of strains tested is linked to their high sterol content, which is an important moderator of membrane fluidity and is also a chemotaxonomic compound.<sup>354</sup> This link between fungal sensitivity to HUFA and sterol content supports the proposed hypothesis that antifungal HUFA interact with fungal membranes,<sup>13, 363</sup> although an exception was also found for *Candida albicans* which has low sterol content and high tolerant of antifungal HUFA. This suggests that other mechanisms might be involved in the resistance of some fungal species to HUFA. It was

hypothesized that the interaction of HUFA and fungal membrane increased the membrane fluidity of sensitive fungi, but interestingly this was not observed in the Laurdan experiment. So, it is possible that the effect of HUFA on membranes could be localized, without changing the overall membrane fluidity. Further studies need to investigate the exact interaction of HUFA with fungal membranes of differing sterol content, both in a membrane model and *in situ*. Additionally, it should be pointed out that, by building structure-function relationships, representative antifungal HUFA can be used to investigate the modes of action, and the possible applications, of other similar compounds. A comprehensive structure-function relationship therefore provides a great advantage for the further investigation and prediction of the properties of similar compounds.

## **8.2 Potential application of HUFA in food preservation**

The proposed structure-antifungal activity relationship for HUFA suggests a possible application of HUFA in food. According to this relationship, 2-OH C18:1 requires a concentration of over  $1.50 \pm 0.87$  g/L to be antifungal against the molds tested. According to the quantitation of HUFA in fermented beef sample, the concentration of 2-OH C18:1 is  $0.12 \pm 0.034$  g/L, which doesn't support its function as an anti-mold agent, but it is compatible with the common application of mold as a ripening agent in fermented meat products.<sup>490, 491, 492</sup> Other hydroxy fatty acids detected in the sausage sample are mainly saturated, which are not antifungal forms.<sup>15</sup> Therefore, the functions of 2-OH fatty acids in fermented sausage remain to be further investigated.

In addition, the HUFA with hydroxyl groups in the C9-C13 position can be used to inhibit the growth of filamentous fungi but not of yeasts. This for example, could be applied to a food

fermentation process that requires the viability and activity of yeasts but not molds. This explains the success of yeast fermentation in bread even with the addition of 0.15% coriolic acid (13-OH C18:1) or the *in situ* production of 10-OH C18:1 (0.7 g/L) via fermentation, as observed before.<sup>15</sup> The addition of 0.15% coriolic acid can extend the shelf-life of white-flour non-fermented bread against *Penicillium roqueforti*, but inhibits *Aspergillus niger* to much lower extent.<sup>15</sup>

Food components can exert synergistic, additive or antagonistic effects on the antifungal activities of HUFA. To be specific, in contrast to results for non-fermented bread, even at lower concentration, ricinoleic acid extended the shelf life of sourdough bread, suggesting the synergistic effect exists between HUFA and the metabolites of *Lactobacillus* fermentation, such as acetate.<sup>33</sup> In addition, one or more of the other *Lactobacillus* metabolites can also contribute to any synergetic or additive effects with HUFA; examples of these metabolites might include short-chain organic acids like lactic acid, phenolic compounds, and dipeptides or proteinaceous compounds.<sup>41</sup> Interestingly, the inhibition of spoilage fungi by ricinoleic acid was only found on wheat-flour sourdough bread, but not flaxseed-flour sourdough bread, which again indicates that the structure-antifungal activities relationship of HUFA may also depend on the food matrix, as a result of which the effect of HUFA can be compromised. For example, mucilage in flaxseed possesses a high water binding capacity,<sup>424</sup> and the resulting hydrocolloids may increase water activity and therefore benefit fungal growth.<sup>33</sup> Meanwhile, flaxseed has higher manganese content compared to wheat flour,<sup>506, 507, 508</sup> and manganese, as an antioxidant mineral at high concentration,<sup>509, 510</sup> may support the growth of fungi.<sup>511</sup> In addition, since the sensitivity of fungi to HUFA is related to their sterol content, food components that effect the sterol synthesis of fungi<sup>512, 513</sup> may also impact the antifungal activity of HUFA *in situ*.

In order to be used as food antifungal additive, their safety in foods, their impact on food sensory properties, and their impact on “clean-label” requirements should also be assessed. Considering safety, the acceptable daily intake of ricinoleic acid has been estimated to be 2.4 g/person (average 60 kg),<sup>412</sup> which is equivalent to 1.7 kg of food with HUFA added at a level of 0.15%, a concentration which exerts antifungal activity.<sup>15</sup> This tolerance may allow the application of HUFA in active concentration as potential antifungal in food. HUFA may also influence the taste of foods. Coriolic acid (the 13-hydroxy-*cis,trans*-9,11-octadecadienoic acid isomer) has a bitter taste with a threshold of about 8 mmol/L, about 2 – 4 times higher than its MIC and also higher than the 0.15% addition rate applied in sourdough bread. Its monoglyceride form has a much lower threshold for bitter taste, about 1 mmol / L, whereas its hydroperoxy analogues has no bitter flavor at 14 mmol/L.<sup>445</sup> In addition, a bitter taste threshold of 0.8 g / L for a mixture of 9-OH C18:2 and 13-OH C18:2 was measured in water suspended oat flour, but it was measured with the co-presence of 62 mg/kg of tri-hydroxy fatty acids .<sup>357</sup> Additionally, other taste contributions from HUFA, especially the non-antifungal HUFA with low concentration in food, e.g. the 2-OH fatty acids found in fermented beef sausage in this thesis, remain unknown. These oxylipins may interact with or contribute to other kokumi-enhancing compounds.<sup>514</sup> Therefore, the taste properties of each different mono-HUFA or their conversion products by food processing, and their synergistic effects with other components in food need to be further studied in the future. These further studies are especially desirable because HUFA, and especially HUFA produced *in situ*, remains an important food antifungal candidate for the pursuit of “clean-label” additives for the food industry.<sup>34, 33</sup>

Many strains of lactic acid bacteria can convert unsaturated fatty acid into HUFA,<sup>425</sup> which may contribute to the antifungal applications of these bacteria.<sup>20, 43, 44</sup> Previously, the antifungal

properties of *Lactobacillus* cultures of different strains and their cell-free supernatant (CFS) were investigated in several perishable or processed food matrices that are vulnerable to fungal spoilage.<sup>20</sup> For dairy products, commercial antifungal *Lactobacillus* spp. have been developed mainly using *L. plantarum*, *L. rhamnosus* and *L. paracasei*,<sup>20</sup> and the antifungal metabolites of these species have also been characterized.<sup>41</sup> However, it is also agreed that the further development of antifungal *Lactobacillus* cultures is restricted, at least for now, by the gap between the antifungal properties of *Lactobacillus in vitro* and *in situ*, their effects on food sensory properties and most importantly, their modes of action.<sup>20</sup> It is commonly concluded from other studies that the synergistic effects of various compounds are the basis of the antifungal mechanism<sup>20</sup> but the exact antifungal compositions giving rise to these synergetic effects were poorly studied. To investigate the contribution of hydroxy fatty acids this synergetic effect, strains of lactic acid bacteria were screened for their antifungal activities, followed by gene extraction and genome sequencing performed on the highly antifungal and less antifungal strains. However, here I found that the presence of the linoleate hydratases-encoding gene didn't explain the difference of antifungal phenotypes, and the presence of hydroxy fatty acids in their fermented cultures are still yet to be confirmed. Therefore, the contribution of linoleate hydratases to the antifungal activities of LAB is likely to be limited. In addition, differences between the antifungal activities of LAB was also observed in media compared to milk and yogurt (unpublished data). The mMRS media are rich supplements of amino acid, while dairy products can provide a high amount of lipid. Therefore, the fermentation substrate may change bacterial metabolites, and therefore change their antifungal activities. These substrate-dependent antifungal activities require further investigation of comparative metabolite analysis and genomic analysis.

### 8.3 Potential application of HUFA in plant protection

In addition to food application, HUFA are suitable anti-pathogenic candidates in plant protection due to their close association with plant self-defense mechanisms. They are produced in response to infection. For example, rice plants produce coriolic acid in response to *Pyricularia oryzae* infection,<sup>515</sup> and *Arabidopsis* produces 2-hydroxy linolenic acid upon *Colletotrichum higginsianum* infection.<sup>37</sup> In plants, 13-OH C18:3 HUFA is produced by 13-lipoxygenase (13-LOX) induced by the plant hormones salicylate and jasmonate.<sup>516</sup> These hormones regulate the plant self-defense in response to pathogens and induce the local or systemic resistance of a plant against pathogens.<sup>517, 518, 519, 520, 521, 522</sup> Despite these close relations between HUFA and plant defense, the structure-antifungal activity function relationship of HUFA was only partially elucidated *in vitro* or *in vivo*.<sup>12</sup> To address this knowledge gap, in collaborate work, using gram-levels of coriolic acid purified by HSCCC in this thesis, it was possible to explore the antifungal activities of coriolic acid *in vitro* and *in vivo* in plants compared with its analogue ricinoleic acid.<sup>523</sup> Analogous to that observed for the food spoilage fungi *Aspergillus niger* and *Penicillium roqueforti*, coriolic acid has a similar MIC to ricinoleic acid against phytopathogens including *Leptosphaeia maculans*, *Pyrenophora teres* f. *teres*, *Pyrenophora tritici-repentis*, *Sclerotinia sclerotiorum* and *Fusarium graminearum*. The MIC of coriolic acid, however, varies among fungal species and phytopathogens were generally more resistant when compared to food spoilage fungi. This variation of fungal sensitivity to HUFA was observed before,<sup>12, 355</sup> but the mechanisms of resistance remain to be elucidated. In addition, HUFA have different levels of fungal interactions at various stages of fungal development, such as asexual spore germination, hyphae development and sexual production.<sup>355, 148, 150</sup> How these additional regulations of HUFA on fungi interact with their antifungal properties is not well understood, especially in a more



realistic model of environment that involves more than one fungus. This requires further analysis of these fungi at different stages, which would be important for pinpointing the mechanism of fungal resistance to HUFA.

The structure-function relationship of HUFA against phytopathogens becomes even more intriguing *in vivo*, as they not only showed different effects against various phyto-pathogens, but also among various dicotyledon and monocotyledon plants. Foliar-sprayed coriolic acid (CA) or ricinoleic acid (RA) at 0.12 g/L-1 g/L didn't decrease the disease severity of *Brassica napus* cv. 'Westar' (canola, dicotyledons) caused by *Leptosphaeria maculans* (MIC=0.72-0.84 g/L for CA and RA) nor *Sclerotinia sclerotiorum* (MIC=2.92±1.09 g/L for CA). Furthermore, 2 g/L of CA or RA caused wilting and formed necrotic lesions on canola leaves, but they have no effect on seed germination. The cause of this plant- and physiological stage- specific toxicity effect is unknown, but it was also observed on other important phyto-defense molecules such as salicylic acid (SA),<sup>524</sup> indicating the delicate requirement for concentration, time, location and plant on applying these phyto-defense molecules as anti-pathogenic agents. Meanwhile, this collaborative work<sup>523</sup> also observed that the phyto-toxicity of HUFA is associated with the generation of H<sub>2</sub>O<sub>2</sub>. In fact, the programmed hypersensitive cell death triggered by H<sub>2</sub>O<sub>2</sub> likely played a critical roles in plant defense,<sup>525</sup> since the hypersensitive response (HR) indicates the successful recognition of pathogens, and the triggered localized cell death is usually linked to restricting the infection spread.<sup>526, 527</sup> More importantly, HR is usually associated with the development of systemic acquired resistance (SAR), a broad-spectrum systemic mechanism of resistance to pathogenic infection.<sup>528</sup> This process is mediated by phyto-hormone salicylic acid (SA), and the production of H<sub>2</sub>O<sub>2</sub> is both upstream and downstream of SA synthesis.<sup>529</sup> Nevertheless, whether CA, RA and their induced H<sub>2</sub>O<sub>2</sub> in such a concentration indeed directly contribute to the

activation of HR and SAR, and whether it will support the development of a local application of HUFA, require much further investigation. Contrary to CA and RA's potential to activate HR, it is interesting to note that 2-OH linoleic acid protects the plant from cell death during HR induced by bacterial infection,<sup>530</sup> although this effect is specific to plant species.<sup>110</sup> A further study on the phyto-toxicity or protection of various HUFA structures, the induction of hypersensitive response (HR) by HUFA, and their antifungal function on dicotyledons, remains highly desirable.

Very different from that observed for dicotyledons, surprisingly, 0.5 g/L-2 g/L of CA, but not RA, oleic acid or lower concentrations of CA, significantly reduced the disease symptoms caused by *Pyrenophora tritici-repentis* (MIC=1.64±0.46 g/L) in *Triticum aestivum* cv. 'Katepwa' (wheat, monocotyledons) and *Pyrenophora teres* f. *teres* (MIC=1.66±0.20 g/L) in *Hordeum vulgare* cv. 'Xena'. (barley, monocotyledons). This reduction of disease severity was observed only on the whole plants but not seed treatments, again indicating the influence of plant physiological stage on the efficacy of HUFA. Meanwhile, the effective concentrations of HUFA in these cases are even lower than their MIC *in vitro*. This mismatch between MIC *in vitro* and effective concentration *in vivo* suggests the possible activation of another plant defense mechanism by HUFA. In fact, the MIC of HUFA *in vitro* cannot always explain their anti-pathogenic performance in plants. For example, 2-OH linolenic acid (2-OH C18:3) exhibited a tissue-protective effect against phytopathogenic bacterial infection,<sup>530</sup> but this protective effect wasn't attributed to its direct bacteriostatic or bactericidal effects against *Pseudomonas syringae* pv *syringae* and *P. pv tabaci*.<sup>530, 12</sup> Similarly, the lack of response of plants to 9-OH C18:3 was linked to their increasing susceptibility against *Pseudomonas syringae*.<sup>359</sup> This maybe because while 9-OH C18:3 is not responsible for the direct inhibition of this pathogen,<sup>12</sup> it may

be responsible for the brassinosteroid-signaled cell wall-based defense, and thus the development of physical protection against *P. syringae*.<sup>360</sup> Most importantly, HUFA can function as signaling compounds to trigger further pathogenic-related gene expression that regulates further pathogenic response.<sup>516, 14</sup> For example, an exogenously applied 10  $\mu$ M solution of 13-OH C18:3, 13*S*-hydroxy-9*Z*,11*E*,15*Z*-octadecatrienoic acid can induce pathogenic-related gene *PR1b* expression in barley leaf segments,<sup>516</sup> and the PR1b proteins are antifungals (minimal concentration of 100  $\mu$ g/mL to inhibit the germination of zoospores by more than 90%).<sup>531</sup>

In summary, our collaborative study suggests that HUFA is a promising candidate in plant protection, but the function of HUFA *in vivo* are complicated by various factors. These factors include: 1) the species and the physiological stage of pathogens; 2) the species and physiological stage of plants; and 3) other functions of HUFA, such as signaling and regulation on protective structures; and 4) the location and the time window of applying HUFA onto plants. Notably, the direct antifungal activity of HUFA and the activation of a further response (both hypersensitivity and development of resistance) by HUFA seem to be delicately dose-dependent. Therefore, it would be extremely interesting to investigate this elegant result of evolution, and to develop a novel HUFA-based plant protection method. The methodologies developed or used in this thesis for the characterization, purification and antifungal testing of HUFA *in vitro* and *in situ* provide a useful foundation to investigate the functions of HUFA, as well as other important bioactive lipids.

## 8.4 Limitation and further research

### 8.4.1 Further development of structure-function relationship and application of HUFA *in situ/in vivo*

Although a structure-function relationship has been developed for food against food spoilage and phytopathogenic fungi *in vitro*, the more comprehensive one *in vivo* has yet to be validated. It was observed in this thesis that different HUFA with a comparable *in vitro* MIC against fungi exhibited different antifungal properties in food and in plants. The antagonistic, additive or synergetic effects of HUFA with other food or plant components are worthy of further investigation to explain these structure-function variations, and to develop applications of HUFA combining other complementary antifungals in specific matrixes. At the same time, in plants, the impact of HUFA on the interplay of different plant signaling pathways, such as salicylate (SA)-mediated systemic acquired resistance (SAR), jasmonate (JA)-mediated induced systemic resistance (ISR), ROS mediated hypersensitive response (HR), and brassinosteroid signaling (cell wall-based defense), need further study. A better understanding is also required to explain the effect of matrixes, such as in the case of wheat-flour vs. flaxseed-flour sourdough bread, or for dicotyledons vs. monocotyledons. In addition, it was observed that the antifungal properties of HUFA are also specific to species and the physiological stage of the fungi and the plants. Therefore, the *in vivo* structure-function relationship of HUFA and their antifungal applications also needs to be accompanied by information about the fungal pathogens, as well as the specific application windows of the time and locations.

#### **8.4.2 Comprehensive characterization and quantitation of HUFA in fermented food matrixes**

Microbes used in fermentation have potential to convert food components into antifungal compounds like HUFA. Methods have been developed for the characterization and quantitation of HUFA in fermented sausage and bread. However, the production of HUFA *in situ* is yet to be analyzed in other food matrixes such as fermented dairy or other cereal products. These types of data will be essential to understand the functions of HUFA in food, as well as the required addition of HUFA in order to achieve antifungal properties. Along with the comprehensive analysis of HUFA in diverse fermented food, the profile of sensory properties or other functions of food can also be related to the structure and the quantity of HUFA, which help pinpoint the functions of specific HUFA structure.

#### **8.4.3 Further study on the mode of action and the resulting development of co-antifungal compounds**

The antifungal activities of HUFA against food-related fungi, mainly grouped as filamentous fungi and yeasts, are partially explained by their ergosterol contents. In this work, the role of sterols was investigated due to their critical roles in maintaining membrane fluidity; furthermore, sterol content was previously related to the resistance of fungi to antifungal unsaturated fatty acids. However, we also found an exception for *Candida albicans*, which had lower ergosterol content but high resistance to HUFA. Hence, more analysis needs to be done on other membrane fluidity moderators, such as the fungal fatty acid and phospholipid compositions, to explain this exception. As well as food-related fungi, compositional analysis of phyto-pathogenic fungi also needs to be acquired to explain their difference of fungal sensitivity to HUFA.

The association of HUFA sensitivity and ability of fungi to adjust their membrane fluidity under stress indicates the potential for co-application of HUFA and antifungal compounds that target membrane composition. For example, combining HUFA with an ergosterol biosynthesis inhibitor may result in a synergetic effect, and therefore a reduced amount of both antifungals might be effective. This would be valuable due to the common pursuit of reduced use of antimicrobials in the food and agricultural industry.

## References

1. Yang, J.; Dong, H.; Hammock, B. D. Profiling the regulatory lipids: another systemic way to unveil the biological mystery. *Curr. Opin. Lipidol.* **2011**, *22*, 197-203.
2. Shevchenko, A.; Simons, K. Lipidomics: coming to grips with lipid diversity. *Nat. Rev. Mol. Cell Biol.* **2010**, *11*, 593-598.
3. Doria, M. L.; Cotrim, Z.; Macedo, B.; Simoes, C.; Domingues, P.; Helguero, L.; Domingues, M. R. Lipidomic approach to identify patterns in phospholipid profiles and define class differences in mammary epithelial and breast cancer cells. *Breast Cancer Res. Treat.* **2012**, *133*, 635-648.
4. Alessenko, A. V. The role of sphingomyelin cycle metabolites in transduction of signals of cell proliferation, differentiation and death. *Membrane & Cell Biology* **2000**, *13*, 303-20.
5. Petursdottir, A. L.; Farr, S. A.; Morley, J. E.; Banks, W. A.; Skuladottir, G. V. Effect of dietary n-3 polyunsaturated fatty acids on brain lipid fatty acid composition, learning ability, and memory of senescence-accelerated mouse. *J. Gerontol., Ser. A* **2008**, *63*, 1153-1160.
6. Troncoso-Ponce, M. A.; Cao, X.; Yang, Z. L.; Ohlrogge, J. B. Lipid turnover during senescence. *Plant Sci.* **2013**, *205*, 13-19.
7. Van der Steen, T.; Kemble, G.; Lupu, R. Targeting fatty acid synthase induces apoptosis and senescence. *Cancer Res.* **2019**, *79*.
8. Deans, J. P.; Li, H. D.; Polyak, M. J. CD20-mediated apoptosis: signalling through lipid rafts. *Immunology* **2002**, *107*, 176-182.
9. Hou, Q. C.; Ufer, G. D.; Bartels, D. Lipid signalling in plant responses to abiotic stress. *Plant, Cell Environ.* **2016**, *39*, 1029-1048.

10. Upchurch, R. G. Fatty acid unsaturation, mobilization, and regulation in the response of plants to stress. *Biotechnol. Lett.* **2008**, *30*, 967-977.
11. Hancock, S. E.; Poad, B. L. J.; Batarseh, A.; Abbott, S. K.; Mitchell, T. W. Advances and unresolved challenges in the structural characterization of isomeric lipids. *Anal. Biochem.* **2017**, *524*, 45-55.
12. Prost, I.; Dhondt, S.; Rothe, G.; Vicente, J.; Rodriguez, M. J.; Kift, N.; Carbonne, F.; Griffiths, G.; Esquerré-Tugayé, M. T.; Rosahl, S.; Castresana, C.; Hamberg, M.; Fournier, J. Evaluation of the antimicrobial activities of plant oxylipins supports their involvement in defense against pathogens. *Plant Physiol.* **2005**, *139*, 1902-1913.
13. Pohl, C. H.; Kock, J. L. F.; Thibane, V. S. Antifungal free fatty acids: a review. In *Science against microbial pathogens: current research and technological advances*, Méndez-Vilas, A., Ed. 2011; Vol. 1, pp 61-71.
14. Weber, H. Fatty acid-derived signals in plants. *Trends Plant Sci.* **2002**, *7*, 217-224.
15. Black, B. A.; Zannini, E.; Curtis, J. M.; Gänzle, M. G. Antifungal hydroxy fatty acids produced during sourdough fermentation: microbial and enzymatic pathways, and antifungal activity in bread. *Appl. Environ. Microbiol.* **2013**, *79*, 1866-1873.
16. Chen, Y. Membrane lipid homeostasis and stress resistance in *Escherichia coli* and *Lactobacillus plantarum*. University of Alberta, 2017.
17. Volkov, A.; Liavonchanka, A.; Kamneva, O.; Fiedler, T.; Goebel, C.; Kreikemeyer, B.; Feussner, I. Myosin cross-reactive antigen of *Streptococcus pyogenes* M49 encodes a fatty acid double bond hydratase that plays a role in oleic acid detoxification and bacterial virulence. *J. Biol. Chem.* **2010**, *285*, 10353-10361.



18. Hunter, M. C.; Smith, R. G.; Schipanski, M. E.; Atwood, L. W.; Mortensen, D. A. Agriculture in 2050: Recalibrating targets for sustainable intensification. *Bioscience* **2017**, *67*, 385-390.
19. FAO. Save food: global initiative on food loss and waste reduction—key findings. <http://www.fao.org/save-food/resources/keyfindings/en/> (accessed 12 August 2019).
20. Salas, M. L.; Mounier, J.; Valence, F.; Coton, M.; Thierry, A.; Coton, E. Antifungal microbial agents for food biopreservation—a review. *Microorganisms* **2017**, *5*.
21. Pitt, J. I.; Hocking, A. D. *Fungi and food spoilage*. 3rd ed.; Springer Dordrecht Heidelberg London New York: New York, 2009; pp v-519.
22. Mitchell, N. J.; Bowers, E.; Hurburgh, C.; Wu, F. Potential economic losses to the US corn industry from aflatoxin contamination. *Food Addit. Contam., Part A* **2016**, *33*, 540-550.
23. Gbashi, S.; Madala, N. E.; Adekoya, I.; Adebo, O.; De Saeger, S.; De Boevre, M.; Njobeh, P. B. The socio-economic impact of mycotoxin contamination in Africa. In *Mycotoxins-Impact and management strategies*, IntechOpen: 2018.
24. Oliveira, P. M.; Zannini, E.; Arendt, E. K. Cereal fungal infection, mycotoxins, and lactic acid bacteria mediated bioprotection: from crop farming to cereal products. *Food Microbiol.* **2014**, *37*, 78-95.
25. Paterson, R. R. M.; Lima, N. How will climate change affect mycotoxins in food? *Food Res. Int.* **2010**, *43*, 1902-1914.
26. Fisher, M. C.; Henk, D. A.; Briggs, C. J.; Brownstein, J. S.; Madoff, L. C.; McCraw, S. L.; Gurr, S. J. Emerging fungal threats to animal, plant and ecosystem health. *Nature* **2012**, *484*, 186-194.

27. Almeida, F.; Rodrigues, M. L.; Coelho, C. The still underestimated problem of fungal diseases worldwide. *Front. Microbiol.* **2019**, *10*.
28. Garcia-Solache, M. A.; Casadevall, A. Global warming will bring new fungal diseases for mammals. *Mbio* **2010**, *1*.
29. Casadevall, A.; Kontoyiannis, D. P.; Robert, V. On the emergence of *Candida auris*: climate change, azoles, swamps, and birds. *Mbio* **2019**, *10*.
30. Grandi, M.; Vecchiato, C. G.; Biagi, G.; Zironi, E.; Tondo, M. T.; Pagliuca, G.; Palmonari, A.; Pinna, C.; Zaghini, G.; Gazzotti, T. Occurrence of mycotoxins in extruded commercial cat food. *ACS Omega* **2019**, *4*, 14004-14012.
31. Magnoli, A. P.; Poloni, V. L.; Cavaglieri, L. Impact of mycotoxin contamination in the animal feed industry. *Curr. Opin. Food Sci.* **2019**, *29*, 99-108.
32. Garnier, L.; Valence, F.; Mounier, J. Diversity and control of spoilage fungi in dairy products: an update. *Microorganisms* **2017**, *5*.
33. Quattrini, M.; Liang, N.; Fortina, M. G.; Xiang, S.; Curtis, J. M.; Gänzle, M. Exploiting synergies of sourdough and antifungal organic acids to delay fungal spoilage of bread. *Int. J. Food Microbiol.* **2018**.
34. Asioli, D.; Aschemann-Witzel, J.; Caputo, V.; Vecchio, R.; Annunziata, A.; Næs, T.; Varela, P. Making sense of the “clean label” trends: A review of consumer food choice behavior and discussion of industry implications. *Food Res. Int.* **2017**, *99*, 58-71.
35. Yara, A.; Yaeno, T.; Montillet, J. L.; Hasegawa, M.; Seo, S.; Kusumi, K.; Iba, K. Enhancement of disease resistance to *Magnaporthe grisea* in rice by accumulation of hydroxy linoleic acid. *Biochem. Biophys. Res. Commun.* **2008**, *370*, 344-347.

36. Cantrell, C. L.; Case, B. P.; Mena, E. E.; Kniffin, T. M.; Duke, S. O.; Wedget, D. E. Isolation and identification of antifungal fatty acids from the basidiomycete *Gomphus floccosus*. *J. Agric. Food Chem.* **2008**, *56*, 5062-5068.
37. Shimada, T. L.; Takano, Y.; Shimada, T.; Fujiwara, M.; Fukao, Y.; Mori, M.; Okazaki, Y.; Saito, K.; Sasaki, R.; Aoki, K.; Hara-Nishimura, I. Leaf oil body functions as a subcellular factory for the production of a phytoalexin in *Arabidopsis*. *Plant Physiol.* **2014**, *164*, 105-118.
38. Badami, R. C.; Patil, K. B. Structure and occurrence of unusual fatty acids in minor seed oils. *Prog. Lipid Res.* **1980**, *19*, 119-153.
39. Kim, K. R.; Oh, D. K. Production of hydroxy fatty acids by microbial fatty acid-hydroxylation enzymes. *Biotechnol. Adv.* **2013**, *31*, 1473-1485.
40. Ohlrogge, J.; Thrower, N.; Mhaske, V.; Stymne, S.; Baxter, M.; Yang, W. L.; Liu, J. J.; Shaw, K.; Shorrosh, B.; Zhang, M.; Wilkerson, C.; Matthäus, B. PlantFAdb: a resource for exploring hundreds of plant fatty acid structures synthesized by thousands of plants and their phylogenetic relationships. *Plant J.* **2018**, *96*, 1299-1308.
41. Schnürer, J.; Magnusson, J. Antifungal lactic acid bacteria as biopreservatives. *Trends Food Sci. Technol.* **2005**, *16*, 70-78.
42. Bernardeau, M.; Guguen, M.; Vernoux, J. P. Beneficial lactobacilli in food and feed: long-term use, biodiversity and proposals for specific and realistic safety assessments. *FEMS Microbiol. Rev.* **2006**, *30*, 487-513.
43. Siedler, S.; Balti, R.; Neves, A. R. Bioprotective mechanisms of lactic acid bacteria against fungal spoilage of food. *Curr. Opin. Biotechnol.* **2019**, *56*, 138-146.
44. Crowley, S.; Mahony, J.; van Sinderen, D. Current perspectives on antifungal lactic acid bacteria as natural bio-preservatives. *Trends Food Sci. Technol.* **2013**, *33*, 93-109.

45. Leyva Salas, M.; Thierry, A.; Lemaitre, M.; Garric, G.; Harel-Oger, M.; Chatel, M.; Le, S.; Mounier, J.; Valence, F.; Coton, E. Antifungal activity of lactic acid bacteria combinations in dairy mimicking models and their potential as bioprotective cultures in pilot scale applications. *Front. Microbiol.* **2018**, *9*.
46. Engan, S. Organoleptic threshold values of some organic acids in beer. *J. Inst. Brew.* **1974**, *80*, 162-163.
47. Aunbjerg, S. D.; Honore, A. H.; Marcussen, J.; Ebrahimi, P.; Vogensen, F. K.; Benfeldt, C.; Skov, T.; Knochel, S. Contribution of volatiles to the antifungal effect of *Lactobacillus paracasei* in defined medium and yogurt. *Int. J. Food Microbiol.* **2015**, *194*, 46-53.
48. Martineau, B.; Acree, T. E.; Henickkling, T. Effect of wine type on the detection threshold for diacetyl. *Food Res. Int.* **1995**, *28*, 139-143.
49. Zhang, C. G.; Brandt, M. J.; Schwab, C.; Gänzle, M. G. Propionic acid production by cofermentation of *Lactobacillus buchneri* and *Lactobacillus diolivorans* in sourdough. *Food Microbiol.* **2010**, *27*, 390-395.
50. Blanco, C. A.; Ronda, F.; Perez, B.; Pando, V. Improving gluten-free bread quality by enrichment with acidic food additives. *Food Chem.* **2011**, *127*, 1204-1209.
51. Magnusson, J.; Schnürer, J. *Lactobacillus coryniformis* subsp. *coryniformis* strain Si3 produces a broad-spectrum proteinaceous antifungal compound. *Appl. Environ. Microbiol.* **2001**, *67*, 1-5.
52. Vermeulen, N.; Gänzle, M. G.; Vogel, R. F. Influence of peptide supply and cosubstrates on phenylalanine metabolism of *Lactobacillus sanfranciscensis* DSM20451(T) and *Lactobacillus plantarum* TMW1.468. *J. Agric. Food Chem.* **2006**, *54*, 3832-3839.

53. Schmidt, M.; Lynch, K. M.; Zannini, E.; Arendt, E. K. Fundamental study on the improvement of the antifungal activity of *Lactobacillus reuteri* R29 through increased production of phenyllactic acid and reuterin. *Food Control* **2018**, *88*, 139-148.
54. Ryan, L. A. M.; Dal Bello, F.; Arendt, E. K.; Koehler, P. Detection and quantitation of 2,5-diketopiperazines in wheat sourdough and bread. *J. Agric. Food Chem.* **2009**, *57*, 9563-9568.
55. Messens, W.; De Vuyst, L. Inhibitory substances produced by *Lactobacilli* isolated from sourdoughs-a review. *Int. J. Food Microbiol.* **2002**, *72*, 31-43.
56. Batish, V. K.; Roy, U.; Lal, R.; Grover, S. Antifungal attributes of lactic acid bacteria - A review. *Crit. Rev. Biotechnol.* **1997**, *17*, 209-225.
57. Mandal, V.; Sen, S. K.; Mandal, N. C. Production and partial characterisation of an inducer-dependent novel antifungal compound(s) by *Pediococcus acidilactici* LAB 5. *J. Sci. Food Agric.* **2013**, *93*, 2445-2453.
58. Axel, C.; Brosnan, B.; Zannini, E.; Peyer, L. C.; Furey, A.; Coffey, A.; Arendt, E. K. Antifungal activities of three different *Lactobacillus* species and their production of antifungal carboxylic acids in wheat sourdough. *Appl. Microbiol. Biot.* **2016**, *100*, 1701-1711.
59. Ito, Y. Golden rules and pitfalls in selecting optimum conditions for high-speed counter-current chromatography. *J. Chromatogr. A* **2005**, *1065*, 145-168.
60. Engels, C.; Gänzle, M. G.; Schieber, A. Fractionation of gallotannins from mango (*Mangifera indica* L.) kernels by high-speed counter-current chromatography and determination of their antibacterial activity. *J. Agric. Food Chem.* **2010**, *58*, 775-780.
61. Smith Jr, C. R. Occurrence of unusual fatty acids in plants. *Prog. Chem. Fats Other Lipids* **1971**, *11*, 137-177.

62. Jenske, R.; Lindström, F.; Gröbner, G.; Vetter, W. Impact of free hydroxylated and methyl-branched fatty acids on the organization of lipid membranes. *Chem. Phys. Lipids* **2008**, *154*, 26-32.
63. Spite, M.; Clària, J.; Serhan, C. N. Resolvins, specialized proresolving lipid mediators, and their potential roles in metabolic diseases. *Cell Metab.* **2014**, *19*, 21-36.
64. Christensen, S. A.; Kolomiets, M. V. The lipid language of plant-fungal interactions. *Fungal Genet. Biol.* **2011**, *48*, 4-14.
65. Sjögren, J.; Magnusson, J.; Broberg, A.; Schnürer, J.; Kenne, L. Antifungal 3-hydroxy fatty acids from *Lactobacillus plantarum* MiLAB 14. *Appl. Environ. Microbiol.* **2003**, *69*, 7554-7557.
66. Liang, N.; Cai, P.; Wu, D.; Pan, Y.; Curtis, J. M.; Gänzle, M. G. High-speed counter-current chromatography (HSCCC) purification of antifungal fatty acids from plant-seed oil and *Lactobacillus* cultures. *J. Agric. Food Chem.* **2017**, *65*, 11229-11236.
67. Thomas, D. W.; van Kuijk, F. J.; Stephens, R. J. Quantitative determination of hydroxy fatty acids as an indicator of *in vivo* lipid peroxidation: oxidation products of arachidonic and docosapentaenoic acids in rat liver after exposure to carbon tetrachloride. *Anal. Biochem.* **1992**, *206*, 353-358.
68. Ostermann, A. I.; Schebb, N. H. Effects of omega-3 fatty acid supplementation on the pattern of oxylipins: a short review about the modulation of hydroxy-, dihydroxy-, and epoxy-fatty acids. *Food Funct.* **2017**, *8*, 2355-2367.
69. Moore, K. H.; Radloff, J. F.; Hull, F. E.; Sweeley, C. C. Incomplete fatty acid oxidation by ischemic heart: beta-hydroxy fatty acid production. *Am. J. Physiol.* **1980**, *239*, H257-H265.

70. Feldstein, A. E.; Lopez, R.; Tamimi, T. A. R.; Yerian, L.; Chung, Y. M.; Berk, M.; Zhang, R. L.; McIntyre, T. M.; Hazen, S. L. Mass spectrometric profiling of oxidized lipid products in human nonalcoholic fatty liver disease and nonalcoholic steatohepatitis. *J. Lipid Res.* **2010**, *51*, 3046-3054.
71. Zelles, L. Fatty acid patterns of phospholipids and lipopolysaccharides in the characterisation of microbial communities in soil: a review. *Biol. Fertil. Soils* **1999**, *29*, 111-129.
72. Gangopadhyay, P. K.; Thadepalli, H.; Roy, I.; Ansari, A. Identification of species of *Candida*, *Cryptococcus*, and *Torulopsis* by gas-liquid chromatography. *J. Infect. Dis.* **1979**, *140*, 952-958.
73. Tallent, W. H.; Harris, J.; Spencer, G. F.; Wolff, I. A. Structure and intraglyceride distribution of coriolic acid. *Lipids* **1968**, *3*, 425-430.
74. Dobarganes, M. C. Analysis of Oxidized Fatty Acids.  
<https://lipidlibrary.aocs.org/chemistry/physics/frying-oils/analysis-of-oxidized-fatty-acids>  
(accessed February 4th, 2020).
75. Martinez, J.; Vogler, O.; Casas, J.; Barcelo, F.; Alemany, R.; Prades, J.; Nagy, T.; Baamonde, C.; Kasprzyk, P. G.; Teres, S.; Saus, C.; Escriba, P. V. Membrane structure modulation, protein kinase C alpha activation, and anticancer activity of minerval. *Mol. Pharmacol.* **2005**, *67*, 531-540.
76. Llado, V.; Gutierrez, A.; Martinez, J.; Casas, J.; Teres, S.; Higuera, M.; Galmes, A.; Saus, C.; Besalduch, J.; Busquets, X.; Escriba, P. V. Minerval induces apoptosis in Jurkat and other cancer cells. *J. Cell. Mol. Med.* **2010**, *14*, 659-670.
77. Teres, S.; Llado, V.; Higuera, M.; Barcelo-Coblijn, G.; Martin, M. L.; Noguera-Salva, M. A.; Marcilla-Etxenike, A.; Garcia-Verdugo, J. M.; Soriano-Navarro, M.; Saus, C.; Gomez-

- Pinedo, U.; Busquets, X.; Escriba, P. V. 2-Hydroxyoleate, a nontoxic membrane binding anticancer drug, induces glioma cell differentiation and autophagy. *Proc. Natl. Acad. Sci. U. S. A.* **2012**, *109*, 8489-8494.
78. Martinez, J.; Gutierrez, A.; Casas, J.; Llado, V.; Lopez-Bellan, A.; Besalduch, J.; Dopazo, A.; Escriba, P. V. The repression of E2F-1 is critical for the activity of Minerval against cancer. *J. Pharmacol. Exp. Ther.* **2005**, *315*, 466-474.
79. Escriba, P. V. Membrane-lipid therapy: a new approach in molecular medicine. *Trends Mol. Med.* **2006**, *12*, 34-43.
80. Ibareguren, M.; Lopez, D. J.; Encinar, J. A.; Gonzalez-Ros, J. M.; Busquets, X.; Escriba, P. V. Partitioning of liquid-ordered/liquid-disordered membrane microdomains induced by the fluidifying effect of 2-hydroxylated fatty acid derivatives. *Biochim. Biophys. Acta* **2013**, *1828*, 2553-2563.
81. Vogler, O.; Lopez-Bellan, A.; Alemany, R.; Tofe, S.; Gonzalez, M.; Quevedo, J.; Pereg, V.; Barcelo, F.; Escriba, P. V. Structure-effect relation of C18 long-chain fatty acids in the reduction of body weight in rats. *Int. J. Obes.* **2008**, *32*, 464-473.
82. Teres, S.; Barcelo-Coblijn, G.; Benet, M.; Alvarez, R.; Bressani, R.; Halver, J. E.; Escriba, P. V. Oleic acid content is responsible for the reduction in blood pressure induced by olive oil. *Proc. Natl. Acad. Sci. U. S. A.* **2008**, *105*, 13811-13816.
83. Guo, L.; Zhang, X.; Zhou, D. Q.; Okunade, A. L.; Su, X. Stereospecificity of fatty acid 2-hydroxylase and differential functions of 2-hydroxy fatty acid enantiomers. *J. Lipid Res.* **2012**, *53*, 1327-1335.
84. Edvardson, S.; Hama, H.; Shaag, A.; Gomori, J. M.; Berger, I.; Soffer, D.; Korman, S. H.; Taustein, I.; Saada, A.; Elpeleg, O. Mutations in the fatty acid 2-hydroxylase gene are



associated with leukodystrophy with spastic paraparesis and dystonia. *Am. J. Hum. Genet.* **2008**, *83*, 643-648.

85. Dick, K. J.; Eckhardt, M.; Paisan-Ruiz, C.; Alshehhi, A. A.; Proukakis, C.; Sibtain, N. A.; Maier, H.; Sharifi, R.; Patton, M. A.; Bashir, W.; Koul, R.; Raeburn, S.; Gieselmann, V.; Houlden, H.; Crosby, A. H. Mutation of FA2H underlies a complicated form of hereditary spastic paraplegia (SPG35). *Hum. Mutat.* **2010**, *31*, E1251-E1260.

86. Kruer, M. C.; Paisan-Ruiz, C.; Boddaert, N.; Yoon, M. Y.; Hama, H.; Gregory, A.; Malandrini, A.; Woltjer, R. L.; Munnich, A.; Gobin, S.; Polster, B. J.; Palmeri, S.; Edvardson, S.; Hardy, J.; Houlden, H.; Hayflick, S. J. Defective *FA2H* leads to a novel form of neurodegeneration with brain iron accumulation (NBIA). *Ann. Neurol.* **2010**, *68*, 611-618.

87. Goetzman, E. S. Chapter 10 - Modeling disorders of fatty acid metabolism in the mouse. In *Progress in molecular biology and translational science*, Chang, K. T.; Min, K. T., Eds.; Academic Press: 2011; Vol. 100, pp 389-417.

88. Matsunaga, I.; Ueda, A.; Fujiwara, N.; Sumimoto, T.; Ichihara, K. Characterization of the ybdT gene product of *Bacillus subtilis*: novel fatty acid beta-hydroxylating cytochrome P450. *Lipids* **1999**, *34*, 841-846.

89. Ciccoli, R.; Sahi, S.; Singh, S.; Prakash, H.; Zafiriou, M. P.; Ishdorj, G.; Kock, J. L. F.; Nigam, S. Oxygenation by COX-2 (cyclo-oxygenase-2) of 3-HETE (3-hydroxyeicosatetraenoic acid), a fungal mimetic of arachidonic acid, produces a cascade of novel bioactive 3-hydroxyeicosanoids. *Biochem. J.* **2005**, *390*, 737-747.

90. Takakuwa, N.; Kinoshita, M.; Oda, Y.; Ohnishi, M. Existence of cerebroside in *Saccharomyces kluyveri* and its related species. *FEMS Yeast Res.* **2002**, *2*, 533-538.

91. Tanji, M.; Namimatsu, K.; Kinoshita, M.; Motoshima, H.; Oda, Y.; Ohnishi, M. Content and chemical compositions of cerebrosides in lactose-assimilating yeasts. *Biosci., Biotechnol., Biochem.* **2004**, *68*, 2205-2208.
92. Toledo, M. S.; Levery, S. B.; Straus, A. H.; Takahashi, H. K. Dimorphic expression of cerebrosides in the mycopathogen *Sporothrix schenckii*. *J. Lipid Res.* **2000**, *41*, 797-806.
93. Deva, R.; Ciccoli, R.; Schewe, T.; Kock, J. L. F.; Nigam, S. Arachidonic acid stimulates cell growth and forms a novel oxygenated metabolite in *Candida albicans*. *Biochim. Biophys. Acta, Mol. Cell Biol. Lipids* **2000**, *1486*, 299-311.
94. Kock, J. L. F.; Strauss, C. J.; Pohl, C. H.; Nigam, S. The distribution of 3-hydroxy oxylipins in fungi. *Prostaglandins Other Lipid Mediators* **2003**, *71*, 85-96.
95. Deva, R.; Ciccoli, R.; Kock, L.; Nigam, S. Involvement of aspirin-sensitive oxylipins in vulvovaginal candidiasis. *FEMS Microbiol. Lett.* **2001**, *198*, 37-43.
96. Nigam, S.; Ciccoli, R.; Ivanov, I.; Szczepanski, M.; Deva, R. On mechanism of quorum sensing in *Candida albicans* by 3(R)-hydroxy-tetradecaenoic acid. *Curr. Microbiol.* **2011**, *62*, 55-63.
97. Madu, U. L.; Ogundeji, A. O.; Mochochoko, B. M.; Pohl, C. H.; Albertyn, J.; Swart, C. W.; Allwood, J. W.; Southam, A. D.; Dunn, W. B.; May, R. C.; Sebolai, O. M. Cryptococcal 3-hydroxy fatty acids protect cells against amoebal phagocytosis. *Front. Microbiol.* **2015**, *6*.
98. Sebolai, O. M.; Pohl, C. H.; Botes, P. J.; Strauss, C. J.; Van Wyk, P. W. J.; Botha, A.; Kock, J. L. F. 3-Hydroxy fatty acids found in capsules of *Cryptococcus neoformans*. *Can. J. Microbiol.* **2007**, *53*, 809-812.
99. Strauss, C. J.; Kock, J. L. F.; van Wyk, P. W. J.; Lodolo, E. J.; Pohl, C. H.; Botes, P. J. Bioactive oxylipins in *Saccharomyces cerevisiae*. *J. Inst. Brew.* **2005**, *111*, 304-308.

100. Fourie, R.; Ells, R.; Swart, C. W.; Sebolai, O. M.; Albertyn, J.; Pohl, C. H. *Candida albicans* and *Pseudomonas aeruginosa* interaction, with focus on the role of eicosanoids. *Front. Physiol.* **2016**, *7*.
101. Nagano, M.; Takahara, K.; Fujimoto, M.; Tsutsumi, N.; Uchimiya, H.; Kawai-Yamada, M. *Arabidopsis* sphingolipid fatty acid 2-hydroxylases (AtFAH1 and AtFAH2) are functionally differentiated in fatty acid 2-hydroxylation and stress responses. *Plant Physiol.* **2012**, *159*, 1138-1148.
102. Ishikawa, T.; Aki, T.; Yanagisawa, S.; Uchimiya, H.; Kawai-Yamada, M. Overexpression of BAX INHIBITOR-1 links plasma membrane microdomain proteins to stress. *Plant Physiol.* **2015**, *169*, 1333-1343.
103. Imai, H.; Ohnishi, M.; Kinoshita, M.; Kojima, M.; Ito, S. Structure and distribution of cerebroside containing unsaturated hydroxy fatty acids in plant leaves. *Biosci., Biotechnol., Biochem.* **1995**, *59*, 1309-1313.
104. Imai, H.; Ohnishi, M.; Kojima, M.; Ito, S. Cerebrosides in seed-plant leaves: Composition of fatty acids and sphingoid bases. **1997**, 224-226.
105. Smith, C. R.; Wolff, I. A. Characterization of naturally occurring  $\alpha$ -hydroxylinolenic acid. *Lipids* **1969**, *4*, 9-14.
106. Bohannon, M. B.; Kleiman, R. Unsaturated C18  $\alpha$ -hydroxy acids in *Salvia nilotica*. *Lipids* **1975**, *10*, 703-706.
107. Machado, L.; Castro, A.; Hamberg, M.; Bannenberg, G.; Gaggero, C.; Castresana, C.; de Leon, I. P. The *Physcomitrella patens* unique  $\alpha$ -dioxygenase participates in both developmental processes and defense responses. *BMC Plant Biol.* **2015**, *15*.

108. Hamberg, M.; Sanz, A.; Rodriguez, M. J.; Calvo, A. P.; Castresana, C. Activation of the fatty acid alpha-dioxygenase pathway during bacterial infection of tobacco leaves - Formation of oxylipins protecting against cell death. *J. Biol. Chem.* **2003**, *278*, 51796-51805.
109. Gaquerel, E.; Steppuhn, A.; Baldwin, I. T. *Nicotiana attenuata* α-DIOXYGENASE1 through its production of 2-hydroxylinolenic acid is required for intact plant defense expression against attack from *Manduca sexta* larvae. *New Phytol.* **2012**, *196*, 574-585.
110. Vicente, J.; Cascon, T.; Vicedo, B.; Garcia-Agustin, P.; Hamberg, M.; Castresana, C. Role of 9-lipoxygenase and alpha-dioxygenase oxylipin pathways as modulators of local and systemic defense. *Mol. Plant* **2012**, *5*, 914-928.
111. Watanabe, M.; Miyagi, A.; Nagano, M.; Kawai-Yamada, M.; Imai, H. Characterization of glucosylceramides in the *Polygonaceae*, *Rumex obtusifolius* L. injurious weed. *Biosci., Biotechnol., Biochem.* **2011**, *75*, 877-881.
112. Ozen, H. C.; Bashan, M.; Keskin, C.; Toker, Z. Fatty acid and 3-hydroxy fatty acid composition of two *Hypericum* species from Turkey. *Eur. J. Lipid Sci. Technol.* **2004**, *106*, 68-70.
113. Dumri, K.; Selpold, L.; Schmidt, R.; Gerlach, G.; Dotterl, S.; Ellis, A. G.; Wessjohann, L. A. Non-volatile floral oils of *Diascia* spp. (Scrophulariaceae). *Phytochemistry* **2008**, *69*, 1372-1383.
114. Seipold, L.; Gerlach, G.; Wessjohann, L. A new type of floral oil from *Malpighia coccigera* (Malpighiaceae) and chemical considerations on the evolution of oil flowers. *Chem. Biodiversity* **2004**, *1*, 1519-1528.

115. Racovita, R. C.; Peng, C.; Awakawa, T.; Abe, I.; Jetter, R. Very-long-chain 3-hydroxy fatty acids, 3-hydroxy fatty acid methyl esters and 2-alkanols from cuticular waxes of *Aloe arborescens* leaves. *Phytochemistry* **2015**, *113*, 183-194.
116. Jiang, R. W.; Hay, M. E.; Fairchild, C. R.; Prudhomme, J.; Le Roch, K.; Aalbersberg, W.; Kubanek, J. Antineoplastic unsaturated fatty acids from Fijian macroalgae. *Phytochemistry* **2008**, *69*, 2495-2500.
117. Kawanami, J.; Kimura, A.; Nakagawa, Y.; Otsuka, H. Lipids of *Streptomyces sioyaensis*. V. On 2-hydroxy-13-methyl-tetradecanoic acid from phosphatidylethanolamine. *Chem. Phys. Lipids* **1969**, *3*, 29-38.
118. Yano, I.; Furukawa, Y.; Kusunose, M. Alpha-hydroxy fatty acid-containing phospholipids of *Nocardia leishmanii*. *Biochim. Biophys. Acta* **1970**, *202*, 189-91.
119. Yano, I.; Furukawa, Y.; Kusunose, M. 2-Hydroxy fatty acid-containing phospholipid of *Arthrobacter simplex*. *Biochim. Biophys. Acta* **1970**, *210*, 105-115.
120. Fensom, A. H.; Gray, G. W. The chemical composition of the lipopolysaccharide of *Pseudomonas aeruginosa*. *Biochem. J.* **1969**, *114*, 185-196.
121. Park, C. E.; Berger, L. R. Fatty acids of extractable and bound lipids of *Rhodocyclidium vanniellii*. *J. Bacteriol.* **1967**, *93*, 230-236.
122. Naka, T.; Fujiwara, N.; Yabuuchi, E.; Doe, M.; Kobayashi, K.; Kato, Y.; Yano, I. A novel sphingoglycolipid containing galacturonic acid and 2-hydroxy fatty acid in cellular lipids of *Sphingomonas yanoikuyae*. *J. Bacteriol.* **2000**, *182*, 2660-2663.
123. Matsunaga, I.; Kusunose, E.; Yano, I.; Ichihara, K. Separation and partial characterization of soluble fatty acid alpha-hydroxylase from *Sphingomonas paucimobilis*. *Biochem. Biophys. Res. Commun.* **1994**, *201*, 1554-1560.

124. Nakayama, M. Structure and apoptosis-inducing activity of sphingolipids isolated from *Sphingobacterium spiritivorum*. *SEIKATSU EISEI* **1998**, *42*, 135-148.
125. Wollenweber, H. W.; Rietschel, E. T. Analysis of lipopolysaccharide (lipid A) fatty acids. *J. Microbiol. Methods* **1990**, *11*, 195-211.
126. Galanos, C.; Luderitz, O.; Rietschel, E. T.; Westphal, O.; Brade, H.; Brade, L.; Freudenberg, M.; Schade, U.; Imoto, M.; Yoshimura, H.; Kusumoto, S.; Shiba, T. Synthetic and natural *Escherichia coli* free lipid A express identical endotoxic activities. *Eur. J. Biochem.* **1985**, *148*, 1-5.
127. Nakagawa, Y.; Kishida, K.; Kodani, Y.; Matsuyama, T. Optical configuration analysis of hydroxy fatty acids in bacterial lipids by chiral column high-performance liquid chromatography. *Microbiol. Immunol.* **1997**, *41*, 27-32.
128. Hosono, K.; Suzuki, H. Acylpeptides, the inhibitors of cyclic adenosine 3',5'-monophosphate phosphodiesterase. III. Inhibition of cyclic AMP phosphodiesterase. *J. Antibiot. (Tokyo)* **1983**, *36*, 679-683.
129. Sjögren, J.; Magnusson, J.; Broberg, A.; Schnürer, J.; Kenne, L. Antifungal 3-hydroxy fatty acids from *Lactobacillus plantarum* MiLAB 14. *Appl. Environ. Microbiol.* **2003**, *69*, 7554-7557.
130. Yano, I.; Ohno, Y.; Masui, M.; Kato, K.; Yabuuchi, E.; Ohyama, A. Occurrence of 2-hydroxy and 3-hydroxy fatty acids in high concentrations in extractable and bound lipids of *Flavobacterium Meningosepticum* and *Flavobacterium* IIb. *Lipids* **1976**, *11*, 685-688.
131. Oyaizu, H.; Komagata, K. Grouping of *Pseudomonas* species on the basis of cellular fatty acid composition and the quinone system with special reference to the existence of 3-hydroxy fatty acids. *J. Gen. Appl. Microbiol.* **1983**, *29*, 17-40.

132. Andersson, A. M.; Weiss, N.; Rainey, F.; Salkinoja-Salonen, M. S. Dust-borne bacteria in animal sheds, schools and children's day care centres. *J. Appl. Microbiol.* **1999**, *86*, 622-634.
133. Uhlig, S.; Negard, M.; Heldal, K. K.; Straumfors, A.; Madso, L.; Bakke, B.; Eduard, W. Profiling of 3-hydroxy fatty acids as environmental markers of endotoxin using liquid chromatography coupled to tandem mass spectrometry. *J. Chromatogr. A* **2016**, *1434*, 119-126.
134. Chen, Y. S.; Lin, H. H.; Liu, P. J.; Tsai, H. Y.; Hsueh, P. T.; Liu, H. Y.; Chen, Y. L. Use of 3-hydroxy fatty acid concentrations in a murine air pouch infection model as a surrogate marker for LPS activity: A feasibility study using environmental *Burkholderia cenocepacia* isolates. *J. Microbiol. Methods* **2011**, *87*, 368-374.
135. Wang, C. F.; Bendle, J.; Yang, Y.; Yang, H.; Sun, H. L.; Huang, J. H.; Xie, S. C. Impacts of pH and temperature on soil bacterial 3-hydroxy fatty acids: Development of novel terrestrial proxies. *Org. Geochem.* **2016**, *94*, 21-31.
136. Schütte, O. M.; Patalag, L. J.; Weber, L. M.; Ries, A.; Romer, W.; Werz, D. B.; Steinem, C. 2-Hydroxy fatty acid enantiomers of Gb3 impact shiga toxin binding and membrane organization. *Biophys. J.* **2015**, *108*, 2775-2778.
137. Minamino, M.; Sakaguchi, I.; Naka, T.; Ikeda, N.; Kato, Y.; Tomiyasu, I.; Yano, I.; Kobayashi, K. Bacterial ceramides and sphingophospholipids induce apoptosis of human leukaemic cells. *Microbiology* **2003**, *149*, 2071-2081.
138. Patwardhan, A. M.; Akopian, A. N.; Ruparel, N. B.; Diogenes, A.; Weintraub, S. T.; Uhlson, C.; Murphy, R. C.; Hargreaves, K. M. Heat generates oxidized linoleic acid metabolites that activate TRPV1 and produce pain in rodents. *J. Clin. Invest.* **2010**, *120*, 1617-1626.

139. Richardson, C. E.; Hennebelle, M.; Otoki, Y.; Zamora, D.; Yang, J.; Hammock, B. D.; Taha, A. Y. Lipidomic analysis of oxidized fatty acids in plant and algae oils. *J. Agric. Food Chem.* **2017**, *65*, 1941-1951.
140. Wilson, R.; Lyall, K.; Smyth, L.; Fernie, C. E.; Riemersma, R. A. Dietary hydroxy fatty acids are absorbed in humans: Implications for the measurement of 'oxidative stress' *in vivo*. *Free Radical Bio. Med.* **2002**, *32*, 162-168.
141. Wilson, R.; Smith, R.; Wilson, P.; Shepherd, M. J.; Riemersma, R. A. Quantitative gas chromatography mass spectrometry isomer-specific measurement of hydroxy fatty acids in biological samples and food as a marker of lipid peroxidation. *Anal. Biochem.* **1997**, *248*, 76-85.
142. Kohen, R.; Nyska, A. Oxidation of biological systems: oxidative stress phenomena, antioxidants, redox reactions, and methods for their quantification. *Toxicol. Pathol.* **2002**, *30*, 620-650.
143. Niki, E. Lipid peroxidation: Physiological levels and dual biological effects. *Free Radical Bio. Med.* **2009**, *47*, 469-484.
144. Strassburg, K.; Huijbrechts, A. M. L.; Kortekaas, K. A.; Lindeman, J. H.; Pedersen, T. L.; Dane, A.; Berger, R.; Brenkman, A.; Hankemeier, T.; van Duynhoven, J.; Kalkhoven, E.; Newman, J. W.; Vreeken, R. J. Quantitative profiling of oxylipins through comprehensive LC-MS/MS analysis: application in cardiac surgery. *Anal. Bioanal. Chem.* **2012**, *404*, 1413-1426.
145. Korinek, M.; Tsai, Y. H.; El-Shazly, M.; Lai, K. H.; Backlund, A.; Wu, S. F.; Lai, W. C.; Wu, T. Y.; Chen, S. L.; Wu, Y. C.; Cheng, Y. B.; Hwang, T. L.; Chen, B. H.; Chang, F. R. Anti-allergic hydroxy fatty acids from *Typhonium blumei* explored through ChemGPS-NP. *Front. Pharmacol.* **2017**, *8*.



146. Kuda, O.; Brezinova, M.; Rombaldova, M.; Slavikova, B.; Posta, M.; Beier, P.; Janovska, P.; Veleba, J.; Kopecky, J.; Kudova, E.; Pelikanova, T.; Kopecky, J. Docosahexaenoic acid-derived fatty acid esters of hydroxy fatty acids (FAHFAs) with anti-inflammatory properties. *Diabetes* **2016**, *65*, 3516-3516.
147. See, V. H. L.; Mas, E.; Prescott, S. L.; Beilin, L. J.; Burrows, S.; Barden, A. E.; Huang, R. C.; Mori, T. A. Effects of prenatal *n*-3 fatty acid supplementation on offspring resolvins at birth and 12 years of age: a double-blind, randomised controlled clinical trial. *Br. J. Nutr.* **2017**, *118*, 971-980.
148. Mazur, P.; Nakanishi, K.; Elzayat, A. A. E.; Champe, S. P. Structure and synthesis of sporogenic psi factors from *Aspergillus nidulans*. *J. Chem. Soc., Chem. Commun.* **1991**, 1486-1487.
149. Bowers, W. S.; Hoch, H. C.; Evans, P. H.; Katayama, M. *Thallophytic allelopathy* - Isolation and identification of laetisarinic acid. *Science* **1986**, *232*, 105-106.
150. Scala, V.; Giorni, P.; Cirlini, M.; Ludovici, M.; Visentin, I.; Cardinale, F.; Fabbri, A. A.; Fanelli, C.; Reverberi, M.; Battilani, P.; Galaverna, G.; Dall'Asta, C. LDS1-produced oxylipins are negative regulators of growth, conidiation and fumonisin synthesis in the fungal maize pathogen *Fusarium verticillioides*. *Front. Microbiol.* **2014**, *5*.
151. Waiblinger, K.; Gröger, D. Zur Kenntnis von Alkaloidbildung und Fettsäuregehalt des Mycels in Submerskulturen von *Claviceps*-Arten. *Biochem. Physiol. Pflanz.* **1972**, *163*, 468-476.
152. Křen, V.; Řezanka, T.; Řeháček, Z. Occurrence of ricinoleic acid in submerged cultures of various *Claviceps* sp. *Experientia* **1985**, *41*, 1476-1477.
153. Fischer, G. J.; Keller, N. P. Production of cross-kingdom oxylipins by pathogenic fungi: An update on their role in development and pathogenicity. *J. Microbiol.* **2016**, *54*, 254-264.

154. Powell, R. G.; Smith, C. R.; Wolff, I. A. Geometric configuration and etherification reactions of some naturally occurring 9-hydroxy-10,12- and 13-hydroxy-9,11-octadecadienoic acids. *J. Org. Chem.* **1967**, *32*, 1442-1446.
155. Tallent, W. H.; Harris, J.; Wolff, I. A.; Lundin, R. E. (*R*)-13-hydroxy-*cis*-9, *trans*-11-octadecadienoic acid, the principal fatty acid from *Coriaria nepalensis* Wall. seed oil. *Tetrahedron Lett.* **1966**, *7*, 4329-4334.
156. Ahmad, M. S.; Ahmad, M. U.; Osman, S. M. A new hydroxyolefinic acid from *Plantago* major seed oil. *Phytochemistry* **1980**, *19*, 2137-2139.
157. Mortensen, A.; Aguilar, F.; Crebelli, R.; Di Domenico, A.; Dusemund, B.; Frutos, M. L.; Galtier, P.; Gott, D.; Gundert-Remy, U.; Leblanc, L. C.; Lindtner, O.; Moldeus, P.; Mosesso, P.; Parent-Massin, D.; Oskarsson, A.; Stankovic, I.; Waalkens-Berendsen, I.; Woutersen, R. A.; Wright, M.; Younes, M.; Boon, P.; Chrysafidis, D.; Gurtler, R.; Tobback, P.; Rincon, A. M.; Tard, A.; Lambre, C.; Additives, E. P. F. Re-evaluation of polyglycerol polyricinoleate (E 476) as a food additive. *EFSA J.* **2017**, *15*.
158. Hou, C. T.; Shaw, J. F. *Biocatalysis and agricultural biotechnology*. CRC Press: 2009.
159. Polan, C. E.; McNeill, J. J.; Tove, S. B. Biohydrogenation of unsaturated fatty acids by rumen bacteria. *J. Bacteriol.* **1964**, *88*, 1056-1064.
160. Kishino, S.; Takeuchi, M.; Park, S. B.; Hirata, A.; Kitamura, N.; Kunisawa, J.; Kiyono, H.; Iwamoto, R.; Isobe, Y.; Arita, M.; Arai, H.; Ueda, K.; Shima, J.; Takahashi, S.; Yokozeki, K.; Shimizu, S.; Ogawa, J. Polyunsaturated fatty acid saturation by gut lactic acid bacteria affecting host lipid composition. *Proc. Natl. Acad. Sci. U. S. A.* **2013**, *110*, 17808-17813.
161. Motiuk, K. Wool wax acids: a review. *J. Am. Oil Chem. Soc.* **1979**, *56*, 91-97.

162. Wu, Z.; Shon, J. C.; Kim, J. Y.; Cho, Y.; Liu, K. H. Structural identification of skin ceramides containing omega-hydroxy acyl chains using mass spectrometry. *Arch. Pharmacol Res.* **2016**, *39*, 1426-1432.
163. Blokker, P.; Schouten, S.; Van den Ende, H.; De Leeuw, J. W.; Damste, J. S. S. Cell wall-specific omega-hydroxy fatty acids in some freshwater green microalgae. *Phytochemistry* **1998**, *49*, 691-695.
164. Riederer, M.; Muller, C. *Annual plant Reviews, biology of the plant cuticle*. John Wiley & Sons: 2008; Vol. 23.
165. Lim, G. H.; Singhal, R.; Kachroo, A.; Kachroo, P. Fatty acid- and lipid-mediated signaling in plant defense. *Annu. Rev. Phytopathol.* **2017**, *55*, 505-536.
166. Pollard, M.; Beisson, F.; Li, Y. H.; Ohlrogge, J. B. Building lipid barriers: biosynthesis of cutin and suberin. *Trends Plant Sci.* **2008**, *13*, 236-246.
167. Gupta, S. C.; Gupta, S. S.; Aggarwal, J. S. The component acids of Kamala oil (*Mallotus philippinensis*, Muell. Agr.). *J. Am. Oil Chem. Soc.* **1954**, *31*, 287-289.
168. Aggarwal, J. S. Kamala seed oil. *J. Sci. Food Agric.* **1955**, *6*, 364-368.
169. Zou, A. P.; Fleming, J. T.; Falck, J. R.; Jacobs, E. R.; Gebremedhin, D.; Harder, D. R.; Roman, R. J. 20-HETE is an endogenous inhibitor of the large-conductance  $Ca^{2+}$ -activated  $K^{+}$  channel in renal arterioles. *Am. J. Physiol.: Regul., Integr. Comp. Physiol.* **1996**, *270*, R228-R237.
170. Newman, J. W.; Watanabe, T.; Hammock, B. D. The simultaneous quantification of cytochrome P450 dependent linoleate and arachidonate metabolites in urine by HPLC-MS/MS. *J. Lipid Res.* **2002**, *43*, 1563-1578.

171. Du, L.; Yin, H.; Morrow, J. D.; Strobel, H. W.; Keeney, D. S. 20-Hydroxylation is the CYP-dependent and retinoid-inducible leukotriene B4 inactivation pathway in human and mouse skin cells. *Arch. Biochem. Biophys.* **2009**, *484*, 80-86.
172. Abe, A.; Sugiyama, K. Growth inhibition and apoptosis induction of human melanoma cells by omega-hydroxy fatty acids. *Anticancer drugs* **2005**, *16*, 543-549.
173. Uchida, Y.; Iwamori, M.; Nagai, Y. Activation of keratinization of keratinocytes from fetal-rat skin with N-(O-linoleoyl) omega-hydroxy fatty acyl sphingosyl glucose (lipokeratinogenoside) as a marker of epidermis. *Biochem. Biophys. Res. Commun.* **1990**, *170*, 162-168.
174. Wood, P. L.; Scoggin, K.; Ball, B. A.; Troedsson, M. H.; Squires, E. L. Lipidomics of equine sperm and seminal plasma: Identification of amphiphilic (O-acyl)-omega-hydroxy-fatty acids. **2016**, *86*, 1212-1221.
175. Kaluzikova, A.; Vrkoslav, V.; Harazim, E.; Hoskovec, M.; Plavka, R.; Budesinsky, M.; Bosakova, Z.; Cvacka, J. Cholesteryl esters of omega-(O-acyl)-hydroxy fatty acids in vernix caseosa. *J. Lipid Res.* **2017**, *58*, 1579-1590.
176. Wood, P. L.; Ball, B. A.; Scoggin, K.; Troedsson, M. H.; Squires, E. L. Lipidomics of equine amniotic fluid: Identification of amphiphilic (O-acyl)-omega-hydroxy-fatty acids. *Theriogenology* **2018**, *105*, 120-125.
177. Lam, S. M.; Tong, L.; Duan, X.; Acharya, U. R.; Tan, J. H.; Petznick, A.; Wenk, M. R.; Shui, G. Longitudinal changes in the levels of tear fluid lysophospholipids and O-acyl-omega-hydroxy fatty acids brought about by eyelid-warming treatment in a cohort of Meibomian Gland Dysfunction patients. *J. Lipid Res.* **2014**, jlr. P051185.

178. Loomba, R.; Quehenberger, O.; Armando, A.; Dennis, E. A. Polyunsaturated fatty acid metabolites as novel lipidomic biomarkers for noninvasive diagnosis of nonalcoholic steatohepatitis. *J. Lipid Res.* **2015**, *56*, 185-192.
179. Lynes, M. I.; Leiria, L.; Lundh, M.; Bartelt, A.; Shamsi, F.; Huang, T. L.; Takahashi, H.; Hirshman, M. F.; Schlein, C.; Lee, A.; Baer, L. A.; May, F. J.; Gao, P.; Narain, N. R.; Chen, E. Y.; Kiebish, M. A.; Cypess, A. M.; Bluher, M.; Goodyear, L. J.; Hotamisligil, G. S.; Stanford, K. I.; Tseng, Y. H. The cold-induced lipokine 12,13-diHOME promotes fatty acid transport into brown adipose tissue. *Nat. Med.* **2017**, *23*, 1384-1384.
180. Serhan, C. N. Novel eicosanoid and docosanoid mediators: resolvins, docosatrienes, and neuroprotectins. *Curr. Opin. Clin. Nutr. Metab. Care* **2005**, *8*, 115-121.
181. Liu, M.; Chen, P.; Vericel, E.; Lelli, M.; Beguin, L.; Lagarde, M.; Guichardant, M. Characterization and biological effects of di-hydroxylated compounds deriving from the lipoxygenation of ALA. *J. Lipid Res.* **2013**, *54*, 2083-2094.
182. Levandi, T.; Pussa, T.; Vaher, M.; Toomik, P.; Kaljurand, M. Oxidation products of free polyunsaturated fatty acids in wheat varieties. *Eur. J. Lipid Sci. Technol.* **2009**, *111*, 715-722.
183. Yang, J.; Schmelzer, K.; Georgi, K.; Hammock, B. D. Quantitative profiling method for oxylipin metabolome by liquid chromatography electrospray ionization tandem mass spectrometry. *Anal. Chem.* **2009**, *81*, 8085-8093.
184. Zhang, T.; Chen, S.; Syed, I.; Ståhlman, M.; Kolar, M. J.; Homan, E. A.; Chu, Q.; Smith, U.; Borén, J.; Kahn, B. B.; Saghatelian, A. A liquid chromatography–mass spectrometry-based workflow for measurement of branched fatty acid esters of hydroxy fatty acids (FAHFAs). *Nat. Protoc.* **2016**, *11*, 747-763.

185. Yuan, Z. X.; Rapoport, S. I.; Soldin, S. J.; Remaley, A. T.; Taha, A. Y.; Kellom, M.; Gu, J.; Sampson, M.; Ramsden, C. E. Identification and profiling of targeted oxidized linoleic acid metabolites in rat plasma by quadrupole time-of-flight mass spectrometry. *Biomed. Chromatogr.* **2013**, *27*, 422-432.
186. Christie, W. W. Preparation of lipid extracts from tissues. In *Advances in lipid methodology*, 1993; Vol. 2, pp 195-213.
187. Anderson, G. E. Edible oil processing: solvent extraction. <https://lipidlibrary.aocs.org/edible-oil-processing/solvent-extraction> (accessed February 4th, 2020).
188. Reichardt, C.; Welton, T. *Solvents and solvent effects in organic chemistry*. John Wiley & Sons: 2011.
189. Smallwood, I. M. *Handbook of organic solvent properties*. Arnold; Halsted Press: London; New York, 1996.
190. Dasari, S. R.; Goud, V. V. Comparative extraction of castor seed oil using polar and non polar solvents. *Int. J. Curr. Eng. Technol.* **2013**, *1*, 121-123.
191. Black, B. A.; Sun, C. X.; Zhao, Y. Y.; Gänzle, M. G.; Curtis, J. M. Antifungal lipids produced by *Lactobacilli* and their structural identification by normal phase LC/atmospheric pressure photoionization-MS/MS. *J. Agr. Food Chem.* **2013**, *61*, 5338-5346.
192. Graveland, A. Analysis of lipoxygenase nonvolatile reaction products of linoleic acid in aqueous cereal suspensions by urea extraction and gas chromatography. *Lipids* **1973**, *8*, 599-605.
193. Burgal, J.; Shockey, J.; Lu, C. F.; Dyer, J.; Larson, T.; Graham, I.; Browse, J. Metabolic engineering of hydroxy fatty acid production in plants: RcDGAT2 drives dramatic increases in ricinoleate levels in seed oil. *Plant Biotechnol. J.* **2008**, *6*, 819-831.

194. Dufour, C.; Loonis, M. Regio- and stereoselective oxidation of linoleic acid bound to serum albumin: identification by ESI-mass spectrometry and NMR of the oxidation products. *Chem. Phys. Lipids* **2005**, *138*, 60-68.
195. Levison, B. S.; Zhang, R. L.; Wang, Z. N.; Fu, X. M.; DiDonato, J. A.; Hazen, S. L. Quantification of fatty acid oxidation products using online high-performance liquid chromatography tandem mass spectrometry. *Free Radical Bio. Med.* **2013**, *59*, 2-13.
196. Kimura, H.; Yokota, K. Characterization of metabolic pathway of linoleic acid 9-hydroperoxide in cytosolic fraction of potato tubers and identification of reaction products. *Appl. Biochem. Biotechnol.* **2004**, *118*, 115-132.
197. Xia, W.; Budge, S. M. GC-MS characterization of hydroxy fatty acids generated from lipid oxidation in vegetable oils. *Eur. J. Lipid Sci. Technol.* **2018**, *120*.
198. Diamond, M. J.; Knowles, R. E.; Binder, R. G.; Goldblatt, L. A. Hydroxy unsaturated oils. II. Preparation and characterization of methyl dimorphocolate and methyl lesquerolate from *Dimorphotheca* and *Lesquerella* oils. *J. Am. Oil Chem. Soc.* **1964**, *41*, 430-433.
199. Charlie, S. Chemistry of fatty acids. In *Bailey's Industrial Oil and Fat Products*, Shahidi, F., Ed. Scottish crop research institute: Dundee, Scotland, 2005.
200. Jin, Q. D.; Yu, C. H. The component acids of seed fats of *Coriaria sinica* Maxim. *Acta Bot. Yunnanica* **1980**, *2*, 228-229.
201. Macmurray, T. A.; Morrison, W. R. Composition of wheat-flour lipids. *J. Sci. Food Agric.* **1970**, *21*, 520-528.
202. Hostettmann, K.; Marston, A.; Hostettmann, M. *Preparative chromatography techniques*. Springer: 1986.

203. Frankel, E. N.; Evans, C. D.; McConnell, D. G.; Jones, E. P. Analyses of lipids and oxidation products by partition chromatography - fatty acid hydroperoxides. *J. Am. Oil Chem. Soc.* **1961**, *38*, 134-137.
204. Chen, J. Z.; Green-Church, K. B.; Nichols, K. K. Shotgun lipidomic analysis of human meibomian gland secretions with electrospray ionization tandem mass spectrometry. *Invest. Ophthalmol. Visual Sci.* **2010**, *51*, 6220-6231.
205. Byrdwell, W. C.; Neff, W. E. Analysis of hydroxy-containing seed oils using atmospheric pressure chemical ionization mass spectrometry. *J. Liq. Chromatogr. Relat. Technol.* **1998**, *21*, 1485-1501.
206. Lin, J. T.; Chen, G. Q. Quantification of the molecular species of TAG and DAG in *Lesquerella (Physaria fendleri)* oil by HPLC and MS. *J. Am. Oil Chem. Soc.* **2014**, *91*, 1417-1424.
207. Lin, J. T.; Arcinas, A.; Harden, L. A. Identification of acylglycerols containing dihydroxy fatty acids in castor oil by mass spectrometry. *Lipids* **2009**, *44*, 359-365.
208. Lin, J. T.; Chen, G. Q. Acylglycerols containing trihydroxy fatty acids in castor oil and the regiospecific quantification of triacylglycerols. *J. Am. Oil Chem. Soc.* **2010**, *87*, 1371-1379.
209. Bartle, K. D.; Myers, P. History of gas chromatography. *TrAC, Trends Anal. Chem.* **2002**, *21*, 547-557.
210. Christie, W. W. *Lipid analysis: isolation, separation, identification and structural analysis of lipids*. Oily Press: Bridgwater, England, 2003.
211. Christie, W. W. *Gas chromatography and lipids: a practical guide*. The Oily Press: Dundee, Scotland, 1989; pp 66-69.



212. Moss, C. W.; Shinoda, T.; Samuels, J. W. Determination of cellular fatty acid compositions of various yeasts by gas-liquid chromatography. *J. Clin. Microbiol.* **1982**, *16*, 1073-1079.
213. Kishimoto, Y.; Radin, N. S. Occurrence of 2-hydroxy fatty acids in animal tissues. *J Lipid Res* **1963**, *4*, 139-143.
214. Camp, R. D. R.; Mallet, A. I.; Woollard, P. M.; Brain, S. D.; Black, A. K.; Greaves, M. W. The identification of hydroxy fatty acids in psoriatic skin. *Prostaglandins* **1983**, *26*, 431-447.
215. Ozen, H. C.; Bashan, M.; Toker, Z.; Keskin, C. 3-Hydroxy fatty acids from the flowers of *Hypericum lysimachioides* var. *lysimachioides*. *Turk. J. Chem.* **2004**, *28*, 223-226.
216. Hübschmann, H. J. *Handbook of GC-MS : fundamentals and applications*. 3rd ed. John Wiley & Sons: 2015.
217. Roessner, U., and Dias, D. A. *Metabolomics tools for natural product discovery: methods and protocols*. 2013; Vol. 1055, pp 1-311.
218. Schneider, S.; Wubbolts, M. G.; Sanglard, D.; Witholt, B. Production of chiral hydroxy long chain fatty acids by whole cell biocatalysis of pentadecanoic acid with an *E. coli* recombinant containing cytochrome P450(BM-3) monooxygenase. *Tetrahedron: Asymmetry* **1998**, *9*, 2833-2844.
219. Miller, L. T. Single derivatization method for routine analysis of bacterial whole-cell fatty acid methyl esters, including hydroxy acids. *J. Clin. Microbiol.* **1982**, *16*, 584-586.
220. Lamoureux, G.; Agüero, C. A comparison of several modern alkylating agents. *Arkivoc* **2009**, 251-264.
221. Morrison, W. R.; Smith, L. M. Preparation of fatty acid methyl esters and dimethylacetals from lipids with boron fluoride-methanol. *J. Lipid Res.* **1964**, *5*, 600-608.

222. Kramer, J. K. C.; Fellner, V.; Dugan, M. E. R.; Sauer, F. D.; Mossoba, M. M.; Yurawecz, M. P. Evaluating acid and base catalysts in the methylation of milk and rumen fatty acids with special emphasis on conjugated dienes and total trans fatty acids. *Lipids* **1997**, *32*, 1219-1228.
223. Smith, C. R.; Wilson, T. L.; Melvin, E. H.; Wolff, I. A. Dimorphecolic acid - a unique hydroxydienoid fatty acid. *J. Am. Chem. Soc.* **1960**, *82*, 1417-1421.
224. Kleiman, R.; Spencer, G. F.; Earle, F. R. Boron trifluoride as catalyst to prepare methyl esters from oils containing unusual acyl groups. *Lipids* **1969**, *4*, 118-122.
225. Ulberth, F.; Kamptner, W. Artifact formation during transmethylation of lipid peroxides. *Anal. Biochem.* **1992**, *203*, 35-38.
226. Christie, W. W. Preparation of ester derivatives of fatty acids for chromatographic analysis. In *Advances in lipid methodology*, 1993; Vol. 2, pp 69-111.
227. Gunstone, F.; Sealy, A. 1101. Fatty acids. Part XII. The acetylenic acids of isano (boleko) oil. *J. Chem. Soc.* **1963**, 5772-5778.
228. Marmesat, S.; Velasco, J.; Dobarganes, M. C. Quantitative determination of epoxy acids, keto acids and hydroxy acids formed in fats and oils at frying temperatures. *J. Chromatogr. A* **2008**, *1211*, 129-134.
229. Ngan, F.; Toofan, M. Modification of preparation of diazomethane for methyl esterification of environmental samples analysis by gas-chromatography. *J. Chromatogr. Sci.* **1991**, *29*, 8-10.
230. Struempel, M.; Ondruschka, B.; Daute, R.; Stark, A. Making diazomethane accessible for R&D and industry: generation and direct conversion in a continuous micro-reactor set-up. *Green Chem.* **2008**, *10*, 41-43.

231. Presser, A.; Hufner, A. Trimethylsilyldiazomethane - A mild and efficient reagent for the methylation of carboxylic acids and alcohols in natural products. *Monatsh. Chem.* **2004**, *135*, 1015-1022.
232. Manini, P.; Camera, E.; Picardo, M.; Napolitano, A.; d'Ischia, M. Free radical oxidation of coriolic acid (13-(*S*)-hydroxy-9*Z*, 11*E*-octadecadienoic acid). *Chem. Phys. Lipids* **2005**, *134*, 161-171.
233. Napolitano, A.; Camera, E.; Picardo, M.; d'Ischia, M. Reactions of hydro(pero)xy derivatives of polyunsaturated fatty acids/esters with nitrite ions under acidic conditions. Unusual nitrosative breakdown of methyl 13-hydro(pero)xyoctadeca-9,11-dienoate to a novel 4-nitro-2-oximinoalk-3-enal product. *J. Org. Chem.* **2002**, *67*, 1125-1132.
234. Fox, S. R.; Akpinar, A.; Prabhune, A. A.; Friend, J.; Ratledge, C. The biosynthesis of oxylipins of linoleic and arachidonic acids by the sewage fungus *Leptomitus lacteus*, including the identification of 8*R*-hydroxy-9*Z*,12*Z*-octadecadienoic acid. *Lipids* **2000**, *35*, 23-30.
235. Morris, L. J.; Holman, R. T.; Fontell, K. Alteration of some long-chain esters during gas-liquid chromatography. *J. Lipid Res.* **1960**, *1*, 412-420.
236. Thomas, D. W.; Vankuijk, F. J. G. M.; Dratz, E. A.; Stephens, R. J. Quantitative determination of hydroxy fatty acids as an indicator of *in vivo* lipid peroxidation: gas-chromatography mass-spectrometry methods. *Anal. Biochem.* **1991**, *198*, 104-111.
237. Parker, J. H.; Smith, G. A.; Fredrickson, H. L.; Vestal, J. R.; White, D. C. Sensitive assay, based on hydroxy fatty acids from lipopolysaccharide lipid A, for Gram-negative bacteria in sediments. *Appl. Environ. Microbiol.* **1982**, *44*, 1170-1177.
238. Kuo, T. M.; Nakamura, L. K. Diversity of oleic acid, ricinoleic acid and linoleic acid conversions among *Pseudomonas aeruginosa* strains. *Curr. Microbiol.* **2004**, *49*, 261-266.

239. Halket, J. M.; Zaikin, V. G. Derivatization in mass spectrometry-1. Silylation. *Eur. J. Mass Spectrom.* **2003**, *9*, 1-21.
240. Little, J. L. Artifacts in trimethylsilyl derivatization reactions and ways to avoid them. *J. Chromatogr. A* **1999**, *844*, 1-22.
241. van Kuijk, F. J.; Thomas, D. W.; Stephens, R. J.; Dratz, E. A. Gas chromatography-mass spectrometry method for determination of phospholipid peroxides; I. Transesterification to form methyl esters. *J. Free Radicals Biol. Med.* **1985**, *1*, 215-225.
242. Christie, W. W. The LipidHome. <http://www.lipidhome.co.uk/> (accessed June 19, 2018).
243. Kleiman, R.; Spencer, G. F. Gas chromatography-mass spectrometry of methyl esters of unsaturated oxygenated fatty acids. *J. Am. Oil Chem. Soc.* **1973**, *50*, 31-38.
244. Richter, W.; Burlingame, A. New evidence for the electron-impact induced migration of trimethylsilyl substituents. *Chem. Commun. (London)* **1968**, 1158-1160.
245. Wheelan, P.; Zirrolli, J. A.; Murphy, R. C. Analysis of hydroxy fatty acids as pentafluorobenzyl ester, trimethylsilyl ether derivatives by electron ionization gas chromatography-mass spectrometry. *J. Am. Soc. Mass Spectrom.* **1995**, *6*, 40-51.
246. Ryhage, R.; Stenhagen, E. Mass spectrometric studies. 6. methyl esters of normal chain oxo-acids, hydroxy-acids, methoxy-acids and epoxy-acids. *Arkiv for kemi* **1960**, *15*, 545-560.
247. Tulloch, A. P. Mass spectra of pyrrolidides of oxo, hydroxy and trimethylsilyloxy octadecanoic acids. *Lipids* **1985**, *20*, 652-663.
248. Fay, L.; Richli, U. Location of double bonds in polyunsaturated fatty acids by gas chromatography-mass spectrometry after 4,4-dimethyloxazoline derivatization. *J. Chromatogr.* **1991**, *541*, 89-98.

249. Bucek, A.; Matouskova, P.; Sychrova, H.; Pichova, I.; Hruskova-Heidingsfeldova, O. Delta 12-fatty acid desaturase from *Candida parapsilosis* is a multifunctional desaturase producing a range of polyunsaturated and hydroxylated fatty acids. *Plos One* **2014**, *9*.
250. Meesapyodsuk, D.; Qiu, X. An oleate hydroxylase from the fungus *Claviceps purpurea*: Cloning, functional analysis, and expression in *Aarabidopsis*. *Plant Physiol.* **2008**, *147*, 1325-1333.
251. Smith, M. A.; Zhang, H. X.; Forseille, L.; Purves, R. W. Characterization of novel triacylglycerol estolides from the seed oil of *Mallotus philippensis* and *Trewia nudiflora*. *Lipids* **2013**, *48*, 75-85.
252. Spitzer, V. GC-MS characterization (chemical ionization and electron-impact modes) of the methyl esters and oxazoline derivatives of cyclopropenoid fatty acids. *J. Am. Oil Chem. Soc.* **1991**, *68*, 963-969.
253. Zhang, J. Y.; Yu, Q. T.; Yang, Y. M.; Huang, Z. H. Chemical modification in mass spectrometry. Part 11. Mass spectra of 4, 4-dimethyloxazoline derivatives of hydroxy fatty acids. *ChemInform* **1989**, *20*.
254. Spitzer, V. Structure analysis of fatty acids by gas chromatography--low resolution electron impact mass spectrometry of their 4,4-dimethyloxazoline derivatives--a review. *Prog. Lipid Res.* **1996**, *35*, 387-408.
255. Harvey, D. J. Picolinyl derivatives for the structural determination of fatty acids by mass-spectrometry: applications to polyenoic acids, hydroxy acids, di-acids and related compounds. *Biomed. Mass Spectrom.* **1984**, *11*, 340-347.

256. Capella, P.; Zorzut, C. M. Determination of double bond position in monounsaturated fatty acid esters by mass spectrometry of their trimethylsilyloxy derivatives. *Anal. Chem.* **1968**, *40*, 1458-1463.
257. Ratnayake, W. M. N. Overview of methods for the determination of trans fatty acids by gas chromatography, silver-ion thin-layer chromatography, silver-ion liquid chromatography, and gas chromatography/mass spectrometry. *J. AOAC Int.* **2004**, *87*, 523-539.
258. Christie, W. W.; Sébédio, J. L.; Juanéda, P. A practical guide to the analysis of conjugated linoleic acid (CLA). *Inform* **2001**, *12*, 147-152.
259. Eulitz, K.; Yurawecz, M. P.; Sehat, N.; Fritsche, J.; Roach, J. A. G.; Mossoba, M. M.; Kramer, J. K. G.; Adlof, R. O.; Ku, Y. Preparation, separation, and confirmation of the eight geometrical *cis/trans* conjugated linoleic acid isomers 8,10-through 11,13–18:2. *Lipids* **1999**, *34*, 873-877.
260. Serhan, C. N.; Clish, C. B.; Brannon, J.; Colgan, S. P.; Chiang, N.; Gronert, K. Novel functional sets of lipid-derived mediators with antiinflammatory actions generated from omega-3 fatty acids via cyclooxygenase 2–nonsteroidal antiinflammatory drugs and transcellular processing. *J. Exp. Med.* **2000**, *192*, 1197-1204.
261. Dale, J. A.; Mosher, H. S. Nuclear magnetic resonance enantiomer reagents. Configurational correlations via nuclear magnetic resonance chemical shifts of diastereomeric mandelate, O-methylmandelate, and alpha-methoxy-alpha-trifluoromethylphenylacetate (MTPA) esters. *J. Am. Chem. Soc.* **1973**, *95*, 512-519.
262. Gradowska, W.; Larsson, L. Determination of absolute configurations of 2-hydroxy and 3-hydroxy fatty acids in organic dust by gas chromatography mass-spectrometry. *J. Microbiol. Methods* **1994**, *20*, 55-67.

263. Schurig, V. Enantiomer separation by gas chromatography on chiral stationary phases. *J. Chromatogr. A* **1994**, *666*, 111-129.
264. Sonesson, A.; Larsson, L.; Fox, A.; Westerdahl, G.; Odham, G. Determination of environmental levels of peptidoglycan and lipopolysaccharide using gas chromatography with negative-ion chemical-ionization mass spectrometry utilizing bacterial amino acids and hydroxy fatty acids as biomarkers. *J. Chromatogr. B: Biomed. Sci. Appl.* **1988**, *431*, 1-15.
265. Nithipatikom, K.; Grall, A. J.; Holmes, B. B.; Harder, D. R.; Falck, J. R.; Campbell, W. B. Liquid chromatographic-electrospray ionization-mass spectrometric analysis of cytochrome P450 metabolites of arachidonic acid. *Anal. Biochem.* **2001**, *298*, 327-336.
266. Johnson, D. W. Contemporary clinical usage of LC/MS: Analysis of biologically important carboxylic acids. *Clin. Biochem.* **2005**, *38*, 351-361.
267. Bollinger, J. G.; Rohan, G.; Sadilek, M.; Gelb, M. H. LC/ESI-MS/MS detection of FAs by charge reversal derivatization with more than four orders of magnitude improvement in sensitivity. *J. Lipid Res.* **2013**, *54*, 3523-3530.
268. Zehethofer, N.; Pinto, D. M.; Volmer, D. A. Plasma free fatty acid profiling in a fish oil human intervention study using ultra-performance liquid chromatography/electrospray ionization tandem mass spectrometry. *Rapid Commun. Mass Spectrom.* **2008**, *22*, 2125-2133.
269. Tie, C.; Hu, T.; Jia, Z. X.; Zhang, J. L. Automatic identification approach for high-performance liquid chromatography-multiple reaction monitoring fatty acid global profiling. *Anal. Chem.* **2015**, *87*, 8181-8185.
270. Masoodi, M.; Mir, A. A.; Petasis, N. A.; Serhan, C. N.; Nicolaou, A. Simultaneous lipidomic analysis of three families of bioactive lipid mediators leukotrienes, resolvins,

protectins and related hydroxy fatty acids by liquid chromatography/electrospray ionisation tandem mass spectrometry. *Rapid Commun. Mass Spectrom.* **2008**, *22*, 75-83.

271. Aveldano, M. I.; Vanrollins, M.; Horrocks, L. A. Separation and quantitation of free fatty-acids and fatty-acid methyl-esters by reverse phase high-pressure liquid-chromatography. *J. Lipid Res.* **1983**, *24*, 83-93.

272. Sud, M.; Fahy, E.; Cotter, D.; Brown, A.; Dennis, A. E.; Glass, K. C.; Merrill, H. A.; Murphy, C. J. R.; Raetz, R. H. C.; Russell, W. D.; Subramaniam, S. LMSD: LIPID MAPS structure database, *Nucleic Acids Res.*, **2006**, *35*, D527–D532.

273. Nikolova-Damyanova, B. Silver ion chromatography and lipids. In *Advances in Lipid Methodology-One*, 1992; pp 181-237.

274. Andre, J. C.; Funk, M. O. Determination of stereochemistry in the fatty acid hydroperoxide products of lipoxygenase catalysis. *Anal. Biochem.* **1986**, *158*, 316-321.

275. Myrdal, P. B.; Angersbach, B. S.; Karlage, K.; Kuehl, P. J. Chiral separation of lipoxygenase metabolites utilizing high-performance liquid chromatography. *J. Chromatogr. A* **2006**, *1132*, 315-319.

276. Beuerle, T.; Schwab, W. Metabolic profile of linoleic acid in stored apples: Formation of 13(*R*)-hydroxy-9(*Z*),11(*E*)-octadecadienoic acid. *Lipids* **1999**, *34*, 375-380.

277. Takagi, T.; Itabashi, Y.; Tsuda, T. High-performance liquid chromatographic separation of 2-hydroxy fatty acid enantiomers on a chiral slurry-packed capillary column. *J. Chromatogr. Sci.* **1989**, *27*, 574-577.

278. Lee, H.-R.; Kochhar, S.; Shim, S.-M. Comparison of electrospray ionization and atmospheric chemical ionization coupled with the liquid chromatography-tandem mass spectrometry for the analysis of cholesteryl esters. *Int. J. Anal. Chem.* **2015**, *2015*, 6.



279. Cai, S. S.; Syage, J. A. Comparison of atmospheric pressure photoionization, atmospheric pressure chemical ionization, and electrospray ionization mass spectrometry for analysis of lipids. *Anal. Chem.* **2006**, *78*, 1191-1199.
280. Ikeda, M.; Kusaka, T. Liquid chromatography-mass spectrometry of hydroxy and non-hydroxy fatty acids as amide derivatives. *J. Chromatogr., Biomed. Appl.* **1992**, *575*, 197-205.
281. Lee, S. H.; Williams, M. V.; DuBois, R. N.; Blair, I. A. Targeted lipidomics using electron capture atmospheric pressure chemical ionization mass spectrometry. *Rapid Commun. Mass Spectrom.* **2003**, *17*, 2168-2176.
282. Lee, S. H.; Williams, M. V.; Blair, I. A. Targeted chiral lipidomics analysis. *Prostaglandins Other Lipid Mediators* **2005**, *77*, 141-157.
283. Lee, S. H.; Blair, I. A. Targeted chiral lipidomics analysis of bioactive eicosanoid lipids in cellular systems. *BMB Rep.* **2009**, *42*, 401-410.
284. Murphy, R. C. Chapter 1 - Fatty acids. In *Tandem mass spectrometry of lipids: molecular analysis of complex lipids*, The Royal Society of Chemistry: United Kingdom, 2015; pp 1-39.
285. Wheelan, P.; Zirrolli, J. A.; Murphy, R. C. Electrospray ionization and low energy tandem mass spectrometry of polyhydroxy unsaturated fatty acids. *J. Am. Soc. Mass Spectrom.* **1996**, *7*, 140-149.
286. Wheelan, P.; Zirrolli, J. A.; Murphy, R. C. Low-energy fast atom bombardment tandem mass spectrometry of monohydroxy substituted unsaturated fatty acids. *Biol. Mass Spectrom.* **1993**, *22*, 465-473.
287. Wang, X.; Chen, J.; Xu, J.; Chen, H.; Yan, X.; Zhou, C. Quantitative analysis of oxylipins in *Laminaria japonica* by LC-MS. *Yaowu Fenxi Zazhi (Chin. J. Pharm. Anal)* **2013**, *33*, 1656-1664.

288. Criegee, R. Mechanism of ozonolysis. *Angew. Chem. Int. Ed. Engl.* **1975**, *14*, 745-752.
289. Sun, C. X.; Zhao, Y. Y.; Curtis, J. M. The direct determination of double bond positions in lipid mixtures by liquid chromatography/in-line ozonolysis/mass spectrometry. *Anal. Chim. Acta* **2013**, *762*, 68-75.
290. Sun, C.; Black, B. A.; Zhao, Y. Y.; Gänzle, M. G.; Curtis, J. M. Identification of conjugated linoleic acid (CLA) isomers by silver ion-liquid chromatography/in-line ozonolysis/mass spectrometry ( $\text{Ag}^+$ -LC/ $\text{O}_3$ -MS). *Anal. Chem.* **2013**, *85*, 7345-7352.
291. Harris, R. A.; May, J. C.; Stinson, C. A.; Xia, Y.; McLean, J. A. Determining double bond position in lipids using online ozonolysis coupled to liquid chromatography and ion mobility-mass spectrometry. *Anal. Chem.* **2018**, *90*, 1915-1924.
292. Murphy, R. C.; Okuno, T.; Johnson, C. A.; Barkleyte, R. M. Determination of double bond positions in polyunsaturated fatty acids using the photochemical Paterno-Buchi reaction with acetone and tandem mass spectrometry. *Anal. Chem.* **2017**, *89*, 8545-8553.
293. Han, X. *Lipidomics: Comprehensive mass spectrometry of lipids*. John Wiley & Sons: 2016.
294. Dumlao, D. S.; Buczynski, M. W.; Norris, P. C.; Harkewicz, R.; Dennis, E. A. High-throughput lipidomic analysis of fatty acid derived eicosanoids and N-acyl ethanolamines. *Biochim. Biophys. Acta, Mol. Cell Biol. Lipids* **2011**, *1811*, 724-736.
295. Hu, C. F.; Wang, M.; Han, X. L. Shotgun lipidomics in substantiating lipid peroxidation in redox biology: Methods and applications. *Redox Biol.* **2017**, *12*, 946-955.
296. Lopez-Bascon, M. A.; Calderon-Santiago, M.; Priego-Capote, F. Confirmatory and quantitative analysis of fatty acid esters of hydroxy fatty acids in serum by solid phase extraction

- coupled to liquid chromatography tandem mass spectrometry. *Anal. Chim. Acta* **2016**, *943*, 82-88.
297. Sun, C.; Curtis, J. M. Locating double bonds in lipids—New approaches to the use of ozonolysis. *Lipid Technol.* **2013**, *25*, 279-282.
298. Magnusson, J.; Strom, K.; Roos, S.; Sjogren, J.; Schnurer, J. Broad and complex antifungal activity among environmental isolates of lactic acid bacteria. *FEMS Microbiol. Lett.* **2003**, *219*, 129-135.
299. Hou, C. T.; Forman, R. J. Growth inhibition of plant pathogenic fungi by hydroxy fatty acids. *J. Ind. Microbiol. Biot.* **2000**, *24*, 275-276.
300. Hou, C. T. New bioactive fatty acids. *Asia Pac. J. Clin. Nutr.* **2008**, *17*, 192-195.
301. Kil, K. S.; Cunningham, M. W.; Barnett, L. A. Cloning and sequence-analysis of a gene encoding a 67-kilodalton myosin-cross-reactive antigen of *Streptococcus pyogenes* reveals its similarity with class-II major histocompatibility antigens. *Infect. Immun.* **1994**, *62*, 2440-2449.
302. Koritala, S.; Bagby, M. O. Microbial conversion of linoleic and linolenic acids to unsaturated hydroxy fatty acids. *J. Am. Oil. Chem. Soc.* **1992**, *69*, 575-578.
303. Rosberg-Cody, E.; Liavonchanka, A.; Göbel, C.; Ross, R. P.; O'Sullivan, O.; Fitzgerald, G. F.; Feussner, I.; Stanton, C. Myosin-cross-reactive antigen (MCRA) protein from *Bifidobacterium breve* is a FAD-dependent fatty acid hydratase which has a function in stress protection. *BMC Biochem.* **2011**, *12*.
304. Yang, B.; Chen, H. Q.; Song, Y. D.; Chen, Y. Q.; Zhang, H.; Chen, W. Myosin-cross-reactive antigens from four different lactic acid bacteria are fatty acid hydratases. *Biotechnol. Lett.* **2013**, *35*, 75-81.

305. Volkov, A.; Khoshnevis, S.; Neumann, P.; Herrfurth, C.; Wohlwend, D.; Ficner, R.; Feussner, I. Crystal structure analysis of a fatty acid double-bond hydratase from *Lactobacillus acidophilus*. *Acta Crystallogr. D Biol. Crystallogr.* **2013**, *69*, 648-657.
306. Kim, K. R.; Oh, H. J.; Park, C. S.; Hong, S. H.; Park, J. Y.; Oh, D. K. Unveiling of novel regio-selective fatty acid double bond hydratases from *Lactobacillus acidophilus* involved in the selective oxyfunctionalization of mono- and di-hydroxy fatty acids. *Biotechnol. Bioeng.* **2015**, *112*, 2206-2213.
307. Park, J. Y.; Lee, S. H.; Kim, K. R.; Park, J. B.; Oh, D. K. Production of 13*S*-hydroxy-9(*Z*)-octadecenoic acid from linoleic acid by whole recombinant cells expressing linoleate 13-hydratase from *Lactobacillus acidophilus*. *J. Biotechnol.* **2015**, *208*, 1-10.
308. O'Flaherty, S. J.; Klaenhammer, T. R. Functional and phenotypic characterization of a protein from *Lactobacillus acidophilus* involved in cell morphology, stress tolerance and adherence to intestinal cells. *Microbiology* **2010**, *156*, 3360-3367.
309. Kishino, S.; Park, S. B.; Takeuchi, M.; Yokozeki, K.; Shimizu, S.; Ogawa, J. Novel multi-component enzyme machinery in lactic acid bacteria catalyzing C=C double bond migration useful for conjugated fatty acid synthesis. *Biochem. Biophys. Res. Commun.* **2011**, *416*, 188-193.
310. Zheng, J. S.; Ruan, L. F.; Sun, M.; Gänzle, M. A genomic view of lactobacilli and pediococci demonstrates that phylogeny matches ecology and physiology. *Appl. Environ. Microb.* **2015**, *81*, 7233-7243.
311. Joo, Y. C.; Jeong, K. W.; Yeom, S. J.; Kim, Y. S.; Kim, Y.; Oh, D. K. Biochemical characterization and FAD-binding analysis of oleate hydratase from *Macrococcus caseolyticus*. *Biochimie* **2012**, *94*, 907-15.

312. Su, M. S.; Schlicht, S.; Gänzle, M. G. Contribution of glutamate decarboxylase in *Lactobacillus reuteri* to acid resistance and persistence in sourdough fermentation. *Microb. Cell Fact.* **2011**, *10 Suppl 1*, S8.
313. Molina-Höppner, A.; Doster, W.; Vogel, R. F.; Gänzle, M. G. Protective effect of sucrose and sodium chloride for *Lactococcus lactis* during sublethal and lethal high-pressure treatments. *Appl. Environ. Microbiol.* **2004**, *70*, 2013-2020.
314. Kankaanpää, P.; Yang, B.; Kallio, H.; Isolauri, E.; Salminen, S. Effects of polyunsaturated fatty acids in growth medium on lipid composition and on physicochemical surface properties of lactobacilli. *Appl. Environ. Microbiol.* **2004**, *70*, 129-136.
315. Johnsson, T.; Nikkilä, P.; Toivonen, L.; Rosenqvist, H.; Laakso, S. Cellular fatty acid profiles of *Lactobacillus* and *Lactococcus* strains in relation to the oleic acid content of the cultivation medium. *Appl. Environ. Microbiol.* **1995**, *61*, 4497-4499.
316. Gänzle, M. G.; Hölzel, A.; Walter, J.; Jung, G.; Hammes, W. P. Characterization of reutericyclin produced by *Lactobacillus reuteri* LTH2584. *Appl. Environ. Microbiol.* **2000**, *66*, 4325-4333.
317. Desbois, A. P.; Smith, V. J. Antibacterial free fatty acids: activities, mechanisms of action and biotechnological potential. *Appl. Microbiol. Biotechnol.* **2010**, *85*, 1629-1642.
318. Wyllie, D. H.; Kiss-Toth, E.; Visintin, A.; Smith, S. C.; Boussouf, S.; Segal, D. M.; Duff, G. W.; Dower, S. K. Evidence for an accessory protein function for Toll-like receptor 1 in anti-bacterial responses. *J. Immunol.* **2000**, *165*, 7125-7132.
319. Guerrini, S.; Bastianini, A.; Granchi, L.; Vincenzini, M. Effect of oleic acid on *Oenococcus oeni* strains and malolactic fermentation in wine. *Curr. Microbiol.* **2002**, *44*, 5-9.

320. Jenkins, J. K.; Courtney, P. D. *Lactobacillus* growth and membrane composition in the presence of linoleic or conjugated linoleic acid. *Can. J. Microbiol.* **2003**, *49*, 51-57.
321. Mishra, P.; Prasad, R. Relationship between ethanol tolerance and fatty acyl composition of *Saccharomyces cerevisiae*. *Appl. Microbiol. Biot.* **1989**, *30*, 294-298.
322. O'Connell, K. J.; Motherway, M. O.; Hennessey, A. A.; Brodhun, F.; Ross, R. P.; Feussner, I.; Stanton, C.; Fitzgerald, G. F.; van Sinderen, D. Identification and characterization of an oleate hydratase-encoding gene from *Bifidobacterium breve*. *Bioengineered* **2013**, *4*, 313-321.
323. Bellon-Fontaine, M. N.; Rault, J.; vanOss, C. J. Microbial adhesion to solvents: A novel method to determine the electron-donor/electron-acceptor or Lewis acid-base properties of microbial cells. *Colloid Surface B* **1996**, *7*, 47-53.
324. Rosenberg, M. Microbial adhesion to hydrocarbons: twenty-five years of doing MATH. *FEMS Microbiol. Lett.* **2006**, *262*, 129-134.
325. Pelletier, C.; Bouley, C.; Cayuela, C.; Bouttier, S.; Bourlioux, P.; Bellon-Fontaine, M. N. Cell surface characteristics of *Lactobacillus casei* subsp *casei*, *Lactobacillus paracasei* subsp *paracasei*, and *Lactobacillus rhamnosus* strains. *Appl. Environ. Microb.* **1997**, *63*, 1725-1731.
326. Boonaert, C. J. P.; Rouxhet, P. G. Surface of lactic acid bacteria: Relationships between chemical composition and physicochemical properties. *Appl. Environ. Microb.* **2000**, *66*, 2548-2554.
327. Ly, M. H.; Vo, N. H.; Le, T. M.; Belin, J. M.; Waché, Y. Diversity of the surface properties of lactococci and consequences on adhesion to food components. *Colloid Surface B* **2006**, *52*, 149-153.

328. Muller, J. A.; Ross, R. P.; Sybesma, W. F.; Fitzgerald, G. F.; Stanton, C. Modification of the technical properties of *Lactobacillus johnsonii* NCC 533 by supplementing the growth medium with unsaturated fatty acids. *Appl. Environ. Microbiol.* **2011**, *77*, 6889-6898.
329. Muñoz-Provencio, D.; Llopis, M.; Antolin, M.; de Torres, I.; Guarner, F.; Perez-Martinez, G.; Monedero, V. Adhesion properties of *Lactobacillus casei* strains to resected intestinal fragments and components of the extracellular matrix. *Arch. Microbiol.* **2009**, *191*, 153-161.
330. Walters, D.; Raynor, L.; Mitchell, A.; Walker, R.; Walker, K. Antifungal activities of four fatty acids against plant pathogenic fungi. *Mycopathologia* **2004**, *157*, 87-90.
331. Legan, J. D. Mold spoilage of bread - the problem and some solutions. *Int. Biodeter. Biodegr.* **1993**, *32*, 33-53.
332. Minervini, F.; Celano, G.; Lattanzi, A.; Tedone, L.; De Mastro, G.; Gobbetti, M.; De Angelis, M. Lactic acid bacteria in durum wheat flour are endophytic components of the plant during its entire life cycle. *Appl. Environ. Microb.* **2015**, *81*, 6736-6748.
333. Ellwood, S. R.; Liu, Z. H.; Syme, R. A.; Lai, Z. B.; Hane, J. K.; Keiper, F.; Moffat, C. S.; Oliver, R. P.; Friesen, T. L. A first genome assembly of the barley fungal pathogen *Pyrenophora teres* f. *teres*. *Genome Biol.* **2010**, *11*.
334. Miller, J. D. Mycotoxins in small grains and maize: Old problems, new challenges. *Food Addit. Contam.* **2008**, *25*, 219-230.
335. Dewaard, M. A.; Georgopoulos, S. G.; Hollomon, D. W.; Ishii, H.; Leroux, P.; Ragsdale, N. N.; Schwinn, F. J. Chemical control of plant diseases: problems and prospects. *Annu. Rev. Phytopathol.* **1993**, *31*, 403-421.

336. Tsen, C. C.; Hlynka, I. Flour lipids and oxidation of sulfhydryl groups in dough. *Cereal Chem.* **1963**, *40*, 145.
337. Kato, T.; Yamaguchi, Y.; Hirano, T.; Yokoyama, T.; Uyehara, T.; Namai, T.; Yamanaka, S.; Harada, N. Unsaturated hydroxy fatty-acids, the self defensive substances in rice plant against rice blast disease. *Chem. Lett.* **1984**, *13*, 409-412.
338. Stadler, M.; Mayer, A.; Anke, H.; Sterner, O. Fatty acids and other compounds with nematocidal activity from cultures of Basidiomycetes. *Planta Med.* **1994**, *60*, 128-132.
339. Kobayashi, Y.; Okamoto, S.; Shimazaki, T.; Ochiai, Y.; Sato, F. Synthesis and physiological activities of both enantiomers of coriolic acid and their geometric isomers. *Tetrahedron Lett.* **1987**, *28*, 3959-3962.
340. Nanda, S.; Yadav, J. S. Lipoxygenase biocatalysis: a survey of asymmetric oxygenation. *J. Mol. Catal. B: Enzym.* **2003**, *26*, 3-28.
341. Sim, D. H.; Shin, K. C.; Oh, D. K. 13-Hydroxy-9Z,11E-octadecadienoic acid production by recombinant cells expressing *Burkholderia thailandensis* 13-lipoxygenase. *J. Am. Oil Chem. Soc.* **2015**, *92*, 1259-1266.
342. Kato, T.; Nakai, T.; Ishikawa, R.; Karasawa, A.; Namai, T. Preparation of the enantiomers of hydroxy-C18 fatty acids and their anti-rice blast fungus activities. *Tetrahedron: Asymmetry* **2001**, *12*, 2695-2701.
343. Chen, Y. Y.; Liang, N. Y.; Curtis, J. M.; Gänzle, M. G. Characterization of linoleate 10-hydratase of *Lactobacillus plantarum* and novel antifungal metabolites. *Front. Microbiol.* **2016**, *7*, 1561.
344. Sutherland, I. A. Recent progress on the industrial scale-up of counter-current chromatography. *J. Chromatogr. A* **2007**, *1151*, 6-13.



345. Cao, X. L.; Ito, Y. C. Supercritical fluid extraction of grape seed oil and subsequent separation of free fatty acids by high-speed counter-current chromatography. *J. Chromatogr. A* **2003**, *1021*, 117-124.
346. Li, D. L.; Schroder, M.; Vetter, W. Isolation of 6,9,12,15-hexadecatetraenoic fatty acid (16:4n-1) methyl ester from transesterified fish oil by HSCCC. *Chromatographia* **2012**, *75*, 1-6.
347. Du, Q. Z.; Shu, A. M.; Ito, Y. Purification of fish oil ethyl esters by high-speed countercurrent chromatography using non-aqueous solvent systems. *J. Liq. Chromatogr. Relat. Technol.* **1996**, *19*, 1451-1457.
348. Valcheva, R.; Korakli, M.; Onno, B.; Prevost, H.; Ivanova, I.; Ehrmann, M. A.; Dousset, X.; Gänzle, M. G.; Vogel, R. F. *Lactobacillus hammesii* sp nov., isolated from French sourdough. *Int. J. Syst. Evol. Microbiol.* **2005**, *55*, 763-767.
349. Shahzadi, A. Bio-transformation of fatty acids. University of Alberta, 2012.
350. Ding, L.; Peschel, G.; Hertweck, C. Biosynthesis of archetypal plant self-defensive oxylipins by an endophytic fungus residing in *Mangrove Embryos*. *ChemBioChem* **2012**, *13*, 2661-2664.
351. Nikolaev, V.; Reddanna, P.; Whelan, J.; Hildenbrandt, G.; Reddy, C. C. Stereochemical nature of the products of linoleic acid oxidation catalyzed by lipoxygenases from potato and soybean. *Biochem. Biophys. Res. Commun.* **1990**, *170*, 491-496.
352. Marston, A.; Hostettmann, K. Developments in the application of counter-current chromatography to plant analysis. *J. Chromatogr. A* **2006**, *1112*, 181-194.
353. Cole, G. T. Basic biology of fungi. In *Medical Microbiology*, Baron, S., Ed. Galveston, Texas, 1996.

354. Avis, T. J.; Bélanger, R. R. Specificity and mode of action of the antifungal fatty acid *cis*-9-heptadecenoic acid produced by *Pseudozyma flocculosa*. *Appl. Environ. Microbiol.* **2001**, *67*, 956-960.
355. Granér, G.; Hamberg, M.; Meijer, J. Screening of oxylipins for control of oilseed rape (*Brassica napus*) fungal pathogens. *Phytochemistry* **2003**, *63*, 89-95.
356. Nielsen, P. V.; de Boer, E. Food preservatives against fungi. In *Introduction to food-and airborne fungi*, Samson, R. A.; Hoekstra, E. S.; Frisvad, J. C., Eds.; 2004; pp 357-363.
357. Biermann, U.; Wittmann, A.; Grosch, W. The occurrence of bitter hydroxy fatty acids in oats and wheat. *Fette, Seifen, Anstrichm.* **1980**, *82*, 236-240.
358. Loureiro, V.; Querol, A. The prevalence and control of spoilage yeasts in foods and beverages. *Trends Food Sci. Technol.* **1999**, *10*, 356-365.
359. Vellosillo, T.; Aguilera, V.; Marcos, R.; Bartsch, M.; Vicente, J.; Cascón, T.; Hamberg, M.; Castresana, C. Defense activated by 9-lipoxygenase-derived oxylipins requires specific mitochondrial proteins. *Plant Physiol.* **2013**, *161*, 617-627.
360. Marcos, R.; Izquierdo, Y.; Vellosillo, T.; Kulasekaran, S.; Cascón, T.; Hamberg, M.; Castresana, C. 9-Lipoxygenase-derived oxylipins activate brassinosteroid signaling to promote cell wall-based defense and limit pathogen infection. *Plant Physiol.* **2015**, *169*, 2324-2334.
361. Lacerda, A.; Vasconcelos, É.; Pelegrini, P.; Grossi-de-Sa, M. F. Antifungal defensins and their role in plant defense. *Front. Microbiol.* **2014**, *5*, 116.
362. Farré-Armengol, G.; Filella, I.; Llusia, J.; Peñuelas, J. Bidirectional interaction between phyllospheric microbiotas and plant volatile emissions. *Trends Plant Sci.* **2016**, *21*, 854-860.

363. Pohl, E. E.; Voltchenko, A. M.; Rupprecht, A. Flip-flop of hydroxy fatty acids across the membrane as monitored by proton-sensitive microelectrodes. *Biochim. Biophys. Acta, Biomembr.* **2008**, *1778*, 1292-1297.
364. Adams, B. G.; Parks, L. W. Isolation from yeast of a metabolically active water-soluble form of ergosterol. *J. Lipid Res.* **1968**, *9*, 8-11.
365. Duchateau, G. S. M. J. E.; Janssen, H. G. M.; Louter, A. J. H. Plant sterol analysis in relation to functional foods. In *Phytosterol as Functional Food Components and Nutraceuticals*, Dutta, P. C., Ed. Marcel Dekker, Inc.: New York, 2003; pp 75-132.
366. Sánchez-Maldonado, A. F.; Schieber, A.; Gänzle, M. G. Antifungal activity of secondary plant metabolites from potatoes (*Solanum tuberosum* L.): Glycoalkaloids and phenolic acids show synergistic effects. *J. Appl. Microbiol.* **2016**, *120*, 955-965.
367. Jones, Q.; Earle, F. R. Chemical analyses of seeds II: oil and protein content of 759 species. *Econ. Bot.* **1966**, *20*, 127-155.
368. Gaquerel, E.; Steppuhn, A.; Baldwin, I. T. *Nicotiana attenuata*  $\alpha$ -DIOXYGENASE1 through its production of 2-hydroxylinolenic acid is required for intact plant defense expression against attack from *Manduca sexta* larvae. *New Phytol.* **2012**, *196*, 574-585.
369. Parasassi, T.; Krasnowska, E. K.; Bagatolli, L.; Gratton, E. Laurdan and Prodan as polarity-sensitive fluorescent membrane probes. *J. Fluoresc.* **1998**, *8*, 365-373.
370. Alexandre, H.; Berlot, J. P.; Charpentier, C. Effect of ethanol on membrane fluidity of protoplasts from *Saccharomyces cerevisiae* and *Kloeckera apiculata* grown with or without ethanol, measured by fluorescence anisotropy. *Biotechnol. Tech.* **1994**, *8*, 295-300.

371. Benyagoub, M.; Willemot, C.; Bélanger, R. R. Influence of a subinhibitory dose of antifungal fatty acids from *Sporothrix flocculosa* on cellular lipid composition in fungi. *Lipids* **1996**, *31*, 1077-1082.
372. Dufourc, E. J. Sterols and membrane dynamics. *J. Chem. Biol.* **2008**, *1*, 63-77.
373. Kamp, F.; Hamilton, J. A. pH gradients across phospholipid membranes caused by fast flip-flop of un-ionized fatty acids. *Proc. Natl. Acad. Sci. U. S. A.* **1992**, *89*, 11367-11370.
374. Negelmann, L.; Pisch, S.; Bornscheuer, U.; Schmid, R. D. Properties of unusual phospholipids. III: Synthesis, monolayer investigations and DSC studies of hydroxy octadeca(e)noic acids and diacylglycerophosphocholines derived therefrom. *Chem. Phys. Lipids* **1997**, *90*, 117-134.
375. Ek-von Mentzer, B. A.; Zhang, F. L.; Hamilton, J. A. Binding of 13-HODE and 15-HETE to phospholipid bilayers, albumin, and intracellular fatty acid binding proteins - Implications for transmembrane and intracellular transport and for protection from lipid peroxidation. *J. Biol. Chem.* **2001**, *276*, 15575-15580.
376. Ghannoum, M. A.; Janini, G.; Khamis, L.; Radwan, S. S. Dimorphism-associated variations in the lipid composition of *Candida albicans*. *J. Gen. Microbiol.* **1986**, *132*, 2367-2375.
377. Morozova, E. V.; Kozlov, V. P.; Tereshina, V. M.; Memorskaya, A. S.; Feofilova, E. P. Changes in lipid composition and carbohydrate composition of *Aspergillus niger* conidia during germination. *Appl. Biochem. Microbiol.* **2002**, *38*, 129-133.
378. Shrestha, S. K.; Garzan, A.; Garneau-Tsodikova, S. Novel alkylated azoles as potent antifungals. *Eur. J. Med. Chem.* **2017**, *133*, 309-318.

379. Appleton, G. S.; Kieber, R. J.; Payne, W. J. The sterol content of fungi. II. Screening of representative yeasts and molds for sterol content. *Appl. Microbiol.* **1955**, *3*, 249-251.
380. Kieber, R. J.; Payne, W. J.; Appleton, G. S. The sterol content of fungi. I. Methods for disrupting cells, extracting and determining sterols. *Appl. Microbiol.* **1955**, *3*, 247-248.
381. Hitchcock, C. A.; Barrett-Bee, K. J.; Russell, N. J. The lipid composition of azole-sensitive and azole-resistant strains of *Candida albicans*. *J. Gen. Microbiol.* **1986**, *132*, 2421-2431.
382. Dal Bello, F.; Clarke, C. I.; Ryan, L. A. M.; Ulmer, H.; Schober, T. J.; Ström, K.; Sjögren, J.; van Sinderen, D.; Schnurer, J.; Arendt, E. K. Improvement of the quality and shelf life of wheat bread by fermentation with the antifungal strain *Lactobacillus plantarum* FST 1.7. *J. Cereal Sci.* **2007**, *45*, 309-318.
383. Denyer, S. P.; Baird, R. M. *Guide to microbiological control in pharmaceuticals and medical devices*. 2nd ed.; CRC Press: Boca Raton, Fla., 2006.
384. Belz, M. C. E.; Mairinger, R.; Zannini, E.; Ryan, L. A. M.; Cashman, K. D.; Arendt, E. K. The effect of sourdough and calcium propionate on the microbial shelf-life of salt reduced bread. *Appl. Microbiol. Biot.* **2012**, *96*, 493-501.
385. Gray, J. A.; Bemiller, J. N. Bread staling: molecular basis and control. *Compr. Rev. Food Sci. Food Saf.* **2003**, *2*, 1-21.
386. Smith, J. P.; Daifas, D. P.; El-Khoury, W.; Koukoutsis, J.; El-Khoury, A. Shelf life and safety concerns of bakery products - A review. *Crit. Rev. Food Sci.* **2004**, *44*, 19-55.
387. Salminen, A.; Latva-Kala, K.; Randell, K.; Hurme, E.; Linko, P.; Ahvenainen, R. The effect of ethanol and oxygen absorption on the shelf-life of packed sliced rye bread. *Packag. Technol. Sci.* **1996**, *9*, 29-42.

388. Anonymous. Maple leaf foods food manifesto. <http://mapleleaf.com/our-food-promise/> (accessed 9 May 2018).
389. Anonymous. Transparency and simplicity, clean label consumer study. <https://www.cargill.com/food-beverage/na/clean-label-white-paper-info-page> (accessed 9 May 2018).
390. Gobbetti, M.; Rizzello, C. G.; Di Cagno, R.; De Angelis, M. How the sourdough may affect the functional features of leavened baked goods. *Food Microbiol.* **2014**, *37*, 30-40.
391. Hammes, W. P.; Gänzle, M. G. Sourdough breads and related products. In *Microbiology of Fermented Foods*, Wood, B. J. B., Ed. Springer US: Boston, MA, 1998; pp 199-216.
392. Axel, C.; Zannini, E.; Arendt, E. K. Mold spoilage of bread and its biopreservation: A review of current strategies for bread shelf life extension. *Crit. Rev. Food Sci.* **2017**, *57*, 3528-3542.
393. Quattrini, M.; Bernardi, C.; Stuknyté, M.; Masotti, F.; Passera, A.; Ricci, G.; Vallone, L.; De Noni, I.; Brasca, M.; Fortina, M. G. Functional characterization of *Lactobacillus plantarum* ITEM 17215: A potential biocontrol agent of fungi with plant growth promoting traits, able to enhance the nutritional value of cereal products. *Food Res. Int.* **2018**, *106*, 936-944.
394. Drews, E. Der Einfluß gesteigerter Essigsäurebildung auf die Haltbarkeit des Schrotbrotes. *Brot Gebäck* **1959**, *13*, 113-114.
395. Gerez, C. L.; Torino, M. I.; Rollán, G.; de Valdez, G. F. Prevention of bread mould spoilage by using lactic acid bacteria with antifungal properties. *Food Control* **2009**, *20*, 144-148.

396. Kaditzky, S.; Seitter, M.; Hertel, C.; Vogel, R. F. Performance of *Lactobacillus sanfranciscensis* TMW 1.392 and its levansucrase deletion mutant in wheat dough and comparison of their impact on bread quality. *Eur. Food Res. Technol.* **2008**, *227*, 433-442.
397. Gänzle, M. G. Lactic metabolism revisited: metabolism of lactic acid bacteria in food fermentations and food spoilage. *Curr. Opin. Food Sci.* **2015**, *2*, 106-117.
398. Ryan, L. A. M.; Dal Bello, F.; Czerny, M.; Koehler, P.; Arendt, E. K. Quantification of phenyllactic acid in wheat sourdough using high resolution gas chromatography-mass spectrometry. *J. Agr. Food Chem.* **2009**, *57*, 1060-1064.
399. Nionelli, L.; Pontonio, E.; Gobbetti, M.; Rizzello, C. G. Use of hop extract as antifungal ingredient for bread making and selection of autochthonous resistant starters for sourdough fermentation. *Int. J. Food Microbiol.* **2018**, *266*, 173-182.
400. Rizzello, C. G.; Lavecchia, A.; Gramaglia, V.; Gobbetti, M. Long-term fungal inhibition by *Pisum sativum* flour hydrolysate during storage of wheat flour bread. *Appl. Environ. Microb.* **2015**, *81*, 4195-4206.
401. Rizzello, C. G.; Verni, M.; Bordignon, S.; Gramaglia, V.; Gobbetti, M. Hydrolysate from from a mixture of legume flours with antifungal activity as an ingredient for prolonging the shelf-life of wheat bread. *Food Microbiol.* **2017**, *64*, 72-82.
402. Ryan, L. A. M.; Dal Bello, F.; Arendt, E. K. The use of sourdough fermented by antifungal LAB to reduce the amount of calcium propionate in bread. *Int. J. Food Microbiol.* **2008**, *125*, 274-278.
403. Valcheva, R.; Korakli, M.; Onno, B.; Prevost, H.; Ivanova, I.; Ehrmann, M. A.; Dousset, X.; Gänzle, M. G.; Vogel, R. F. *Lactobacillus hammesii* sp nov., isolated from French sourdough. *Int. J. Syst. Evol. Microbiol.* **2005**, *55*, 763-767.

404. Decimo, M.; Quattrini, M.; Ricci, G.; Fortina, M. G.; Brasca, M.; Silvetti, T.; Manini, F.; Erba, D.; Criscuoli, F.; Casiraghi, M. C. Evaluation of microbial consortia and chemical changes in spontaneous maize bran fermentation. *AMB Express* **2017**, *7*.
405. Gänzle, M. G.; Hertel, C.; Hammes, W. P. Resistance of *Escherichia coli* and *Salmonella* against nisin and curvacin A. *Int. J. Food Microbiol.* **1999**, *48*, 37-50.
406. Sirot, V.; Fremy, J. M.; Leblanc, J. C. Dietary exposure to mycotoxins and health risk assessment in the second French total diet study. *Food Chem. Toxicol.* **2013**, *52*, 1-11.
407. Ryan, L. A. M.; Zannini, E.; Dal Bello, F.; Pawlowska, A.; Koehler, P.; Arendt, E. K. *Lactobacillus amylovorus* DSM 19280 as a novel food-grade antifungal agent for bakery products. *Int. J. Food Microbiol.* **2011**, *146*, 276-283.
408. Axel, C.; Röcker, B.; Brosnan, B.; Zannini, E.; Furey, A.; Coffey, A.; Arendt, E. K. Application of *Lactobacillus amylovorus* DSM19280 in gluten-free sourdough bread to improve the microbial shelf life. *Food Microbiol.* **2015**, *47*, 36-44.
409. Lind, H.; Jonsson, H.; Schnürer, J. Antifungal effect of dairy propionibacteria - contribution of organic acids. *Int. J. Food Microbiol.* **2005**, *98*, 157-165.
410. Stratford, M.; Eklund, T. Organic acids and esters. In *Food Preservatives*, Russell, N. J.; Gould, G. W., Eds.; Springer US: Boston, MA, 2003; pp 48-84.
411. Joint Food and Agriculture Organization (FAO)/World Health Organization (WHO) Expert Committee on Food Additives. Final report on the safety assessment of *Ricinus communis* (castor) seed oil, hydrogenated castor oil, glyceryl ricinoleate, glyceryl ricinoleate se, ricinoleic acid, potassium ricinoleate, sodium ricinoleate, zinc ricinoleate, cetyl ricinoleate, ethyl ricinoleate, glycol ricinoleate, isopropyl ricinoleate, methyl ricinoleate, and octyldodecyl ricinoleate. *Int. J. Toxicol.* **2007**, *26 (Suppl. 3)*, 31-77.



412. Burdock, G. A.; Carabin, I. G.; Griffiths, J. C. Toxicology and pharmacology of sodium ricinoleate. *Food Chem. Toxicol.* **2006**, *44*, 1689-1698.
413. Stolz, P.; Vogel, R. F.; Hammes, W. P. Utilization of electron acceptors by lactobacilli isolated from sourdough .2. *Lactobacillus pontis*, *L. reuteri*, *L. amylovorus*, and *L. fermentum*. *Z. Lebensm. Unters. For.* **1995**, *201*, 402-410.
414. Hansen, Å.; Schieberle, P. Generation of aroma compounds during sourdough fermentation: applied and fundamental aspects. *Trends Food Sci. Tech.* **2005**, *16*, 85-94.
415. Korakli, M.; Rossmann, A.; Gänzle, M. G.; Vogel, R. F. Sucrose metabolism and exopolysaccharide production in wheat and rye sourdoughs by *Lactobacillus sanfranciscensis*. *J. Agr. Food Chem.* **2001**, *49*, 5194-5200.
416. Brandt, M. J. Sourdough products for convenient use in baking. *Food Microbiol.* **2007**, *24*, 161-164.
417. Gänzle, M. G.; Zheng, J. S. Lifestyles of sourdough lactobacilli - Do they matter for microbial ecology and bread quality? *Int. J. Food Microbiol.* **2019**, *302*, 15-23.
418. Lacaze, G.; Wick, M.; Cappelle, S. Emerging fermentation technologies: Development of novel sourdoughs. *Food Microbiol.* **2007**, *24*, 155-160.
419. Tang, K. X.; Zhao, C. J.; Gänzle, M. G. Effect of glutathione on the taste and texture of type I sourdough bread. *J. Agr. Food Chem.* **2017**, *65*, 4321-4328.
420. Dubois, V.; Breton, S.; Linder, M.; Fanni, J.; Parmentier, M. Fatty acid profiles of 80 vegetable oils with regard to their nutritional potential. *Eur. J. Lipid Sci. Tech.* **2007**, *109*, 710-732.
421. Caligiuri, S. P. B.; Aukema, H. M.; Ravandi, A.; Guzman, R.; Dibrov, E.; Pierce, G. N. Flaxseed consumption reduces blood pressure in patients with hypertension by altering

circulating oxylipins via an alpha-linolenic acid-induced inhibition of soluble epoxide hydrolase. *Hypertension* **2014**, *64*, 53-59.

422. Cunnane, S. C.; Hamadeh, M. J.; Liede, A. C.; Thompson, L. U.; Wolever, T. M. S.; Jenkins, D. J. A. Nutritional attributes of traditional flaxseed in healthy young adults. *Am. J. Clin. Nutr.* **1995**, *61*, 62-68.

423. Kajla, P.; Sharma, A.; Sood, D. R. Flaxseed-a potential functional food source. *J. Food Sci. Tech.* **2015**, *52*, 1857-1871.

424. Kaewmanee, T.; Bagnasco, L.; Benjakul, S.; Lanteri, S.; Morelli, C. F.; Speranza, G.; Cosulich, M. E. Characterisation of mucilages extracted from seven Italian cultivars of flax. *Food Chem.* **2014**, *148*, 60-69.

425. Ogawa, J.; Kishino, S.; Ando, A.; Sugimoto, S.; Mihara, K.; Shimizu, S. Production of conjugated fatty acids by lactic acid bacteria. *J. Biosci. Bioeng.* **2005**, *100*, 355-364.

426. Delgado-Pando, G.; Cofrades, S.; Ruiz-Capillas, C.; Jimenez-Colmenero, F. Healthier lipid combination as functional ingredient influencing sensory and technological properties of low-fat frankfurters. *Eur. J. Lipid Sci. Tech.* **2010**, *112*, 859-870.

427. Gandemer, G. Lipids in muscles and adipose tissues, changes during processing and sensory properties of meat products. *Meat Sci.* **2002**, *62*, 309-321.

428. Fuentes, V.; Estevez, M.; Ventanas, J.; Ventanas, S. Impact of lipid content and composition on lipid oxidation and protein carbonylation in experimental fermented sausages. *Food Chem.* **2014**, *147*, 70-77.

429. Ordonez, J. A.; Hierro, E. M.; Bruna, J. M.; de la Hoz, L. Changes in the components of dry-fermented sausages during ripening. *Crit. Rev. Food Sci.* **1999**, *39*, 329-367.

430. Estevez, M. Protein carbonyls in meat systems: A review. *Meat Sci.* **2011**, *89*, 259-279.

431. Amaral, A. B.; da Silva, M. V.; Lannes, S. C. D. Lipid oxidation in meat: mechanisms and protective factors - a review. *Food Sci. Tech.-Brazil* **2018**, *38*, 1-15.
432. Toldra, F. Proteolysis and lipolysis in flavour development of dry-cured meat products. *Meat Sci.* **1998**, *49*, S101-S110.
433. Zuber, A. D.; Horvat, M. Influence of starter cultures on the free fatty acids during ripening in Tea sausages. *Eur. Food Res. Technol.* **2007**, *224*, 511-517.
434. Running, C. A.; Craig, B. A.; Mattes, R. D. Oleogustus: The unique taste of fat. *Chem. Senses* **2015**, *40*, 507-516.
435. Poette, J.; Mekoue, J.; Neyraud, E.; Berdeaux, O.; Renault, A.; Guichard, E.; Genot, C.; Feron, G. Fat sensitivity in humans: oleic acid detection threshold is linked to saliva composition and oral volume. *Flavour Frag. J.* **2014**, *29*, 39-49.
436. Ansorena, D.; Gimeno, O.; Astiasaran, I.; Bello, J. Analysis of volatile compounds by GC-MS of a dry fermented sausage: chorizo de Pamplona. *Food Res. Int.* **2001**, *34*, 67-75.
437. Viallon, C.; Berdague, J. L.; Montel, M. C.; Talon, R.; Martin, J. F.; Kondjoyan, N.; Denoyer, C. The effect of stage of ripening and packaging on volatile content and flavour of dry sausage. *Food Res. Int.* **1996**, *29*, 667-674.
438. Chizzolini, R.; Novelli, E.; Zanardi, E. Oxidation in traditional Mediterranean meat products. *Meat Sci.* **1998**, *49*, S87-S99.
439. Leroy, F.; Verluyten, J.; De Vuyst, L. Functional meat starter cultures for improved sausage fermentation. *Int. J. Food Microbiol.* **2006**, *106*, 270-285.
440. Lizaso, G.; Chasco, J.; Beriain, M. J. Microbiological and biochemical changes during ripening of salchichon, a Spanish dry cured sausage. *Food Microbiol.* **1999**, *16*, 219-228.

441. Molly, K.; Demeyer, D.; Civera, T.; Verplaetse, A. Lipolysis in a Belgian sausage: Relative importance of endogenous and bacterial enzymes. *Meat Sci.* **1996**, *43*, 235-244.
442. Kanauchi, M.; Nagata, A.; Kondo, A. Accumulation of hydroxyl fatty acid in *Lactobacillus sakei* Y-20 cells cultivated under stress conditions and expression of fatty acid hydroxylase. *J. Am. Soc. Brew. Chem.* **2018**, *76*, 62-70.
443. Zagorec, M.; Champomier-Verges, M. C. *Lactobacillus sakei*: A starter for sausage fermentation, a protective culture for meat products. *Microorganisms* **2017**, *5*.
444. Romero-Guido, C.; Belo, I.; Ta, T. M. N.; Cao-Hoang, L.; Alchihab, M.; Gomes, N.; Thonart, P.; Teixeira, J. A.; Destain, J.; Wache, Y. Biochemistry of lactone formation in yeast and fungi and its utilisation for the production of flavour and fragrance compounds. *Appl. Microbiol. Biot.* **2011**, *89*, 535-547.
445. Biermann, U.; Grosch, W. Bitter-tasting monoglycerides from stored oat flour. *Zeitschrift für Lebensmittel-Untersuchung und Forschung* **1979**, *169*, 22-26.
446. Molly, K.; Demeyer, D.; Johansson, G.; Raemaekers, M.; Ghistelinck, M.; Geenen, I. The importance of meat enzymes in ripening and flavour generation in dry fermented sausages. First results of a European project. *Food Chem.* **1997**, *59*, 539-545.
447. López, C. M.; Sentandreu, M. A.; Vignolo, G. M.; Fadda, S. G. Low molecular weight peptides derived from sarcoplasmic proteins produced by an autochthonous starter culture in a beaker sausage model. *EuPA Open Proteomics* **2015**, *7*, 54-63.
448. López, C. M.; Sentandreu, M. A.; Vignolo, G. M.; Fadda, S. G. Proteomic and peptidomic insights on myofibrillar protein hydrolysis in a sausage model during fermentation with autochthonous starter cultures. *Food Res. Int.* **2015**, *78*, 41-49.

449. Chen, Q.; Kong, B. H.; Han, Q.; Xia, X. F.; Xu, L. The role of bacterial fermentation in lipolysis and lipid oxidation in Harbin dry sausages and its flavour development. *Lwt-Food Sci. Technol.* **2017**, *77*, 389-396.
450. Ojha, K. S.; Harrison, S. M.; Brunton, N. P.; Kerry, J. P.; Tiwari, B. K. Statistical approaches to access the effect of *Lactobacillus sakei* culture and ultrasound frequency on fatty acid profile of beef jerky. *J. Food Compos. Anal.* **2017**, *57*, 1-7.
451. Aksu, M. I.; Kaya, M. Effect of commercial starter cultures on the fatty acid composition of pastirma (Turkish dry meat product). *J. Food Sci.* **2002**, *67*, 2342-2345.
452. Blanco-Lizarazo, C. M.; Sotelo-Diaz, I.; Arjona-Roman, J. L.; Adriana, L.-B.; Miranda-Ruvalcaba, R. Effect of starter culture and low concentrations of sodium nitrite on fatty acids, color, and *Escherichia coli* behavior during salami processing. *Int. J. Food Sci.* **2018**, *2018*, 5934305.
453. Casaburi, A.; Di Monaco, R.; Cavella, S.; Toldra, F.; Ercolini, D.; Villani, F. Proteolytic and lipolytic starter cultures and their effect on traditional fermented sausages ripening and sensory traits. *Food Microbiol.* **2008**, *25*, 335-347.
454. Mauriello, G.; Casaburi, A.; Blaiotta, G.; Villani, F. Isolation and technological properties of coagulase negative staphylococci from fermented sausages of Southern Italy. *Meat Sci.* **2004**, *67*, 149-158.
455. Signorini, M.; Ponce-Alquicira, E.; Guerrero-Legarreta, I. Proteolytic and lipolytic changes in beef inoculated with spoilage microorganisms and bioprotective lactic acid bacteria. *Int. J. Food Prop.* **2003**, *6*, 147-163.

456. Song, H.; Wu, H. H.; Geng, Z. M.; Sun, C.; Ren, S.; Wang, D. Y.; Zhang, M. H.; Liu, F.; Xu, W. M. Simultaneous determination of 13-HODE, 9,10-DHODE, and 9,10,13-THODE in cured meat products by LC-MS/MS. *Food Anal. Method* **2016**, *9*, 2832-2841.
457. Flores, M.; Mora, L.; Reig, M.; Toldra, F. Risk assessment of chemical substances of safety concern generated in processed meats. *Food Sci. Hum. Well.* **2019**, *8*, 244-251.
458. Tang, K. X.; Shi, T. G.; Gänzle, M. Effect of starter cultures on taste-active amino acids and survival of pathogenic *Escherichia coli* in dry fermented beef sausages. *Eur. Food Res. Technol.* **2018**, *244*, 2203-2212.
459. Hara, A.; Radin, N. S. Lipid extraction of tissues with a low-toxicity solvent. *Anal. Biochem.* **1978**, *90*, 420-426.
460. Moe, M. K.; Strøm, M. B.; Jensen, E.; Claeys, M. Negative electrospray ionization low-energy tandem mass spectrometry of hydroxylated fatty acids: a mechanistic study. *Rapid Commun. Mass Spectrom.* **2004**, *18*, 1731-1740.
461. Brent Friesen, J.; Pauli, G. F. GUESS—A generally useful estimate of solvent systems for CCC. *J. Liq. Chromatogr. Relat. Technol.* **2005**, *28*, 2777-2806.
462. Capella, P.; Galli, C.; Fumagalli, R. Hydroxy fatty acids from cerebroside of the central nervous system: GLC determination and mass spectrometric identification. *Lipids* **1968**, *3*, 431-438.
463. Talon, R.; Dublet, N.; Montel, M. C.; Cantonnet, M. Purification and characterization of extracellular *Staphylococcus warneri* lipase. *Curr. Microbiol.* **1995**, *30*, 11-16.
464. Kenneally, P. M.; Leuschner, R. G.; Arendt, E. K. Evaluation of the lipolytic activity of starter cultures for meat fermentation purposes. *J. Appl. Microbiol.* **1998**, *84*, 839-846.

465. Flores, M.; Toldra, F. Microbial enzymatic activities for improved fermented meats. *Trends Food Sci. Tech.* **2011**, *22*, 81-90.
466. Papon, M.; Talon, R. Cell location and partial characterization of *Brochothrix thermosphacta* and *Lactobacillus curvatus* lipases. *J. Appl. Bacteriol.* **1989**, *66*, 235-242.
467. Lopes, M. D. S.; Leitao, A. L.; Regalla, M.; Marques, J. J. F.; Carrondo, M. J. T.; Crespo, M. T. B. Characterization of a highly thermostable extracellular lipase from *Lactobacillus plantarum*. *Int. J. Food Microbiol.* **2002**, *76*, 107-115.
468. Bruna, J. M.; Ordonez, J. A.; Fernandez, M.; Herranz, B.; de la Hoz, L. Microbial and physico-chemical changes during the ripening of dry fermented sausages superficially inoculated with or having added an intracellular cell-free extract of *Penicillium aurantiogriseum*. *Meat Sci.* **2001**, *59*, 87-96.
469. Selgas, M. D.; Casas, C.; Toledo, V. M.; Garcia, M. L. Effect of selected mould strains on lipolysis in dry fermented sausages. *Eur. Food Res. Technol.* **1999**, *209*, 360-365.
470. Chaillou, S.; Champomier-Verges, M. C.; Cornet, M.; Crutz-Le Coq, A. M.; Dudez, A. M.; Martin, V.; Beaufile, S.; Darbon-Rongere, E.; Bossy, R.; Loux, V.; Zagorec, M. The complete genome sequence of the meat-borne lactic acid bacterium *Lactobacillus sakei* 23K. *Nat. Biotechnol.* **2005**, *23*, 1527-1533.
471. Hertel, C.; Schmidt, G.; Fischer, M.; Oellers, K.; Hammes, W. P. Oxygen-dependent regulation of the expression of the catalase gene *katA* of *Lactobacillus sakei* LTH677. *Appl. Environ. Microbiol.* **1998**, *64*, 1359-1365.
472. Dominguez, R.; Pateiro, M.; Gagaoua, M.; Barba, F. J.; Zhang, W. G.; Lorenzo, J. M. A Comprehensive review on lipid oxidation in meat and meat products. *Antioxidants* **2019**, *8*.

473. Knauf, H. J.; Vogel, R. F.; Hammes, W. P. Cloning, sequence, and phenotypic expression of *kata*, which encodes the catalase of *Lactobacillus sake* LTH677. *Appl. Environ. Microbiol.* **1992**, *58*, 832-839.
474. An, H.; Zhou, H.; Huang, Y.; Wang, G.; Luan, C.; Mou, J.; Luo, Y.; Hao, Y. High-level expression of heme-dependent catalase gene *kata* from *Lactobacillus sakei* protects *Lactobacillus rhamnosus* from oxidative stress. *Mol. Biotechnol.* **2010**, *45*, 155-160.
475. Amanatidou, A.; Bennik, M. H. J.; Gorris, L. G. M.; Smid, E. J. Superoxide dismutase plays an important role in the survival of *Lactobacillus sake* upon exposure to elevated oxygen. *Arch. Microbiol.* **2001**, *176*, 79-88.
476. De Angelis, M.; Gobbetti, M. Stress responses of lactobacilli. In *Stress responses of lactic acid bacteria*, Springer: 2011; pp 219-249.
477. Pophaly, S. D.; Singh, R.; Pophaly, S. D.; Kaushik, J. K.; Tomar, S. K. Current status and emerging role of glutathione in food grade lactic acid bacteria. *Microb. Cell Fact.* **2012**, *11*.
478. Ning, C.; Bao, P.; Zhang, D.; Li, L.; Chen, L.; Fang, H.; Tang, Y.; Zhou, C. Reduction and coordination properties of l-Lysine/l-arginine/l-cysteine for the improvement of the color of cured sausage. *Food Chem.* **2020**, *312*, 126122.
479. Talon, R.; Walter, D.; Chartier, S.; Barriere, C.; Montel, M. C. Effect of nitrate and incubation conditions on the production of catalase and nitrate reductase by staphylococci. *Int. J. Food Microbiol.* **1999**, *52*, 47-56.
480. Barriere, C.; Leroy-Setrin, S.; Talon, R. Characterization of catalase and superoxide dismutase in *Staphylococcus carnosus* 833 strain. *J. Appl. Microbiol.* **2001**, *91*, 514-519.



481. Barriere, C.; Centeno, D.; Lebert, A.; Leroy-Setrin, S.; Berdague, J. L.; Talon, R. Roles of superoxide dismutase and catalase of *Staphylococcus xylosus* in the inhibition of linoleic acid oxidation. *FEMS Microbiol. Lett.* **2001**, *201*, 181-185.
482. Nikolic, N.; Radulovic, N.; Momcilovic, B.; Nikolic, G.; Lazic, M.; Todorovic, Z. Fatty acids composition and rheology properties of wheat and wheat and white or brown rice flour mixture. *Eur. Food Res. Technol.* **2008**, *227*, 1543-1548.
483. Morrison, W. R. On the free fatty acids of wheat flour. With reference to their contribution to chemical changes which occur during the mixing of doughs. University of Glasgow, 1963.
484. Ogawa, J.; Kishino, S.; Ando, A.; Sugimoto, S.; Mihara, K.; Shimizu, S. Production of conjugated fatty acids by lactic acid bacteria. *J. Biosci. Bioeng.* **2005**, *100*, 355-364.
485. Parker, J. H.; Smith, G. A.; Fredrickson, H. L.; Vestal, J. R.; White, D. C. Sensitive assay, based on hydroxy fatty acids from lipopolysaccharide lipid A, for Gram-negative bacteria in sediments. *Appl. Environ. Microbiol.* **1982**, *44*, 1170-1177.
486. Lee, D. S.; Yamada, A.; Sugimoto, H.; Matsunaga, I.; Ogura, H.; Ichihara, K.; Adachi, S.; Park, S. Y.; Shiro, Y. Substrate recognition and molecular mechanism of fatty acid hydroxylation by cytochrome P450 from *Bacillus subtilis* - Crystallographic, spectroscopic, and mutational studies. *J. Biol. Chem.* **2003**, *278*, 9761-9767.
487. Kishimoto, Y.; Radin, N. S. Microdetermination, isolation, and gas-liquid chromatography of 2-hydroxy fatty acids. *J. Lipid Res.* **1963**, *4*, 130-138.
488. Yoneshige, A.; Matsuda, J. Glycosphingolipids containing 2-hydroxy fatty acid are indispensable for the long-term maintenance of axon and myelin in the nervous system. *Trends Glycosci. Glyc.* **2009**, *21*, 193-195.

489. Engelvin, G.; Feron, G.; Perrin, C.; Molle, D.; Talon, R. Identification of beta-oxidation and thioesterase activities in *Staphylococcus carnosus* 833 strain. *FEMS Microbiol. Lett.* **2000**, *190*, 115-120.
490. García Rico, R.; Chavez, R.; Fierro, F.; Laich, F. Mold-fermented foods: *Penicillium* spp. as ripening agents in the elaboration of cheese and meat products. In *Mycofactories*, Leitão, A. L., Ed. Bentham Science Publisher, 2011; pp 73-98.
491. Vignolo, G.; Fontana, C.; Fadda, S. Semidry and dry fermented sausages. In *Handbook of meat processing*, Toldrá, F., Ed. 2010; pp 379-398.
492. Andersen, S. J. Compositional changes in surface mycoflora during ripening of naturally fermented sausages. *J. Food Prot.* **1995**, *58*, 426-429.
493. An, J. U.; Joo, Y. C.; Oh, D. K. New biotransformation process for production of the fragrant compound gamma-dodecalactone from 10-hydroxystearate by permeabilized *Waltomyces lipofer* cells. *Appl. Environ. Microbiol.* **2013**, *79*, 2636-2641.
494. Montel, M. C.; Reitz, J.; Talon, R.; Berdague, J. L.; RoussetAkrim, S. Biochemical activities of Micrococcaceae and their effects on the aromatic profiles and odours of a dry sausage model. *Food Microbiol.* **1996**, *13*, 489-499.
495. Shureiqi, I.; Jiang, W.; Zuo, X. S.; Wu, Y. Q.; Stimmel, J. B.; Leesnitzer, L. M.; Morris, J. S.; Fan, H. Z.; Fischer, S. M.; Lippman, S. M. The 15-lipoxygenase-1 product 13-*S*-hydroxyoctadecadienoic acid down-regulates PPAR-delta to induce apoptosis in colorectal cancer cells. *P. Natl. Acad. Sci. USA* **2003**, *100*, 9968-9973.
496. Llado, V.; Teres, S.; Higuera, M.; Alvarez, R.; Noguera-Salva, M. A.; Halver, J. E.; Escriba, P. V.; Busquets, X. Pivotal role of dihydrofolate reductase knockdown in the anticancer activity of 2-hydroxyoleic acid. *P. Natl. Acad. Sci. USA* **2009**, *106*, 13754-13758.

497. Unlocking the lipid labyrinth. *Nat. Chem. Biol.* **2010**, *6*, 471.
498. Hennebelle, M.; Otoki, Y.; Yang, J.; Hammock, B. D.; Levitt, A. J.; Taha, A. Y.; Swardfager, W. Altered soluble epoxide hydrolase-derived oxylipins in patients with seasonal major depression: An exploratory study. *Psychiat. Res.* **2017**, *252*, 94-101.
499. Mattes, R. D. Fat taste and lipid metabolism in humans. *Physiol. Behav.* **2005**, *86*, 691-697.
500. Meynier, A.; Genot, C. Molecular and structural organization of lipids in foods: their fate during digestion and impact in nutrition. *OCL Oils. Fat. Crop Li.* **2017**, *24*.
501. The LIPID MAPS Lipidomics Gateway. <http://www.lipidmaps.org/> (accessed February 4th, 2020).
502. Liu, H.; Yuan, Q. P.; Li, C. F.; Huang, T. X. Isolation and purification of silychristin, silydianin and taxifolin in the co-products of the silybin refined process from the silymarin by high-speed counter-current chromatography. *Process Biochem.* **2010**, *45*, 799-804.
503. Zhu, S.; Li, Y.; Ma, C. Y.; Chen, S. W.; Dai, J.; Lou, Z. X.; Wang, H. X. Lipase catalyzed acetylation of EGCG, a lipid soluble antioxidant, and preparative purification by high-speed counter-current chromatography (HSCCC). *Sep. Purif. Technol.* **2017**, *185*, 33-40.
504. Gu, M.; Fan, O. Y.; Su, Z. G. Comparison of high-speed counter-current chromatography and high-performance liquid chromatography on fingerprinting of Chinese traditional medicine. *J. Chromatogr. A* **2004**, *1022*, 139-144.
505. Schroder, M.; Vetter, W. Detection of 430 fatty acid methyl esters from a transesterified butter sample. *J. Am. Oil. Chem. Soc.* **2013**, *90*, 771-790.
506. Hussain, S.; Anjum, F.; Butt, M.; Sheikh, M. Chemical composition and functional properties of flaxseed (*Linum usitatissimum*) flour. *Sarhad J. Agric.* **2008**, *24*, 649-653.

507. Kajla, P.; Sharma, A.; Sood, D. Effect of germination on proximate principles, minerals and antinutrients of flaxseeds. *Asian Journal of Dairy and Food Research* **2017**, *36*.
508. Araujo, R. G. O.; Dias, F. D. S.; Macedo, S. M.; dos Santos, W. N. L.; Ferreira, S. L. C. Method development for the determination of manganese in wheat flour by slurry sampling flame atomic absorption spectrometry. *Food Chem.* **2007**, *101*, 397-400.
509. Gerwien, F.; Skrahina, V.; Kasper, L.; Hube, B.; Brunke, S. Metals in fungal virulence. *FEMS Microbiol. Rev.* **2018**, *42*, 1-21.
510. Siedler, S.; Rau, M. H.; Nielsen, S. D. A. Inhibition of fungal growth by manganese depletion. WO/2019/202003, October 24th, 2019.
511. Leal, S. M.; Vareechon, C.; Cowden, S.; Cobb, B. A.; Latge, J. P.; Momany, M.; Pearlman, E. Fungal antioxidant pathways promote survival against neutrophils during infection. *J. Clin. Invest.* **2012**, *122*, 2482-2498.
512. OuYang, Q. L.; Tao, N. G.; Jing, G. X. Transcriptional profiling analysis of *Penicillium digitatum*, the causal agent of citrus green mold, unravels an inhibited ergosterol biosynthesis pathway in response to citral. *BMC Genomics* **2016**, *17*.
513. Parveen, M.; Hasan, M. K.; Takahashi, J.; Murata, Y.; Kitagawa, E.; Kodama, O.; Iwahashi, H. Response of *Saccharomyces cerevisiae* to a monoterpene: evaluation of antifungal potential by DNA microarray analysis. *J. Antimicrob. Chemother.* **2004**, *54*, 46-55.
514. Degenhardt, A. G.; Hofmann, T. Bitter-tasting and kokumi-enhancing molecules in thermally processed Avocado (*Persea americana* Mill.). *J. Agric. Food Chem.* **2010**, *58*, 12906-12915.
515. Shimura, M.; Mase, S.; Iwata, M.; Suzuki, A.; Watanabe, T.; Sekizawa, Y.; Sasaki, T.; Furihata, K.; Seto, H.; Otake, N. Anti-conidial germination factors induced in the presence of

probenazole in infected host leaves. III. Structural elucidation of substances A and C. *Agric. Biol. Chem.* **1983**, *47*, 1983-1989.

516. Weichert, H.; Stenzel, I.; Berndt, E.; Wasternack, C.; Feussner, I. Metabolic profiling of oxylipins upon salicylate treatment in barley leaves - preferential induction of the reductase pathway by salicylate. *FEBS Lett.* **1999**, *464*, 133-137.

517. Tamaoki, D.; Seo, S.; Yamada, S.; Kano, A.; Miyamoto, A.; Shishido, H.; Miyoshi, S.; Taniguchi, S.; Akimitsu, K.; Gomi, K. Jasmonic acid and salicylic acid activate a common defense system in rice. *Plant Signaling Behav.* **2013**, *8*, e24260.

518. Thaler, J. S.; Humphrey, P. T.; Whiteman, N. K. Evolution of jasmonate and salicylate signal crosstalk. *Trends Plant Sci.* **2012**, *17*, 260-270.

519. Paolacci, A. R.; Catarcione, G.; Ederli, L.; Zadra, C.; Pasqualini, S.; Badiani, M.; Musetti, R.; Santi, S.; Ciaffi, M. Jasmonate-mediated defence responses, unlike salicylate-mediated responses, are involved in the recovery of grapevine from bois noir disease. *BMC Plant Biol.* **2017**, *17*, 118.

520. Conrath, U. Systemic acquired resistance. *Plant Signaling Behav.* **2006**, *1*, 179-184.

521. Derksen, H.; Rampitsch, C.; Daayf, F. Signaling cross-talk in plant disease resistance. *Plant Sci.* **2013**, *207*, 79-87.

522. Dempsey, D. A.; Klessig, D. F. SOS - too many signals for systemic acquired resistance? *Trends Plant Sci.* **2012**, *17*, 538-545.

523. Yasari, A. Investigating the potential use of unsaturated fatty acids as antifungal crop protective agents. University of Alberta, 2018.

524. Hayat, Q.; Hayat, S.; Irfan, M.; Ahmad, A. Effect of exogenous salicylic acid under changing environment: A review. *Environ. Exp. Bot.* **2010**, *68*, 14-25.

525. Levine, A.; Tenhaken, R.; Dixon, R.; Lamb, C. H<sub>2</sub>O<sub>2</sub> from the oxidative burst orchestrates the plant hypersensitive disease resistance response. *Cell* **1994**, *79*, 583-593.
526. Zurbriggen, M. D.; Carrillo, N.; Hajirezaei, M. R. ROS signaling in the hypersensitive response: when, where and what for? *Plant Signaling Behav.* **2010**, *5*, 393-396.
527. Morel, J. B.; Dangl, J. L. The hypersensitive response and the induction of cell death in plants. *Cell Death Differ.* **1997**, *4*, 671-683.
528. Balint-Kurti, P. The plant hypersensitive response: concepts, control and consequences. *Mol. Plant Pathol.* **2019**, *20*, 1163-1178.
529. Herrera-Vasquez, A.; Salinas, P.; Holuigue, L. Salicylic acid and reactive oxygen species interplay in the transcriptional control of defense genes expression. *Front. Plant Sci.* **2015**, *6*, 171.
530. Hamberg, M.; Sanz, A.; Rodriguez, M. J.; Calvo, A. P.; Castresana, C. Activation of the fatty acid  $\alpha$ -dioxygenase pathway during bacterial infection of tobacco leaves - Formation of oxylipins protecting against cell death. *J. Biol. Chem.* **2003**, *278*, 51796-51805.
531. Niderman, T.; Genetet, I.; Bruyere, T.; Gees, R.; Stintzi, A.; Legrand, M.; Fritig, B.; Mosinger, E. Pathogenesis-related PR-1 proteins are antifungal (isolation and characterization of three 14-kilodalton proteins of tomato and of a basic PR-1 of tobacco with inhibitory activity against *Phytophthora infestans*). *Plant Physiol.* **1995**, *108*, 17-27.
532. Yu, R. K.; Tsai, Y. T.; Ariga, T.; Yanagisawa, M. Structures, biosynthesis, and functions of gangliosides-An overview. *J. Oleo Sci.* **2011**, *60*, 537-544.
533. Vajn, K.; Viljetic, B.; Degmecic, I. V.; Schnaar, R. L.; Heffer, M. Differential distribution of major brain gangliosides in the adult mouse central nervous system. *Plos One* **2013**, *8*.

534. Ledeen, R. W.; Yu, R. K.; Rapport, M. M.; Suzuki, K. *Ganglioside Structure, Function, and Biomedical Potential*. Springer US: Boston, MA, 1984; online resource.
535. McJarrow, P.; Schnell, N.; Jumpsen, J.; Clandinin, T. Influence of dietary gangliosides on neonatal brain development. *Nutr. Rev.* **2009**, *67*, 451-463.
536. Fong, B. Y.; Ma, L.; Khor, G. L.; van der Does, Y.; Rowan, A.; McJarrow, P.; MacGibbon, A. K. H. Ganglioside composition in beef, chicken, pork, and fish determined using liquid chromatography high-resolution mass spectrometry. *J. Agr. Food Chem.* **2016**, *64*, 6295-6305.
537. Ledeen, R.; Wu, G. Gangliosides of the nervous system. *Methods Mol Biol.* **2018**, *1804*, 19-55.
538. Zappia, M.; Crescibene, L.; Bosco, D.; Arabia, G.; Nicoletti, G.; Bagala, A.; Bastone, L.; Napoli, I. D.; Caracciolo, M.; Bonavita, S.; Di Costanzo, A.; Gambardella, A.; Quattrone, A. Anti-GM1 ganglioside antibodies in Parkinson's disease. *Acta Neurol. Scand.* **2002**, *106*, 54-57.
539. Kaida, K.; Ariga, T.; Yu, R. K. Antiganglioside antibodies and their pathophysiological effects on Guillain-Barre syndrome and related disorders-025EFA review. *Glycobiology* **2009**, *19*, 676-692.
540. Di Pardo, A.; Maglione, V.; Alpaugh, M.; Horkey, M.; Atwal, R. S.; Sassone, J.; Ciammola, A.; Steffan, J. S.; Fouad, K.; Truant, R.; Sipione, S. Ganglioside GM1 induces phosphorylation of mutant huntingtin and restores normal motor behavior in Huntington disease mice. *Proc. Natl. Acad. Sci. U. S. A.* **2012**, *109*, 3528-3533.
541. Ariga, T.; McDonald, M. P.; Yu, R. K. Role of ganglioside metabolism in the pathogenesis of Alzheimer's disease - a review. *J. Lipid Res.* **2008**, *49*, 1157-1175.

542. Miklavcic, J. J.; Hart, T. D. L.; Lees, G. M.; Shoemaker, G. K.; Schnabl, K. L.; Larsen, B. M. K.; Bathe, O. F.; Thomson, A. B. R.; Mazurak, V. C.; Clandinin, M. T. Increased catabolism and decreased unsaturation of ganglioside in patients with inflammatory bowel disease. *World J. Gastroentero.* **2015**, *21*, 10080-10090.
543. Kregel, U.; Bousquet, P. A. Molecular recognition of gangliosides and their potential for cancer immunotherapies. *Front. Immunol.* **2014**, *5*, 1-11.
544. Schneider, J. S.; Sendek, S.; Daskalakis, C.; Cambi, F. GM1 ganglioside in Parkinson's disease: Results of a five year open study. *J. Neurol. Sci.* **2010**, *292*, 45-51.
545. Svennerholm, L.; Brane, G.; Karlsson, I.; Lekman, A.; Ramstrom, I.; Wikkelso, C. Alzheimer disease - Effect of continuous intracerebroventricular treatment with GM1 ganglioside and a systematic activation programme. *Dement. Geriatr. Cogn.* **2002**, *14*, 128-136.
546. Alpaugh, M.; Galleguillos, D.; Forero, J.; Morales, L. C.; Lackey, S. W.; Kar, P.; Di Pardo, A.; Holt, A.; Kerr, B. J.; Todd, K. G.; Baker, G. B.; Fouad, K.; Sipione, S. Disease-modifying effects of ganglioside GM1 in Huntington's disease models. *EMBO Mol. Med.* **2017**, *9*, 1537-1557.
547. Miklavcic, J. J.; Schnabl, K. L.; Mazurak, V. C.; Thomson, A. B.; Clandinin, M. T. Dietary ganglioside reduces proinflammatory signaling in the intestine. *J. Nutr. Metab.* **2012**, *2012*, 280286.
548. Kundu, S. K.; Scott, D. D. Rapid separation of gangliosides by high-performance liquid chromatography. *J. Chromatogr. B: Biomed. Sci. Appl.* **1982**, *232*, 19-27.
549. Gazzotti, G.; Sonnino, S.; Ghidoni, R.; Kirschner, G.; Tettamanti, G. Analytical and preparative high-performance liquid chromatography of gangliosides. *J. Neurosci. Res.* **1984**, *12*, 179-192.



550. van Echten-Deckert, G. Sphingolipid extraction and analysis by thin-layer chromatography. *Methods Enzymol.* **2000**, *312*, 64-79.
551. Sonnino, S.; Ghidoni, R.; Gazzotti, G.; Kirschner, G.; Galli, G.; Tettamanti, G. High-performance liquid-chromatography preparation of the molecular-species of GM1 and GD1a gangliosides with homogeneous long-chain base composition. *J. Lipid Res.* **1984**, *25*, 620-629.
552. Kato, T.; Hatanaka, K. Purification of gangliosides by liquid-liquid partition chromatography. *J. Lipid Res.* **2008**, *49*, 2474-2478.
553. Oikawa, N.; Matsubara, T.; Fukuda, R.; Yasumori, H.; Hatsuta, H.; Murayama, S.; Sato, T.; Suzuki, A.; Yanagisawa, K. Imbalance in fatty-acid-chain length of gangliosides triggers alzheimer amyloid deposition in the precuneus. *Plos One* **2015**, *10*.
554. Gobburi, A. L. P. An LC-MS/MS approach for gangliosides profiling in brain and retinal tissue of mice: application to glaucoma mice age studies. Cleveland State University, 2017.
555. Ikeda, K.; Shimizu, T.; Taguchi, R. Targeted analysis of ganglioside and sulfatide molecular species by LC/ESI-MS/MS with theoretically expanded multiple reaction monitoring. *J. Lipid Res.* **2008**, *49*, 2678-2689.
556. Masson, E. A. Y.; Sibille, E.; Martine, L.; Chaux-Picquet, F.; Bretillon, L.; Berdeaux, O. Apprehending ganglioside diversity: a comprehensive methodological approach. *J. Lipid Res.* **2015**, *56*, 1821-1835.
557. Garcia, A. D.; Chavez, J. L.; Mechref, Y. Rapid and sensitive LC-ESI-MS of gangliosides. *J. Chromatogr. B: Anal. Technol. Biomed. Life Sci.* **2014**, *947*, 1-7.
558. Wang, X.; Wei, D.; Zhou, L.; Yin, Z. Simple method for large-scale isolation and purification of gangliosides by non-ionic adsorption chromatography. *Prep. Biochem. Biotechnol.* **2004**, *34*, 305-313.

559. Berthod, A.; Friesen, J. B.; Inui, T.; Pauli, G. F. Elution-extrusion countercurrent chromatography: Theory and concepts in metabolic analysis. *Anal. Chem.* **2007**, *79*, 3371-3382.
560. Cazes, J.; Ewing, G. W. *Ewing's analytical instrumentation handbook*. 3rd ed.; Marcel Dekker: New York, 2005.
561. Oka, H.; Ito, Y. Systematic selection of solvent systems for high speed countercurrent chromatography. In *Encyclopedia of Chromatography*, Cazes, J., Ed. Taylor & Francis Group: Boca Raton, 2004; Vol. 2, pp 1628-1634.
562. Billardello, B. *Countercurrent chromatography, the support-free liquid stationary phase*. 2002; Vol. 38.
563. Berthod, A.; Maryutina, T.; Spivakov, B.; Shpigun, O.; Sutherland, I. A. Countercurrent chromatography in analytical chemistry (IUPAC technical report). *Pure Appl. Chem.* **2009**, *81*, 355-387.
564. Agnely, M.; Thiebaut, D. Dual-mode high-speed counter-current chromatography: retention, resolution and examples. *J. Chromatogr. A* **1997**, *790*, 17-30.
565. Brent Friesen, J.; Pauli, G. F. G.U.E.S.S.—A generally useful estimate of solvent systems for CCC. *J. Liq. Chromatogr. Relat. Technol.* **2005**, *28*, 2777-2806.
566. Berthod, A.; Mekaoui, N. Distribution ratio, distribution constant and partition coefficient. Countercurrent chromatography retention of benzoic acid. *J. Chromatogr. A* **2011**, *1218*, 6024-6030.
567. Zhao, C. X.; He, C. H. Mass transfer and separation criteria for high-speed countercurrent chromatography. *AIChE J.* **2011**, *57*, 359-372.
568. Ito, Y.; Conway, W. D. Experimental observations of the hydrodynamic behavior of solvent systems in high-speed counter-current chromatography: III. Effects of physical properties

of the solvent systems and operating temperature on the distribution of two-phase solvent systems. *J. Chromatogr. A* **1984**, *301*, 405-414.

569. Berthod, A. Countercurrent chromatography and the journal of liquid chromatography: A love story. *J. Liq. Chromatogr. Relat. Technol.* **2007**, *30*, 1447-1463.

570. Matsuda, K.; Ma, Y.; Barghout, V.; Ito, Y.; Chatterjee, S. Isolation of less polar alkali-labile glycolipids of human brain by high-speed countercurrent chromatography. *J. Liq. Chromatogr. Relat. Technol.* **1998**, *21*, 103-110.

571. Matsuda, K.; Matsuda, S.; Saito, M.; Ito, Y. Separation of phospholipids and glycolipids using analytical toroidal-coil countercurrent chromatography. I. Separation of human brain lipids. *J. Liq. Chromatogr. Relat. Technol.* **2002**, *25*, 1255-1269.

572. Leitao, G. G.; de Souza, P. A.; Moraes, A. A.; Brown, L. Step-gradient CCC separation of phenylpropanoid and iridoid glycosides from roots of *Stachytarpheta cayennensis* (Rich.) Vahl. *J. Liq. Chromatogr. Relat. Technol.* **2005**, *28*, 2053-2060.

573. Jerz, G.; Gutzeit, D.; Winterhalter, P. Characterization of acylated flavonoid glycosides from sea buckthorn (*Hippophae rhamnoides*) juice concentrate by preparative HSCCC/ESI-MS-MS. In *Flavor and Health Benefits of Small Fruits*. **2010**, American Chemical Society, pp. 253-265.

574. Paget, C.; Deng, S.; Soulard, D.; Priestman, D. A.; Speca, S.; von Gerichten, J.; Speak, A. O.; Saroha, A.; Pewzner-Jung, Y.; Futerman, A. H., TLR9-mediated dendritic cell activation uncovers mammalian ganglioside species with specific ceramide backbones that activate invariant natural killer T cells. *PLoS Biol.* **2019**, *17*, e3000169.

575. Palestini, P.; Masserini, M.; Fiorilli, A.; Calappi, E.; Tettamanti, G. Age-related changes in the ceramide composition of the major gangliosides present in rat brain subcellular fractions enriched in plasma membranes of neuronal and myelin origin. *J. Neurochem.* **1993**, *61*, 955-960.
576. Vetter, W.; Hammannl, S.; Müller, M.; Englert, M.; Huang, Y. N. The use of countercurrent chromatography in the separation of nonpolar lipid compounds. *J. Chromatogr. A* **2017**, *1501*, 51-60.
577. Liu, D.; Hong, Z. L.; Gao, M. Z.; Wang, Z. X.; Gu, M.; Zhang, X. Z.; Xiao, H. B. Polarity, selectivity and performance of hydrophilic organic/salt-containing aqueous two-phase system on counter-current chromatography for polar compounds. *J. Chromatogr. A* **2016**, *1448*, 49-57.
578. Guzlek, H. Counter-current chromatography for the purification of high value natural compounds: performance modelling and solvent selection. Imperial College London, **2011**.
579. Sonnino, S.; Kirschner, G.; Ghidoni, R.; Acquotti, D.; Tettamanti, G. Preparation of GM1 ganglioside molecular species having homogeneous fatty acid and long chain base moieties. *J. Lipid Res.* **1985**, *26*, 248-257.

## **Appendix 1: Advances in the preparative separation of gangliosides by high-speed counter-current chromatography (HSCCC)**

### **A1.1 Introduction**

Gangliosides are glycosphingolipids containing sialic acid(s).<sup>532, 533</sup> They are widely distributed within organisms, most notably in the nervous, haematopoietic and digestive systems.<sup>534</sup> So far, almost 200 gangliosides have been found in vertebrates, with diverse structures of carbohydrate and ceramide moieties.<sup>532, 535</sup> Among them, monosialogangliosides (GM1), disialogangliosides (GD1a and GD1b), and trisialogangliosides (GT1) are the major species found in brains,<sup>533</sup> which differ by their composition or arrangement of saccharide monomers (glycoforms). In addition, various ceramides can be linked to each of these saccharide moieties (species), for example the (d36:1) and (d38:1) homologues.<sup>536</sup>

Many important biological functions of gangliosides have been identified.<sup>532, 533</sup> In particular, they play roles in the pathology of neurodegenerative diseases<sup>537</sup> such as Parkinson's disease,<sup>538</sup> Guillain-Barré syndrome,<sup>539</sup> Huntington's disease,<sup>540</sup> and Alzheimer's disease,<sup>541</sup> and other progressive diseases like inflammatory bowel disease<sup>542</sup> and cancer.<sup>543</sup> Accordingly, ganglioside supplementation has been used as treatments for these diseases.<sup>544, 545, 546, 547</sup>

Despite the increasing number of investigations that involve gangliosides, the relationship between an individual ganglioside structure (which combines a unique species of ganglioside with a unique ceramide structure) and its biological function or potential therapeutic effect, is not well studied. A significant challenge to progress in such studies is the low availability of individual ganglioside standards; these purified standards are needed in sufficient quantities for

functional tests *in vitro* or *in vivo*. This is also especially important to the further development of ganglioside-based pharmaceuticals or dietary supplements.<sup>535</sup>

Purified individual ganglioside standards are also required for use in ganglioside structural characterization and their absolute quantification by LC/MS or other analytical techniques. Ideally, quantification would be achieved without assuming that similar gangliosides have identical response factors, which is a necessary assumption in the absence of pure compounds. In summary, the development of efficient purification methods to isolate individual ganglioside compounds is highly desirable.

Previously both liquid and solid stationary phases have been used in the separation of individual gangliosides, through liquid-solid chromatography (LC)<sup>548, 549, 550, 551</sup> and liquid-liquid chromatography (LLC).<sup>552</sup> Gangliosides were separated using reversed-phase HPLC for analytical<sup>553, 554</sup> and preparative purposes<sup>549, 551</sup> mainly based on the carbon number.<sup>555, 556</sup> Separations of gangliosides species differing in their saccharide moieties were performed using normal-phase,<sup>553, 556</sup> hydrophilic interaction LC (HILIC)<sup>557, 556</sup> or non-ionic absorbance resin columns.<sup>558</sup> However, preparative LC has limitations when separating complicated gangliosides mixtures, which combine multiple glycoforms and ceramides. For analytical purposes, the resulting overlapping of analytes can be complemented by additional selectivity towards each compound using highly selective detection methods, such as multiple reaction monitoring modes in mass spectrometry. However, for preparative applications, this is not applicable.

Compared to LC, LLC has certain advantages in that it can be operated in a low pressure system, with a high sample loading capacity, and with high analyte recovery.<sup>66, 144, 559, 59</sup> High-speed counter-current chromatography (HSCCC) is a commonly used hydrodynamic LLC system that uses the advantage of a high partition efficiency that arises from the larger interfacial

area between the stationary and mobile phases, compared to its hydrostatic counterparts.<sup>560</sup>

Although HSCCC has been explored in ganglioside separations,<sup>552</sup> only limited resolution of the various ganglioside species was achieved using the previous developed conditions. Furthermore, the separation of ganglioside homologues that only differs in their ceramides was not investigated in that work.<sup>552</sup>

Here, we aimed to improve the HSCCC preparative separation of gangliosides 1) classes that differ in saccharide monomer compositions, 2) species that differ in saccharide monomer arrangements and 3) homologues that differ in ceramide compositions. A mixture of porcine gangliosides which contain mainly GM1 (d36:1), GD1a (d36:1), GD1b (d36:1) and their (d38:1) homologues, was used in this method development. HSCCC parameters, such as the choice of two-phase solvent system, the addition of solvent modifier and the elution mode, were selected to achieve separation of individual porcine gangliosides. FIA-MS/MS was first used to analyze the composition of the fractions collected from HSCCC separations. Fractions with a similar composition were then combined and re-analyzed by LC-MS/MS to measure the relative abundance of analytes, and thus evaluate the separation performance.

## **A1.2 Materials and methods**

### **A1.2.1 Reagents**

HPLC-grade reagents (including acetonitrile, methanol, 2-propanol and methyl tert-butyl ether (MTBE)), ammonium acetate, deionized ultra-filtered water, and Optima® LC-MS grade water were purchased from Fisher Scientific (Ottawa, Ontario, Canada). “Chromasolv® Plus for HPLC” 1-Butanol was obtained from Sigma-Aldrich (St. Louis, MO, USA). Acetic acid (glacial) was purchased from CALEDON (Halton Hills, Ontario, Canada).

Mixed porcine gangliosides ( $\text{NH}_4^+$  salt, >98% by TLC) was obtained from Matreya, Lipids and Biochemical LLC (PA, USA). GM1 mixture from porcine was provided by the courtesy of Dr. Simonetta Sipione, University of Alberta.

### **A1.2.2 LC-MS/MS analysis of gangliosides**

Hydrophilic interaction liquid chromatography (HILIC) analysis was used to separate gangliosides differing by glycoform. An XBridge<sup>®</sup> HILIC column (15 cm  $\times$  2.1 mm, 3  $\mu\text{m}$ , Waters, Milford, MA, USA) was used with a gradient elution of mobile phase solvent A (acetonitrile/50 mM aqueous ammonium acetate, 1:1 (v/v)) and solvent B (acetonitrile) as follows: 0-20 min, 5-80% solvent A; held at 80% solvent A to 22 min; re-equilibrated to 5% A for 8 min. The flow rate was kept at 0.3 mL/min. A 10  $\mu\text{L}$  sample was injected and the data acquisition window of 5-22 min was programmed using the automated column valve.

Fractions were prepared for flow-injection (FIA)-MS/MS analysis as described in Section 2.4 below. The mobile phase consisted of 50% solvent A (2% methanol and 5mM acetic acid in water) and 50% solvent B (methanol: isopropanol, 1:1 (v/v) with addition of 5mM acetic acid). The flow rate was set to 0.3 mL/min and the total run time was 2 min.

All LC analyses were performed on an Agilent 1200 Series LC system equipped with a degasser, an autosampler and a binary pump (Agilent Technologies, CA, US). Gangliosides were detected by tandem mass spectrometry (MS/MS) using a 3200 QTRAP mass spectrometer (AB SCIEX, ON, Canada) coupled to an electrospray ionization (ESI) source operating in negative mode. Nitrogen was used as curtain gas, nebulizing gas, and drying gas. The mass spectrometer was run using the following parameters: curtain gas, GS1 and GS2 at 20, 40 and 50 arbitrary units, ion spray voltage (IS) at -4500 V, ion source temperature at 400  $^{\circ}\text{C}$ , and collision cell exit



potential (CXP) at -4.00. Multiple reaction monitoring (MRM) experiments were run using the optimized settings to monitor individual gangliosides (see **Table A1-1**). Data processing was performed on Analyst 1.4.2 software.

### **A1.2.3 Selection of the solvent system for HSCCC separation of gangliosides**

The components of the solvent system for ganglioside separation was initially based on the recommendation of the previous literature.<sup>552, 561, 59</sup> These solvent systems, which consist of butanol (BuOH)/methyl tert-butyl ether (MTBE)/acetonitrile (ACN)/water, are expected to provide a suitable partition for amphiphilic compounds like gangliosides.<sup>552, 561, 59</sup> Acetic acid, a volatile (i.e. easily removed by rotary evaporation) acidic solvent system modifier was added into solvent system to test its effect on the ganglioside elution profile.

To understand the possible elution profile of individual gangliosides, the partition coefficient ( $K$  value) was determined as follows.<sup>59</sup> The GM1 mixture was dissolved in water, and the mixed ganglioside sample from porcine was dissolved in chloroform/methanol/water (2:1:0.1, v/v/v) to make a 30 mg/mL stock solution. An aliquot (25  $\mu$ L) of each chosen stock solution was dried in a 2 mL micro-centrifuge tube under nitrogen. Then a flask containing approximately 5 mL of each of the mobile and stationary phases was prepared. From this, equal aliquots of the upper and lower phases were added to the micro-centrifuge tube to create a small partition system. After vigorously mixing, the small partition system was allowed to settle, and was centrifuged if necessary, to separate the two phases completely. Equal amounts of the upper and lower phases were separately taken to individual HPLC vials. These samples were dried under nitrogen, re-dissolved in 1 mL methanol, and analyzed for ganglioside content by LC-MS/MS analysis, as described above. The remaining partition system was then adjusted using different levels of

acetic acid (0.008%, 0.5%, 1%, 2% and 4%) to evaluate the effect of solvent acidification on the  $K$  value for gangliosides. LC-MS analyses were used to determine the partition coefficient between the two phases of each solvent system, calculated as:

$$K \equiv A_{upper}/A_{lower}$$

where  $K$ ,  $A_{upper}$  and  $A_{lower}$  are the partition coefficient, the peak area of the analyte from upper and lower phases, respectively.

#### **A1.2.4 High-speed counter-current chromatography (HSCCC) separation of gangliosides**

The TBE-300B HSCCC system used in this study was coupled with a Model 501 PrimeLine solvent delivery module (Analytical Scientific Instruments, California, USA), a 260 mL multilayer-coiled column ( $\beta=0.5-0.8$ ; 1.9 mm i.d. tubing) (Tauto Biotech, Shanghai, China) and a CHF 122SC fraction collector (Avantec Toyo Kaisha Ltd., Tokyo, Japan).<sup>66</sup> The preparation of the solvent system and the head-to-tail mode HSCCC separation procedure followed the established literature,<sup>66</sup> except when the dual-elution mode<sup>562, 563, 564</sup> was applied as described below. Briefly, a solvent system was mixed, allowed to separate into two phases, and equilibrated overnight. The two phases were then separately collected and sonicated before use. To start the HSCCC separation, head-to-tail mode was applied: the HSCCC column was first filled up with upper phase (stationary phase), and then rotated at 1000 rpm while introducing lower phase as mobile phase at a constant flow rate of 3 mL/min, except when the solvent system was BuOH/MTBE/ACN/water 3:1:1:5 ( $v/v/v/v$ ), where 2mL/min was used. The stock solution of ganglioside sample (100  $\mu$ L, 30 mg/mL) was dried under nitrogen, dissolved in 5 mL of upper phase and 5 mL of lower phase, and injected into the equilibrated system. Fractions were

collected over either 1 min or 3 min time windows after sample injection. Retention of the stationary phase was calculated as

$$R = [(V_{whole} - V_{pushed}) / (V_{whole} - V_{sample\ loop})] * 100\%$$

where  $V_{whole}$ ,  $V_{pushed}$  and  $V_{sample\ loop}$  represent the whole HSCCC pipeline volume (260 mL), the volume of the stationary phase pushed out during equilibrium of solvent system, and the volume of the sample loop (20 mL), respectively. When dual-elution mode was applied, the separation was performed as above except that at 150 min after sample injection, the column was switched to tail-to-head mode and the mobile phase was changed to the previous stationary phase (the upper phase).

After the HSCCC separation of up to 5 hours, 100  $\mu$ L aliquots taken from each of every 10 successive fractions were combined, dried, re-dissolved in 1 mL methanol, and analyzed by FIA-MS/MS to identify the elution window for gangliosides in the HSCCC experiment. For this elution window, a 20  $\mu$ L aliquot of each collected fraction was diluted by addition of 80  $\mu$ L methanol and analyzed by FIA-MS/MS analysis, where the peak areas were used to construct HSCCC chromatogram. The collected fractions with similar ganglioside compositions were combined, dried and re-dissolved in 1 mL of 1:1 (v/v) acetonitrile-methanol. The combined fraction was further diluted 1: 60 (v/v) in 1:1 (v/v) acetonitrile-methanol and analyzed by LC-MS/MS for ganglioside identification and measurement of relative abundances. Relative abundance was calculated as the LC-MS/MS peak area of a target analyte divided by the sum of all peak areas detected for the MRM transitions monitored (**Table A1-1**).

**Table A1- 1. Multiple reaction monitoring (MRM) experiments of ganglioside individuals**

Compounds	Q <sub>1</sub>	Q <sub>3</sub>	DP*	EP*	CEP*	CE*	Retention
	( <i>m/z</i> )	( <i>m/z</i> )	(V)	(V)	(V)	(V)	Time (min)
GM1 (d36:1)	1544.7	290.1	-165	-8	-68.8	-95	13.9
GM1 (d38:1)	1572.8	290.1	-165	-8	-69.9	-100	13.9
GD1a (d36:1)	917.4	290.1	-95	-10	-28	-54	14.9
GD1a (d38:1)	931.5	290.1	-90	-10	-34	-54	15.0
GD1b (d36:1)	917.4	290.1	-95	-10	-28	-54	15.8
GD1b (d38:1)	931.5	290.1	-90	-10	-34	-54	15.8
GT1b (d36:1)	1063.0	290.1	-70	-10	-36	-44	16.5
GT1b (d38:1)	1077.1	290.1	-100	-10	-51.5	-62	16.5

\*: *DP, EP, CEP and CE are abbreviation for declustering potential, entrance potential, collision cell entrance potential and collision energy, respectively.*

### **A1.3 Results**

#### **A1.3.1 LC-MS analysis of gangliosides to determine their partition coefficient ( $K_D$ value) in BuOH/MTBE/ACN/water solvent systems**

The  $K$  values of ganglioside in a range of BuOH/MTBE/ACN/water systems without the addition of acetic acid were first investigated (**Table A1-2**). It was observed that for the ganglioside mixture (supplied in the form of ammonium salts), the systems 2:4:3:8 and 2:2:1:5 (where these numbers refer to BuOH/MTBE/ACN/water ratios,  $v/v/v/v$ ) resulted in  $K$  values of

<0.4 for most of the gangliosides (i.e. GD1a, GD1b and GT1). A previous study had also obtained similar  $K < 0.4$  for the 3:1:1:5 system.<sup>552</sup> This indicates that without further modification, these solvent systems can't retain most of the gangliosides tested in their upper phases, which would be the stationary phase in the head-to-tail elution of CCC. Other commonly used HSCCC solvent systems with higher contents of hydrophobic solvents, are expected to have even lower retention of gangliosides.<sup>552, 561, 59</sup>

In order to increase these  $K$  values and so achieve greater separation, acetic acid was added to the solvent systems. Acetic acid was chosen due to its volatility, making it compatible with mass spectrometry, and also possible to remove conveniently by rotary evaporation. With the increased addition of acetic acid in a system, the  $K$  value of each ganglioside also increased. For example, the  $K$  value of GM1 (d36:1) increased from 0.74 to 17.6 with acetic acid addition from 0% to 4% (v/v). All gangliosides followed the same trend in all of the solvent systems tested. This means that the added acid, only a small amount of which was consumed to convert ganglioside ammonium salts into their more non-polar acidic form, acted to greatly increase the partition of analytes into the upper phase.

**Table A1- 2.** Partition coefficient (*K* value) of gangliosides in the solvents system of butanol (BuOH)/methyl tert-butyl ether (MTBE)/acetonitrile (ACN)/water with/without addition of acetic acid

Solvent ratio	Acid addition (v/v)	<i>K</i> value							
		GM1 (d36:1)	GM1 (d38:1)	GD1a (d36:1)	GD1a (d38:1)	GD1b (d36:1)	GD1b (d38:1)	GT1b (d36:1)	GT1b (d38:1)
3:1:1:5	0.50%	5.6	6.4	/	/	/	/	/	/
2:2:1:5	0.00%	0.7	0.8	<=0.1	<=0.1	<=0.1	<=0.1	<=0.1	<=0.1
	0.01%	1.1	1.1	<=0.1	<=0.1	0.3	0.3	<=0.1	<=0.1
	0.50%	4.0	4.4	0.7	0.7	1.3	1.3	0.2	0.2
	1.00%	7.4	8.4	1.3	1.6	2.9	2.7	0.4	0.4
	2.00%	13	14	3.3	3.6	6.6	7.4	1.1	1.4
	4.00%	18	21	5.9	7.9	9.2	11	2.0	2.8
2:4:3:8	0.00%	0.4	0.5	<=0.1	<=0.1	<=0.1	<=0.1	<=0.1	<=0.1
	0.01%	0.7	0.8	<=0.1	<=0.1	0.2	0.2	<=0.1	<=0.1
	0.50%	2.1	2.3	0.3	0.4	0.7	0.8	<=0.1	<=0.1
	1.00%	3.2	3.8	0.7	0.8	1.2	1.3	0.2	0.2

Often, a  $K=0.4-2.5$  window is considered to be the “sweet spot” in HSCCC separations, i.e. the elution window that usually achieves the optimal peak resolution<sup>565</sup>. However, due to the wide-ranging partition behaviours of diverse gangliosides, it was difficult to achieve a single solvent system that resulted in all of the gangliosides falling into the *K* value window of 0.4-2.5.

For example, when 0.5% (v/v) acetic acid was added into the 2:2:1:5 system, the *K* values of four GD1 homologues were between 0.4-2.5. However, the *K* value of both GM1 were >2.5, which means the retention of these compounds in the stationary phase of such a system might become too strong. In this case, other HSCCC strategies, such as dual mode HSCCC<sup>564</sup> or elution-extrusion HSCCC,<sup>559</sup> can be used to expand the “sweet spot” window, shorten the operational time and improve the peak shape. In the same system, the *K* value of GT1 was <0.4, which indicates GT1 was expected to elute much faster compared to other gangliosides in head-to-tail mode, and thus get well separated from other gangliosides. As the amount of acid further increased, the *K* values of analytes became much higher (**Table A1-2**) but not necessary more feasible for the HSCCC separation, due to the excessively strong partition into the upper phase, resulting in very long run time and peak broadening effect in head-to-tail mode.<sup>565</sup>

### **A1.3.2 HSCCC separation of ganglioside with head-to-tail mode**

Despite the fact that the measured partition coefficient is a critical parameter to predict the elution of analytes, the actual HSCCC separation also relies on the other experiment conditions.<sup>59, 566, 567</sup> Hence, an optimised HSCCC separation method should be evaluated based on its actually achieved separation profile, rather than mere prediction via *K* values. In this work, a suitable HSCCC separation for gangliosides was thus developed as follows.

Before purification, porcine gangliosides were analyzed (**Figure A1-1**). From the LC-MS/MS analysis, the 6 major gangliosides and their relative abundances were as follow: GM1 (d36:1) 12%, GM1 (d38:1) 11%, GD1a (d36:1) 13%, GD1a (d38:1) 21%, GD1b (d36:1) 10% and GD1b (d38:1) 17%. In order to develop HSCCC protocols to separate these individual gangliosides (i.e. to increase the relative abundances of each target analyte after purification, compared to the

original porcine ganglioside mixture), the HSCCC separations using 3 different BuOH/MTBE/ACN/water solvent systems were evaluated. Achieving an optimum HSCCC separation requires the consideration of various aspects including  $K$  values, the retention of the stationary phase in the CCC column and the overall operational time.

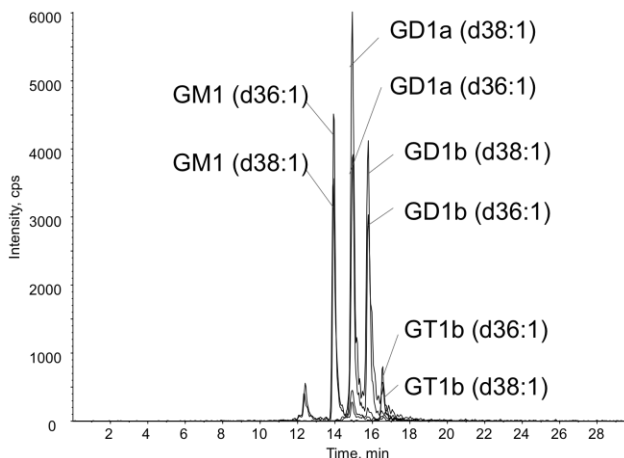


**Figure A1-1.** LC-MS/MS chromatogram of the porcine ganglioside mixture used in this work

The  $K$  value tested here and in the previous report<sup>552</sup> indicated that 3:1:1:5 results in the strongest retention of gangliosides in the upper phase among the 3 solvent systems, and therefore this system was first evaluated. The two GM1 homologues GM1 (d36:1) and GM1(d38:1) could not be separately monitored by the thin layer chromatography (TLC) technique used previously<sup>552</sup> could now be separately detected by MS/MS. The previously reported HSCCC conditions, i.e. rotation of 1000 rpm and flow rate of 2 ml/min in the 3:1:1:5 system with a head-to-tail mode, was then re-evaluated. Acetic acid was added to 10 mL of solvent mixture (5 mL of the upper phase and 5 mL of the lower phase) to a final concentration of 0.5%, v/v. This was used to dissolve the sample prior to injection, so that ganglioside ammonium salts were acidified, unless otherwise noted. As found in the previous report,<sup>552</sup> GM1 was well separated from other



ganglioside classes. It was also found that this system did indeed separate GM1 (d36:1) from GM1 (d38:1).

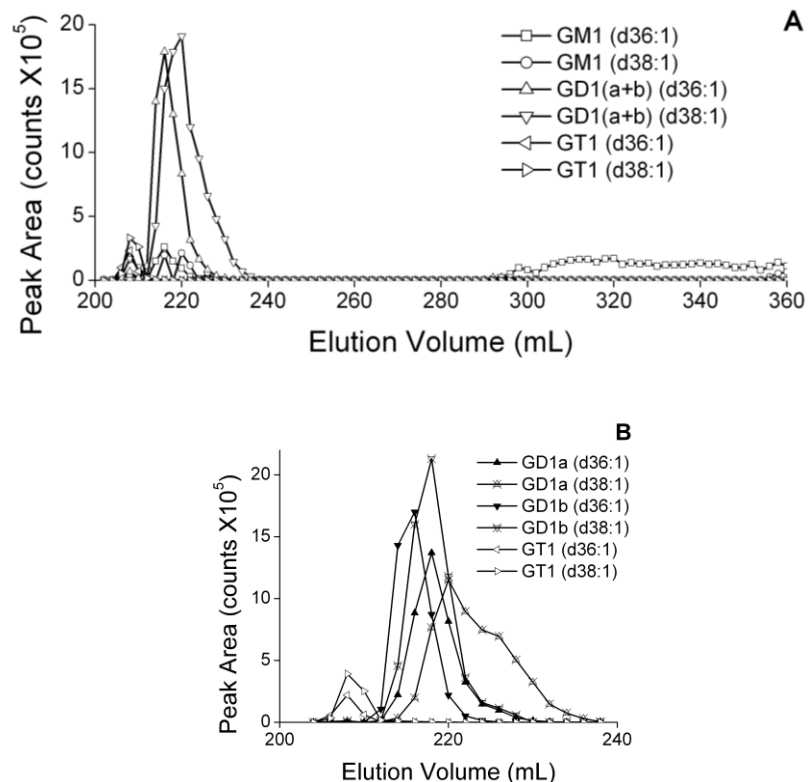


**Figure A1-2.** Head-to-tail mode HSCCC chromatograms of the ganglioside mixture using a BuOH/MTBE/ACN/water 3:1:1:5, v/v/v/v solvent system with acetic acid added in the sample solution to 0.5% (v/v).

The flow rate was 2ml/min and fraction collection frequency was 1 min/tube. **Figure A1-2 A** was resulted from ganglioside measurement by FIA-MS/MS analysis while in **Figure A1-2 B** LC-MS/MS was used in order to separate GD1a and GD1b within each HSCCC fraction.

In **Figure A1-2A**, the elution of GM1 (d36:1) can be seen over the elution volumes of 296-358mL, whereas GM1(d38:1) appeared at higher elution volumes (not shown). The collected fractions, selected on the basis of FIA-MS/MS analysis as described above, were combined and re-analyzed by LC-MS/MS (**Figure A1-3**). These results show that separation of GM1 (d36:1) (**Figure A1-3 F**) from GM1 (d38:1) (**Figure A1-3G**) has been achieved; the combined GM1 (d36:1) fraction (**Figure A1-3 F**) showed only 4% of GM1 (d38:1) and the combined GM1 (d38:1) fraction (**Figure A1-3 G**) contained only 12% of GM1 (d36:1). There was also good separation of the classes of GT1 (**Figure A1-3 A**) from GD1 (**Figure A1-3 B, C, D and E**). However, the homologues within the GD1 species (i.e., GD1b (d36:1), GD1b (d38:1), GD1a (d36:1) and GD1a (d38:1)) were not fully separated, as illustrated by the co-elution of GD1b (d38:1) and GD1a (d36:1) (**Figures A1-3 B, S1 C and D**). Therefore, for better separation of GD1 species, the separation method needed to be further optimized. In addition, it was noticed that the retention of stationary phase only reached 36 % (n=2) in the 3:1:1:5 solvent system with the current conditions (rotation of 1000 rpm and flow rate of 2 ml/min). One of the strategies used to improve peak resolution is to increase the retention of stationary phase by applying more hydrophobic solvent systems.<sup>568</sup>

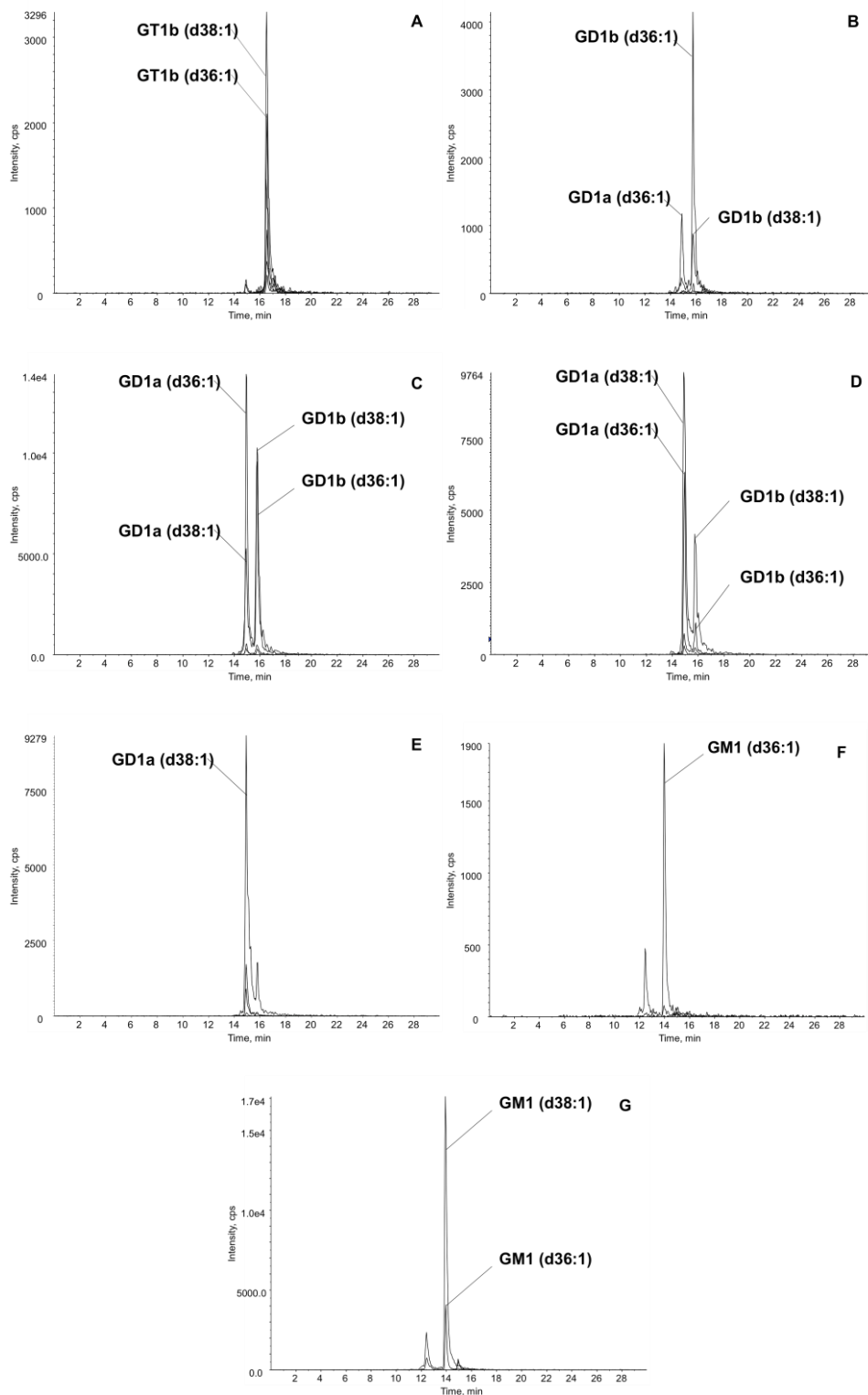


**Figure A1-3.** LC-MS/MS analysis of fractions collected from the head-to-tail mode HSCCC separation using the 3:1:1:5 solvent system shown in **Figure A1-2**.

(The enriched fractions were collected over the following specific elution volume windows: A) GT1b at 206 mL→212 mL; B) GD1b (d36:1) at 212 mL→216 mL; C) GD1a (d36:1), GD1b (d38:1) and GD1b (d36:1) at 216 mL→220 mL; D) GD1a (d38:1), GD1a (d36:1) and GD1b (d38:1) at 220 mL→224 mL; E) GD1a (d38:1) at 224 mL→238 mL; F) GM1 (d36:1) at 296 mL→358 mL; G) GM1 (d38:1) at 360 mL→422 mL.)

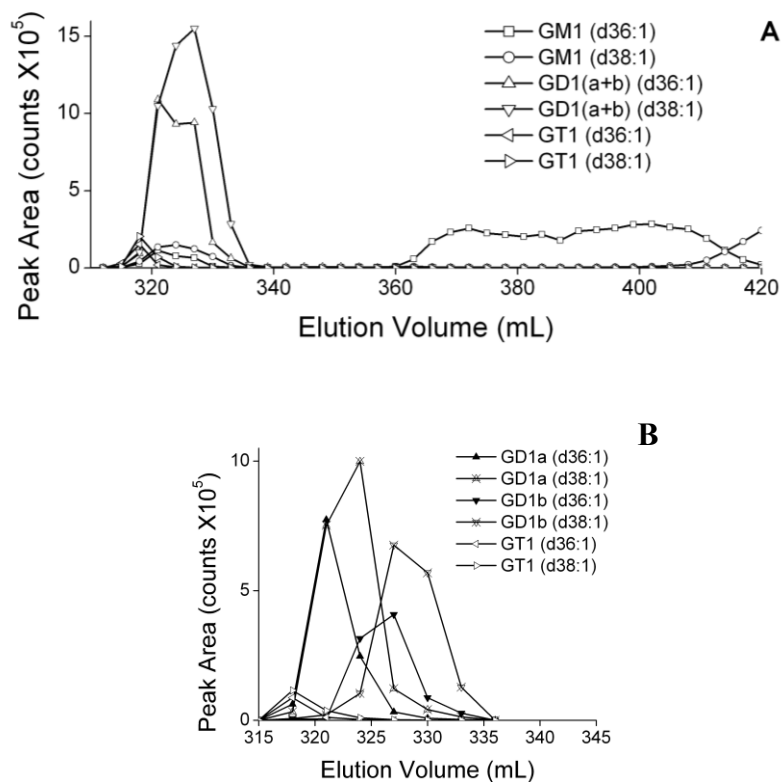


**Figure A1-4.** Head-to-tail mode HSCCC chromatogram of gangliosides mixture using a BuOH/MTBE/ACN/water 2:2:1:5, v/v/v/v solvent system with acetic acid added in the sample solution to 0.5% (v/v).

(The flow rate was 3ml/min and fraction collection frequency was 1 min/tube. **Figure A1-4A** was measured using FIA analysis, while **Figure A1-4B** used LC to distinguish the separation of GD1a and GD1b during specific elution window.)

Following this direction, the more hydrophobic BuOH/MTBE/ACN/water 2:2:1:5 (v/v/v/v) system (greater proportion of MTBE)<sup>552, 561</sup> was then tested to separate this ganglioside mixture (**Figure A1-4A**). As a result, improved resolutions of GD1a and GD1b, for both d36:1 and d38:1 ceramide (**Figure A1-4B**) were observed compared to the 3:1:1:5 experiment (**Figure A1-2B**). This is consistent with an increased retention of the stationary phase. Although the separation of GD1 homologues within the same species (i.e. GD1a (d36:1) from (d38:1), and GD1b (d36:1) from (d38:1)) remained limited with this method (**Figure A1-4B**), semi-purified fractions of GD1a (d38:1) (**Figure A1-5C**) and GD1b (d38:1) (**Figure A1-5E**) were still successfully collected. In addition, the two GM1 homologues GM1 (d36:1) and (d38:1) were also found to be well separated, similar to the observation in the 3:1:1:5 experiment (**Figure A1-4A, A1-5F and A1-5G**). As a result, these collected fractions consist of different compositions of gangliosides homologues (**Figure A1-5A to A1-5G**), including the fractions enriched in abundances of, was achieved: A) GT1b (d36:1+d38:1) and GD1a (d36:1+38:1) (41%, 31%), B) GD1a (d36:1) and (d38:1) (44%, 43%), C) GD1a (d38:1) (56%), D) GD1b (d38:1) and (d36:1) (47%, 27%), E) GD1b (d38:1) (71%), F) GM1 (d36:1) (62%), and G) GM1 (d38:1) (83%) fraction.

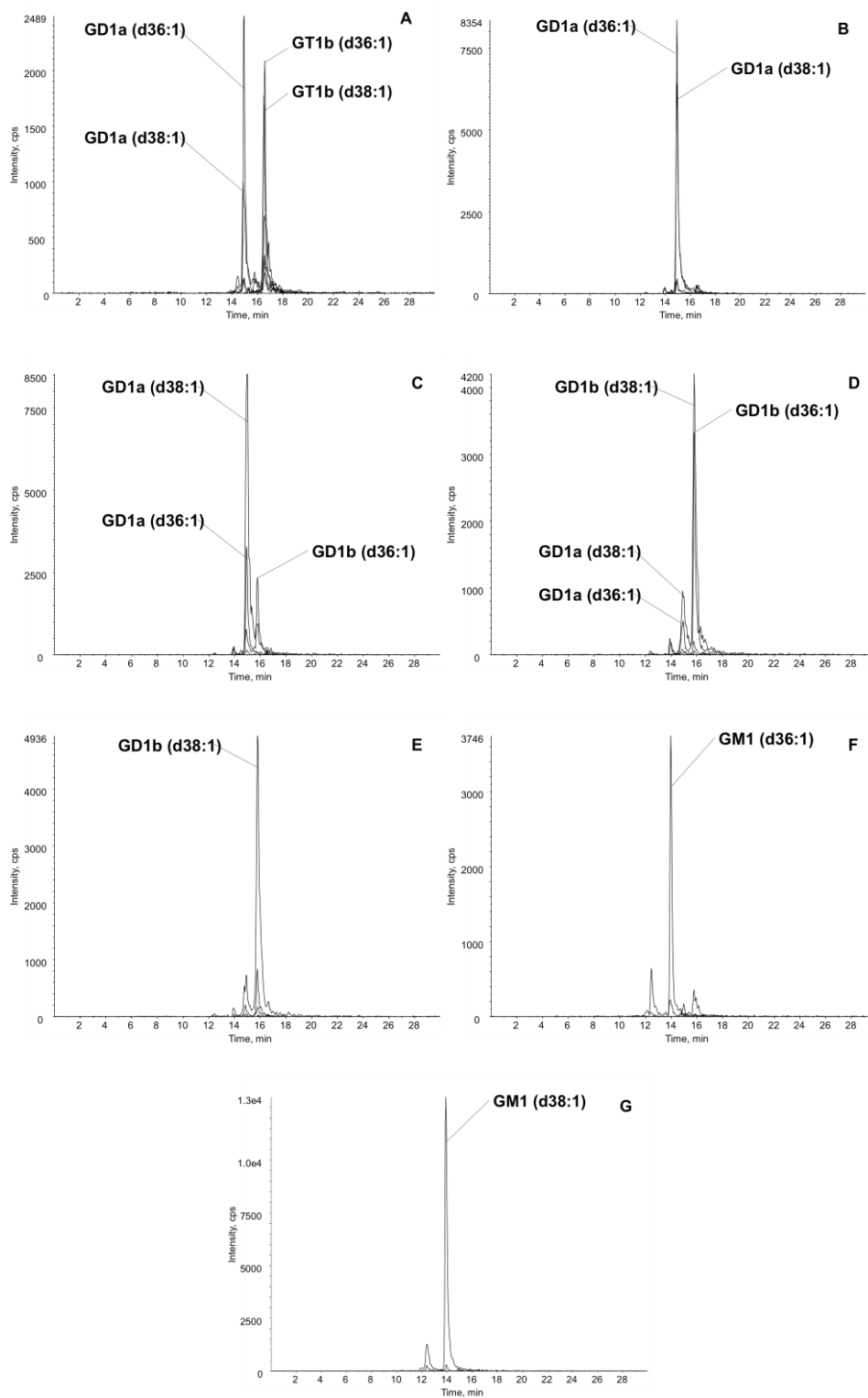


**Figure A1-5.** LC-MS/MS analysis of fractions collected from the HSCCC separation using the 2:2:1:5 solvent system indicated in **Figure A1-4**.

(The enrichment fractions were collected over the following specific elution volume windows:  
A) GT1b and GD1a at 318 mL→321 mL; B) GD1a (d36:1) and (d38:1) at 321 mL→324 mL; C)  
GD1a (d38:1) at 324 mL→327 mL; D) GD1b (d38:1) and (d36:1) at 327 mL→330 mL; E)  
GD1b (d38:1) at 330 mL→336 mL; F) GM1 (d36:1) at 360 mL→411 mL; G) GM1 (d38:1) at  
423 mL→603 mL)

An additional 2:2:1:5 HSCCC experiment was performed using 3mg of a GM1 (d36:1) and (d38:1) mixture (**Figure A1-6**). The purified fractions collected were analysed by LC-MS/MS as seen in **Figure A1-7**. This GM1 mixture contains approximately 4 times the amount of GM1 (d36:1) and (d38:1) compared to the mixture used in the earlier experiments (e.g. that used in **Figures A1-3** and **A1-4**). It can be seen that the separation achieved between GM1 (d36:1) and (d38:1) (**Figure A1-7**) is very similar to that seen in **Figure A1-5F** and **Figure A1-5G**, demonstrating that under the HSCCC conditions used, the separation is scalable, at least over about the 0.375 to 1.5 mg per component range. This would be an important area to study in future research in order to maximise the amount of each ganglioside that could be collected per run.

In conclusion, the 2:2:1:5 system was successful in separating multiple gangliosides classes (GT1, GD1 and GM1) and species (GD1a and GD1b), as well as homologues in some species (GM1 (d36:1) and (d38:1)). The separation of GM1 (d36:1) and (d38:1) was also shown to be scalable. Despite this achievement, further optimization on the separation of GD1 homologues within the same species is still highly desirable.

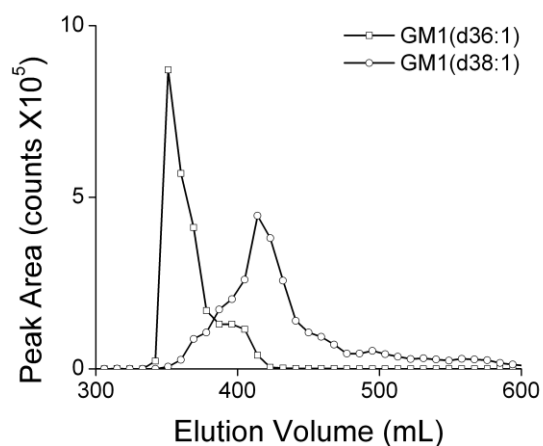


**Figure A1-6.** Head-to-tail mode HSCCC chromatogram of GM1 mixture using a BuOH/MTBE/ACN/water 2:2:1:5, v/v/v/v solvent system with acetic acid added in the sample solution to 0.5% (v/v). The flow rate was 3 ml/min and fraction collection frequency was 3 min/tube.

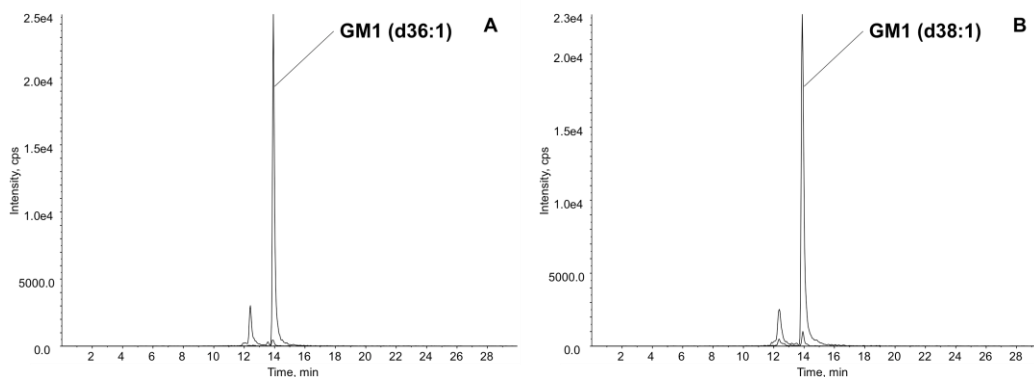


**Figure A1-7.** LC-MS/MS analysis of A) GM1 (d36:1) and B) GM1 (d38:1) fractions separated using the BuOH/MTBE/ACN/water, 2:2:1:5 v/v/v/v solvent system indicated in **Figure A1-6**. (A) and (B) were fractions collected during the elution volume of 342-369 mL, and 414-900 mL.



### **A1.3.3 HSCCC separation of gangliosides in acidified solvent systems with dual-mode elution**

In order to further improve the resolution of gangliosides homologues in the 2:2:1:5 solvent system, we attempted to further increase the interaction between gangliosides and the stationary phase (upper phase) by adding acetic acid into the overall solvent system. Initially, we added acetic acid in the equilibrated 2:2:1:5 system to a final concentration of 0.5% (v/v). This did indeed result in greatly increased interaction between the upper phase and all of the ganglioside species tested, as indicated by the prolonged retention times (no gangliosides eluted within the first 810mL of elution volume) compared to the non-acidified 2:2:1:5 system (**Figure A1-4A**, gangliosides elution at 318-603 mL). In order to overcome this problem of excessively long analyte retention times, and to improve the elution profile, dual-mode HSCCC<sup>564</sup> was then applied.

When the 2:2:1:5 system, acidified with acetic acid, was applied in dual-mode HSCCC, the mobile phase was changed to the stationary phase, and the head-to-tail mode switched to tail-to-head mode at an elution volume of 450 mL (**Figure A1-8 A**). Note that in the following studies, GT1 was not included due to its lower abundance in the mixture combined with the observed peak broadening at larger elution volumes. The chromatogram in **Figure A1-8 A** shows that the classes of GM1 and GD1 species were then separated. In addition, some separation of GD1a and GD1b occurred, as indicated by the peak-widths in the HSCCC chromatogram and confirmed by LC-MS/MS analysis (data not shown). However, the (d36:1) and (d38:1) homologues within each species weren't resolved from each other. We then hypothesized that a solvent system allowing slightly less retention of gangliosides into the non-polar (upper) phase (i.e. a more hydrophobic solvent system) would be a suitable approach to further improve the separation.

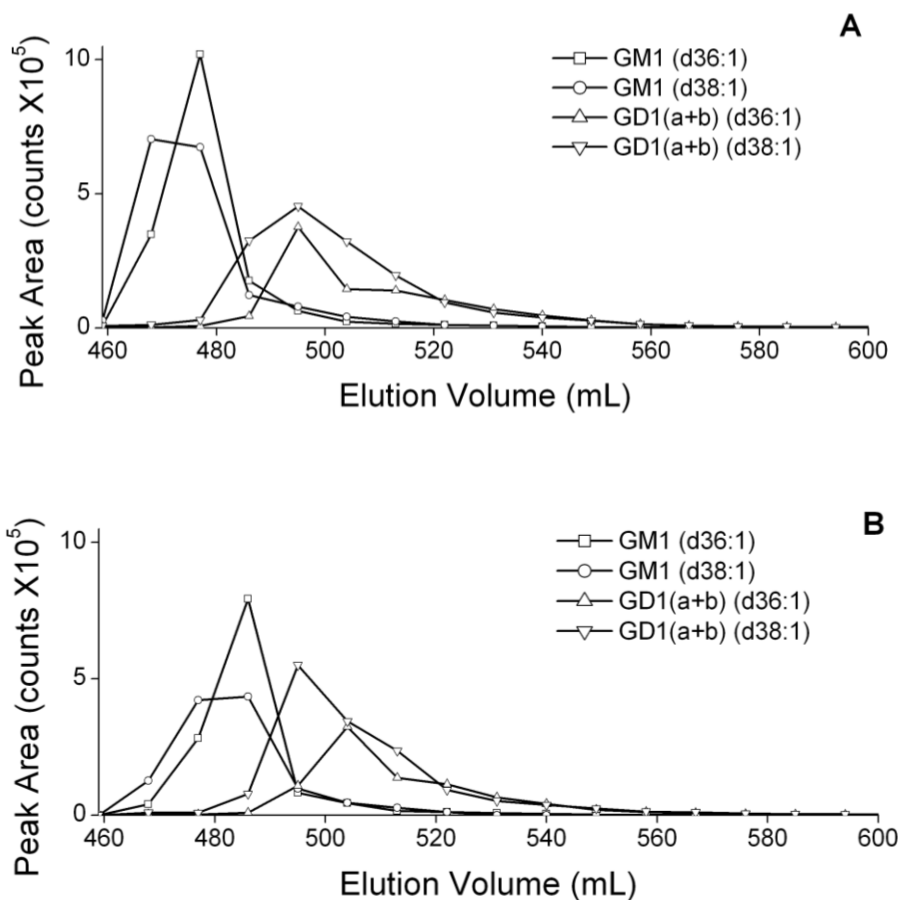


**Figure A1-8.** Dual-mode HSCCC chromatogram of gangliosides mixture using a BuOH/MTBE/ACN/water 2:2:1:5, v/v/v/v solvent system with acetic acid added in the solvent system (A) or only in the lower phase (B) to 0.5% (v/v).

(The flow rate was 3 mL/min and fraction collection frequency was 3 min/tube. To perform dual-mode HSCCC, at the elution volume point of 450 mL, the CCC column was switch to “tail-to-head” mode and upper phase was introduced as mobile phase.)

Following this hypothesis, we aimed to 1) decrease the acid addition in the solvent system, and 2) choose a solvent system resulting in smaller *K* value of the gangliosides tested (**Table A1-2**). First, the acetic acid addition was decreased by only adding it to lower phase, to a

concentration of 0.5% (v/v). This resulted in improved separation of (d36:1) and (d38:1) in both GD1a and GD1b, as indicated by elution volumes of GD1 (a+b) (d36:1) compared to (d38:1) (**Figure A1-8 B**), which are more separated than those seen before this change was applied (**Figure A1-8 A**).

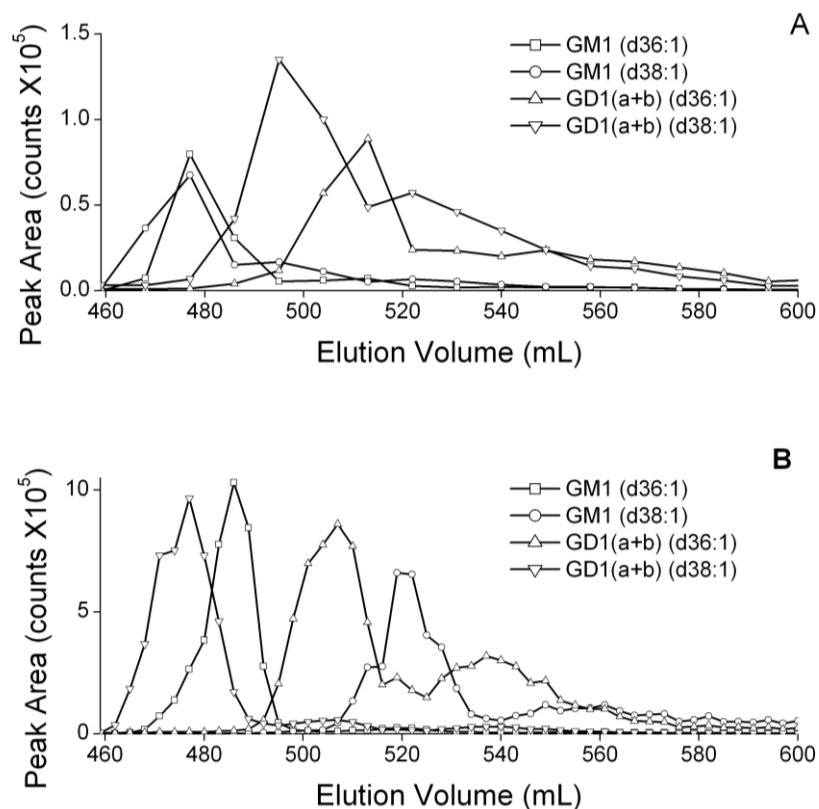


**Figure A1-9.** Dual-mode HSCCC chromatogram of gangliosides mixture using a BuOH/MTBE/ACN/water 2:4:3:8, v/v/v/v solvent system with acetic acid added in the lower phase to 0.5% (v/v).

(The flow rate was 3 mL/min and fraction collection frequency was (A) 3 min/tube and (B) 1 min/tube. To perform dual-mode HSCCC, at the elution volume point of 450 mL, the CCC column was switch to “tail-to-head” mode and upper phase was introduced as mobile phase.)

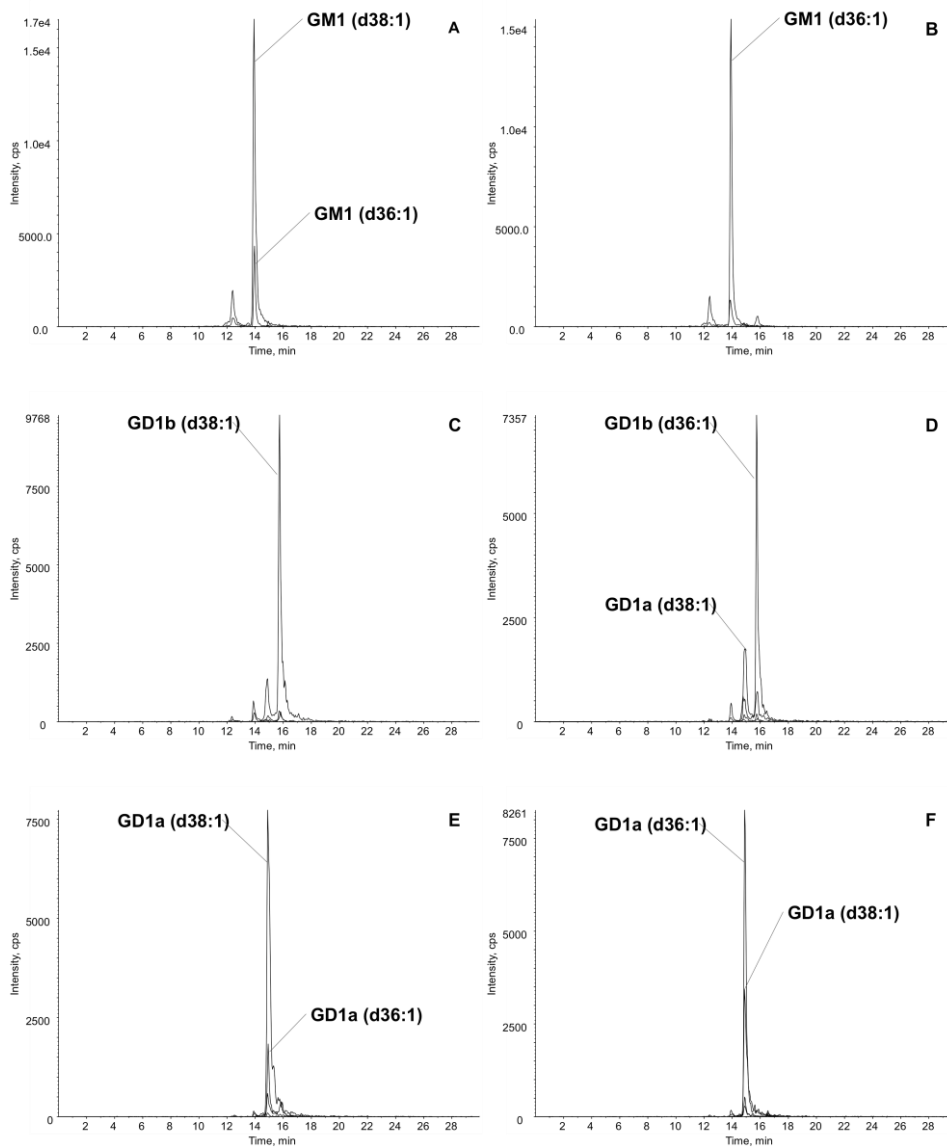


**Figure A1-10.** LC-MS/MS analysis of fractions collected from the dual-mode HSCCC separation using the 2:4:3:8 solvent system indicated in **Figure A1-9**.

(The enriched fractions were collected during the following specific elution volume windows: A) GM1 (d38:1) at 462 mL→480 mL; B) GM1 (d36:1) at 486 mL→495 mL; C) GD1b (d38:1) at 498 mL→507 mL; D) GD1b (d36:1) at 519 mL→528 mL; E) GD1a (d38:1) at 534 mL→549 mL; F) GD1a (d36:1) and GD1a (d38:1) at 561 mL→609 mL;)

Keeping the same concentration of acid addition in the lower phase, we then applied the more hydrophobic solvent system 2:4:3:8 (**Figure A1-9 A**). Compared to the 2:2:1:5 system, a further improvement in peak resolution was observed, such as the appearance of better resolved peaks in the GD1 (a+b) (d38:1) trace (GD1b at 495 mL; GD1a at 522 mL) and in GD1 (a+b) (d36:1) (GD1b at 513 mL; GD1a at 549 mL). Then, by repeating this experiment but with more frequent fraction collection (**Figure A1-9 B**, collecting fractions at 1min/tube compared to 3 min/tube), it became possible to collect fractions enriched in GM1 (d38:1), GM1 (d36:1), GD1b (d38:1), GD1b (d36:1), GD1a (d38:1) and GD1a (d36:1). The ganglioside compositions and their relative abundances of these fractions were illustrated by their LC-MS/MS-MRM traces (**Figure A1-10 A-F**), which were 70%, 73%, 72%, 55%, 72% and 58%, respectively. Note that in an LC-MS/MS (MRM) experiment only the targeted compounds are observed, but this is sufficient to determine the level of fractionation achieved from a mixture containing only gangliosides. Hence, the final HSCCC method was able to separate both GD1 species (GD1a and GD1b) and the homologues ((d36:1) and (d38:1)) within each species, which is a significant advance. Overall, this method was able to fractionate 6 different gangliosides within an elution window of 150 mL, equivalent to a retention time of 50 min.

#### A1.4 Discussion

This study developed an HSCCC method to separate a mixture of porcine gangliosides at the mg-level. MS/MS detection was used to monitor the HSCCC separation of ganglioside homologues that only differ in their ceramide chains. The ganglioside species GM1, GD1a and GD1b, as well as the (d36:1) and (d38:1) homologues of each species were separated within one dual-mode HSCCC experiment, performed using a solvent system of BuOH/MTBE/ACN/water (2:4:3:8, v/v/v/v). Enriched fractions of GM1 (d36:1), GM1 (d38:1), GD1a (d36:1), GD1a (d38:1), GD1b (d36:1) and GD1b (d38:1) were obtained with relative abundances of 55-73%, compared to the 10-21% in the original porcine ganglioside mixtures. These enriched fractions of individual gangliosides were collected, ready to be used for further studies, such as of their structure-dependent functions.

As a powerful separation tool complementary to conventional solid-support methods, liquid-liquid chromatography has many advantages.<sup>66, 144, 559, 59, 569</sup> HSCCC in particular has been used in efficiently separating natural products, including lipids, proteinaceous compounds, alkaloids and many others.<sup>59</sup> In particular, HSCCC has also been reported to separate several types of glycolipids. The less polar alkali-labile glycolipids (i.e. ester cerebroside and monoglucosyldiacylglycerol) were separated using hexane/ethanol/water (5:4:1, v/v/v) system.<sup>570</sup> Sphingolipids and cerebroside were separated via hexane/ethyl acetate/ethanol/0.1% aqueous ammonia (5:5:5:4) using a toroidal-coil model of CCC.<sup>571</sup> In addition to glycolipids, CCC separations of other glycosides have also been reported.<sup>572 573</sup> Pioneering work on the HSCCC separation of gangliosides, especially GM1, was described.<sup>552</sup> However, the detection of ganglioside homologues only differing in their ceramide moieties was not possible in that work, but may be important when discussing structure-dependent functions.<sup>574, 575</sup> Additionally, in the

same study, centrifugal partition chromatography (CPC) achieved better separation compared to HSCCC for GM1, GD1a, GD1b and GT1,<sup>552</sup> possibly due to the better retention of the liquid stationary phase in CPC.<sup>569</sup> However, due to the hydrodynamic nature of HSCCC, in principle, it has advantages of better separation efficiency and low pressure compared to a hydrostatic system like CPC.<sup>560</sup> Therefore, we hypothesized that HSCCC could be further optimized to achieve a better level of separation among gangliosides, not only in class, but also at the species and homologue level.

Although HSCCC can save the cost of stationary phase and increase efficiency by allowing bigger sample loading in each experiment, a major challenge in developing an HSCCC method is the selection of the solvent system.<sup>576, 568</sup> Therefore, systematic selection methods of solvent systems for HSCCC have been reported,<sup>59</sup> especially for predicting the elution pattern based on the *K* value.<sup>59</sup> However, the actual HSCCC separation performance can be affected by many other factors such as sample loading,<sup>566</sup> pH,<sup>566</sup> axial dispersion, mass transfer,<sup>567</sup> and reasonable operation time.<sup>59</sup> Thus, in HSCCC the solvent system and other parameters must be tested for each application. The previously reported HSCCC solvent system used for separation of gangliosides, 3:1:1:5 system is a relatively hydrophilic system,<sup>552</sup> but we found it produced limited separation of GD1 species and homologues. This may be due to the low retention of the stationary phase, resulting in little interaction with the analytes. A low retention of stationary phase has been observed previously in highly hydrophilic systems without additional solvent modifiers, due to the low difference in density between two phases.<sup>568, 577</sup>

We then considered a more hydrophobic solvent system (2:2:1:5)<sup>568</sup> that has been suggested to improve retention of the stationary phase.<sup>59</sup> As a result, the separation of the GD1a and GD1b was indeed improved, but the separation of homologues in both species was still limited. In

another approach, acetic acid directly added into the solvent system resulted in very strong interaction between gangliosides and the upper phase, likely due to the resulting charge state of the acidic gangliosides. To avoid such prolonged elution time, dual-mode elution was then applied in the experiment, in which the system changed from head-to-tail mode to tail-to-head *mode*. After the system switches between these modes of operation, gangliosides continue to partition between both phases in the system and elute in the reverse order. This technique is expected to achieve higher resolution of compounds that are highly retained in upper phase, compared to the simple extrusion of lower phase.<sup>559, 564</sup> In this work, it was found that with this method, most of the individual gangliosides in the mixture could be separated. We further adjusted the addition of acetic acid (0.5%, *v/v* acetic acid in the lower phase) and solvent system ratio to 2:4:3:8 (*v/v/v/v*), which resulted in improved peak resolution.

The importance of maintaining ionizable compounds in the appropriate form for their separation was also apparent. In their non-acidic form (e.g. the ganglioside mixtures were obtained as ammonium salts), gangliosides GM1 (d36:1) and (d38:1) were not separated by the solvent system of BuOH/MTBE/ACN/water (2:2:1:5, *v/v/v/v*) (data not shown). By acidification, the ganglioside ammonium salts were protonated, resulting in a change in their partition behaviour, and leading to the improved separation that was observed. Another strategy that has been applied is the use of an ion exchange cartridge, to obtain similar objectives.<sup>552</sup> pH control as a sample pre-treatment is simple, but is critically important for the separation of ionizable compounds.<sup>578</sup> Additionally, considering the ionizable properties of gangliosides, other strategies targeting ion-pairing and ionic strength can be considered,<sup>578</sup> including a useful HSCCC method, pH-zone-refining counter-current chromatography.<sup>59</sup> However, these strategies usually require



additional clean-up processes after separation (e.g. de-salting process) and hence these methods were not selected in this study.

The purification achieved in this work is the result of selection of the solvent system, solvent modifier and elution mode. This HSCCC method has the advantage of a high sample loading potential, for the preparative separation of ganglioside extracts. In addition, the separation methods described can be combined with semi-synthetic preparations of gangliosides to purify individual compounds.<sup>579</sup>

## **A1.5 Conclusions**

In summary, the main advances achieved by this HSCCC study of gangliosides include the separation of: 1) classes that differ in their sizes of saccharide moieties, e.g. the separation of acidified GM1, GD1 and GT1; 2) species that differ in their saccharide monomer arrangements, e.g. the separation of acidified GD1a and GD1b; and 3) homologues that differ by their ceramide structures, e.g. the separation of GM1 (d38:1) from GM1 (d36:1), GD1a (d38:1) from GD1b (d36:1), and GD1b (d38:1) from GD1b (d36:1).

The versatility of HSCCC to combine different strategies, such as employing pH modifiers to sample or solvent system, different elution modes (head-to-tail, tail-to-head or dual-mode), and a wide range of solvent systems, make it powerful to separate closely similar molecules in a ready-to-scale-up and cost-efficient manner. The application of dual-mode mode here demonstrates the complementarity of liquid-liquid chromatography to solid-support chromatography, where dual elution mode is not easily available. These ganglioside fractionation methods will enable the further characterization of unknown gangliosides, the preparation of analytical standards, and the investigations of their specific biological functions.